

QUARTZ CRYSTAL STUDIES AT VHF AND UHF

A THESIS

Presented to
the Faculty of the Graduate Division

by

Samuel Newton Witt, Jr.

In Partial Fulfillment
of the Requirements for the Degree
Doctor of Philosophy in the School
of Electrical Engineering

Georgia Institute of Technology

June, 1962

"In presenting the dissertation as a partial fulfillment of the requirements for an advanced degree from the Georgia Institute of Technology, I agree that the Library of the Institution shall make it available for inspection and circulation in accordance with its regulations governing materials of this type. I agree that permission to copy from, or to publish from, this dissertation may be granted by the professor under whose direction it was written, or, in his absence, by the dean of the Graduate Division when such copying or publication is solely for scholarly purposes and does not involve potential financial gain. It is understood that any copying from, or publication of, this dissertation which involves potential financial gain will not be allowed without written permission.

DEDICATION

This thesis is gratefully dedicated to my wife, Knoxie, who has somehow survived many years of lonely nights with patience and encouragement, without which the thesis would not have been completed.

ACKNOWLEDGEMENTS

The work reported here represents a combination of research activities sponsored by the United States Army Signal Corps under various contracts and by the Engineering Experiment Station of the Georgia Institute of Technology. The author gratefully acknowledges the use of Signal Corps equipment for much of the work. He is also gratefully indebted to Mr. W. B. Wrigley for arranging the sponsorship by the Engineering Experiment Station.

The volume of work presented would not have been possible without the able assistance of Mr. V. K. Woodcox, who aided in the development of the measurement equipment and in the reduction of the data, and of Mr. J. E. Lane, who tirelessly collected much of the quartz crystal data.

The conversion of the volumes of data into an organized document would not have been possible without the patience and assistance of Dr. D. L. Finn, the author's thesis advisor. The author also acknowledges the contributions of the other members of the reading committee, Dr. B. J. Dasher and Dr. W. B. Jones.

The author also expresses thanks to his many other associates, especially to Mr. W. H. Hicklin, who offered helpful suggestions; to Savoy Electronics of Griffin, Georgia, who supplied some of the necessary quartz crystal blanks; to Dr. W. F. Atchison of the Rich Electronic Computer Center, who arranged for the use of digital computer facilities; and to Mrs. Betty McKelvey, who transcribed the manuscript to plates for reproduction.

TABLE OF CONTENTS

	Page
ACKNOWLEDGEMENTS.	iii
LIST OF TABLES.	v
LIST OF ILLUSTRATIONS	vi
SUMMARY	xii
Chapter	
I. INTRODUCTION	1
II. THE CONVENTIONAL QUARTZ CRYSTAL RESONATOR.	13
III. THE COAXIAL CRYSTAL HOLDER	69
IV. CRYSTAL CONTROL OF OSCILLATORS AT VHF AND UHF.	107
V. CONCLUSIONS AND RECOMMENDATIONS	121
Appendix	
I. MEASUREMENT SYSTEMS AND PROCEDURES	124
II. MATHEMATICAL PROCEDURES AND COMPUTER PROGRAMS.	167
III. SYMBOLS AND ABBREVIATIONS.	182
IV. LITERATURE CITED	184
VEEA.	187

LIST OF TABLES

Table	Page
1. Summary of Responses Measured by the Crystal Measurement Standard.	30
2. Summary of Crystal Holder Calculations by Various Methods	45
3. Summary of Conventional and Hafner Holder Calculations on Several Crystal Responses.	49
4. Comparison of Motional-Arm Resistances in the Coaxial and Conventional Holders.	85
5. Comparison of Calculated Values of C_0 at Various Overtone Frequencies.	88
6. Crystal W254 in the Model 3 Holder.	96
7. Crystal W351 in the Model 3 Holder.	96
8. Crystal W504 in the Model 3 Holder.	99
9. Crystal W507 with the Recessed Electrodes	100
10. Electronic Computer Corrections of National Bureau of Standards Data on General Radio Termination Type 874-W100, Serial No. 111.	128
11. The Harmonic Generation of a Radio-Frequency Amplifier	152
12. Transmission Line Subtraction Program	170
13. Calculate Network Admittance Function Program	173
14. Crystal Holder Analysis	178
15. Crystal Holder Subtraction.	180

LIST OF ILLUSTRATIONS

Figure	Page
1. Several Types of Conventionally-Mounted Quartz Crystal Units.	5
2. Two Types of Internal Construction Employed with the HC-6 Crystal Mount.	5
3. An Equivalent Circuit for a High-Frequency Crystal Unit.	8
4. Coaxial Quartz Crystal Holders	9
5. An Equivalent Circuit of a Coaxial Crystal Holder.	10
6. The Van Dyke Equivalent Circuit for a Low-Frequency Crystal Resonator.	15
7. The Smith Chart Representation of a Simple Series Resonant Circuit	17
8. The Perfect Circle Representation of a Laboratory Crystal.	18
9. Two Equivalent Circuits for a High-Frequency Crystal Unit	20
10. A Crystal Holder Equivalent Circuit.	23
11. An Equivalent Circuit Representing Several Overtone Responses.	23
12. The Actual Laboratory Response of the Crystal of Figure 8	25
13. An Equivalent Circuit to Represent Spurious Responses.	26
14. The Block-Diagram of the Crystal Measurements Standard System.	28
15. Admittance Characteristics of Test Crystal No. C-1	31
16. Admittance Characteristics of Test Crystal No. C-2	32
17. Admittance Characteristics of Test Crystal No. C-3	33
18. The Analysis Circuit for High-Frequency Crystal Units.	34

LIST OF ILLUSTRATIONS (Continued)

Figure	Page
19. Perfect Circle Approximations of the Data of Figure 15. . .	35
20. Admittance Characteristics of Crystal No. C-1 with the Conventional Holder Subtracted.	38
21. Hafner Equivalent Circuit for a High-Frequency Crystal Unit.	39
22. Admittance Characteristics of Crystal No. C-1 with the Hafner Holder Subtracted.	40
23. Circle Approximations of the Holders of Crystal Nos. C-2 and C-3	42
24. Motional-Arm Circles for Crystal No. C-2 as Obtained by Several Methods.	47
25. Motional-Arm Circles for Crystal No. C-3 as Obtained by Several Methods.	48
26. Motional-Arm Response of Crystal No. C-11	52
27. Rectangular Representation of Responses of Crystal No. C-11.	53
28. Motional-Arm Resistance of Several Crystals as a Function of Frequency.	55
29. Motional-Arm Resistance of Several Crystals as a Function of Overtone Number.	56
30. Motional-Arm Q of Several Crystals as a Function of Frequency	57
31. Motional-Arm Q of Several Crystals as a function of Overtone Number	58
32. Values of Q and R_1 for the Motional Arm of a High- Frequency Quartz Crystal.	59
33. Typical Overtone Responses for High-Frequency Crystals at Several Frequencies.	60
34. A Typical Overtone Response at 200 Mc/Sec	61
35. A Typical Overtone Response at 300 Mc/Sec	62

LIST OF ILLUSTRATIONS (Continued)

Figure	Page
36. A Typical Overtone Response at 400 Mc/Sec	63
37. A Typical Overtone Response at 500 Mc/Sec	64
38. The Model 1 Coaxial Crystal Holder.	70
39. Air-Gap Electrodes for the Coaxial Crystal Holder	72
40. Admittance Characteristics of the Model 1 Coaxial Holder and of the Conventional HC-6 Holder.	73
41. Admittance Characteristics of Crystal No. 20 in an HC-6 Holder	75
42. Recessed Quartz Air-Gap Electrodes.	76
43. The Model 2 Coaxial Crystal Holder.	78
44. An Assembly Diagram of the Model 2 Coaxial Crystal Holder .	79
45. Plating Mask for the Preparation of Crystals for the Model 2 Holder.	80
46. Overtone Responses of Crystal Blank A-1 in the Model 1 Holder.	82
47. Responses of Crystal Blank A-1 in an HC-6/U Holder.	83
48. Motional-Arm Responses of Crystal Blank A-1 as Deter- mined from Measurements with an HC-6/U Holder	84
49. Responses of Crystal W351 in the Model 1 Holder	87
50. The Component Parts of the Model 3 Coaxial Crystal Holder .	89
51. The Model 3 Coaxial Holder without the Antiresonating Transmission-Line Stub.	89
52. A Cross-Sectional Sketch of the Model 3 Holder.	90
53. Air-Gap Electrodes and Plating Clip for the Model 3 Holder.	91
54. Responses of Crystal W254 in the Model 3 Holder at 225 Mc/Sec.	93

LIST OF ILLUSTRATIONS (Continued)

Figure	Page
74. Susceptance Corrections for General Radio Admittance Meter, Serial Number 1401	131
75. Calibration of General Radio Resistive Terminations with Serial Numbers as Shown	132
76. Admittance Meter Measurements on Resistive Terminations with Minimum Line Length.	133
77. Loci of Points which can be Calibrated with a 9.69-Cm Line Length	135
78. Admittance Meter Measurements on Resistive Terminations with a Dual Directional Coupler Inserted in the Coaxial Line.	137
79. Admittance Meter Measurements on Resistive Terminations with a 40-Cm Line Length.	138
80. Network Approximation of a Transmission Line.	139
81. Impedance Level Compensation of 40-Cm Transmission Line Data.	145
82. Admittance Meter Measurements on Resistive Terminations with a Half-Wavelength Line	148
83. Power Gain Characteristics of the Instruments for Industry Wide-Band Amplifiers Model 530	151
84. Frequency Characteristics of Three Low-Pass Radio-Frequency Filters	153
85. Null-Detection Sensitivity of the Eddystone Receiver Type 770U	155
86. Stray-Signal Shielding Used with the Eddystone Receiver Type 770U	156
87. Spurious-Signal Reception of the Eddystone Receiver Type 770U	158
88. Signal-Level Meter Sensitivity of the Eddystone Receiver at 250 Mc/Sec	160
89. A Typical Setup of the Crystal Measurements Standard.	164

LIST OF ILLUSTRATIONS (Continued)

Figure	Page
90. System for Locating Crystal Overtone Responses.	165
91. Circuit Diagram for Computer Program 2.	171
92. Circuit Diagram for Computer Program 3.	176

SUMMARY

Quartz crystals have, for many years, been used to control the frequency of electronic oscillators to provide frequency-stable sources of radio-frequency energy. Since the earliest applications, rapid progress has been made in extending the frequency range of quartz crystal control. However, before this research, the state of the art permitted the effective applications of quartz crystals at frequencies only as high as about 150 mc/sec. Many attempts have been made to increase the frequency range of conventionally mounted high-frequency quartz crystal units, but they have achieved only limited success.

The primary purpose of this research was to increase the frequency range of applications of quartz crystals by developing a novel method of mounting the quartz to realize its ultimate properties. Fulfilling this purpose first required a thorough investigation of the properties of the more conventional units. Such an investigation, in turn, necessitated the development of specialized equipment capable of measuring the detailed properties of the conventional units.

A measurement system, given the name of the Crystal Measurements Standard System, was developed for measuring the two-terminal driving-point characteristics of quartz crystal units. The system was complicated by the fact that a crystal displays a very narrow-band resonance characteristic which is dependent upon excitation level. Highly stable signal sources and sensitive detector systems as well as methods for measuring the excitation level were required. A system with the neces-

sary characteristics was developed and calibrated. Insofar as possible, commercially available instruments were employed. Modifications and special calibrations were required in some instances.

Detailed analyses of the two-terminal driving-point characteristics of many conventional quartz crystal units were necessary for the determination of typical internal quartz characteristics. A knowledge of these internal characteristics was necessary for the eventual evaluation of improved mounting techniques. Numerous digital computer programs were written for the automated analyses of the large volume of data obtained with the Crystal Measurements Standard System. In addition, the characteristics of quartz at VHF and UHF were tabulated to obtain a typical representation. The findings indicated that substantial improvements in over-all quartz crystal unit characteristics were possible by the reduction of losses and undesirable reactive effects of the conventional mountings.

The nature of the losses of conventional crystal mountings and the frequency range involved indicated the possible application of coaxial techniques in the construction of an improved crystal mount. Many configurations were investigated with numerous samples of quartz before suitable combinations of material and techniques were found. Eventually, a compensated coaxial quartz crystal holder was developed to provide a crystal unit with the desirable characteristics. This holder was essentially lossless and provided means for the cancellation of reactive effects. Measurements and mathematical calculations indicated that the coaxially mounted quartz crystal units should be useful at frequencies as high as 500 mc/sec.

The superiority of the coaxial crystal holder over the conventional holder at the higher frequencies was substantiated by a series of crystal-controlled oscillator experiments. Crystals mounted in both types of holders were alternately used to control the frequency of various oscillator units. Although the oscillator units were specially designed for use with the conventional crystal units, the frequency stabilities were appreciably better with the coaxial units.

The results of the research are summarized with suggestions for other applications of the measurement equipment and procedures. Direct applications of the conventional quartz crystal data are also suggested.

Recommendations for future work include suggestions of methods for making further improvements in the characteristics of the coaxial holder. Possible oscillator circuit configurations for the more effective application of the desirable characteristics of the coaxial crystal units are also discussed.

CHAPTER I

INTRODUCTION

Since the earliest applications of electronics, the need has existed for improved methods of controlling the frequency of electronic energy inverters. The degree of precision required is dependent upon the applications and may range from permissible variations in frequency of several per cent to an order of precision of one part in 10^{10} per day (1).*

Where very low orders of precision are satisfactory, the frequency may be controlled by the discharge of a capacitor through a resistance network or by the resonance phenomena of an inductance-capacitance network. Greater precision in control is readily accomplished at low frequencies by the application of tuning forks or other mechanically resonant systems (2). Under carefully controlled conditions, inductance-capacitance combinations can provide frequency control to better than one part in 10^5 at frequencies of several hundreds of megacycles per second (mc/sec) for periods of time of several hours or days. At higher frequencies, comparable control is possible through the application of tuned electrical cavities. With these various methods, precise environmental control is generally necessary to achieve the maximum of stability.

* Arabic numerals in parenthesis refer to Cited Literature, APPENDIX IV.

Most of the frequency control methods mentioned above permit frequency changes and adjustments with relative ease. This facility may or may not be an advantage, depending upon the applications. For example, in controlling the frequency of a radio broadcast transmitter, methods for changing or adjusting the frequency are not required as long as the frequency remains stable within a prescribed tolerance. For such applications, piezoelectric control devices have long been used. The most common of these devices is the quartz crystal resonator (or more simply a quartz crystal).

The quartz crystal is capable of controlling the frequency of an audio or radio frequency source with precisions ranging from a few parts in 10^4 to better than one part in 10^{11} for short periods of time. At low radio frequencies, stabilities of the order of one part in 10^8 per week have been accomplished by commercially available instruments (1). Some instruments are capable of longer-term stabilities of a few parts in 10^8 per year. Where ultra-precision moderate-term and long-term stabilities are required, use has recently been made of atomic and molecular resonance phenomena. Atomic resonance devices are capable of maintaining very high degrees of precision for indefinite periods of time.

Although widespread interest exists in the development of ultra-precision frequency control devices, the vast majority of applications call for moderate precisions ranging from one part in 10^5 to one part in 10^7 . For such applications, the quartz crystal is ideally suited. Until about 20 years ago, direct frequency control with quartz crystals was possible only at frequencies up to several megacycles per second.

When control at higher frequencies was required, use was made of frequency multiplication techniques, which generally required extensive electronic circuitry. Recent advances in crystal manufacturing techniques and circuitry techniques have made possible the direct application of quartz crystals at frequencies as high as 150 to 200 mc/sec with low to moderate stabilities (3). Very little has been accomplished, however, in commercial manufacture of crystals or commercial applications of crystal units at higher frequencies.

The primary purpose of this research was to extend the useful frequency range of quartz crystals. This has been accomplished by, first, gaining a better understanding of the characteristics of presently available commercial crystal units and, second, by developing an improved method of mounting quartz crystal plates.

The frequency controlling capabilities of a quartz crystal arise from an electrically-excited mechanical vibration. Since the resonance phenomena are actually mechanical, the frequency is dependent upon the physical dimensions of the crystal and upon the mode of vibration. Electrical coupling is accomplished through the piezoelectric property of quartz, that is, any mechanical deformation of the quartz produces an electrical charge or, conversely, any electrical charge produces a mechanical deformation. The electrical charge is coupled to an external circuit by means of conducting plates between which the quartz crystal is "sandwiched."

For high-frequency applications, the quartz plate is made to vibrate in the thickness-shear mode in which case the thickness of the quartz plate determines the frequency of vibration. The frequency is

inversely proportional to the thickness and is approximately 50 mc/sec for a thickness of one one-thousandth of an inch (4). In addition to the vibrations at the fundamental frequency, the quartz plate may also be made to vibrate at certain overtone frequencies. For thickness-shear crystals, the overtone frequencies fall near the odd harmonics of the fundamental frequency. This condition is comparable to the vibrational characteristics of a stretched string.

The mounting of and coupling to the quartz plate must be such that the mechanical vibrations are not excessively damped. In most cases this may be accomplished by a metallic plating placed directly in contact with the surface of the quartz plate. The plating must, however, be very thin and of light weight metal for satisfactory high-frequency operation.

The highest fundamental frequency available in commercially mounted quartz crystals is of the order of 35 mc/sec. The frequency limitation is imposed by the difficulties in plating, cleaning, and mounting the very thin quartz plates. Oscillator crystal control at higher frequencies is accomplished by operating the crystals at their overtone frequencies.

Several conventionally mounted quartz crystals and some of the component parts are shown in Figure 1. Of the types presently available, the military type HC-6 mount produces the most useful characteristics at the higher frequencies. Thus, only this type will be considered in the present discussions.

A close-up view of the internal construction of the HC-6 crystal mount is shown in Figure 2. Metallic plated electrodes are generally

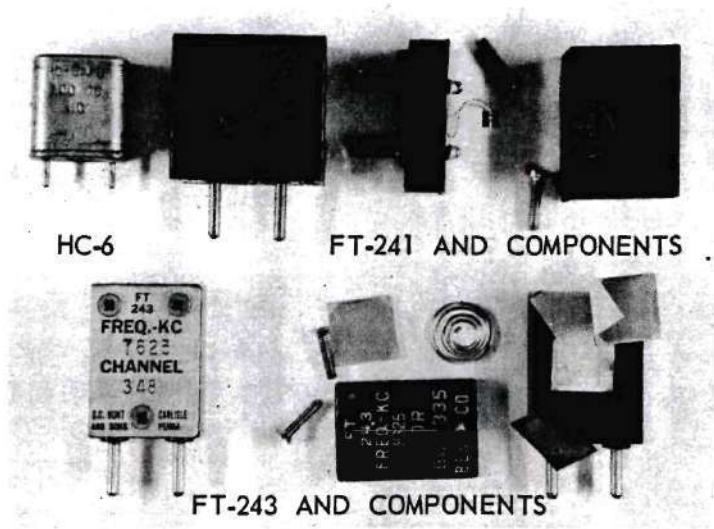


Figure 1. Several Types of Conventionally-Mounted Quartz Crystal Units.

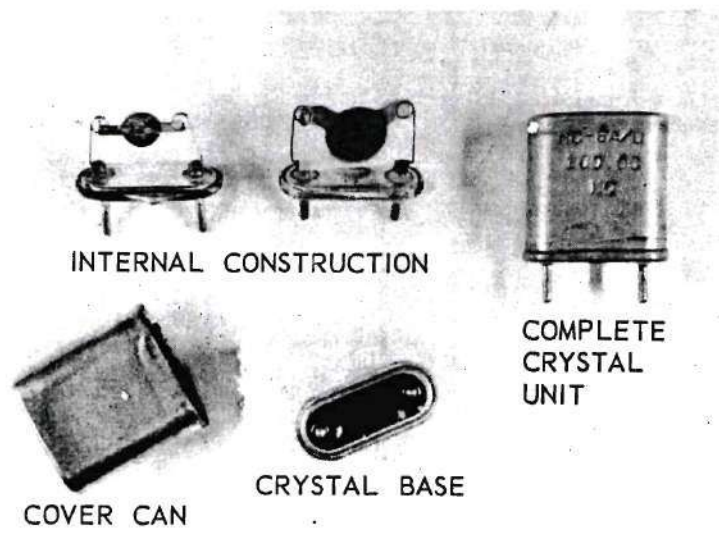


Figure 2. Two Types of Internal Construction Employed with the HC-6 Crystal Mount.

employed to provide electrical coupling to the piezoelectric phenomenon displayed by the quartz. The supporting leads are mechanically and electrically attached to the quartz plates by spring clips as may be seen in Figure 2. Silver cement bonds are generally used to assure good electrical contact. The springs must be constructed of small diameter wire to permit insertion of the edge of the quartz plate without breakage. The supporting wires must also be small to provide some degree of shock mounting.

The piezoelectric phenomenon of quartz in thickness-shear vibration provides an electrical impedance characteristic almost identical to that of an ideal electrical series-resonant circuit. The electrical coupling to the mechanical vibration is, therefore, often represented by a motional-arm equivalent circuit consisting of a relatively small resistance, an extremely small capacitance and an extremely large inductance (5). Thus, the quality factor (Q) of the motional-arm resonance is very high. The values of the equivalent electrical elements can be made to remain highly stable for wide variations in environmental conditions.

The terminal properties of most crystal units are not adequately described by the simple motional-arm equivalent circuit. Various additional circuit elements are required because of the electrical properties of the crystal mounting structure. For example, the capacitance between the plated electrodes, the quartz serving as a dielectric material, is usually included in parallel with the motional-arm circuit (4). The reactance of the capacitance is relatively large at the lower frequencies and, therefore, of little concern. At

frequencies of several mc/sec, the effects of the capacitive reactance can be substantially canceled at any particular frequency by paralleling the crystal unit with a suitable inductance to produce a high-impedance antiresonance.

At frequencies above about 50 mc/sec, an additional circuit effect is introduced by conventional crystal mounts. This effect, which is primarily a property of the supporting wires shown in Figure 2, may be represented as an inductance in series with the motional-arm elements and plating capacitance. Since the inductive reactance is generally smaller than the plating-capacitance reactance, the complete crystal remains capacitive at these frequencies and the net capacitance can still be antiresonated by an inductance. This results in a transformation in the impedance level of the resonance characteristic, a condition which may be either desirable or undesirable, depending upon the intended circuit applications.

At still higher frequencies, generally around 150 mc/sec, the equivalent resistance of the supporting wires becomes appreciable, compared to the lower reactance of the plating capacitance. At frequencies above about 150 mc/sec, the supporting wires may no longer be accurately represented by a simple lumped-parameter circuit. They may, however, be considered as a lossy transmission line with a typical characteristic impedance of about 200 ohms. At most frequencies of present interest, the distributed capacitance between the supporting wires may be lumped with the plating capacitance or, in some cases, divided between the plating capacitance and a terminal capacitance to again yield a lumped-parameter circuit. An equivalent

electrical circuit such as shown in Figure 3 may then be used to represent the complete crystal unit. In the figure, R_L , L_L , and C_L represent the motional-arm equivalent elements while C_O , C_O' , R_L , and L_L represent the holder or mounting equivalent elements.

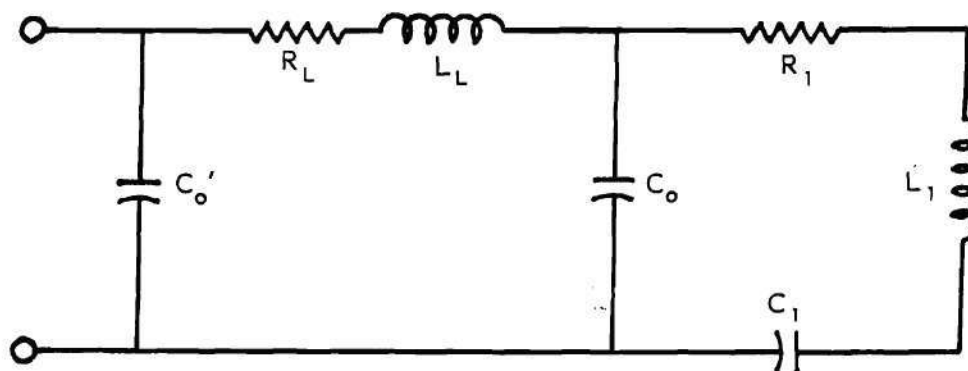


Figure 3. An Equivalent Circuit for a High-Frequency Crystal Unit.

For typical crystal units at frequencies below about 400 mc/sec, the net input terminal reactance of the equivalent circuit of Figure 3 is capacitive when the motional-arm is resonant. If attempts are now made to cancel this reactance with an antiresonating inductance, the resulting terminal characteristics may no longer closely resemble those of an ideal series resonant circuit, even in the vicinity of crystal resonance, since the holder elements may produce both impedance-magnitude and phase-angle distortions and also greatly reduce the effective Q . Thus the usefulness of the device may be severely limited. Practical applications of the presently available quartz crystal units are limited generally to frequencies below 200 mc/sec. Some carefully selected units are occasionally useful at much higher frequencies.

If only the effects of series holder resistance, represented by R_L of Figure 3, could be eliminated, the crystal unit could be made useful at much higher frequencies. The impedance magnitude and phase angle distortions would, however, still limit the upper frequency applications. If the equivalent holder inductance effect could also be eliminated, the plating capacitance could then be antiresonated so that the complete crystal unit assembly could again be represented by the motional-arm equivalent circuit in the vicinity of the motional-arm resonance.

The primary purpose of this research has been to develop crystal mounting techniques to reduce the undesirable mounting effects of the conventional units described above. A novel crystal holder, using a coaxial configuration, has been developed. Three models of this holder are shown in Figure 4. An equivalent circuit that adequately describes the terminal characteristics of the model 3 holder is shown in Figure 5.

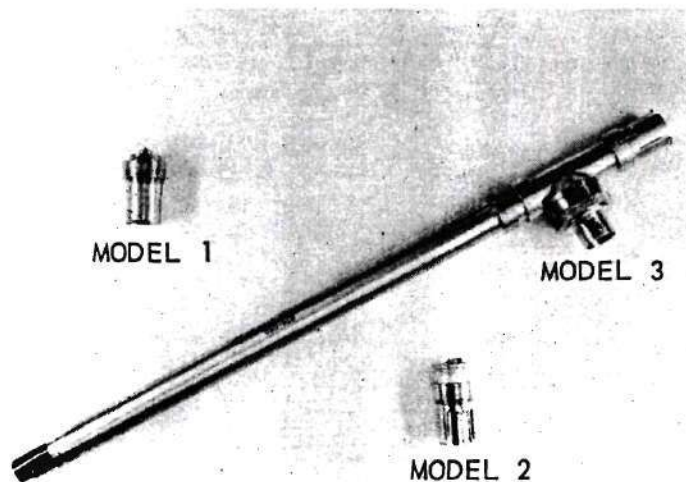


Figure 4. Coaxial Quartz Crystal Holders.

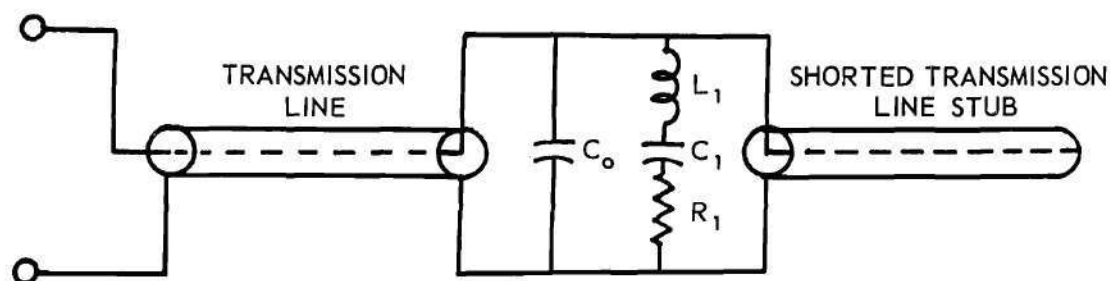


Figure 5. An Equivalent Circuit of a Coaxial Crystal Holder.

Since the plating capacitance, C_o , of the crystal has not been eliminated, its reactance must be antiresonated by the shorted transmission line. A low-loss half-wavelength transmission line is used to couple the crystal unit to external circuits, thus eliminating lead inductance from consideration.

The characteristics of the coaxial crystal holder have been found to be almost ideal at all useful crystal frequencies. Oscillators designed for use with conventional crystals at frequencies as high as 350 mc/sec have been adapted for use with the coaxial holder. The coaxially mounted crystal has provided crystal frequency control superior to the best obtained with conventional crystals. Various considerations have indicated that with the design of crystal controlled coaxial oscillator circuits, reliable and stable frequency control can be accomplished at frequencies well above 400 mc/sec.

Three factors were important in establishing a method of approach to this research problem: (1) the potential usefulness of quartz at frequencies above 300 mc/sec had not been determined, (2) a suitable explanation for the poor performance of conventional crystals at high frequencies was not available, and (3) suitably polished

crystal plates were not available for testing the initially proposed coaxial crystal holder.

Early measurements on conventional quartz crystal units indicated that at least some resonant properties existed even at frequencies as high as 450 mc/sec. Such properties were, however, essentially useless for oscillator control purposes. With the knowledge then available, the degradation of useful properties at the higher frequencies could have been attributed entirely to the characteristics of the quartz, entirely to the parameters of the crystal holders, or partially to each. If the degradation were attributed entirely to the quartz, the design of improved holders would have been a useless endeavor.

The initial phase of this research was concerned primarily with the determination of typical characteristics of conventional crystals. This analysis phase involved, first, developing equipment for measuring the terminal characteristics of such crystals, second, collecting large volumes of data on such crystals, and third, analyzing the data to determine separately the holder characteristics and the motional-arm characteristics. Some of the conventional crystals, after the analyses were completed, were disassembled, the quartz plate mounted in a coaxial holder, and the resulting characteristics compared with the calculated motional-arm characteristics.

Chapter II describes the analyses of conventionally mounted crystal units. Justifications for the assumptions required in presenting the equivalent circuit of Figure 3 are developed. Statistical characteristics of conventional crystal units and of quartz motional-arm parameters are described. Appendix I describes the equipment and

measurement procedures used in collecting the data for Chapter II. Appendix II describes some of the digital computer programs which were most useful in reducing the data.

During a later phase of the research, polished crystal blanks became available in sufficient quantity to permit the design and construction of prototype coaxial crystal holders. Chapter III describes and evaluates these various holders. A final coaxial holder design which essentially eliminates all of the undesirable parameters of the conventional holder is described.

After suitable methods of coaxially mounting quartz plates were developed, some experiments were conducted with applications to oscillator circuits. Probably the more useful, but also more time consuming, approach would have been to design coaxial oscillators for use with the coaxial holders. Since the applications of coaxially mounted crystals were not considered to be the major purpose of the research, conventional high-frequency oscillator circuits were modified to accept the coaxial holder. This procedure permitted the operation of such oscillator circuits with both the conventional and the coaxially mounted crystals for direct comparisons. Thus any differences in performance could be attributed only to the crystals and not to the circuits. The superiority of the coaxial holder is indicated by the experiments with crystal oscillator circuits as described in Chapter IV.

Chapter V, in addition to summarizing the results of the research, indicates some of the possible methods of improving the coaxial crystal holder and associated circuits.

CHAPTER II

THE CONVENTIONAL QUARTZ CRYSTAL RESONATOR

W. G. Cady (5) in his book "Piezoelectricity" states:

Man's earliest production of an electrical effect came through the agency of mechanical forces. A mysterious attractive power was known by the ancient Greeks to be a property of elektron (amber) when rubbed. (Although a knowledge of this property of amber is frequently attributed to Thales in the sixth century B.C., the first authentic account that has come down to us appears to be in Plato's "Timaeus," 427-347 B.C.) In later centuries, as more was learned about electricity, its various manifestations were distinguished by special prefixes, as galvanic, voltaic, animal, frictional, contact, faradic, thermo-, photo-, ballo-, tribo-, actino-, pyro-, piezo-, or strepho-, some of which are now obsolete or abandoned.

The discovery that electrical charges can be produced by compression of certain crystals is attributed to Pierre and Jacques Curie in 1880 (6, 7). Woldemar Voigt (8) first pointed out the difference between the closely related pyroelectric and piezoelectric effects. The Curies and others showed that the piezoelectric effects were reciprocal; that is, the piezoelectric coefficient for quartz is the same for the conversion of deformation to charge as it is in the conversion of charge to deformation. Voigt was the first to mathematically describe the many forms of piezoelectric effects.

Piezoelectric effects were almost entirely ignored, serving only as material for a few doctoral theses, until during World War I when crystals were used as acoustic transducers for underwater sound transmission and reception. Cady, in 1918, first examined the properties of crystals at frequencies near mechanical resonances. In

1922, Cady published a paper on the application of his theory to piezoelectric resonators. Several hundred papers have since been published dealing with applications and geometric configurations of various types of piezoelectric materials.

The possible modes of vibration of a crystal are numerous and extremely complicated due to the several forms of strain (flexural, torsional, shear, and others), each of which depend upon the elastic constants, dimensions, and density of the material and each of which may exist on several surfaces of the material, either independently or coupled to the other modes. Cady (5) states: "No complete and rigorous theory of vibrations in solids, even for the simpler forms of isotropic bodies, has ever been formulated. A full treatment of all coupling effects and boundary conditions defies analysis."

For high-frequency applications of quartz crystals, the shear modes of vibration are of greatest interest for various reasons which will not be discussed here. In particular, the thickness-shear mode, where the lateral dimensions of the plate are great compared to the thickness, is of prime interest. For a perfect plate of infinite lateral dimensions, the shear mode will not be coupled to the other modes and, for the thickness-shear mode, the frequency will be determined only by the thickness of the plate (9). This condition is approached by practical quartz plates of reasonable dimensions.

The equations for the mechanical vibration of quartz in thickness shear can be written and solved with reasonable accuracy. When the mechanical equations are combined with the piezoelectric equations, an equivalent electrical circuit for the quartz plate can be formulated.

Van Dyke (10, 11, 12), using the equations of Cady, has shown that an equivalent electrical circuit for a crystal operating near its mechanical resonance is as shown in Figure 6. In this figure, all of the ele-

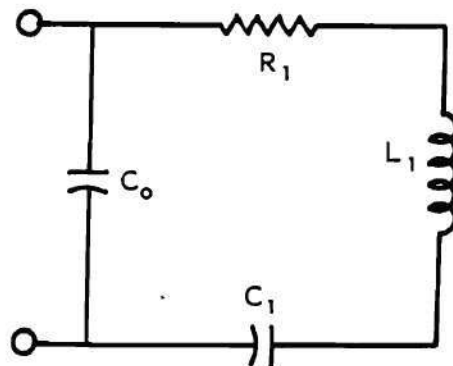


Figure 6. The Van Dyke Equivalent Circuit for a Low-Frequency Crystal Resonator.

ment values are independent of frequency, the series RLC branch representing the electrical equivalent of the mechanical resonance and the shunt capacitance, C_0 , representing the capacitance of the electrodes with the crystal as a dielectric. Butterworth (13) independently predicted the same circuit configuration even before crystals were first used as resonators. Later, Dye (14), using the Butterworth theory, derived the Van Dyke equivalent circuit. Van Dyke (15), after discussing the validity of the equivalent circuit, states:

Although the detailed theory has not been worked out for other types of resonators, there can hardly be any doubt of the universal validity of Butterworth's theorem as applied to piezoelectric vibrators, in that a piezo resonator of any type can be represented by the same form of equivalent network.

Since this research was concerned only with the mounting of existing quartz resonator plates, the circuit of Figure 6 will be assumed to satisfactorily represent the piezoelectric coupling to the plates.

The elements of this circuit will be assumed, as is justified in the literature (10, 11, 12), to be of constant value with respect to frequency, except as will be discussed in specific examples later. The author recognizes, however, that temperature, pressure, and mechanical loading will affect the element values.

The analyses to be presented can best be studied when the responses are graphically represented in terms of impedance or admittance. In particular, the use of Smith charts (16) greatly simplifies the analyses. The admittance characteristics of a simple series resonant circuit as plotted on a Smith chart are shown in Figure 7. If the Q of the circuit is extremely high, the range of frequencies which may be resolved on the circle is extremely small. Thus, if the circuit is shunted by a capacitor as in Figure 6, the susceptance of the capacitance may be considered to be constant over most of the range of the circle. An excellent approximation to the response of Figure 6 is then also a circle as shown dotted in Figure 7. This response circle is appreciably in error only in the region near zero conductance, a region of little concern in the present analysis.

For well mounted crystals, using the conventional high-frequency military type HC-6 mount, the equivalent circuit and admittance diagrams of Figures 6 and 7 are satisfactory for frequencies below about 50 mc/sec. Laboratory measurements have shown, however, that at higher frequencies, the resonance characteristics may no longer be represented by circles such as the dotted example of Figure 7. Perfect circle approximations for an actual laboratory crystal are shown for several overtone frequencies in Figure 8. The actual data points occur in a

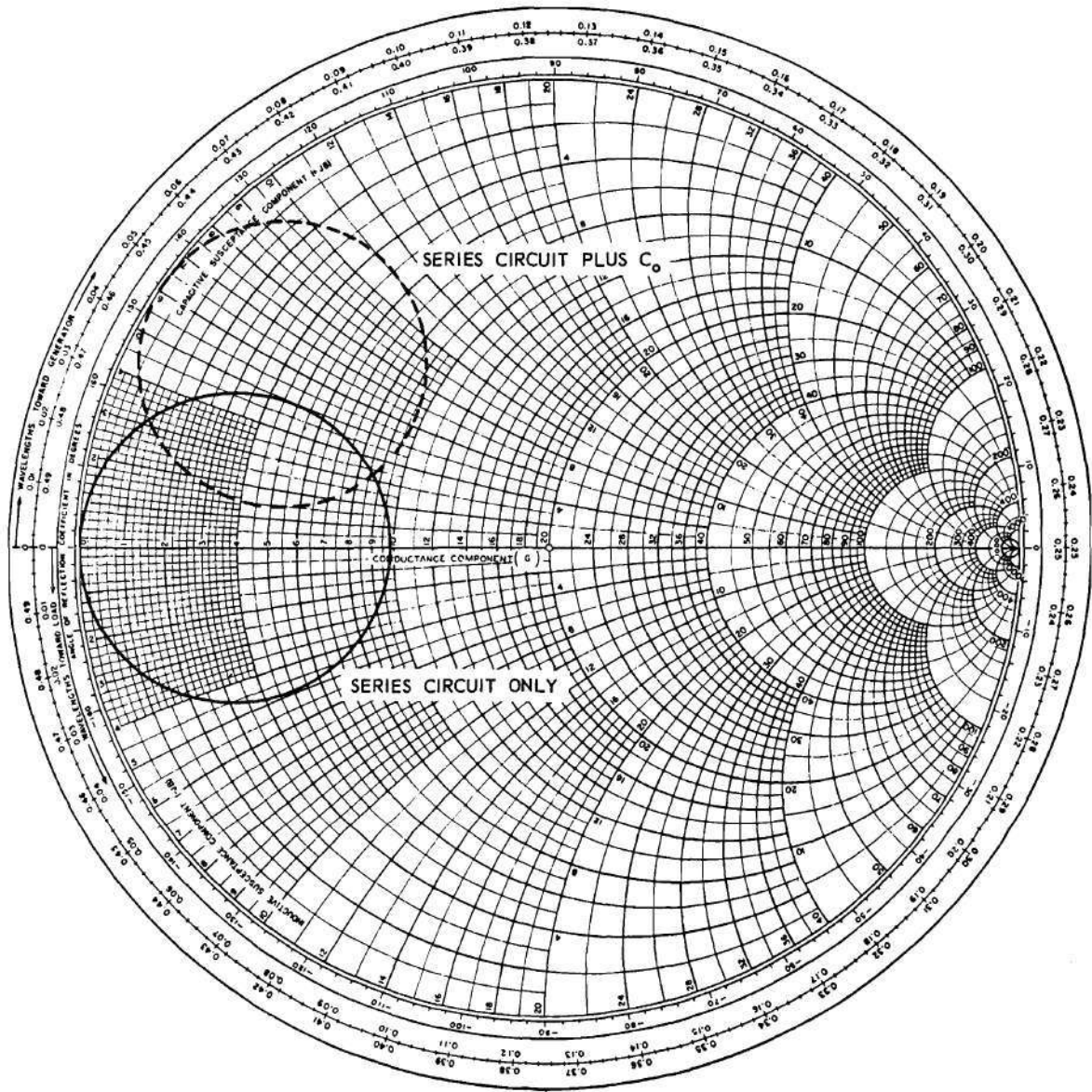


Figure 7. The Smith Chart Representation of a Simple Series Resonant Circuit.

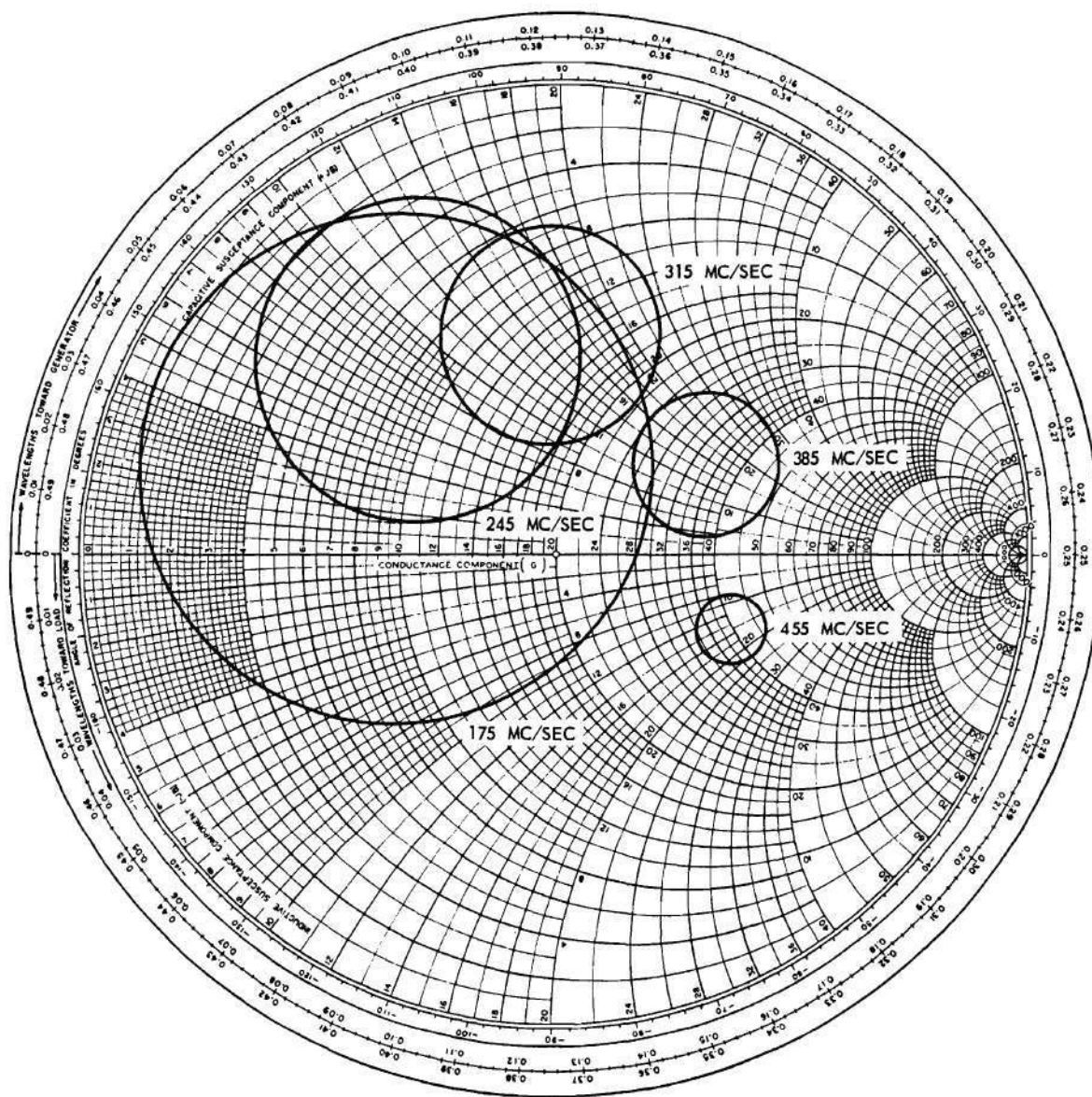


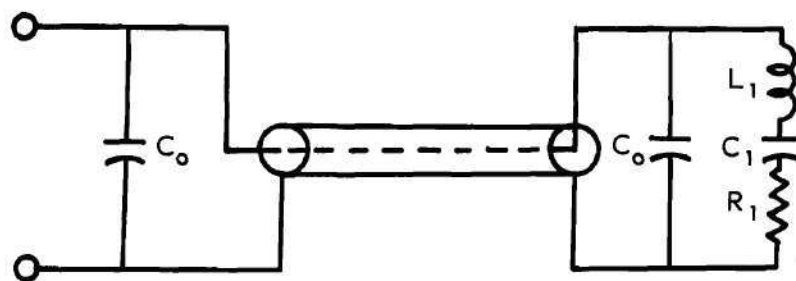
Figure 8. The Perfect Circle Representation of a Laboratory Crystal.

more random manner; however, the perfect circles of the figure (as will be discussed later) are appropriate for the present illustrations.

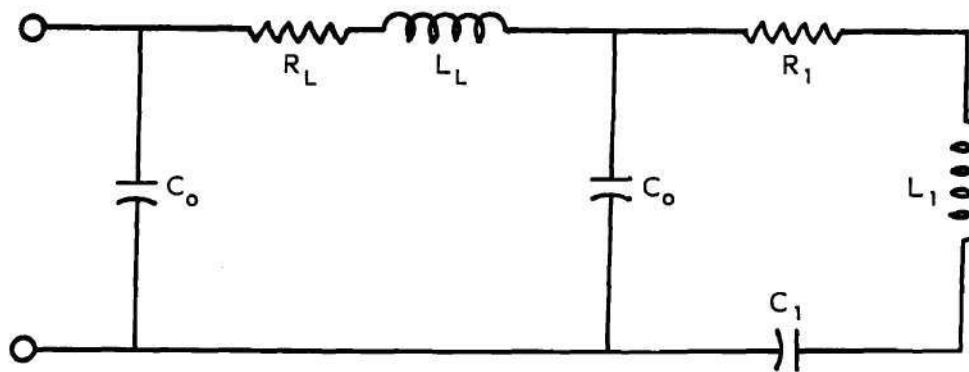
No choice of parameter values exist such that the circuit of Figure 6 will duplicate the characteristics of the individual circles of Figure 8. Thus, additional elements must be added to the circuit. A wide variety of circuits will approximate the desired characteristics; however, a circuit which can be physically justified from the construction of the crystal mount is desirable. Several such circuits exist, each approximating the desired characteristics to various degrees.

In order to separate the piezoelectric effects from the holder effects, the equivalent series-resonant circuit of Figure 6 will hereafter be called the motional-arm circuit. Since no reason has been found to doubt the conclusions of Butterworth, Van Dyke, and others, as previously referred to, the motional-arm circuit configuration will be assumed to be invariant. The remaining circuit elements, as necessary to satisfactorily represent the complete crystal unit, will be referred to as the holder equivalent circuit. The holder circuit will include the plating capacitance, C_0 , of Figure 6.

Of several possible circuits which might be considered, the two circuits of Figure 9 have been chosen for further analyses for the following reasons: (1) they are sufficiently simple for practical mathematical analysis, (2) the choice of configuration can be physically justified from the mechanical and electrical holder configuration, and (3) the circuits generally provide sufficiently accurate approximations to the measured characteristics of laboratory crystals.



(a) A TRANSMISSION LINE CIRCUIT.



(b) A LUMPED-ELEMENT CIRCUIT.

Figure 9. Two Equivalent Circuits for a High-Frequency Crystal Unit.

The circuit of Figure 9a can be physically justified from the examination of the military type HC-6 mount. The supporting wires of this mount form a transmission line with a characteristic impedance of approximately 200 ohms. The terminating capacitor, C_o , represents the crystal plating capacitance while the other terminating capacitor, C_o' , represents a discontinuity at the point where the supporting wires pass through the hermetic seal at the base of the mount. The methods described by King (17) are applicable here. In order for this circuit to provide the characteristics of Figure 8, the transmission line must be lossy.

One of the purposes of the analyses of conventional high-frequency crystals was to determine the motional-arm parameters of typical crystal units. Only the two-terminal characteristics of the units can be measured without destroying the hermetic seal. Thus, the equivalent circuit and the analysis method must be chosen so that all element values can be determined from this very limited data.

The practical usefulness of the circuit of Figure 9a is questionable since the electrical length of the transmission line is small compared to a quarter-wavelength at the highest frequencies of interest. Thus, the transmission line can be approximated by lumped elements in either "Tee", "pi", or "L" configurations. If the "pi" configuration is chosen, the transmission line is approximated by a series inductor and two shunt capacitors. The circuit of Figure 9a may then be replaced by the circuit of Figure 9b, where C_o and C_o' will have slightly different values in the two circuits. The circuit of Figure 9b may also be directly justified by ignoring the possible transmission line

effects of the physical holder and considering the supporting wires merely as inductors. The high-frequency resistance of the wires replaces the transmission-line loss by a lumped resistance, R_L , as shown in Figure 9b.

Since the motional-arm capacitance, C_1 , is extremely small, the admittance of the motional-arm circuit is appreciable only at frequencies near an overtone response. The complete crystal may, therefore, be represented by the holder equivalent circuit alone, as shown in Figure 10, over most of the frequency spectrum. This circuit may be recognized as a series resonant circuit consisting of C_0 , L_L , and R_L , shunted by a capacitor, C_0' . Matching of the circuit of Figure 9b to the measured laboratory data is thus substantially simplified. (The term matching as here applied to equivalent electrical circuits implies the process of choosing circuit element values so that the impedance or admittance function is, as nearly as possible, identical to the measured laboratory characteristic).

The simplified equivalent circuits discussed thus far have assumed that only one motional-arm response exists for each crystal. In reality, a response exists at each overtone frequency (corresponding approximately to the fundamental frequency and each odd-numbered harmonic frequency). Therefore, a more nearly exact representation of the crystal would be as shown in Figure 11. Here, motional-arm responses, sufficient in number to represent the crystal of Figure 8, are shown.

An additional complication in representing a laboratory crystal by an equivalent circuit arises from imperfections in the quartz and

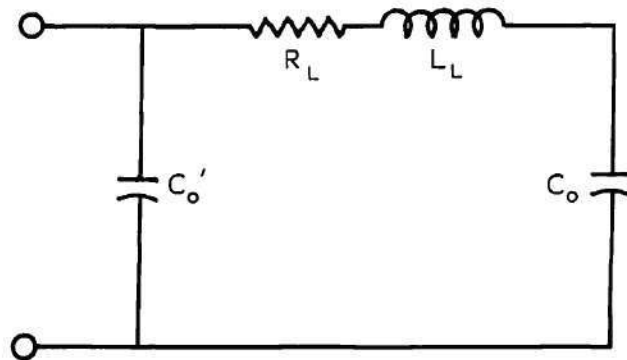


Figure 10. A Crystal Holder Equivalent Circuit.

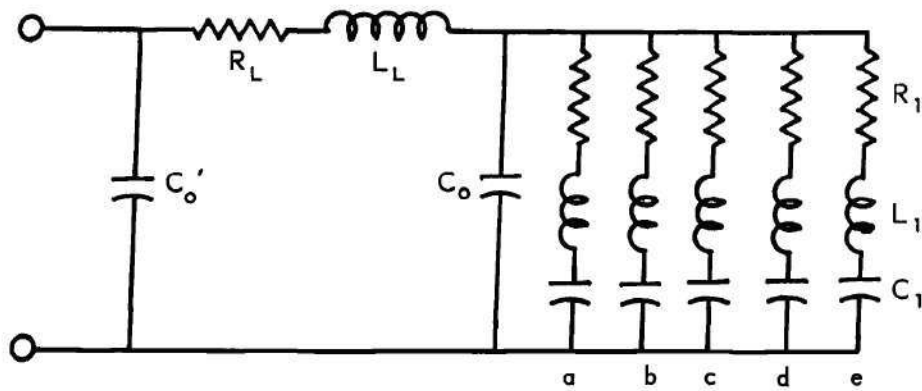


Figure 11. An Equivalent Circuit Representing Several Overtone Responses.

lack of symmetry in electrode structure. This complication is illustrated in Figure 12, which is the point-by-point data plot for the corresponding response of Figure 8. The larger circular curve at 175 mc/sec is defined as the desired or main response and the smaller circular curves near the same frequency are defined as spurious or unwanted responses. Similar spurious responses exist at the other overtone frequencies but are not shown because of the complexity of the diagram. One equivalent circuit which may approximate the characteristics of Figure 12 is illustrated in Figure 13. Each spurious response is characterized by its resistance, Q , and resonant frequency. For a crystal to be acceptable for use in oscillator circuits, all spurious responses must have resistances much greater than that of the main response and the resonant frequencies of the spurious responses must be well separated from that of the main response. If these conditions are realized, the main responses will be approximately circular in shape as shown in Figure 12. In particular, the spurious responses almost always occur at frequencies above the resonant frequency of the main response. Thus, at frequencies below resonance, little distortion of the main response occurs.

Only the main response of the motional arm is of interest for the analysis purposes. The spurious responses may be conveniently disregarded by approximating the main response with a perfect circle. Graphically, a circle is constructed through as many of the main response data points as possible with more weight given to the points below the resonant frequency than to the points nearer the spurious responses. Such circles will hereafter be referred to as the perfect circle approximations of the motional-arm response.

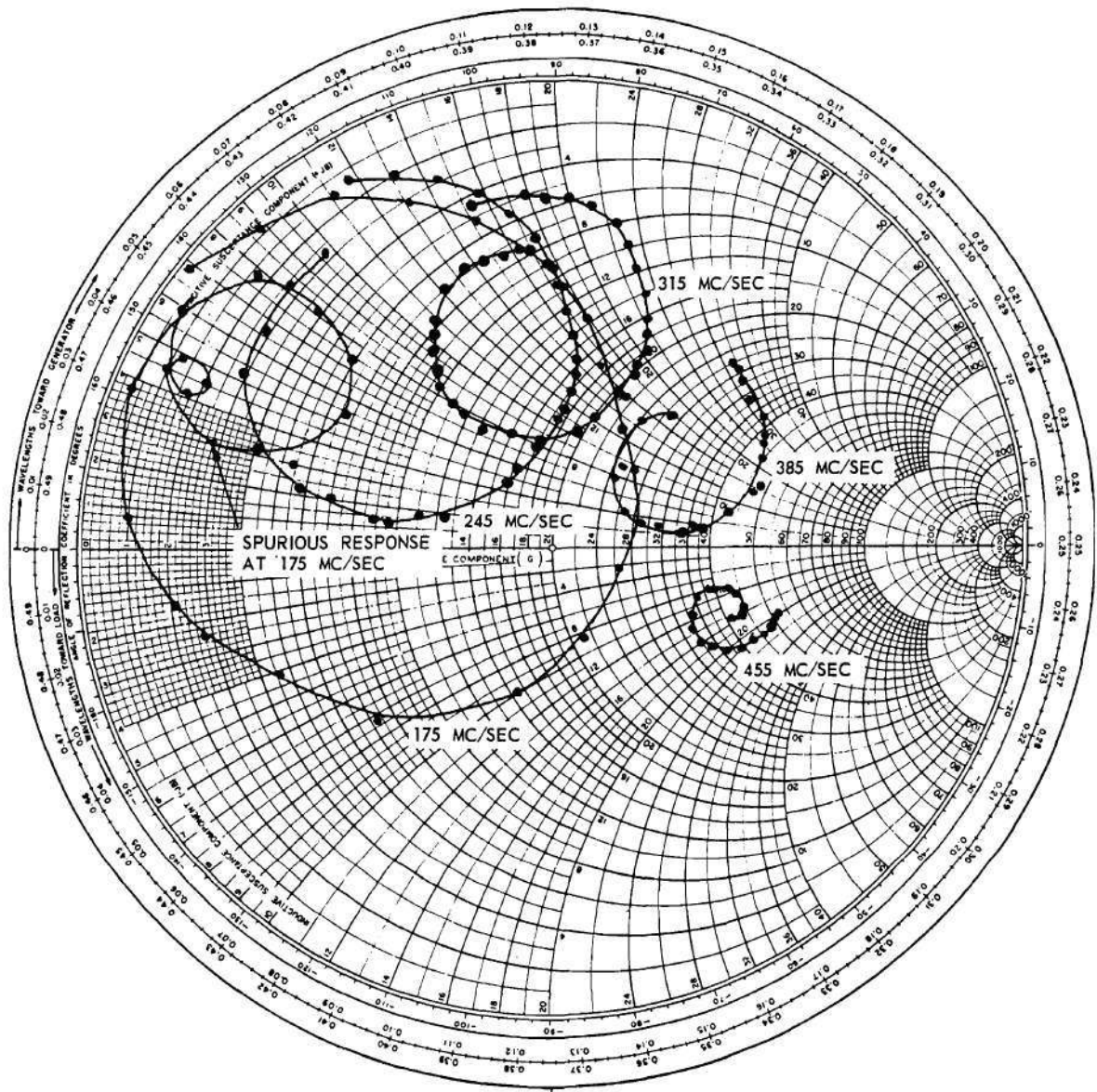


Figure 12. The Actual Laboratory Response of the Crystal of Figure 8.

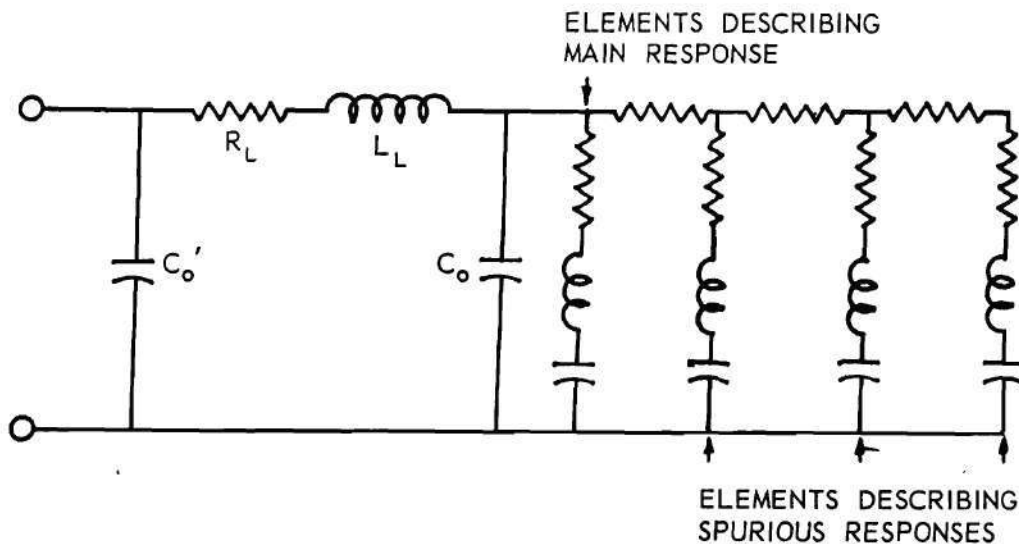


Figure 13. An Equivalent Circuit to Represent Spurious Responses.

At any particular overtone response frequency, the combined net reactance of all other responses, both main and spurious, is generally negligible or can be represented by slight variations in the value of capacitor C_o . Thus, the simplified equivalent circuit of Figure 9b, indicating only one overtone response for a particular set of parameter values, is satisfactory for most purposes.

Equivalent circuits similar to that of Figure 9b have frequently been proposed in the literature. However, the desirability of including the element C_o' has not generally been recognized, probably due to poor laboratory measurement resolution. The use of a more refined equivalent circuit with additional elements cannot be justified with the present limitations on measurement accuracy. The circuit of Figure 9b will hereafter be referred to as the conventional equivalent circuit of a high-frequency quartz crystal.

Since a principle objective of this research was to determine the potential usefulness of quartz crystals at the higher frequencies, methods had to first be found for measuring the external parameters of the crystals and then various analysis procedures had to be developed to separate the holder and motional-arm parameters.

Crystal Impedance Meters have long been available for measuring the parameters of low-frequency crystals. Currently available instruments of this type are capable of measuring some of the parameters of crystals at frequencies as high as 200 mc/sec (18). These measurements are, however, restricted to such quantities as equivalent resistance and overtone frequency and are of very limited accuracy.

Other possible measurement methods include bridge (19), transmission (20), and substitution methods (21). The substitution methods were investigated but found to be of little usefulness at the higher frequencies except for very limited accuracy applications (22). Most of the transmission methods are capable of supplying only a limited quantity of information concerning the crystal. The bridge methods, however, are capable of supplying complete information concerning the two-terminal characteristics of the crystal.

A large portion of the early stages of this research was devoted to the development of suitable measurement procedures. The resulting system, which will be referred to as the Crystal Measurements Standard System (22), is block-diagrammed in Figure 14. A complete description and evaluation of the system including operating procedures appears in Appendix I.

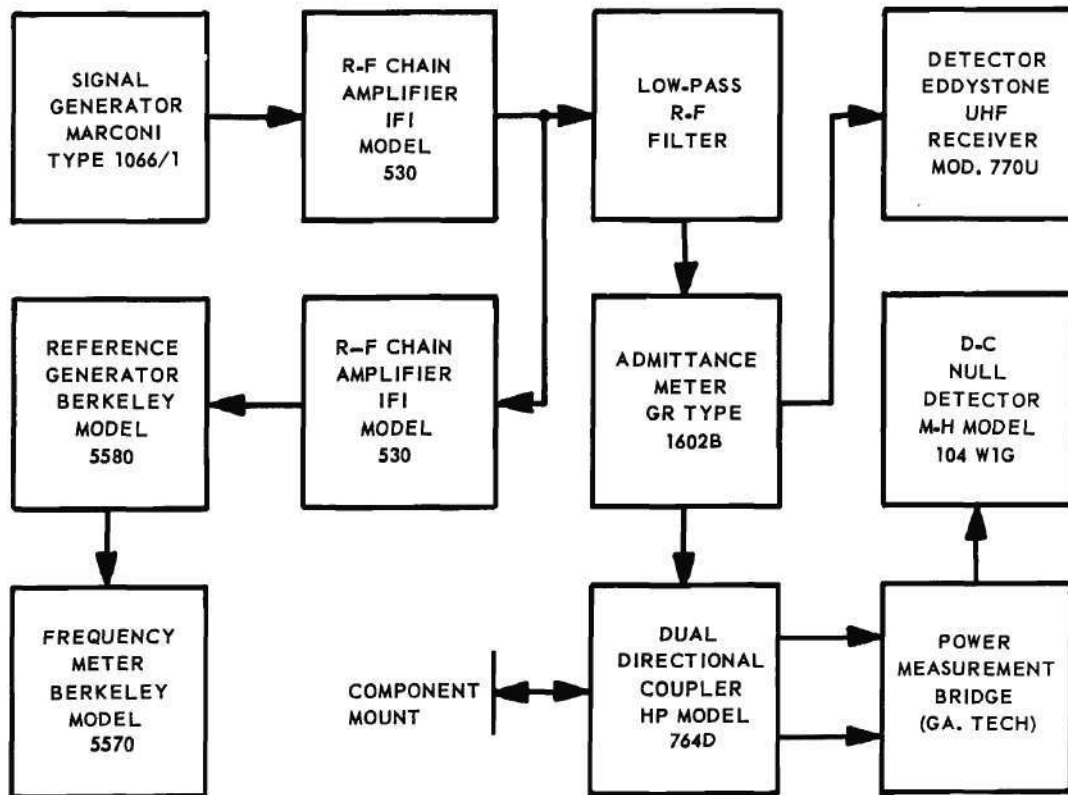


Figure 14. The Block-Diagram of the Crystal Measurements Standard System.

During the conventional crystal analysis phase of the research, crystal measurement data were obtained on approximately 50 VHF HC-6 quartz crystals at overtone frequencies from below 150 to above 300 mc/sec. All measurements were made with the Crystal Measurements Standard System with a crystal drive level of 2 mw or less as indicated by a high-frequency vacuum-tube voltmeter connected across the crystal. That variations in drive level affects the various parameters of quartz crystals is well known (23); however, the exact effects depend greatly upon the individual crystal characteristics. Thus, the drive level was kept small to minimize these effects.

More than one-half of the measurements were made during the development stages of the Measurements Standard and will not be considered in the analyses because of the limited measurement accuracies. Table 1 shows a summary of the more accurately measured responses. Thirty to fifty data points were obtained for each of the overtone responses indicated.

The corrected responses (see Appendix I and computer program number 1 of Appendix II) of three of the better crystals are shown in Figures 15, 16, and 17. Several possible methods exist for reducing the two-terminal crystal data, such as represented by these figures, to crystal equivalent circuits. The methods differ both in theory and results; however, each of the methods is based on a particular assumed equivalent circuit. For reasons already presented, the circuit of Figure 9b was chosen for the initial analyses. This circuit is redrawn as Figure 18 to stress the defined separation between the holder elements and the motional-arm elements.

Table 1. Summary of Responses Measured
by the Crystal Measurement Standard

Crystal Number	Fundamental Frequency In Mc/Sec	Overtone Responses Measured										Highest Overtone Frequency Measured In Mc/Sec	
		5	7	9	11	13	15	17	19	21	23		
C-9	16.67			X	X	X	X	X	X	X	X	X	384
C-4	16.67			X	X	X	X	X	X	X	X	X	384
C-12	19.96			X	X	X	X	X	X	X			420
C-13	19.97			X	X	X	X						300
C-2	29.93	X	X	X	X								330
C-3	32.93	X	X	X	X	X	X						429
C-10	34.93	X	X	X	X	X							455
C-5	16.17				X	X	X	X	X				308
C-6	16.17				X	X	X	X	X				308
C-25	16.18				X	X	X	X	X				308
C-26	16.17				X	X	X	X	X				308
C-35	16.17				X	X	X	X	X				308
C-36	16.17				X	X	X	X	X				308
C-37	16.17				X	X	X	X	X				308
C-50	17.96			X	X	X	X	X					306
C-51	17.96			X	X	X	X	X					306
C-52	17.96			X	X	X	X	X	X				342
C-7	14.97				X	X	X	X	X				285
C-70	17.96			X	X	X	X	X	X	X	X	X	414
C-8	17.96			X	X	X	X	X	X	X	X	X	414
C-72	17.96			X	X	X	X	X	X	X	X	X	414
C-1	35.00	X	X	X	X	X							455
C-38	16.67				X								184
C-39	16.67				X								184
C-68	17.96			X	X	X	X						270
C-69	17.96			X	X	X	X						270

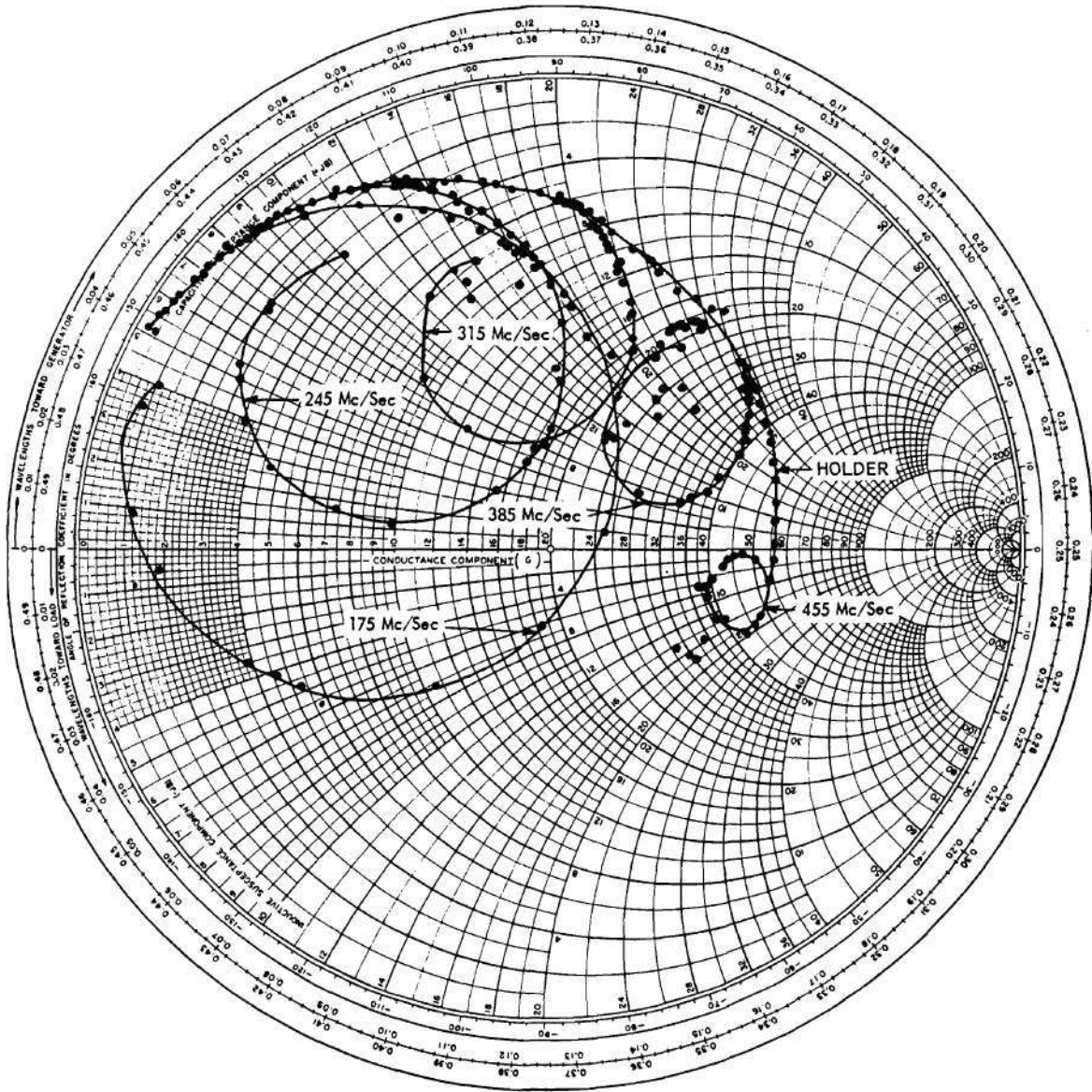


Figure 15. Admittance Characteristics of Test Crystal No. C-1.

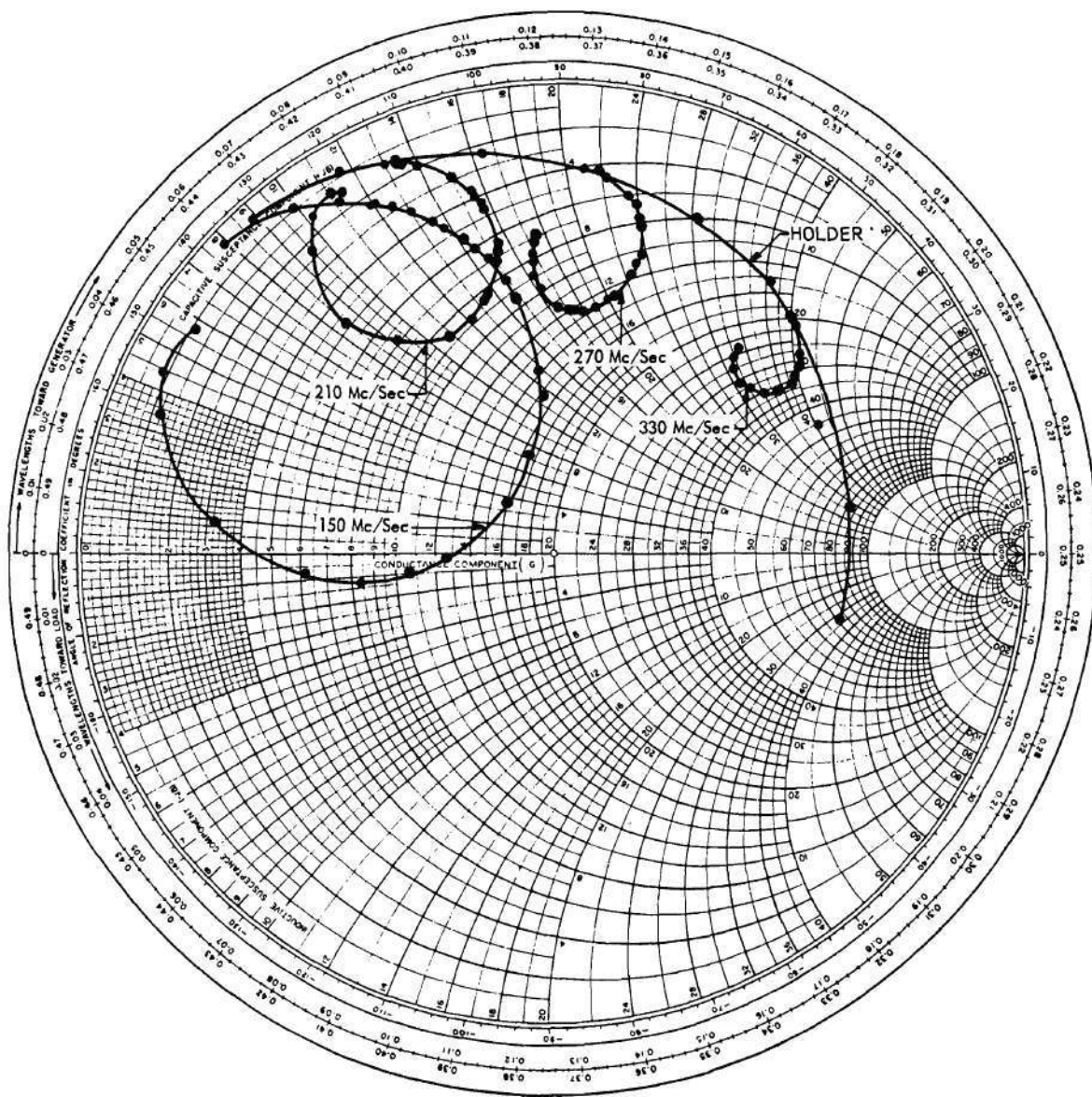


Figure 16. Admittance Characteristics of Test Crystal No. C-2.

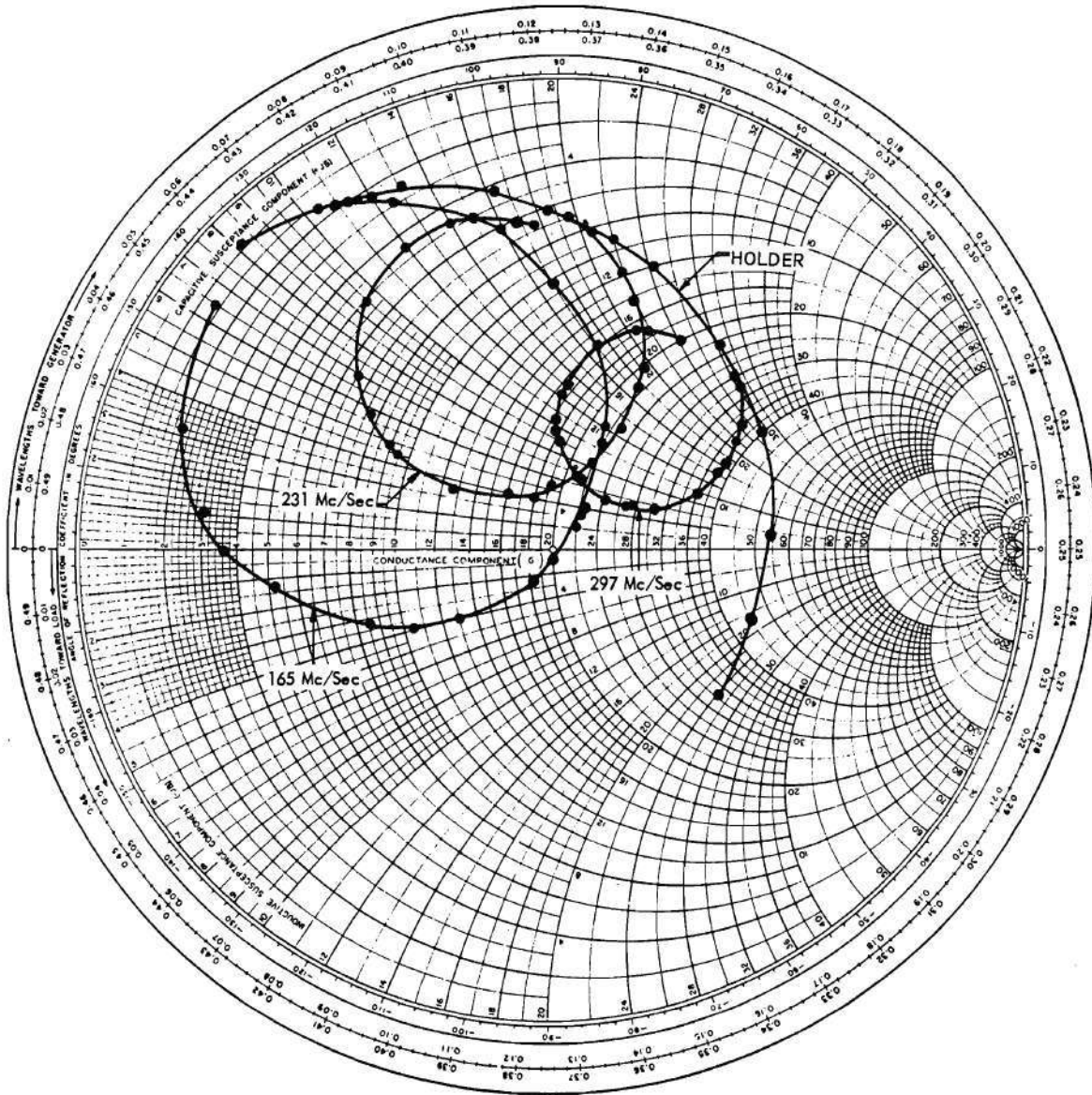


Figure 17. Admittance Characteristics of Test Crystal No. C-3.

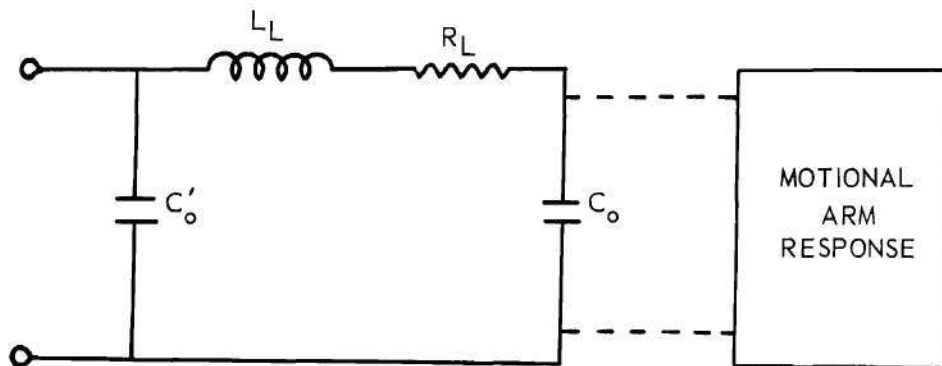


Figure 18. The Analysis Circuit for High-Frequency Crystal Units.

The principal object of the analyses of conventional HC-6 crystal units was to determine typical element values for the holder equivalent circuit of Figure 18 and to determine the typical variations in motional-arm parameters with frequency. The first step normally taken in making an analysis for this purpose is to reduce the original measurement data to perfect circle approximations. For Crystal No. C-1, the perfect circle approximations of the data of Figure 15 are shown in Figure 19. The data points on the low-frequency sides of the motional-arm responses were considered more significant in making the circle approximations because of the distortion which occurs on the high-frequency sides due to spurious responses.

As mentioned previously in connection with Figure 10, the response characteristic of a crystal holder alone may be measured by avoiding the frequencies near overtone responses. Holder characteristics obtained in this way are plotted in Figures 15, 16, and 17. As would be expected from the holder equivalent circuit, the holder responses can also be

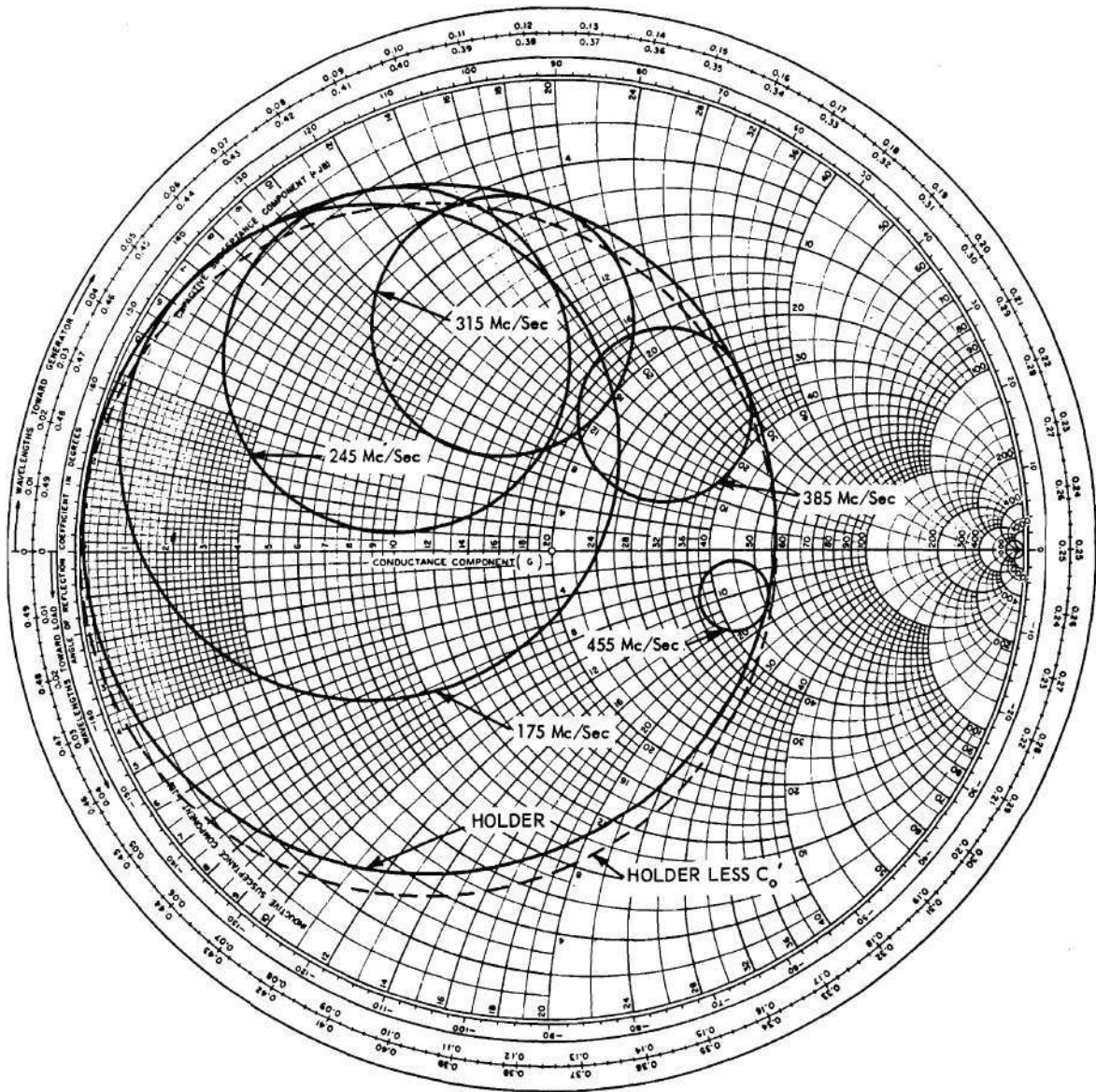


Figure 19. Perfect Circle Approximations of the Data of Figure 15.

approximated by perfect circles (by at first ignoring the presence of C_o') as indicated by the example of Figure 19. The circle, however, is not perfectly centered about the zero-susceptance axis because of the shunt effects of C_o' . If a circle with the same maximum conductance is now constructed about a center on the zero-susceptance axis, the separation between this circle and the original data points may be used to calculate the value of C_o' . For typical crystals, the value of C_o' was found to be approximately the same regardless of the frequency, within the range from 100 to 400 mc/sec, chosen for the calculation. For Figure 19, the value of the C_o' was found to be approximately 0.69 mmfd.

The other holder circuit parameter values may be calculated from the "holder less C_o' " circle of Figure 19 together with the frequency distribution data. The resistance, R_L , is the reciprocal of the maximum conductance of the circle. The values of L_L and C_o may be determined by conventional methods from the frequencies at the half-power points of the circle.

The calculations for the holder of Figure 19 yielded values as follows: $R_L = 17.5$ ohms, $L_L = 29.9$ μ h, and $C_o = 4.393$ mmfd. When the holder parameter values were substituted into an appropriate computer program and the terminal admittance characteristic calculated and subtracted from the appropriate original data points of Figure 15, residuals averaging 0.07 millimhos for conductance and 0.02 millimhos for susceptance were obtained after omitting several points which were determined to be erroneous. Computer program number 2 of Appendix II was used for calculating the rectangular form of the admittances from the calculated holder element values.

An alternate method of calculating the holder element values was provided by computer program 3 of Appendix II. A complete mathematical description of this program appears in the appendix. This program calculates the holder parameters by using only three input data points; one, the point of maximum holder conductance, two, an arbitrary point at a frequency higher than holder resonance, and three, an arbitrary point at a frequency below holder resonance. Exact holder match, within the capabilities of the computer, is provided at either the point below holder resonance or the point above holder resonance. The arbitrary points must be points which lie on smooth curves of conductance and susceptance versus frequency.

For properly chosen input points, computer program number 3 gave essentially the same results as were obtained from the half-power point calculations. The results varied only slightly as different input points were used with the computer program.

After satisfactory holder element values were found, the holder was mathematically subtracted from each of the crystal overtone responses by computer program 4 of Appendix II. The admittances of the remaining functions should represent series resonant circuits.

When the calculated holder parameters for the crystal of Figure 15 were subtracted from the 175 mc/sec response, the resulting admittance function of Figure 20 was obtained. The admittance magnitude and phase angle were used for these curves because of the greater convenience in comparing the data with universal resonance curves for series resonant circuits. Shown also in Figure 20 are the universal resonance curves calculated for best match with the crystal curves. The phase angle

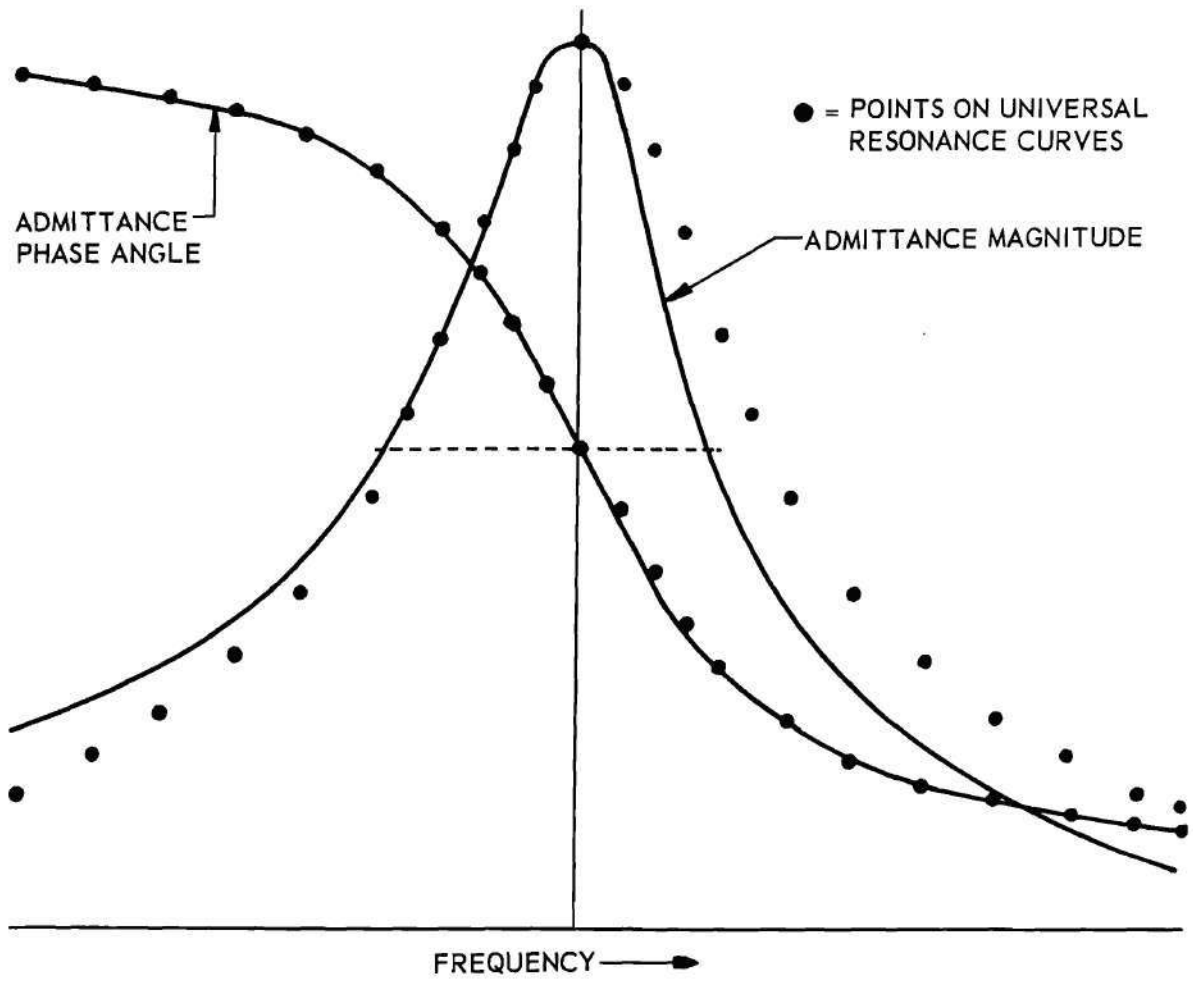


Figure 20. Admittance Characteristics of Crystal No. C-1 with the Conventional Holder Subtracted.

curves match almost perfectly, while the magnitude curves show disagreement on both sides of resonance. The larger disagreement at frequencies above resonance can be attributed to the effects of spurious responses; however, the low-frequency disagreement is unexplained. Any error in the holder equivalent circuit could, of course, account for the disagreement.

During the search for better methods of mathematically representing the crystal holder, an analysis method proposed by Dr. E. Hafner (24) of the United States Army Signal Research and Development Laboratories was investigated. His method divides the holder resistance as shown in Figure 21. By using the Hafner method, values for R_L and R_o of 0.7 and

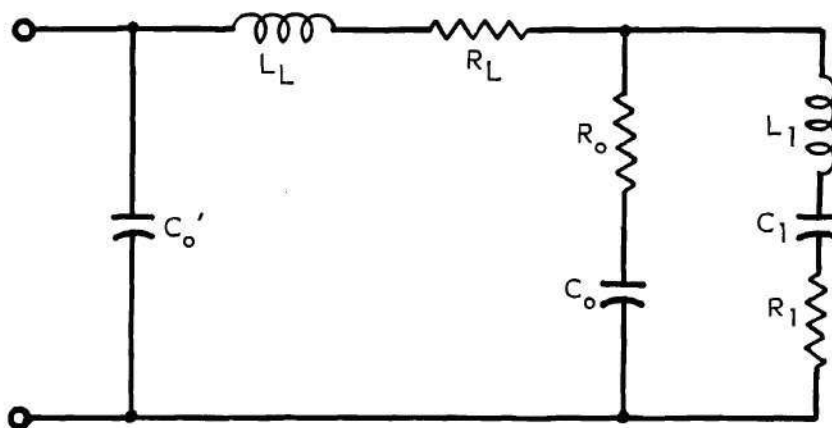


Figure 21. Hafner Equivalent Circuit for a High-Frequency Crystal Unit.

16.8 ohms, respectively, were found for the crystal of Figure 15. Other element values were the same as for the conventional holder. When this holder was subtracted from the 175 mc/sec response of Figure 15, the resulting admittance function of Figure 22 was obtained. Both the phase angle and magnitude curves were displaced slightly from the curves of Figure 20.

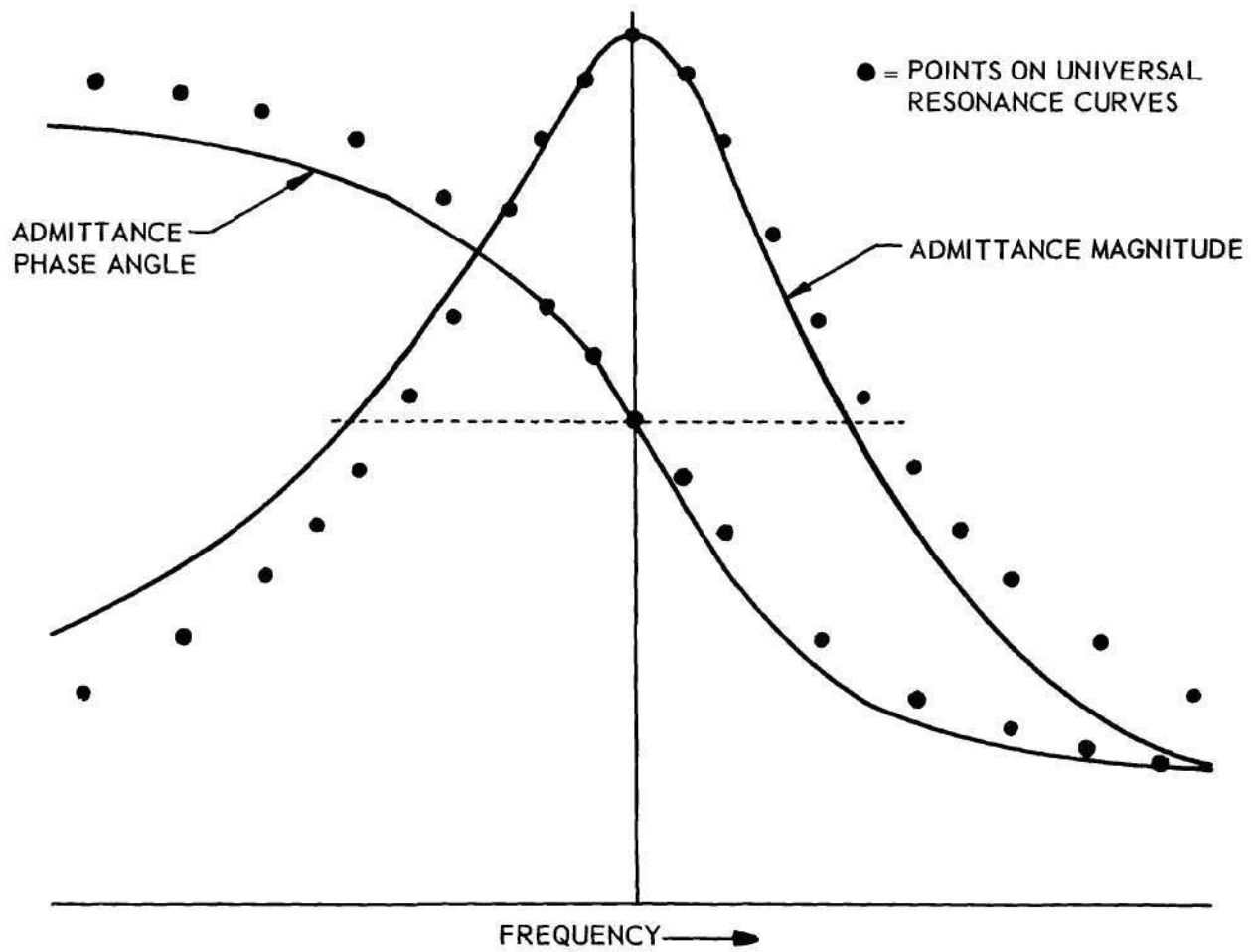


Figure 22. Admittance Characteristics of Crystal No. C-1 with the Hafner Holder Subtracted.

Again, attempts were made to match the characteristics with universal resonance curves, as shown dotted in Figure 22. This attempt resulted, however, in a poorer match than was obtained for Figure 20. Therefore, a possible conclusion is that the Hafner procedure results in a poorer representation of the motional arm of this particular crystal than does the conventional holder. However, one source of error is introduced by the Hafner analysis method that does not appear with the conventional method. Since the Hafner method is purely graphical, the required Smith Chart calculations introduce appreciable errors due to limited chart resolution. With the conventional analysis, the digital computer was used for practically all calculations.

The remaining crystals on which data had been obtained were extensively analyzed by various combinations of the Hafner and conventional methods.

The first step in each case was to examine the holder responses to determine whether or not they could be represented with reasonable accuracy by simple equivalent circuits. The data for crystals C-2 and C-3, as shown in Figures 16 and 17, were typical of the better crystals. The circle approximations of the holders of these crystals are shown in Figure 23. Again, the centers of these circles do not fall on the zero susceptance axis. If the assumption is made that the displacement is due to a C_0 and the holder parameters are calculated for each holder, a theoretical circle may be obtained which agrees very closely on the Smith Chart with the original circle approximation. However, an examination of the frequency distribution around the circle shows some disagreement, indicating that an accurate equivalent circuit has not been

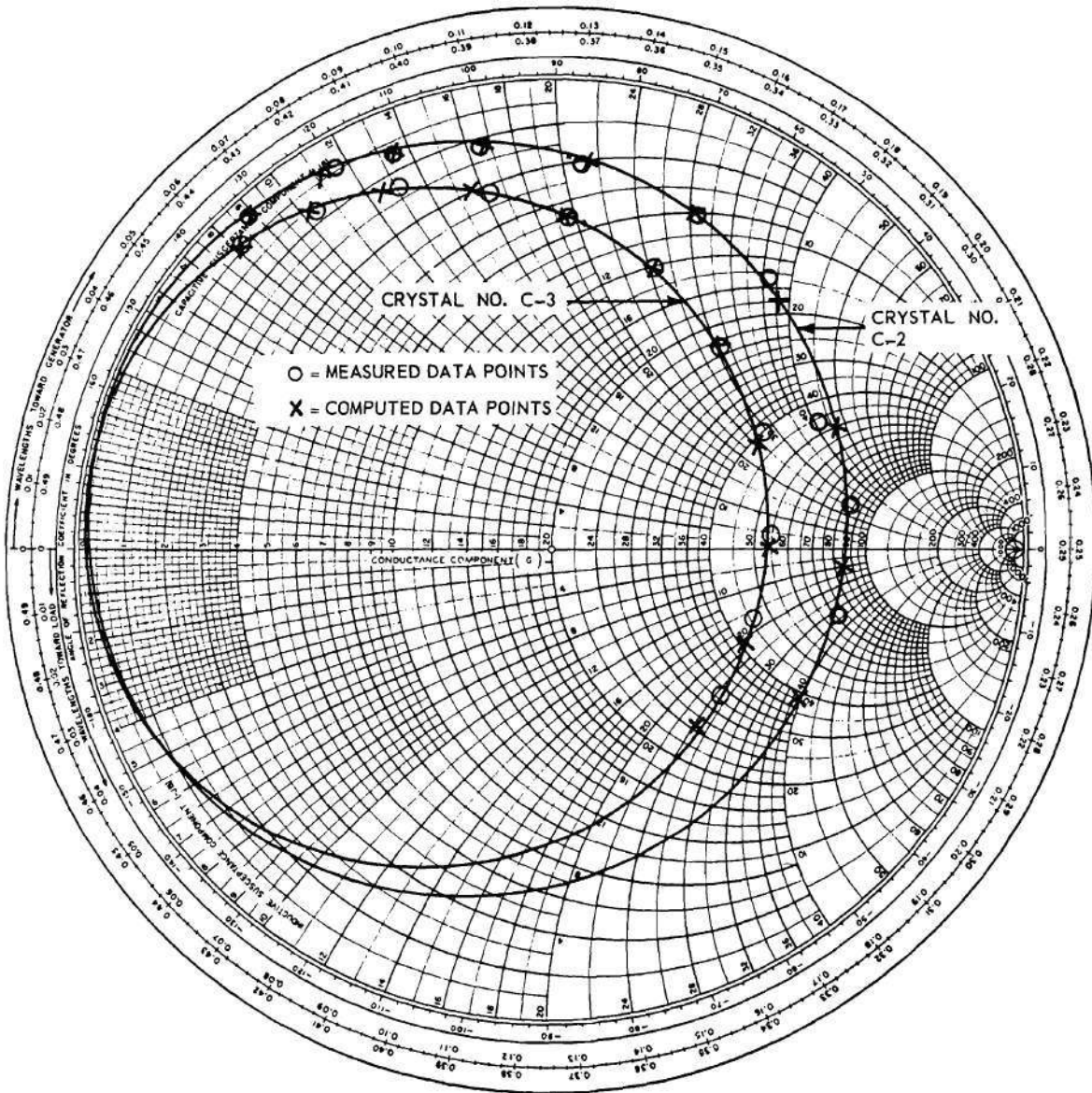


Figure 23. Circle Approximations of the Holders of Crystal Nos. C-2 and C-3.

found. This disagreement is illustrated by the small circles and crosses, which should fall at the same points on the holder circles of Figure 23. Since this result was typical of most of the crystals measured, the need for further studies of the holder characteristics was indicated.

One possible cause of the holder circuit disagreements was the subtraction of an incorrect line length in the measurement system as described in Appendix I. The electrical length between the crystal and the Admittance Meter was known to be 9.69 cm; however, the effective length could be greater due to fringing at the crystal terminals. Thus, a series of 14 line lengths from 9.69 cm to 12.5 cm were subtracted from the original data for crystals C-2 and C-3. Equivalent holder circuit parameters including C_0' were then calculated at each line length. The theoretical circles were plotted against the measured circles with approximately the same frequency disagreements as shown in Figure 23.

Several other efforts were made to find a more precise equivalent circuit representation of the holder. All such efforts, however, gave the same order of disagreements as has been illustrated. This either implies that no linear holder equivalent circuit exists (i.e., the element values are not constant) or that a suitable circuit must be basically different from or considerably more complicated than that of Figure 10. That C_0 varies slightly with frequency because of the shunting effects of the motional-arm responses has been recognized; however, this variation is insufficient to account for the discrepancies observed.

When only the crystal holder response is of concern, the conventional holder and the Hafner holder become identical since the sum of

the resistances, R_O and R_L , for the Hafner holder should equal R_L for the conventional holder. Thus, the holder analysis discussed above is not dependent upon the type of analysis to be used on the crystal overtone response.

Rather than add additional elements to the holder equivalent circuit at this time, the decision was made to continue the conventional and Hafner analyses of crystal overtone responses, using the holder element values and line lengths which gave the least holder circle errors. Analyses were performed with results as indicated in Table 2. Only two crystal responses, Crystal C-2 at 150 mc/sec and Crystal C-3 at 165 mc/sec, are represented in this table. Two line-length subtractions were used for each of these crystals; (a) the standard length of 9.69 cm which required the use of a C_O' to correct the position of the holder circle and (b) a length which corrected the position of the holder with a minimum value of C_O' . A line length could have been found which would require a zero value for C_O' ; however, the calculations would have required an excessive amount of computer time with the particular programs which were used. Very little error is introduced into the final results by the negative value of C_O' resulting from the chosen line length.

The conventional holder parameters were calculated as indicated under Runs Nos. 5, 6, 12, and 13 in Table 2. The values of R_L under these runs should represent the total holder resistance as determined by the diameter of the holder circles. They should also represent the sums of R_O and R_L for the respective Hafner calculations if graphical errors can be completely avoided.

Table 2. Summary of Crystal Holder Calculations by Various Methods.

Run No.	C_o' (mmfd)	R_L (ohms)	L_L (m μ hy)	C_o (mmfd)	R_o (ohms)	Line Length (cm)	Method
Crystal No. C-2				Overtone Frequency 150 Mc/Sec			
1	1.71	1.25	36.5	5.05	17.6	9.69	Hafner
2	----	10.0	23.2	7.00	-3.75	9.69	Hafner
3	----	10.5	27.2	5.55	1.0	12.1	Hafner
4	-0.06	5.75	32.6	5.01	8.25	12.1	Hafner
5	-0.06	11.5	32.6	5.01	0.0	12.1	Conventional
6	1.71	11.5	36.5	5.05	0.0	9.69	Conventional
Crystal No. C-3				Overtone Frequency 165 Mc/Sec			
7	0.97	16.25	33.1	6.31	0.47	9.69	Hafner
8	0.97	12.0	33.1	6.31	8.8	9.69	Hafner
9	----	13.25	26.4	7.3	3.15	9.69	Hafner
10	----	13.25	29.0	6.52	7.9	11.3	Hafner
11	-0.186	12.0	30.5	6.29	10.0	11.3	Hafner
12	-0.186	18.5	30.5	6.29	0.0	11.3	Conventional
13	0.97	18.5	33.08	6.31	0.0	9.69	Conventional

Remaining runs in Table 2 were performed by the Hafner method. For Run Nos. 1, 4, 7, 8, and 11, the digital computer was used to calculate values of C_o and L_L . For Run Nos. 2, 3, 9, and 10, two points were chosen on the holder circle and holder parameters were chosen by the method described by Hafner, ignoring the possible presence of a C_o' . The division of R_o and R_L , as determined from the construction sheets, is tabulated for each run. The sum of R_o and R_L for each run generally disagrees appreciably with R_L for the respective conventional holder. In one case, a negative value of R_o was given by the Hafner calculations.

The principle reason for conducting the crystal holder analyses as have been described was to permit the determination of the crystal motional-arm parameters. Accordingly, the holder parameters described in Table 2

were subtracted by computer program 4 of Appendix II from the respective overtone responses for each run indicated. The resulting perfect circle approximations are shown in Figures 24 and 25. The numbers associated with the circles correspond to the Run Nos. of Table 2. The two sets of dots on the circles of the figures represent points of equal frequency for each set. Thus, Figures 24 and 25 show the maximum variations in motional-arm parameters that may be expected from different analyses procedures. For crystal C-2, the maximum variation in R_1 for the various methods was ± 10 per cent. For crystal C-3, the maximum variation was ± 7.5 per cent. Although the resonant frequency of the motional arm is dependent upon the method of analysis, the Q of the motional arm is affected very little, as indicated by the corresponding frequency points of the figures.

The two conventional holder subtractions for each crystal resulted in essentially identical circles in Figures 24 and 25. Thus, the effects of a C_0 and a short line length error are almost indistinguishable.

Typical holder data by the conventional and Hafner methods are shown for several other crystals in Table 3. From these data, the holder circuit was subtracted from each overtone response indicated in the table. At each overtone response, the maximum difference in motional-arm resistance and Q as given by the two methods was less than 10 per cent. This difference was determined by plotting the motional-arm responses from the two methods on normalized resistance and frequency scales. The disagreements were estimated without actually calculating the resistance and Q.

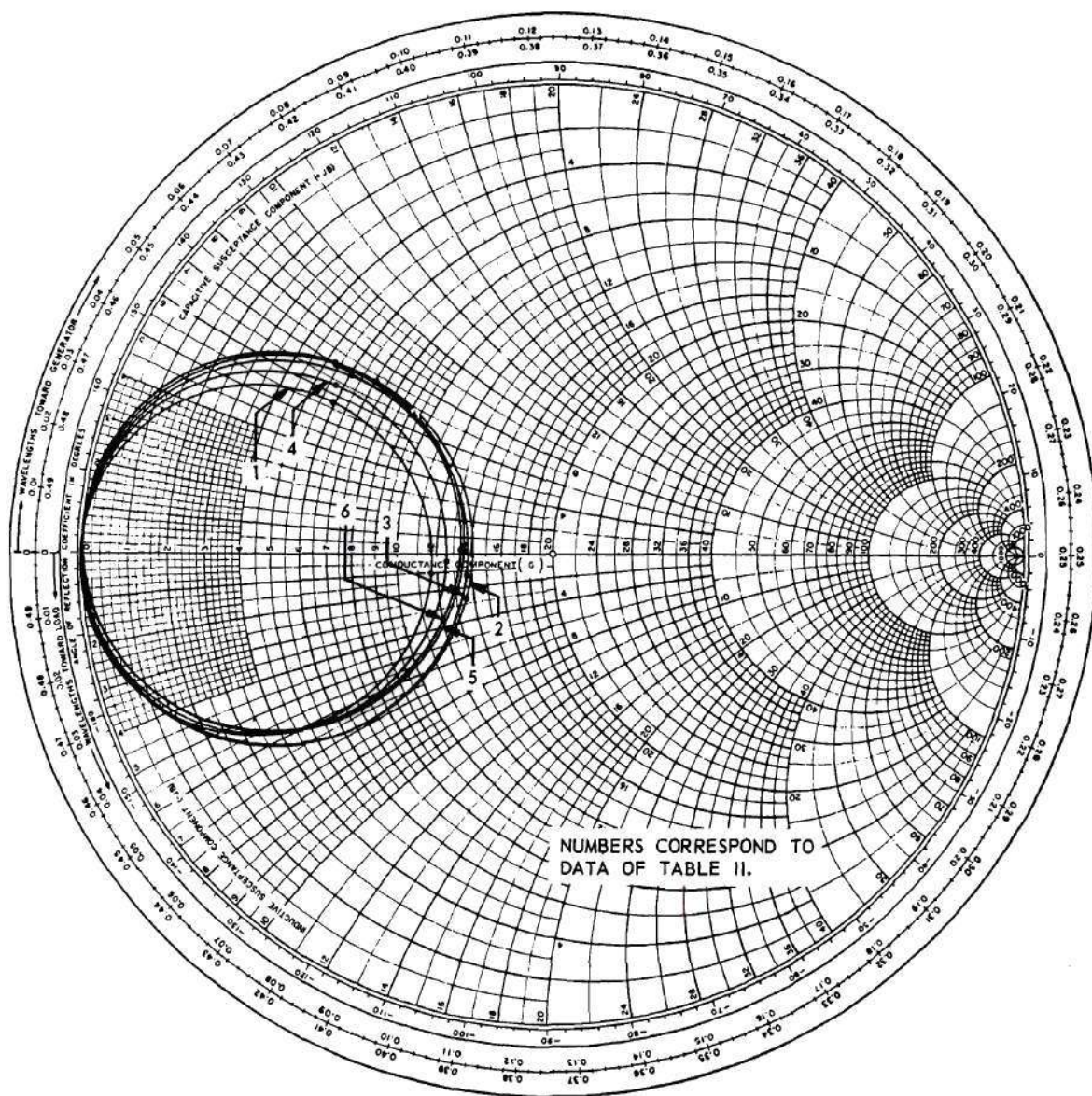


Figure 24. Motional-Arm Circles for Crystal No. C-2 as Obtained by Several Methods.

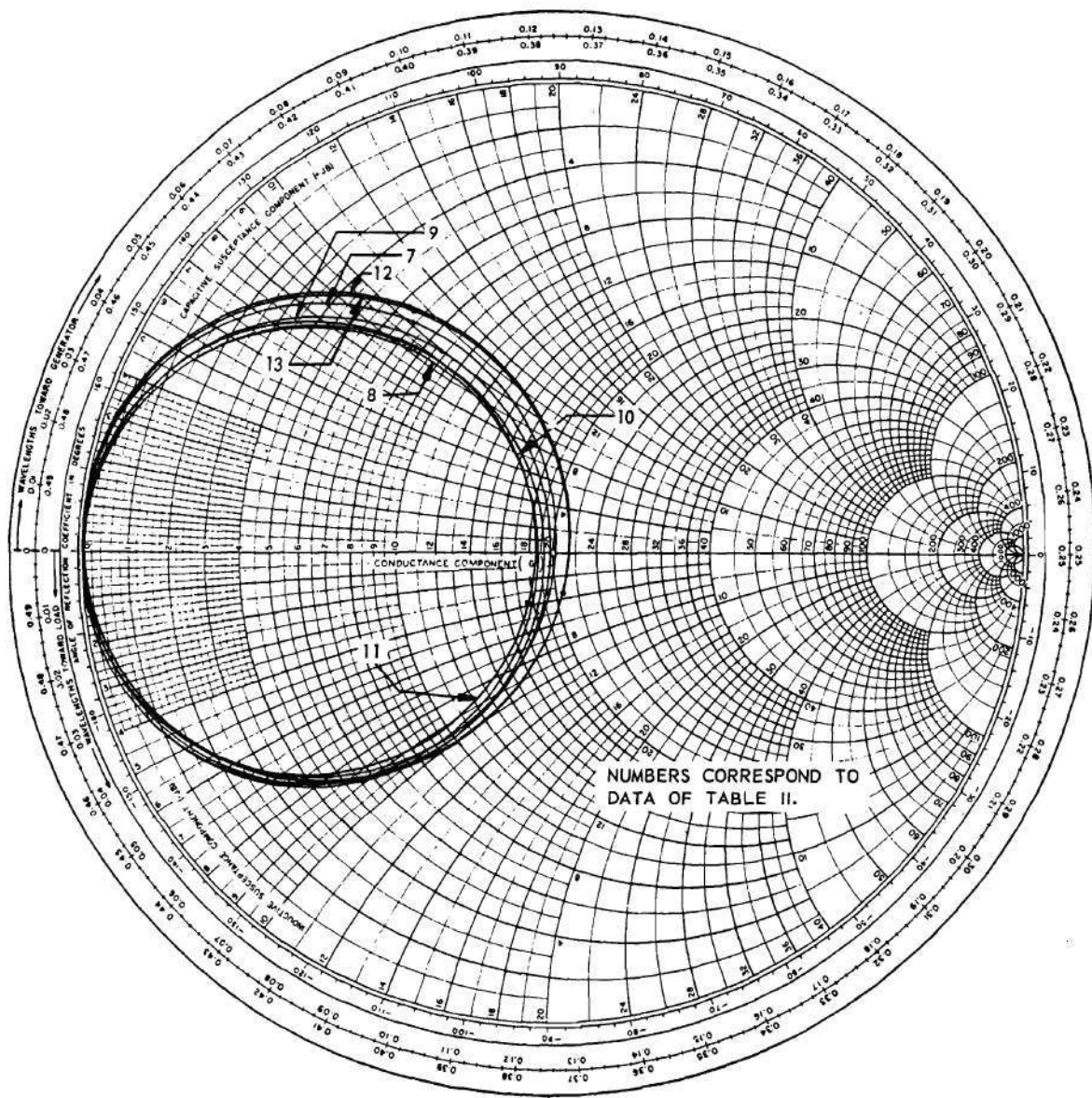


Figure 25. Motional-Arm Circles for Crystal No. C-3 as Obtained by Several Methods.

These results indicate that, where inaccuracies of 10 per cent or less are acceptable, the relative division of holder resistance is unimportant. Where greater accuracies in calculating motional-arm parameters are necessary, neither the conventional nor the Hafner holder equivalent circuits have been proven to be satisfactory by the results obtained with these particular crystals.

Table 3. Summary of Conventional and Hafner Holder Calculations on Several Crystal Responses.

Crystal No.	Overtone Frequency mc/sec	Computer Calculated				Hafner Calculations	
		C_o' mmfd	C_o mmfd	L_L mhy	R_T ohms	R_L ohms	R_o ohms
C-4	150	1.91	4.51	35.6	10.2	1.00	13.90
C-4	184	1.91	4.51	35.6	10.2	0.00	16.00
C-4	217	1.91	4.51	35.6	10.2	0.00	13.30
C-4	250	1.91	4.51	35.6	10.2	-8.75	21.85
C-5	178	1.58	4.59	35.2	12.3	0.50	13.70
C-5	210	1.58	4.59	35.2	12.3	*	*
C-6	178	1.32	4.39	37.3	11.6	-26.50	37.90
C-7	165	1.54	5.40	33.5	11.1	9.50	6.40
C-8	198	1.54	5.51	31.6	11.6	2.08	11.93
C-8	198	1.54	5.51	31.6	11.6	-13.75	35.10
C-10	175	1.17	5.75	31.5	18.2	14.25	5.50
C-10	245	1.17	5.75	31.5	18.2	11.25	7.00
C-10	315	1.17	5.75	31.5	18.2	12.50	6.55

* Crystal circle degenerated to a point at one stage in the analysis causing the method to fail completely.

Since the results obtainable by the analysis methods described were more than satisfactory for the intended purpose, the methods were applied to several more of the original 25 crystals for which complete

data were available. In each case, a holder was found which matched the original data reasonably well. Both the conventional and Hafner analyses and combinations of the two were used. The holders were then subtracted from the overtone responses by the appropriate computer program. The overtone responses (motional-arm only) were then plotted to determine if additional holder corrections were required. For some crystals, where a single set of holder parameters did not match the original data sufficiently well over the entire frequency spectrum, new values of holder parameters were calculated for each overtone response. These calculations were possible since the computer program used in the holder calculations provided exact holder match with the laboratory data at any one chosen frequency. In most cases, however, one set of holder parameters gave a satisfactory match for several overtone responses.

As an additional check of the holder data, the holder responses for each crystal were remeasured using the Crystal Measurements Standard. Some corrections in holder parameters resulted; however, in most cases, the original data were found to be satisfactory.

Additional attempts were made to improve the holder matches by empirical means. These means included such efforts as changing the maximum holder conductance (at holder resonance) to be used in the computer program and changing the value of C_0' manually in the computer calculations. In most cases, only very slight improvements could be obtained by these procedures.

From the total holder data, the one set of holder parameters which gave the best over-all match to the original holder data and the one set of parameters which gave the best match at frequencies near each

overtone response were selected. The various holder parameters were then subtracted from the overtone responses by computer program 4 of Appendix II. Subtraction of different holders at most of the responses again indicated that the details of the holders have only minor effects on the values of motional-arm Q and R_1 . Some few of the responses were not analyzed because of their very high values of R_1 .

The resulting overtone responses, which should now represent only the motional-arm responses, were plotted both on Smith Admittance Charts and on linear graph paper, the latter as functions of frequency. The values for R_1 were determined from the points of maximum conductance on the Smith Charts. The approximate Q 's of the motional arms were determined from the half-power points on the rectangular plots.

One of the better motional arm responses, plotted on a Smith Chart, is shown in Figure 26. The maximum conductance is seen to be 19 millimhos, corresponding to an R_1 value of 52.5 ohms. This response is not centered perfectly about the conductance axis. A more nearly perfect centering could have been obtained by repeating the analysis procedure with appropriate adjustments; however, this was not considered necessary since only slightly different R_1 and Q values would have been obtained.

A rectangular plot of the data of Figure 26 is shown in Figure 27. As was expected, the response resembles that of a series resonant circuit. For a series resonant circuit, the Q can be determined from the frequency separation of the half-power points. The half-power points occur at the two peaks of the susceptance curve and at the half-conductance values of the conductance curve. For an ideal series resonant circuit, these pairs

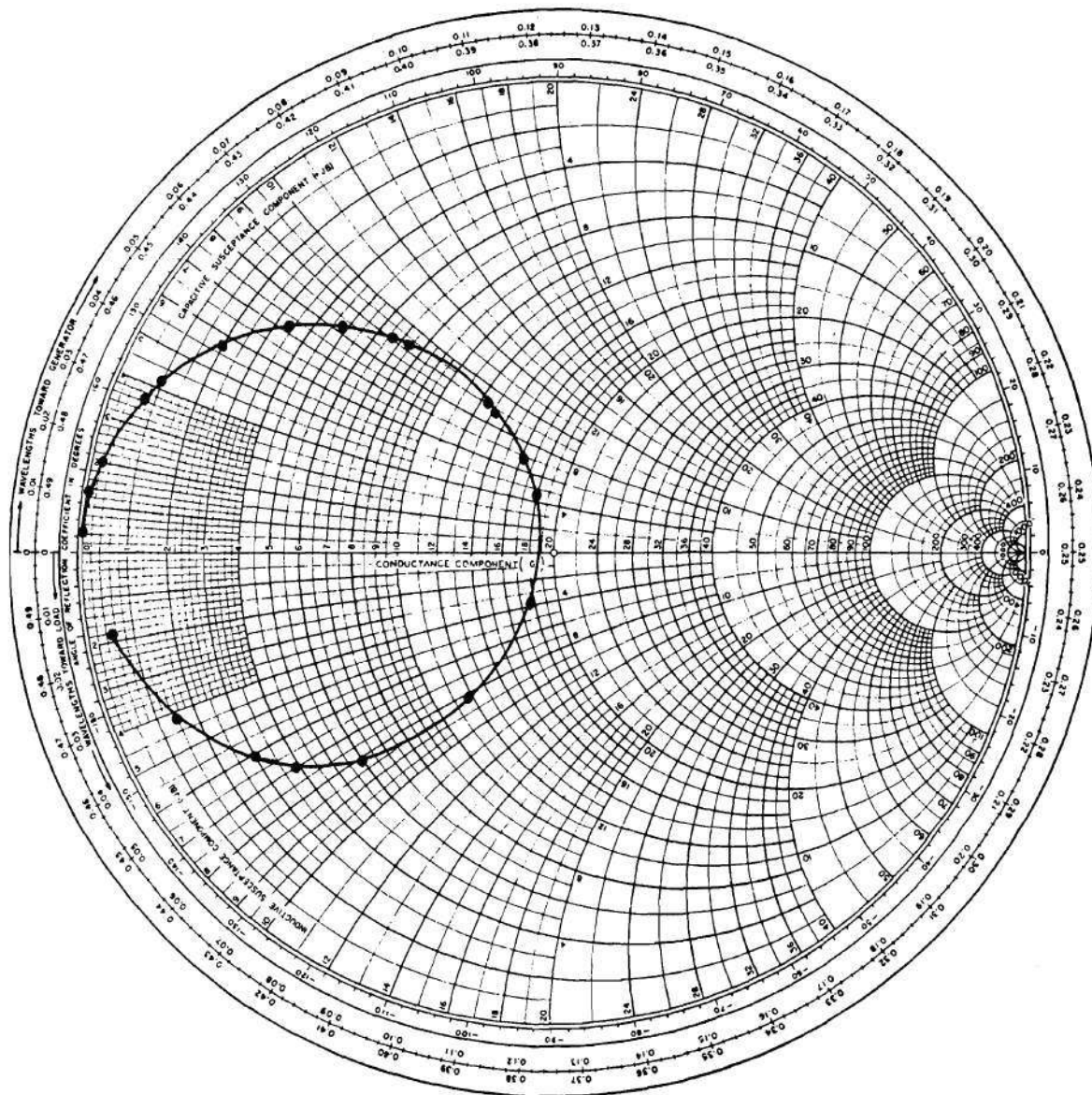


Figure 26. Motional-Arm Response of Crystal No. C-11.

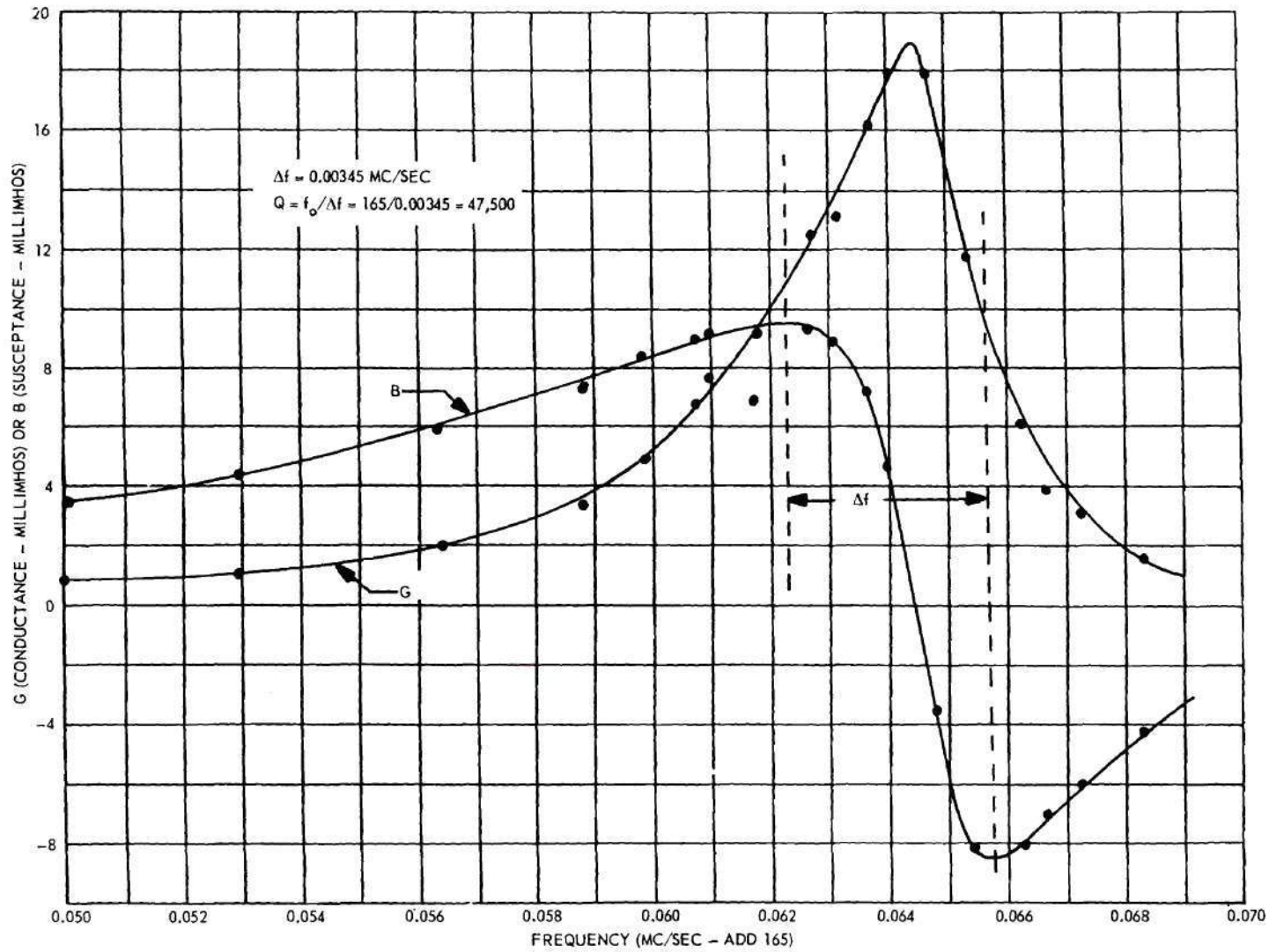


Figure 27. Rectangular Representation of Responses of Crystal No. C-11.

of points should occur at the same pair of frequencies. The frequency errors of Figure 27 are typical of the errors encountered with many of the overtone responses and are not considered excessive when all of the possible sources of error are examined. The dotted lines of Figure 27 indicate the frequencies used in calculating the Q of the response. The calculation is also shown in the figure. This process was repeated for each of the overtone responses.

A compilation of all available data on the values of Q and R_1 for several crystals is shown in Figures 28, 29, 30, and 31. In Figures 28 and 29, R_1 is plotted as functions of frequency and overtone number, respectively. In Figures 30 and 31, Q is plotted as functions of frequency and overtone number, respectively.

From the crystal analysis data which have been presented, holder parameter values were chosen as being average for the HC-6 quartz crystal holder at VHF, as listed in Figure 32.

For the available crystals, the values of R_1 and Q appeared to be more dependent upon frequency than upon overtone number, as indicated by the curves of Figures 28, 29, 30, and 31. Thus, a single smooth curve was drawn to represent the better crystals of each of Figures 28 and 30. Each curve was found to be approximately a straight line when plotted on semi-logarithmic graph paper. The resulting values of R_1 and Q as functions of frequency are shown in Figure 32.

Computer program 2 of Appendix II was used to plot the terminal characteristics of the crystal described by Figure 32 for any chosen frequency. Typical terminal admittance characteristics are shown in Figure 33. (It is recognized that an actual crystal could not have responses at the

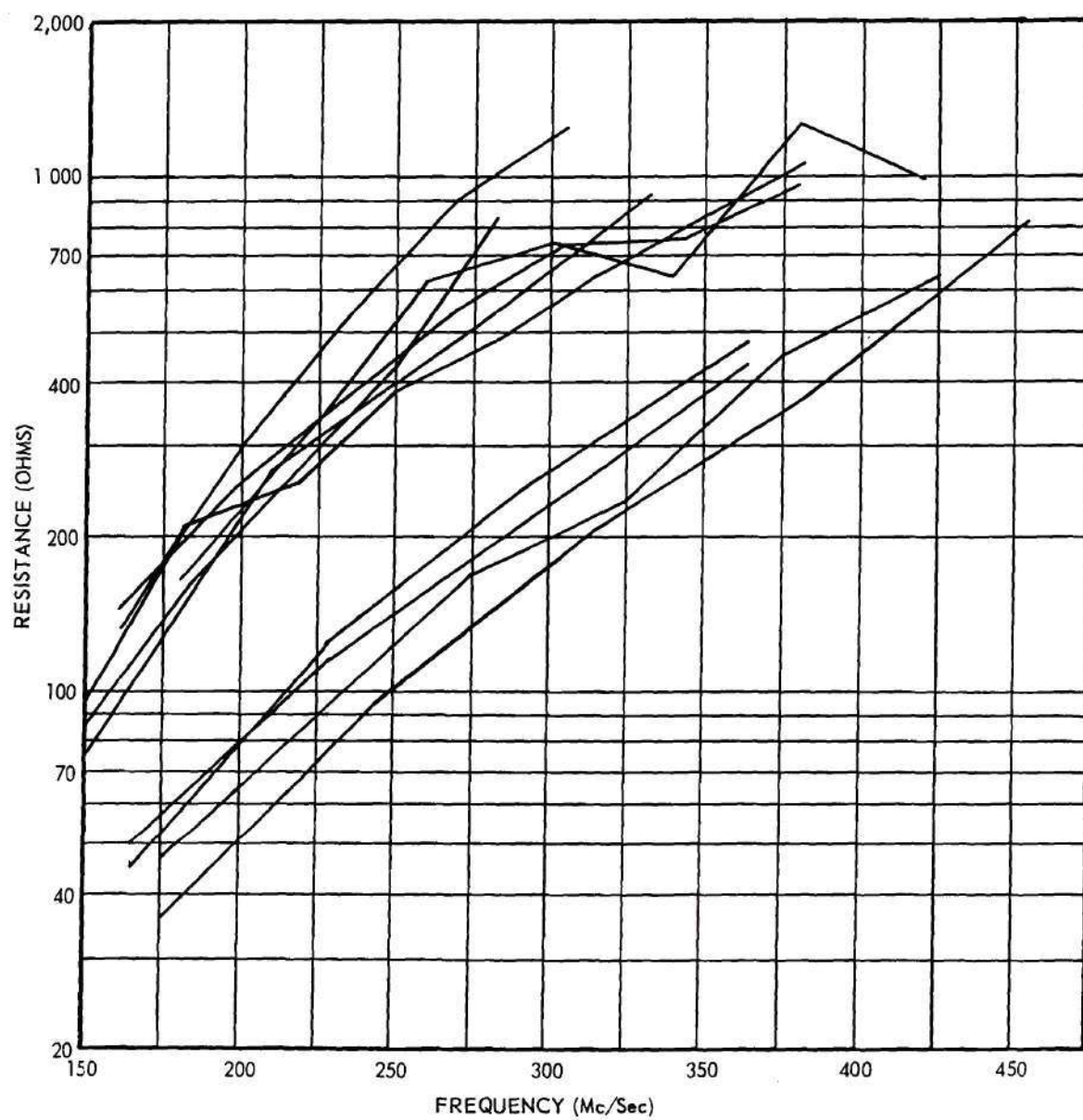


Figure 28. Motional-Arm Resistance of Several Crystals as a Function of Frequency.

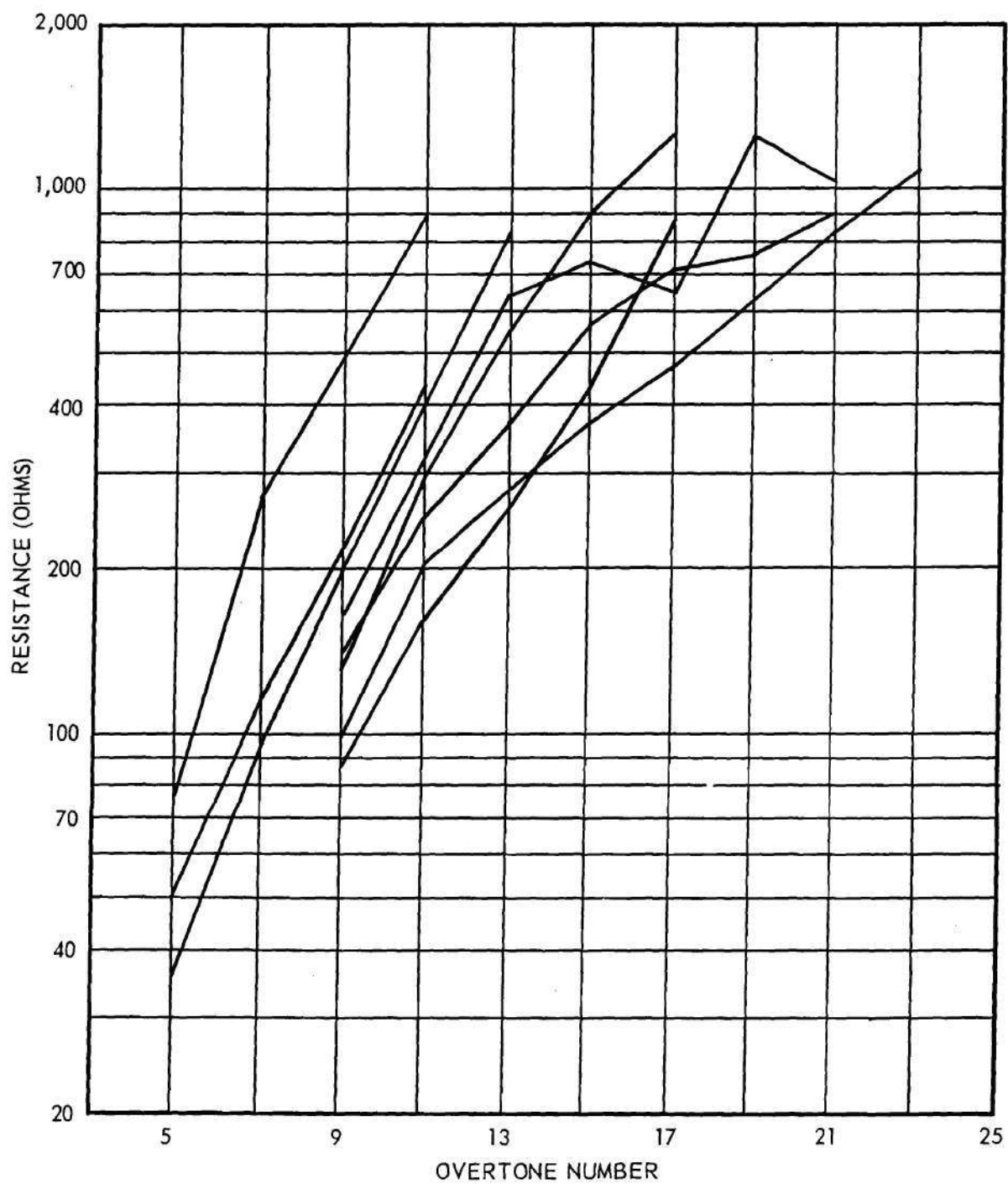


Figure 29. Motional-Arm Resistance of Several Crystals as a Function of Overtone Number.

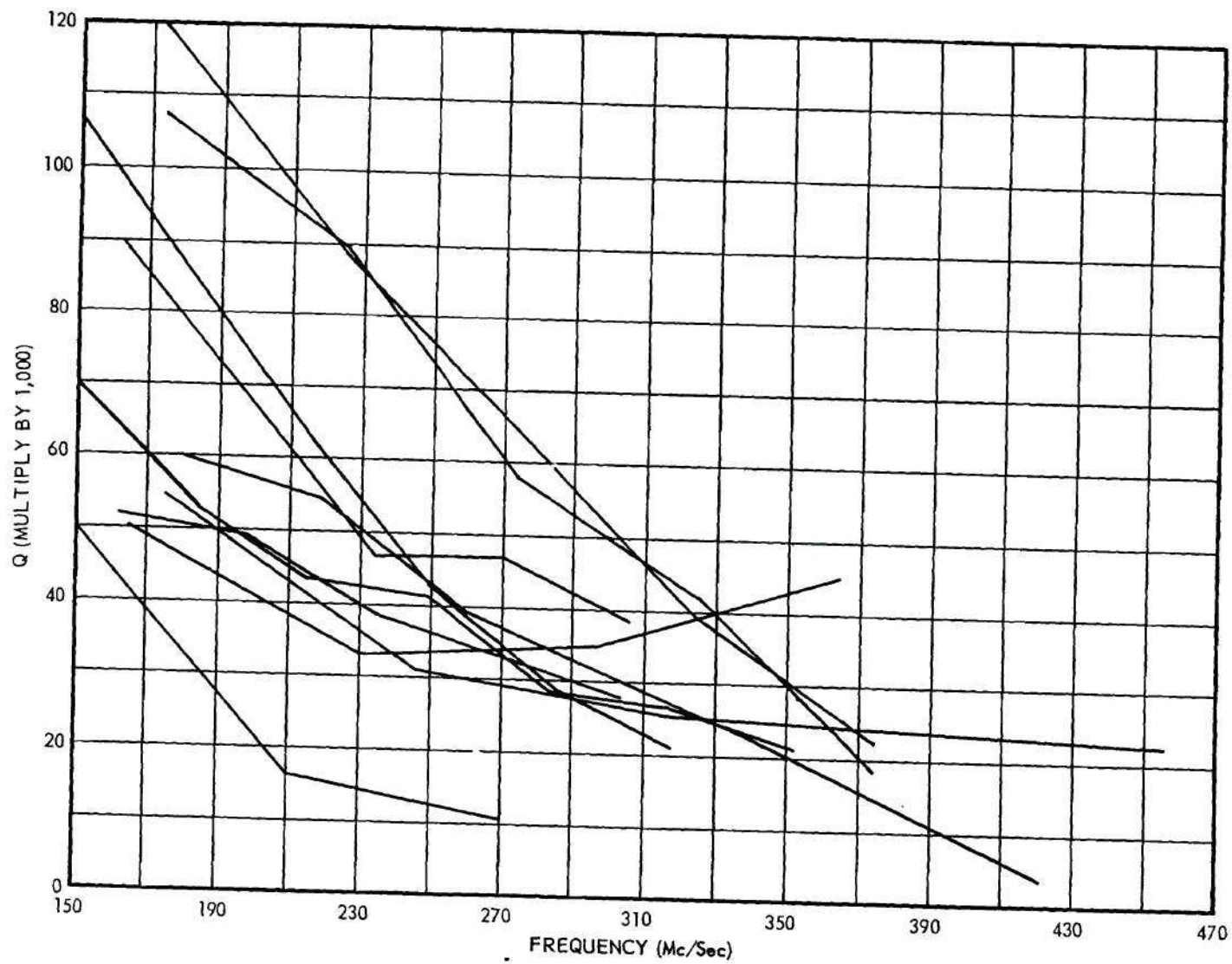


Figure 30. Motional-Arm Q of Several Crystals as a Function of Frequency.

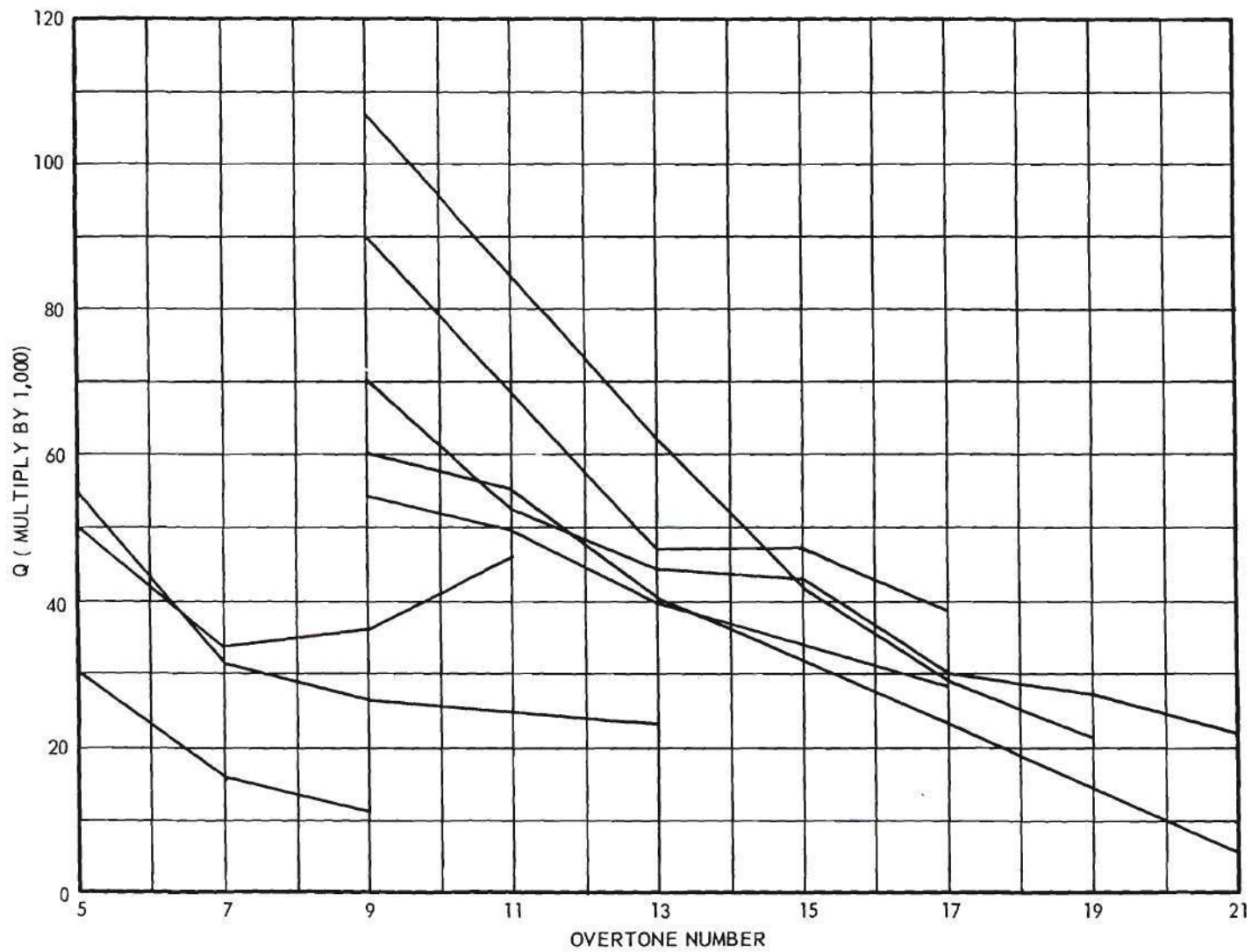


Figure 31. Motional-Arm Q of Several Crystals as a Function of Overtone Number.

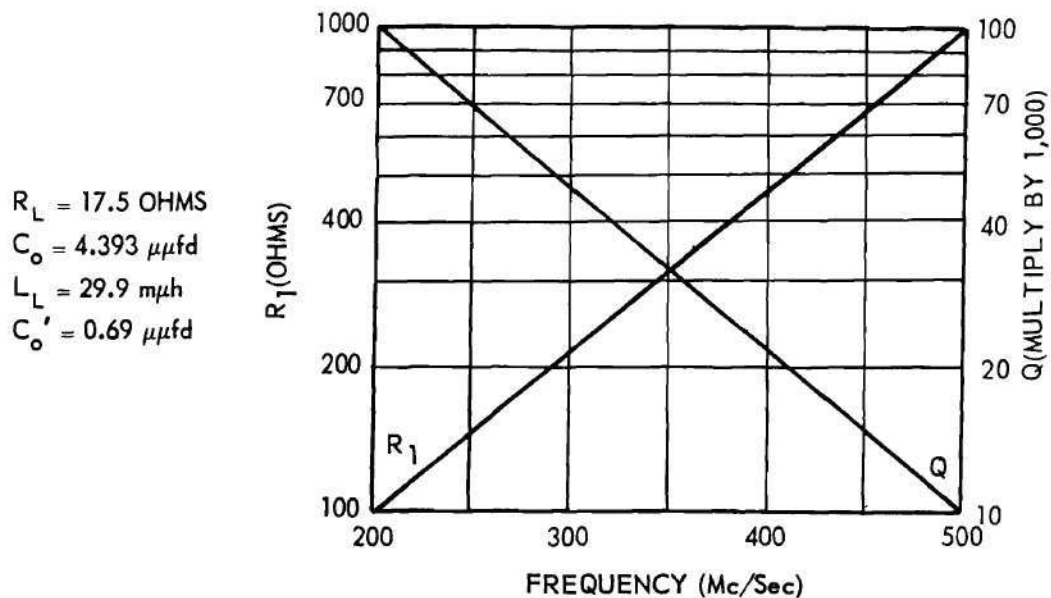


Figure 32. Values of Q and R_1 for the Motional Arm of a High-Frequency Quartz Crystal.

particular combination of frequencies chosen for this figure; however, these frequencies were desirable for interpolative purposes.) To each overtone response was added a fixed susceptance to simulate the process of anti-resonating the effective capacitance or inductance of the crystal. An inductive susceptance was required at 200, 300, and 400 mc/sec while a capacitive susceptance was required at 500 mc/sec. The resulting data in terms of admittance magnitude and phase angle were plotted against rectangular coordinates as shown in Figures 34, 35, 36, and 37. Shown on the same figures are the conductance and susceptance data before susceptance corrections were made.

At 200 and 300 mc/sec, the curves can be seen to resemble the conventional curves for a series resonant circuit. At the higher frequencies, the curves become radically different. If the curves are assumed to represent a series resonant condition, the values for Q can be calculated

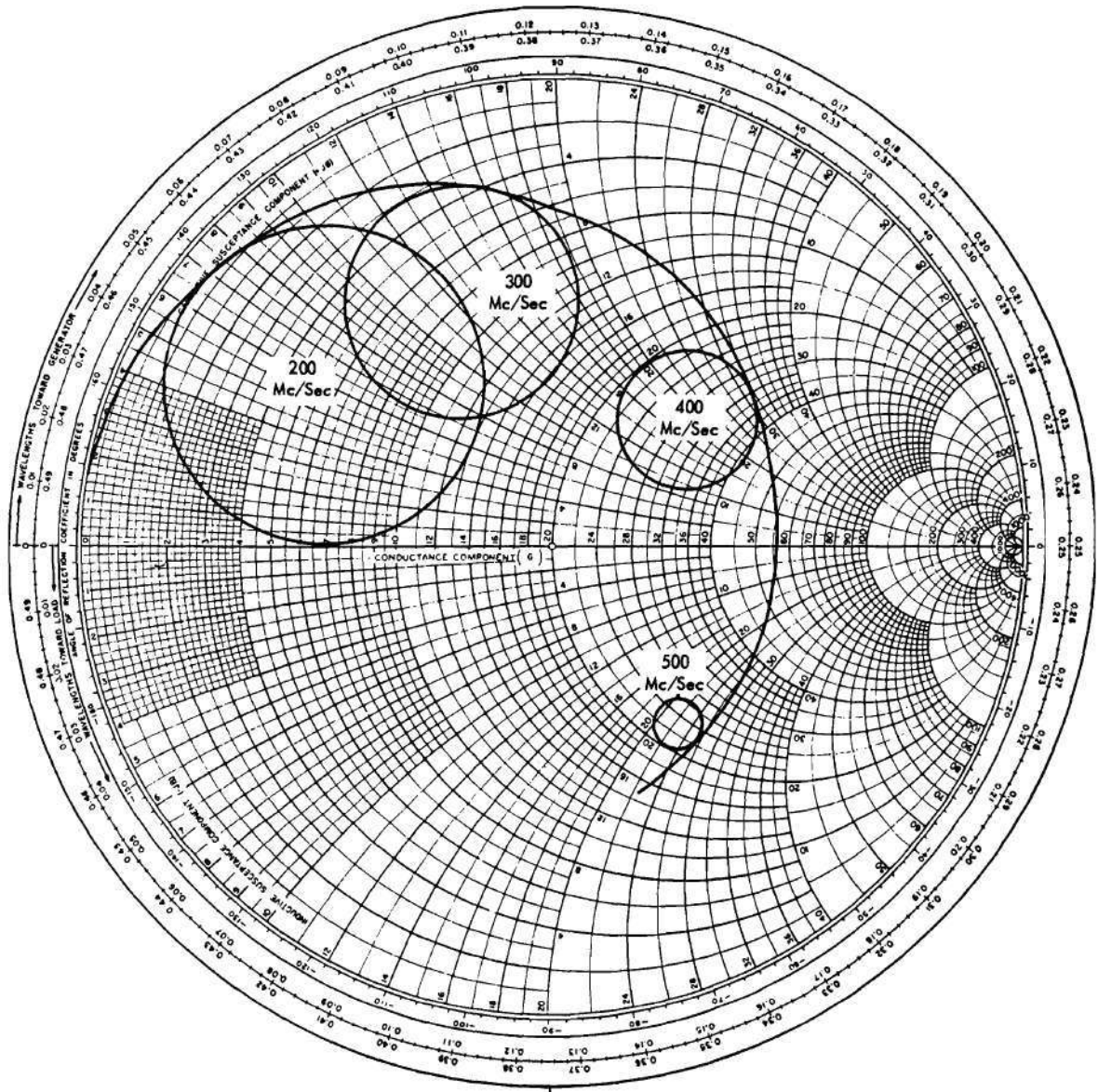


Figure 33. Typical Overtone Responses for High-Frequency Crystals at Several Frequencies.

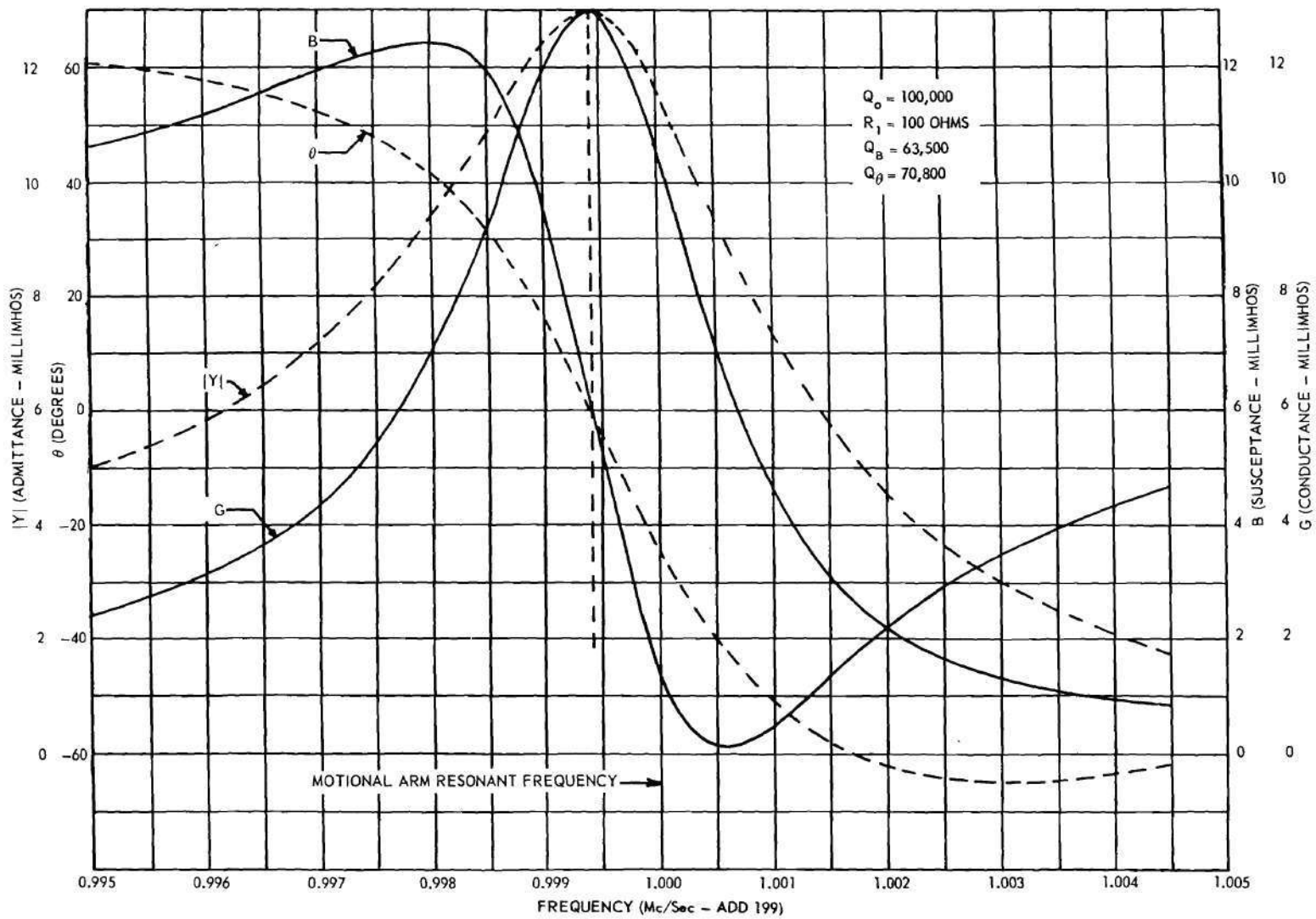


Figure 34. A Typical Overtone Response at 200 Mc/Sec.

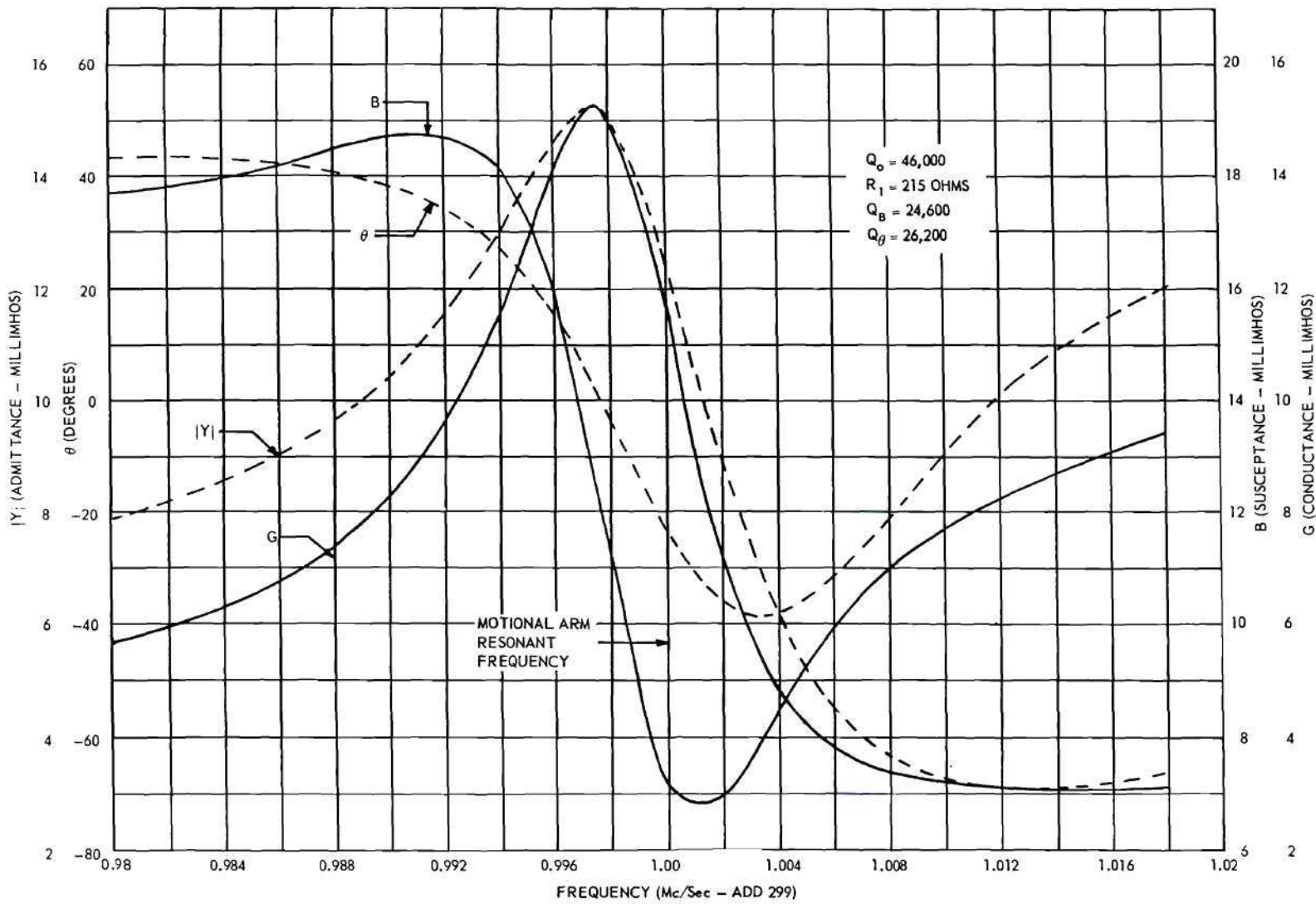


Figure 35. A Typical Overtone Response at 300 Mc/Sec.

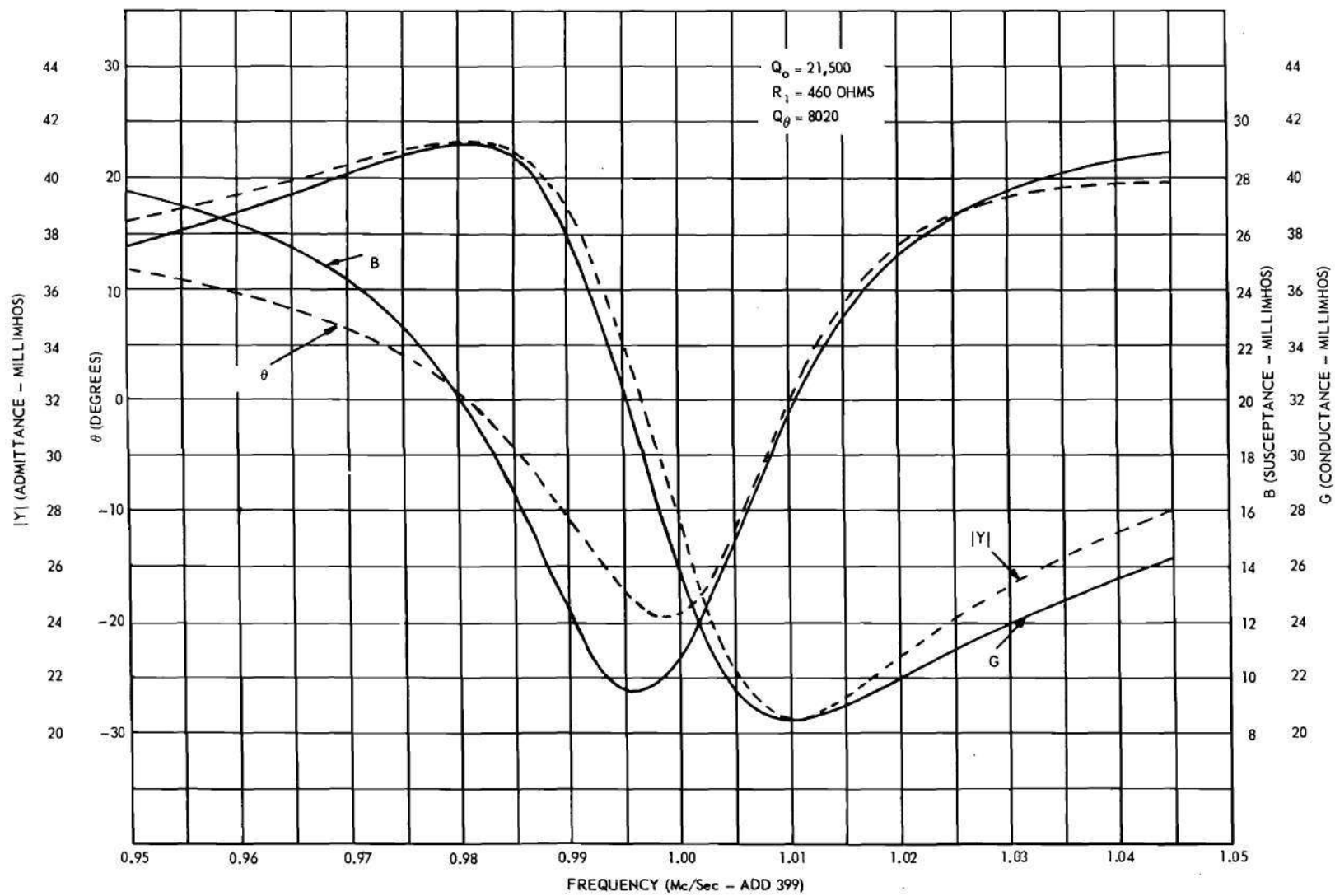


Figure 36. A Typical Overtone Response at 400 Mc/Sec.

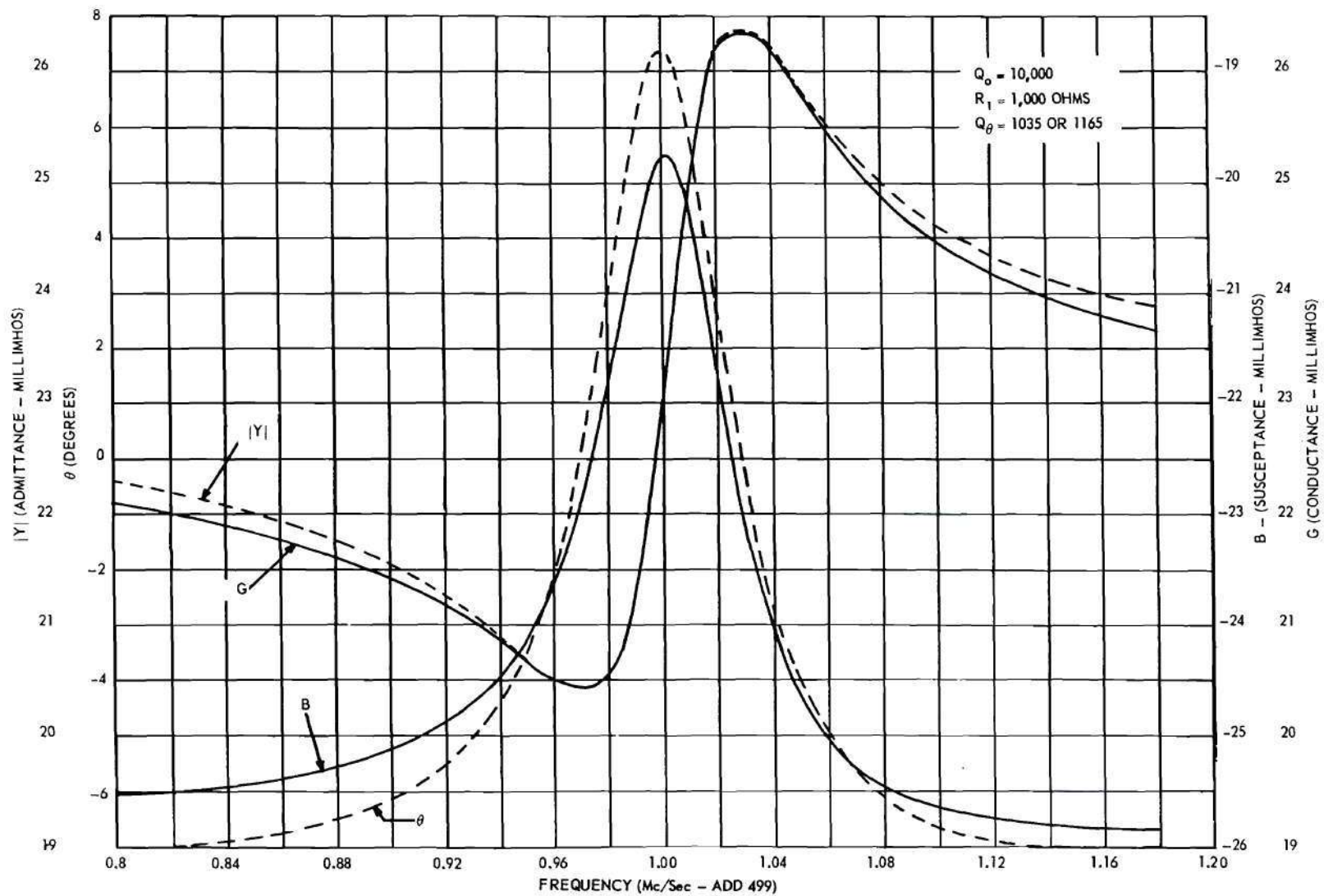


Figure 37. A Typical Overtone Response at 500 Mc/Sec.

from the expression

$$Q_{\theta} = \frac{f_0}{2} \cdot \frac{d\theta}{df},$$

and

$$Q_B = \frac{f_0}{2G} \cdot \frac{dB}{df},$$

where f_0 is the frequency at the maximum rate of change of phase ($d\theta/df$) or at the point of maximum conductance (G).

For a true series resonant circuit, maximum conductance will occur at the same frequency as the maximum rate of change of susceptance (dB/df). For the curves shown, however, the Q can be maximized by choosing the point of maximum rate of change of susceptance rather than the exact point of maximum conductance.

At 200 mc/sec, the Q_0 of the motional arm (the symbol Q_0 will be used to identify the Q of the motional arm) is 100,000. The effective values of Q calculated from the above equations are $Q_B = 63,500$ and $Q_{\theta} = 70,800$. At 300 mc/sec, the Q_0 is 46,000 with calculated $Q_B = 24,600$ and $Q_{\theta} = 26,200$. The slight disagreements between Q_B and Q_{θ} are caused by the fact that the curves do not represent true series resonant circuits.

At both 200 and 300 mc/sec, the resonant frequency of the crystal is displaced from the resonant frequency of the motional arm. At the higher frequencies, no clearly defined resonance point can be chosen since the maximum admittance magnitude does not occur at the point of greatest rate of change of phase. At 400 and 500 mc/sec, two clearly defined maxima occur for the rate of change of phase. In each case, a maximum or minimum of admittance magnitude occurs near the frequency of

maximum rate of change of phase. Thus, each overtone response possesses characteristics resembling both series and parallel resonant circuits. The definition of Q on the basis of variations in susceptance is no longer applicable; however, the definition based on rate of change of phase is still the primary factor determining the stability of an oscillator.

At 400 mc/sec, the rate of change of phase near the admittance magnitude minimum yields an equivalent value for Q_{θ} of 8020 compared to 21,500 for Q_0 . The equivalent Q_{θ} near the point of maximum conductance is only 2800.

At 500 mc/sec, and for a Q_0 of 10,000, an equivalent Q_{θ} of 1035 is obtained near the admittance minimum. The equivalent Q_{θ} near the admittance maximum is 1165.

At the higher frequencies (above about 250 mc/sec), Q_{θ} is substantially less than Q_0 ; however, with suitable circuits, crystal oscillator control should still be possible with conventional crystal units, even at frequencies as high as 500 mc/sec. The stabilities of such oscillators would be considerably poorer than could be obtained if the full values of Q_0 could be utilized for oscillator control. Thus, any method of reducing the degradation of the motional-arm characteristics by modifying the holder design would be worthy of consideration. This fact was of considerable importance to the research since previous knowledge had not indicated the degree to which the holder was responsible for poor crystal performance at the higher frequencies.

Several other important deductions and accomplishments were realized from the analyses of conventional HJ-6 quartz crystals. Each of these is summarized in a following paragraph.

A measurement system was developed which permitted the reasonably accurate determination of the two-terminal parameters of quartz crystals. The system would be useful for any similar type of measurement problem where high-Q or low-power limitations make the more conventional collection of equipment practically useless.

A sufficient number of crystals were analyzed to permit the determination of typical values of motional-arm Q and resistance at the higher frequencies. Various claims have been made that a relaxation effect occurs in quartz at frequencies above 300 mc/sec. This had been disproven for the particular collections of crystals which were measured. The motional-arm Q's of typical crystals were found to be sufficiently high to indicate the desirability of a better crystal mount.

The typical HC-6 crystal was represented by an equivalent circuit with values assigned, the characteristics of which should permit the optimum design of high-frequency oscillators on a theoretical basis. Previously, high-frequency oscillator design was primarily a laboratory procedure. Although the particular set of crystals which were measured were carefully selected, indications are that current manufacturing procedures can produce such crystals in reasonably large quantities. Rapid progress is currently being made in manufacturing techniques.

The degrading properties of the HC-6 holder were found to be primarily caused by series resistance in the holder structure. This resistance can be reduced by alternate mounting techniques. If some of the holder losses are due to plating resistance, R_0 , (as the Hafner equivalent circuit would indicate) such losses can also be reduced by the use of air-gap mounting techniques. Thus, the analyses of conventional

crystals indicated the paths of approach for the development of the coaxial crystal holder.

CHAPTER III

THE COAXIAL CRYSTAL HOLDER

A primary purpose of this research was to develop improved methods of mounting quartz crystal plates. The conventional HC-6 crystal holder has been shown to have undesirable loss characteristics which generally make the conventional crystals nearly useless at frequencies above 250 mc/sec. In many cases, the crystal characteristics are appreciably degraded, even at lower frequencies.

The principle factor producing this limited usefulness was found to be the equivalent series resistance of the holder. That the effects of an internal series resistance cannot practically be cancelled by external circuitry was indicated in Chapter II. If, however, the series resistance were eliminated, the harmful effects of shunt capacitance or of series inductance of the holder would be reduced.

The primary sources of series resistance in the conventional holders are series resistance of the support leads, series resistance of the cement bond between the support leads and the crystal slab plating, and resistance of the plated electrodes. The first two resistance sources might be essentially eliminated by using very large support leads and alternate bonding arrangements. Such supports, however, are not generally practical because of the extreme delicacy of the quartz slab. The third source of resistance, that of the plated electrodes, is not generally appreciable except at very-high-frequencies, where the electrodes must be extremely thin and light weight to prevent loading of

the mechanical vibrations. At frequencies above 200 mc/sec, the plated electrode is generally prepared by sputtering or evaporating aluminum to a maximum thickness of about 1500 angstroms.

By the adoption of a coaxial configuration with air-gap rather than plated electrodes, all of the resistance losses described above can be significantly reduced at moderately high frequencies. This fact was first demonstrated by means of the mechanical arrangement of Figure 38.

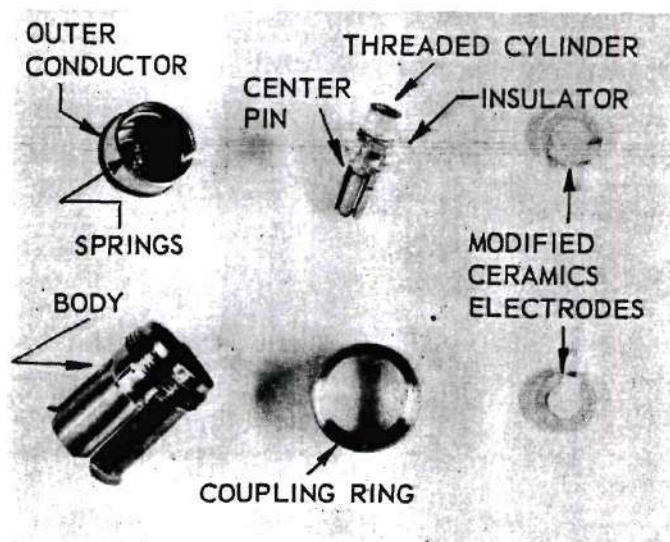


Figure 38. The Model 1 Coaxial Crystal Holder.

Pictured in this figure are the various parts of the first prototype coaxial crystal holder. This holder was constructed from parts of a General Radio Type 874 Basic Connector. The body, center connector pin, mechanical coupling ring, and insulator disk of the connector were used without modification. The center connector pin was attached to the insulator disk by a short threaded cylinder. The rear section of the holder was constructed from a short section of outer conductor tubing removed from a General Radio air-dielectric transmission line. The end

of this outer section was closed by a metal plate and provided with spiral springs to provide mechanical pressure and electrical connection.

Plated ceramic air-gap electrodes, removed from a CR-24/U crystal unit (25), were used for mounting the quartz slab. Sketches of these electrodes, with plating thickness exaggerated, are shown in Figure 39. The arrangement of the parts, when properly assembled, was shown as Model 1 of Figure 4.

In operation, the quartz slab was placed between the two air-gap electrodes. The center or active conductors of the electrodes did not make physical contact with the quartz slab but were separated from it by plated circular arcs a few ten-thousandths of an inch thicker than the center electrodes. Because of this separation, mechanical loading of the quartz by the electrode plating was absent and the electrodes could thus be constructed of deposited silver sufficiently thick to greatly reduce resistive losses. Other holder resistive losses were essentially eliminated by the large physical size of the supporting and conducting structures.

A quartz slab was mounted in this structure and the admittance characteristic of the holder determined by the Crystal Measurements Standard System. The resulting data are plotted in Figure 40. Shown also in this figure are the typical admittance characteristics of a conventional HC-6 holder. The location of the model 1 coaxial holder curve on the periphery of the Smith Chart indicated that the resistive losses of the coaxial holder were essentially zero. Therefore, the holder characteristics were nearly ideal provided suitable coupling to the quartz slab could be obtained.

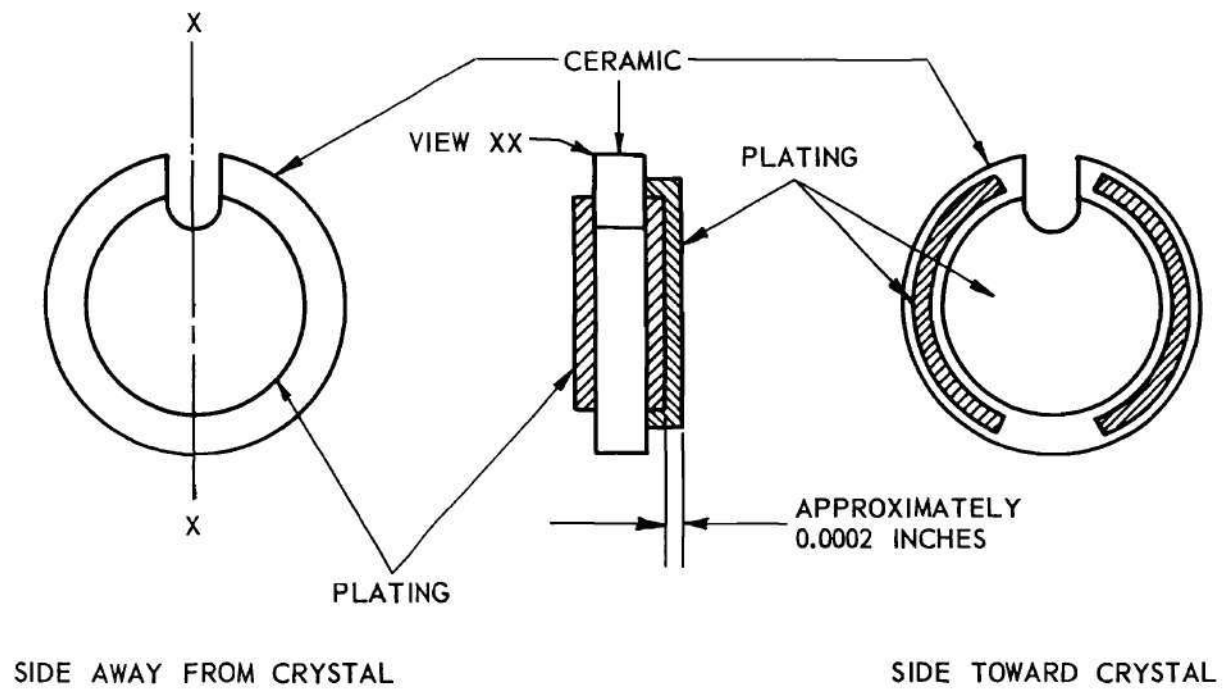


Figure 39. Air-Gap Electrodes for the Coaxial Crystal Holder.

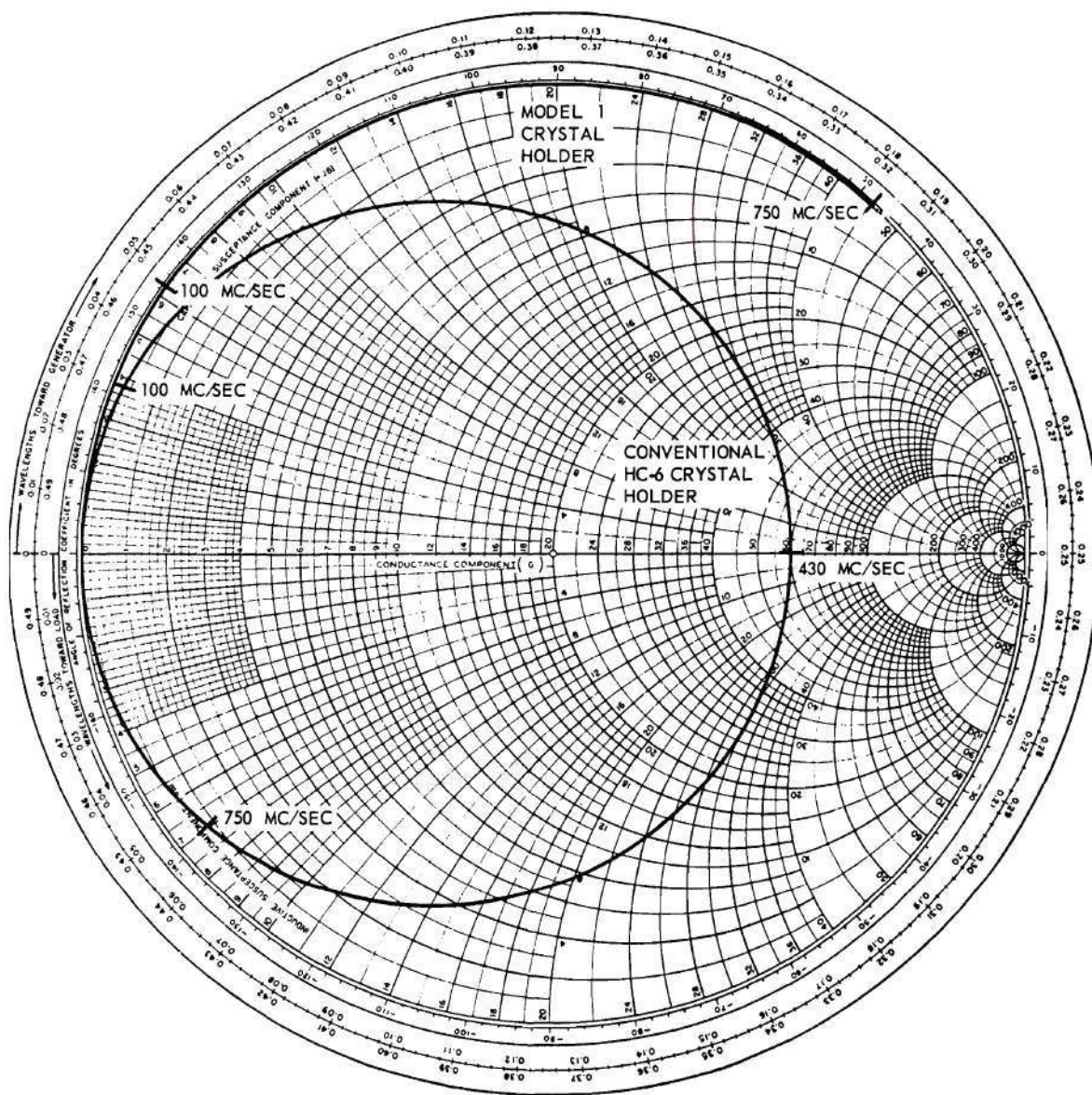


Figure 40. Admittance Characteristics of the Model 1 Coaxial Holder and of the Conventional HC-6 Holder.

Attempts were made to locate a crystal overtone response with this holder arrangement. No high-frequency responses could be found. The particular quartz blank used in this initial experiment was one which had been removed from the CR-24/U crystal holder mentioned above and was ground for use with the particular ceramic pressure mounting electrodes; however, it was not an optically polished blank.

Several additional quartz slabs with fundamental frequencies between 16 and 25 mc/sec were tested in the holder. No appreciable responses at frequencies above about 100 mc/sec were obtained. Several of these slabs were obtained by disassembling commercially fabricated HC-6 crystal units. One of the crystal units had been previously measured, with results as shown in Figure 41, to confirm its activity.

The reason for the failure of these electrodes to produce satisfactory responses was not fully determined; however, it was believed to be due to incorrect electrode diameter and air-gap spacing for high-overtone frequency operation. Accordingly, several experimental air-gap mounted HC-6 crystal units were obtained and disassembled for parts to be used in the coaxial holder. Sketches of one of the parts of interest are shown in Figure 42. These parts had been fabricated from quartz, recessed and plated as shown.

These quartz mounting electrodes were cemented to the original ceramic electrodes to form a good mechanical and electrical bond (the modified electrodes were shown in Figure 38). The plane sides of the quartz electrodes were placed toward the ceramic electrodes.

Again, all of the quartz blanks previously tested were remounted and again they failed to show any appreciable responses. Since the

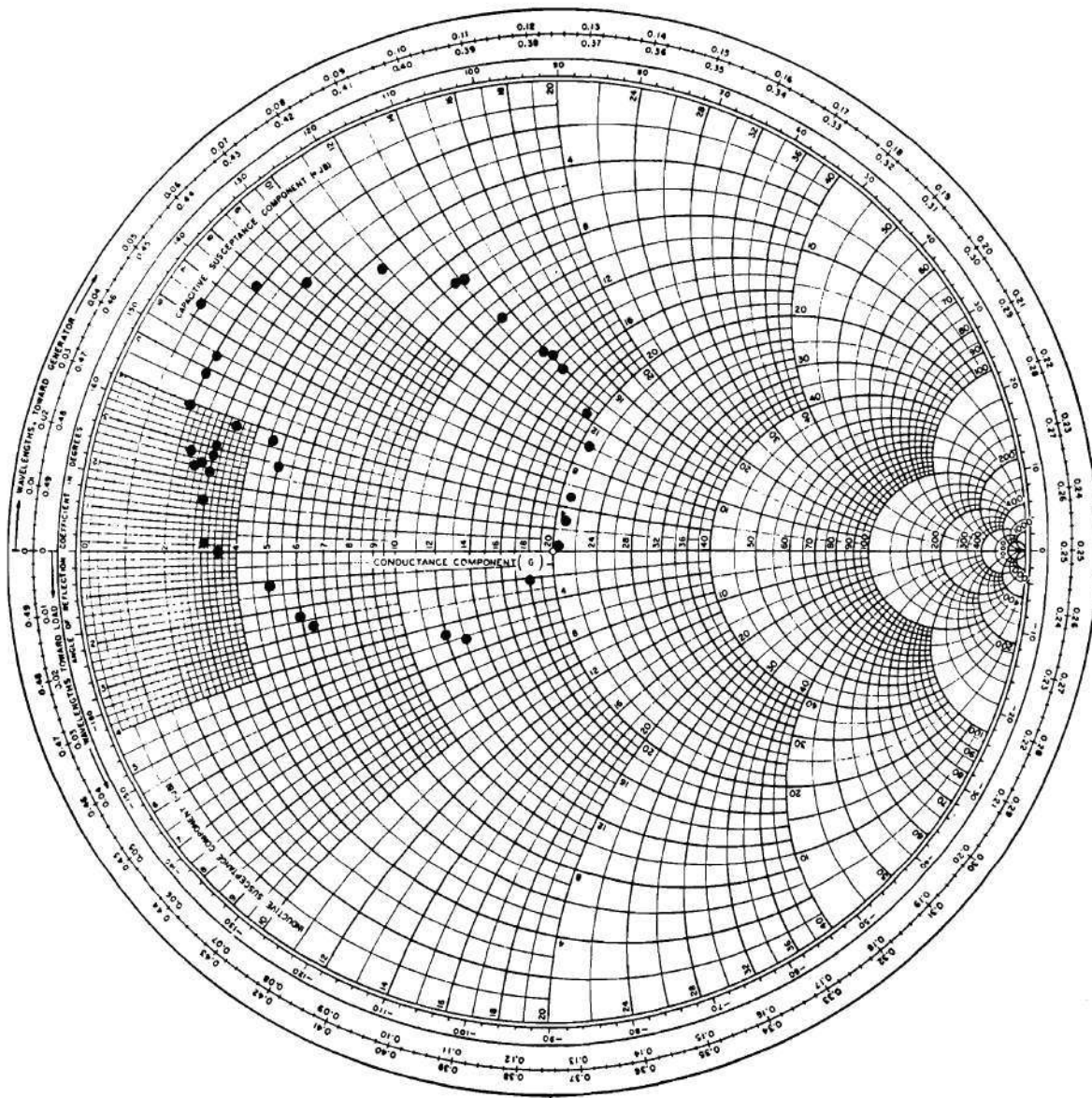


Figure 41. Admittance Characteristics of Crystal No. 20 in an HC-6 Holder.

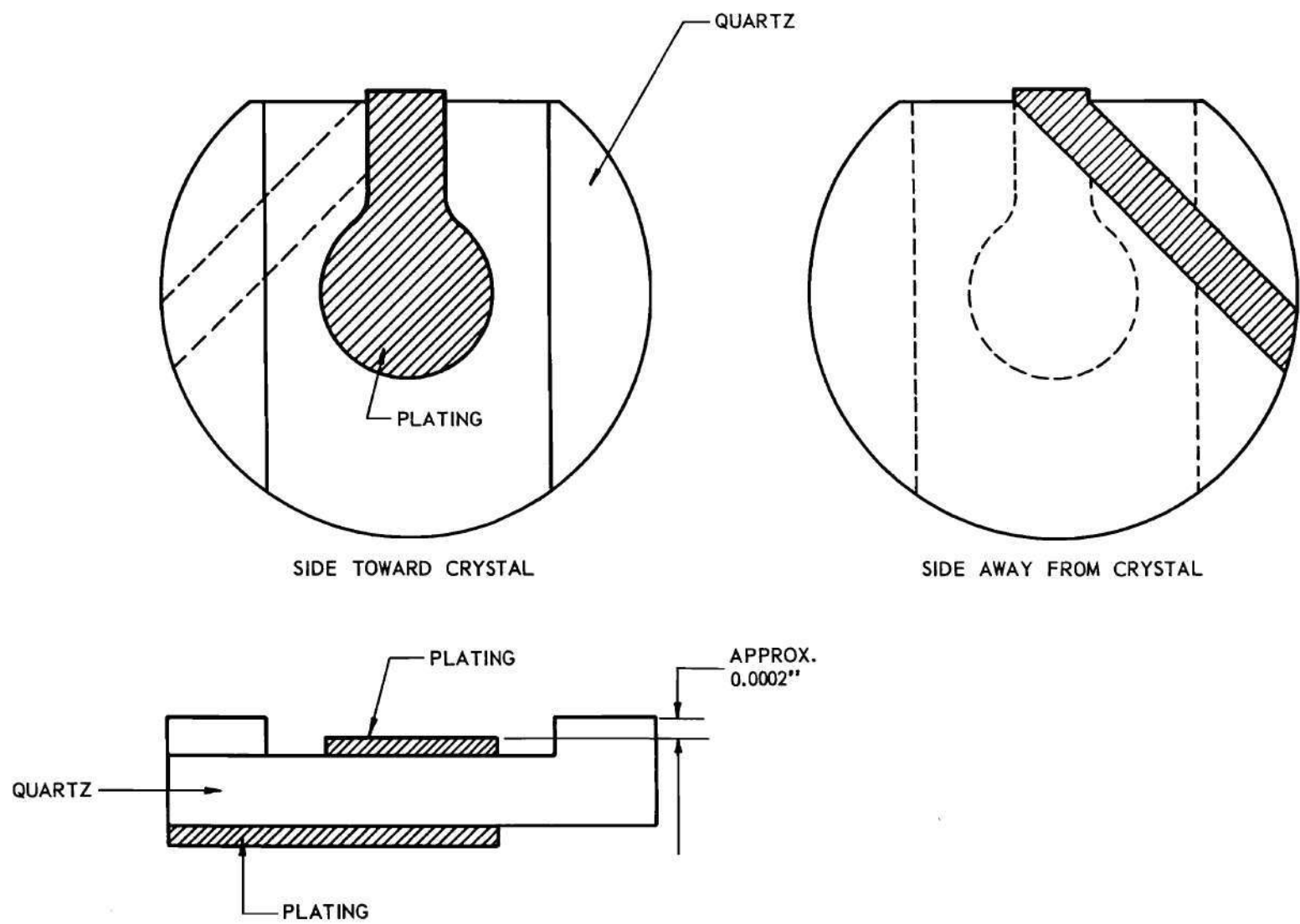


Figure 42. Recessed Quartz Air-Gap Electrodes.

quartz mounting electrodes were specifically designed for high-frequency applications, the crystal blanks were assumed to be inactive at the higher frequencies. At least one exception should have been the blank removed from the crystal whose characteristics were shown in Figure 41. Apparently, this quartz blank had been damaged when it was removed from its original holder.

All of the other quartz blanks available at the time were of too small a diameter for test with the electrodes of Figure 42. Attempts were made to prepare a set of electrodes for use with smaller quartz blanks by removing the plating from a pair of the CR-24/U ceramic electrodes and counter-sinking the centers of these electrodes a few ten-thousandths of an inch with an ultrasonic drill. The electrodes were replated and tested with several smaller quartz blanks having known activity. However, no appreciable responses were found. The lack of success this time was apparently due to the lack of mechanical precision in forming the electrodes.

As has been previously mentioned, a crystal mount employing air-gap electrodes is preferred over a mount requiring direct plating on the surface of the quartz slab because of reduced mechanical loading of the former. However, because of the difficulties experienced in obtaining responses with the prototype coaxial air-gap mount and because of the lack of facilities for precision machining of suitable air-gap electrodes, further attempts at air-gap mounting were temporarily abandoned.

A second coaxial crystal holder was constructed for use with plated quartz blanks. A photograph of the parts of this holder is shown in Figure 43. An assembly diagram for the holder is shown in Figure 44. The

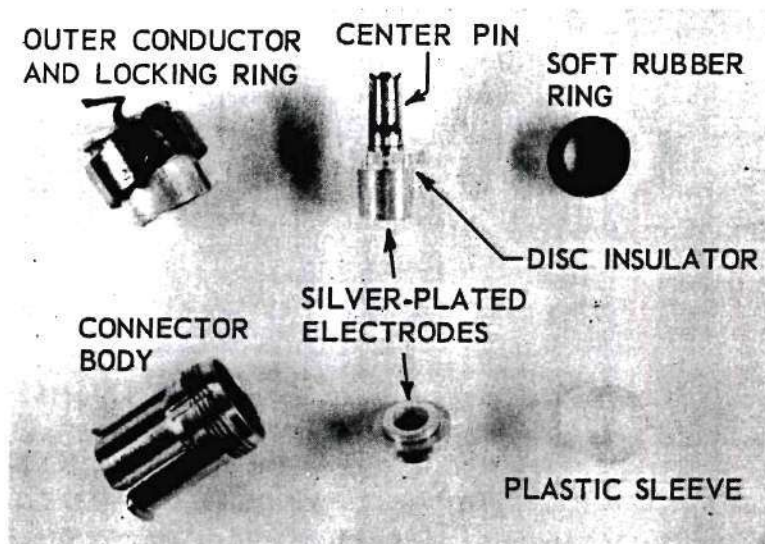


Figure 43. The Model 2 Coaxial Crystal Holder.

holder was arranged so that the plated quartz blank could be sandwiched between two silver plated brass electrodes while being properly centered by a plastic sleeve. One of the electrodes was attached to the center pin of a General Radio Type 874 Basic Connector while the other electrode was connected to the outer surface of the connector by a shield braid. Pressure was applied by means of a soft rubber ring. The holder was designed especially to fit a stock of 50 optically polished quartz blanks which were available for test purposes. The fundamental frequency of these blanks was 20 mc/sec. The assembled holder was shown as Model 2 of Figure 4.

A special plating mask for plating the quartz blanks was constructed. A photograph of the mask is shown in Figure 45.

Twenty of the blanks were plated in the prepared mask by evaporation of aluminum. Of the 20, only 3 were successfully registered because of improper fit in the mask. Several additional blanks were plated

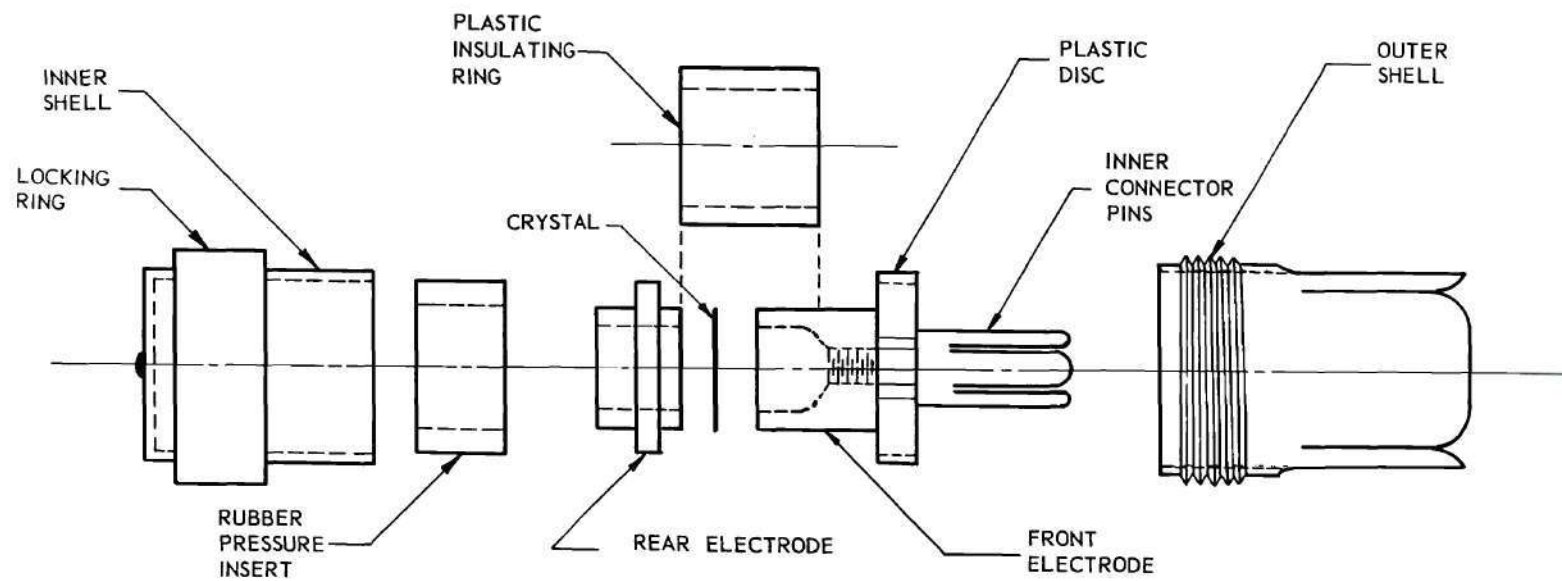


Figure 44. An Assembly Diagram of the Model 2 Coaxial Crystal Holder.

over their entire surfaces on both sides. The plating of each of the latter was then removed in areas to leave a key-way configuration by etching the blank in a sodium hydroxide solution. Several different key-way configurations, similar to those shown in Figure 45, were tried.

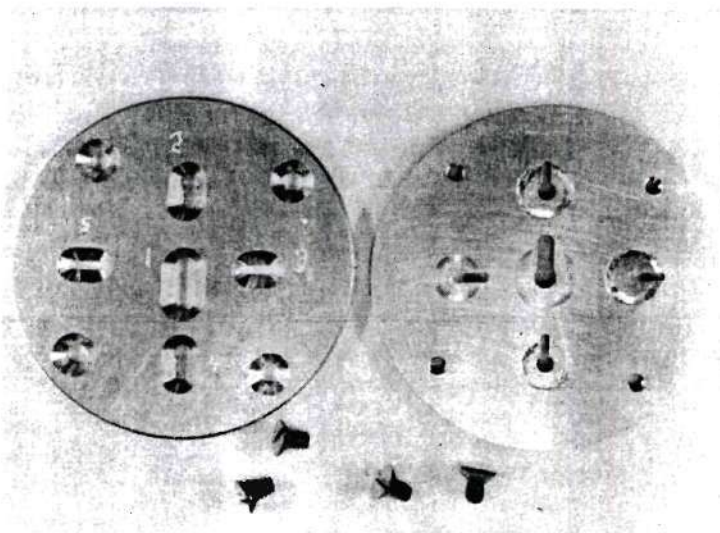


Figure 45. Plating Mask for the Preparation of Crystals for the Model 2 Holder.

All of the satisfactorily prepared blanks were cleaned and mounted successively in the Model 2 holder for test. None of the crystals showed appreciable high-frequency responses.

The remaining blanks of the original 50 were plated and prepared for mounting in conventional HC-6 holders to determine if responses could be obtained. Only two were successfully mounted without breakage. These two showed no appreciable responses even in the conventional holders. Thus, this set of crystal blanks was also assumed to be inactive at high frequencies. Also, by this time, practically all of the original 50 blanks had been damaged or broken.

Again a search was made for suitable quartz blanks. Several HC-6 crystal units which were available for disassembly were tested in the Crystal Measurements Standard for overtone responses. Disassembly without damage to the crystal blank was successful for only two of the units. One of these blanks was of a size suitable for use with the Model 1 air-gap holder of Figure 38. The blank, which had a fundamental frequency of approximately 33 mc/sec, was cleaned and mounted in the air-gap holder. Appreciable responses were obtained in a coaxial holder for the first time. Plots of the responses, corrected for line length and C_0 , are shown in Figure 46. The curves indicate that the holder was essentially lossless, except at the 363 mc/sec response where small resistive holder components were indicated.

Severe spurious responses in close proximity to the main response were observed. These responses were probably due to dirt or dissymmetry in mounting.

The original overtone responses for this crystal blank while mounted in an HC-6 holder are shown in Figure 47 for comparison with the responses obtained in the coaxial holder. The responses shown in Figure 47 are corrected for line length only. The two higher frequency responses are of little use in oscillator control because of the excessive holder losses.

Figure 48 shows the motional-arm responses for this crystal in the HC-6 mount as calculated from the responses of Figure 47 using the methods described in Chapter II. The values of motional-arm resistance (R_1) as determined from Figures 46 and 48 are tabulated in Table 4. The motional-arm resistance (and, therefore, the Q) was degraded relatively

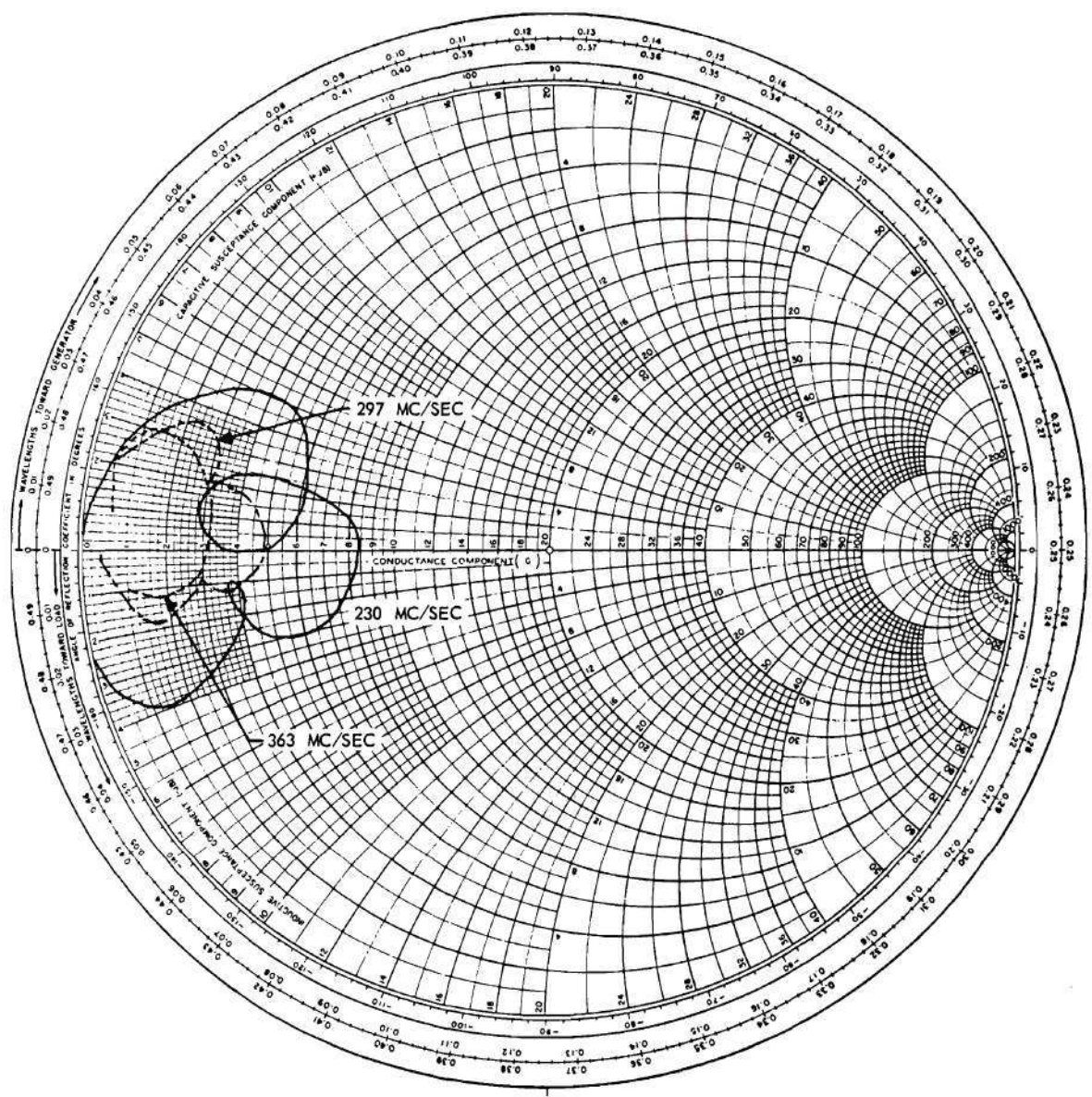


Figure 46. Overtone Responses of Crystal Blank A-1 in the Model 1 Holder.

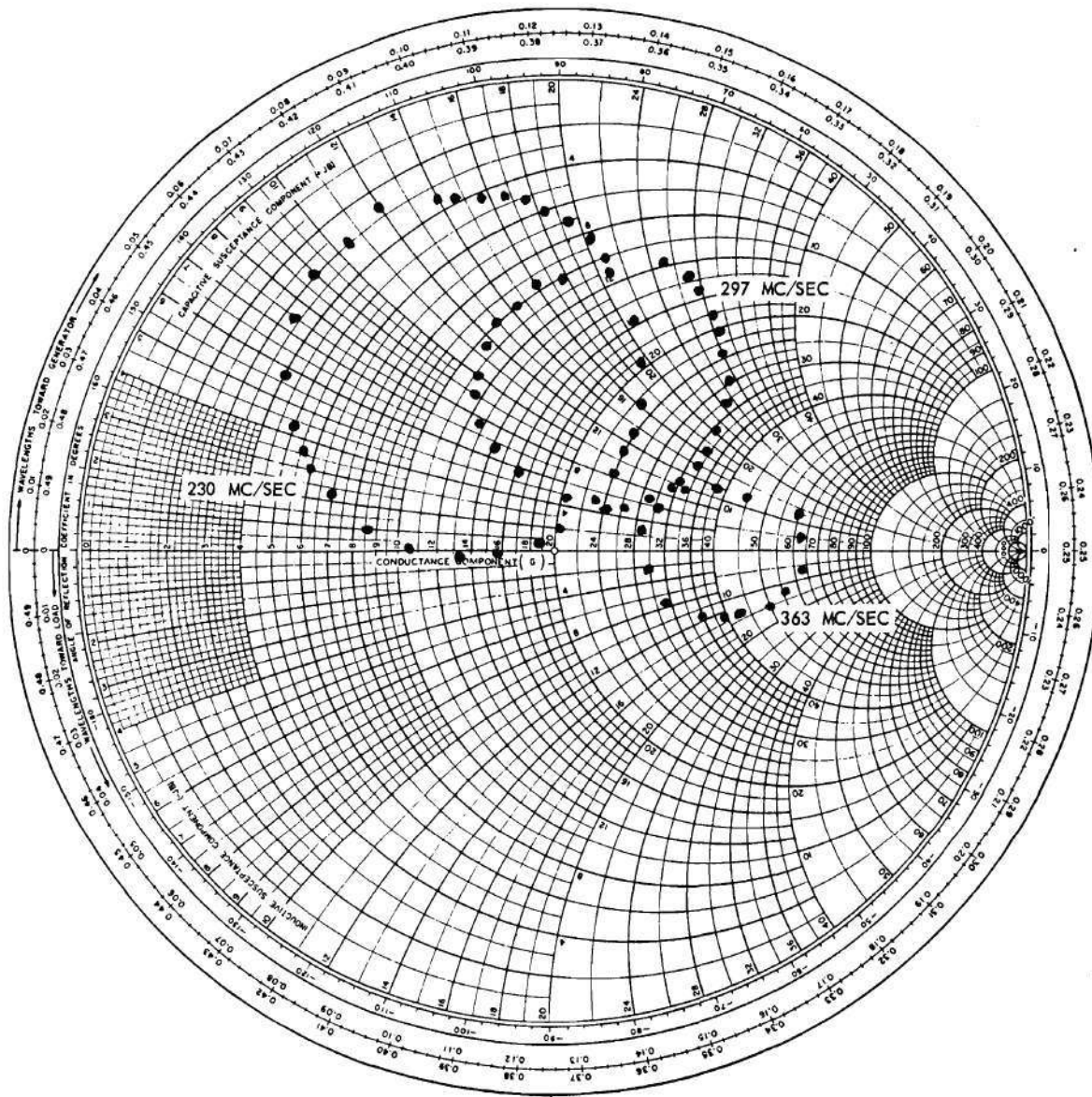


Figure 47. Responses of Crystal Blank A-1 in an HC-6/U Holder.

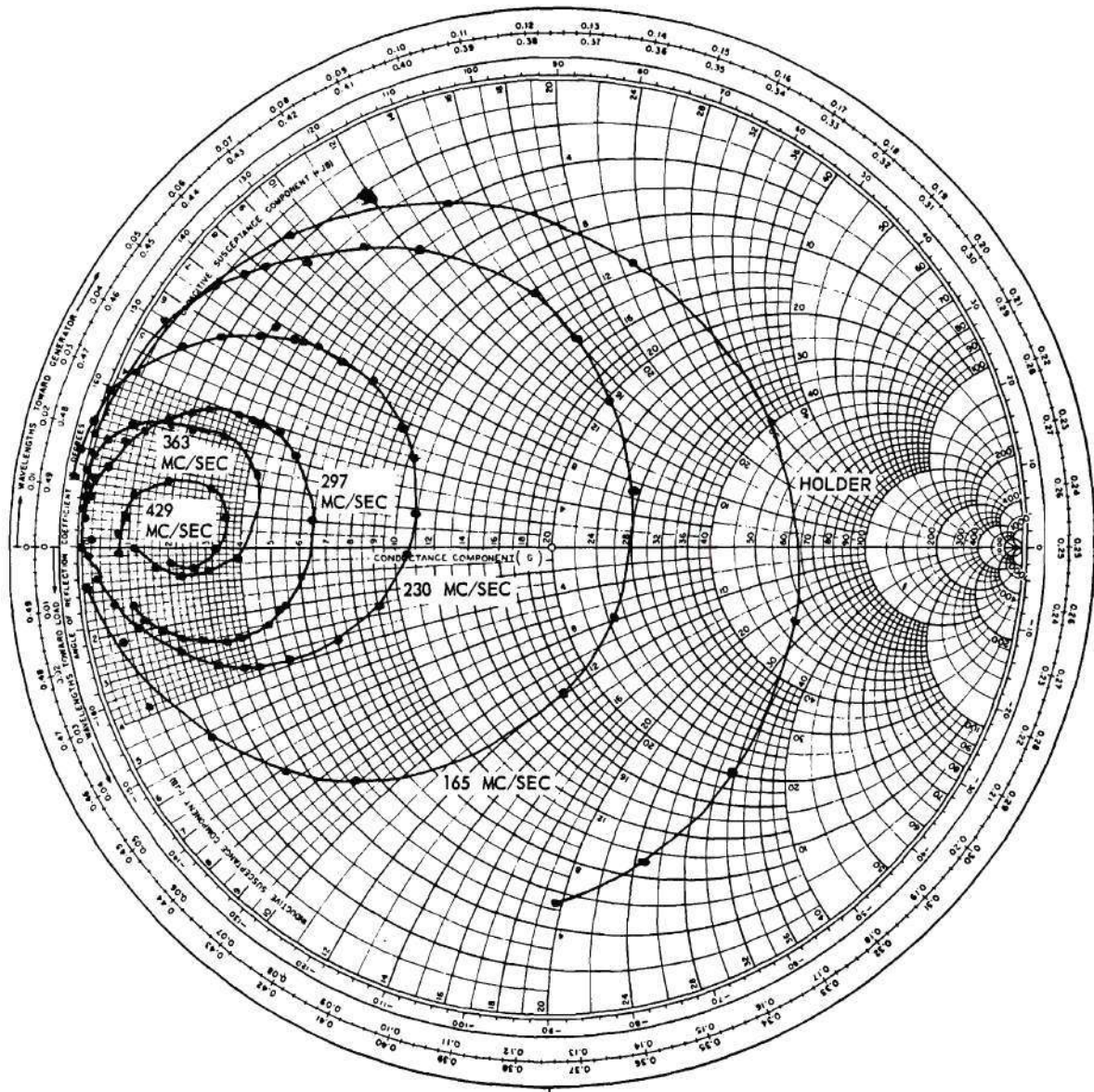


Figure 48. Motional-Arm Responses of Crystal Blank A-1 as Determined from Measurements with an HC-6/U Holder.

little by the coaxial holder, while at the same time the holder losses were almost entirely eliminated. The observed increases in R_1 in the coaxial mount may have been due either to the presence of the severe spurious responses near the main responses or to poorer coupling between the quartz blank and the electrodes. Theoretically, at least, the air-gap electrodes with optimum spacings could produce smaller values of R_1 than the plated electrodes due to the absence of mechanical loading by the plated electrodes.

Table 4. Comparison of Motional-Arm Resistances in the Coaxial and Conventional Holders.

Overtone Frequency (Mc/Sec)	R_1 in Coaxial Holder (Ohms)	R_1 in HC-6/U Holder (Ohms)
230	128	91
297	205	154
363	310	220

The equivalent shunt capacitance, C_o , of this coaxial holder (15.5 mmfd) was somewhat larger than that of the conventional HC-6 mount; however, this capacitance could theoretically be antiresonated to raise the shunt impedance whereas such was not possible with the HC-6 mount because of resistive losses.

At this time, a larger quantity of high quality optically polished quartz blanks was obtained. Included were blanks of various diameters and with fundamental frequencies of 16, 25, 35, and 50 mc/sec. Many experiments, which included the construction of special plating masks and mounting fixtures, were performed while attempting to obtain responses by plating various of these blanks and mounting them in the holder of

Figure 43. No appreciable responses were obtained. Examination of the blanks in each case showed faults in the plating. Satisfactory bondings between the plating and blanks were not obtained because of the extremely smooth surface of the blanks.

Several of the 35 mc/sec blanks were cleaned and mounted in the air-gap holder of Figure 38. Low-resistance responses were obtained in many cases; however, all responses showed severe spurious responses. A typical example is shown in Figure 49. In this figure, the responses were corrected for holder line length but not for C_0 . Again, the loss-free characteristics of the coaxial holder may be observed. The C_0 of this holder was calculated at each of the responses shown to determine whether or not elements, in addition to the transmission line and C_0 , must be included in the holder equivalent circuit. The results are tabulated in Table 5.

The small discrepancy between the capacitance values of Table 5 (except at 454 mc/sec, where the instrument resolution was poor because of the very large susceptance) indicated that the complete coaxial crystal could be satisfactorily represented as a motional-arm circuit paralleled by a constant C_0 and coupled to external terminals by a lossless transmission line.

The severe spurious responses of Figure 49 were attributed to lack of symmetry in the construction of the mount. Since these spurious responses were apparently inherent in this particular coaxial holder, further tests with this unit were discontinued.

Because of the difficulties encountered with the two original coaxial holders and since they did not include provisions for antiresonating

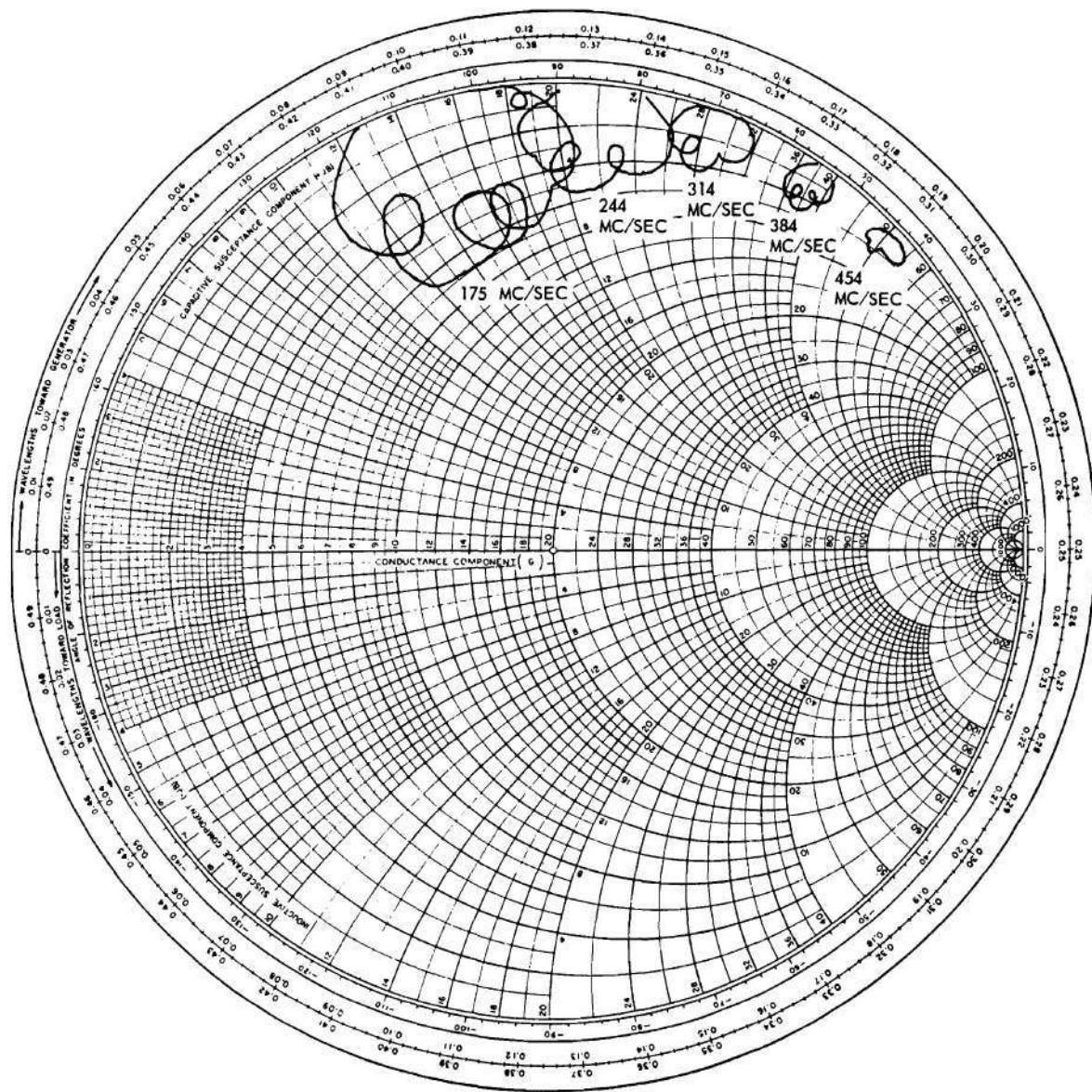


Figure 49. Responses of Crystal W351 in the Model 1 Holder.

C_o , a third and final coaxial holder was designed and constructed. A photograph of this holder was shown as Model 3 of Figure 4. The various disassembled parts are shown in Figure 50. A close-up view of the holder proper is shown in Figure 51.

Table 5. Comparison of Calculated Values of C_o at Various Overtone Frequencies.

Frequency (Mc/Sec)	Susceptance (Millimhos)	C_o (Mmfd)
175	15.5	14.1
244	22.0	14.4
314	29.0	14.7
384	38.5	15.9
454	52.0	18.3
0.335*	----	14.9

* Measured with a Boonton Q-Meter Type 160-A.

Figure 52 is a cross-sectional sketch of Figure 51. The external terminals of the holder are at A. At the opposite end of the holder, a shorted stub, C, with an adjustable length short at B acts as a transmission line inductance for antiresonating the C_o of the crystal mount. The lower electrode, L, is supported by the center conductor, J, through part E. The upper electrode, K, is grounded to the outer conductor of the assembly through part F and spring clips, H, which apply the necessary pressure to the quartz blank, G. The insulator, D, serves to center the quartz assembly and prevent short circuits.

The original intention was to form the electrodes, K and L, for the quartz blank from plated insulators of the same diameters. Several

Page missing from thesis

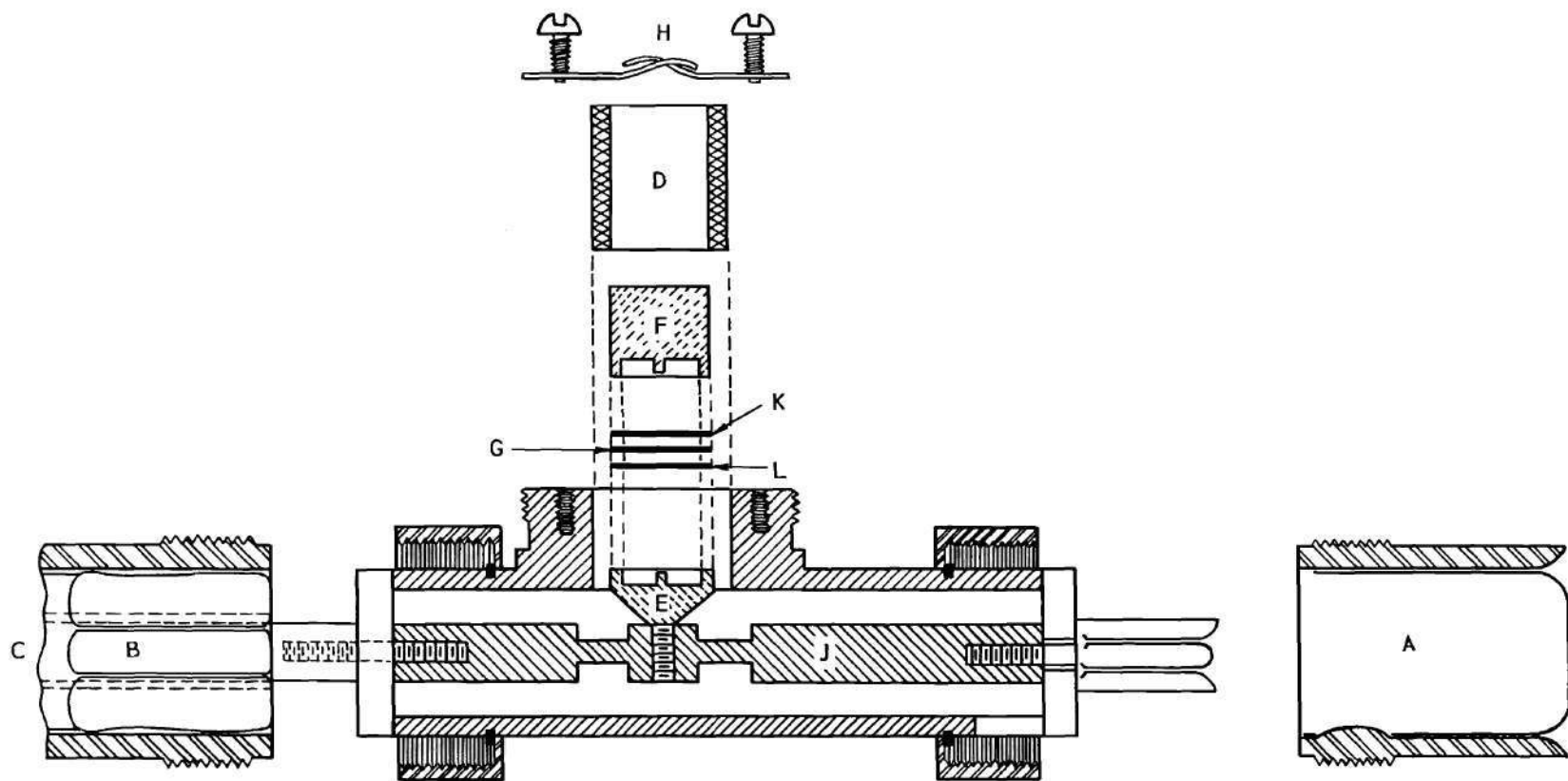


Figure 52. A Cross-Sectional Sketch of the Model 3 Holder.

large diameter semi-polished quartz blanks with a fundamental frequency of 8 mc/sec were edge-ground to a diameter of 0.345 inches (the diameter of the test crystals). These blanks were then plated with the configuration shown in Figure 53 by evaporation of silver. Attempts were then

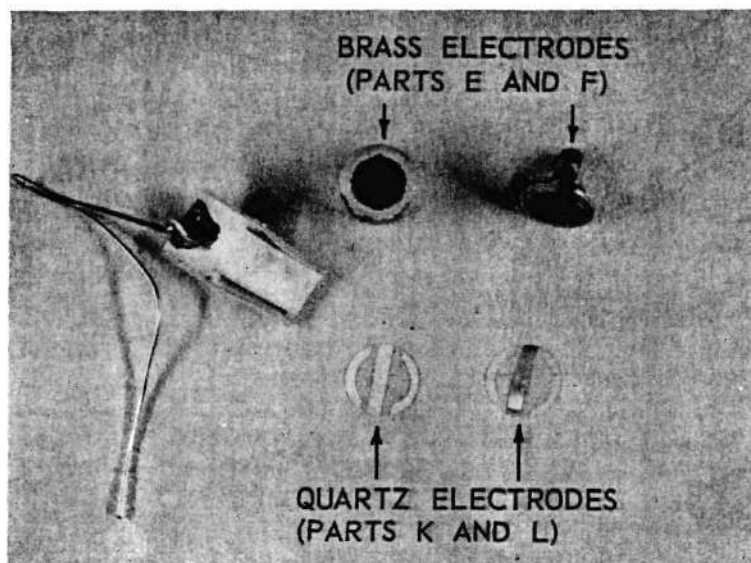


Figure 53. Air-Gap Electrodes and Plating Clip for the Model 3 Holder.

made to overplate the two outer circular arcs in a liquid silver-plating solution by mounting the discs in the fixture shown also in Figure 53. The evaporated silver was, however, stripped off by the silverplating bath. Several other concentrations of silver-plating solution, including a strike solution, were tried with varying current densities. The evaporated silver was stripped off in all cases.

Evaporated nickel and sputtered nickel were both tried as base platings. The adherence was slightly better when overplating with silver was attempted; however, no successfully overplated blanks were obtained. Several other attempts at overplating were also unsuccessful.

An alternate electrode forming procedure was tried. Parts K and L were eliminated and parts E and F of Figure 52 were plated with rings at the outer diameters as shown in Figure 53. The plated rings were built up to a thickness of approximately 0.0002 inch to form the necessary air-gap. A 25 mc/sec quartz blank was mounted and an overtone response was obtained at 225 mc/sec. This response, however, was very poor.

The coaxial holder was disassembled and the parts E and F were repolished to reduce the air-gap. The crystal blank was remounted and again tested. The data obtained are shown in Figures 54, 55, and 56. At the three lower overtone frequency responses (225, 275, and 325 mc/sec), the C_0 of the unit was antiresonated by the inductive stub. The line length from the T-junction of the holder to the internal terminals of the Admittance Meter was made one-half wavelength at each overtone frequency so that the data shown are those obtained directly from the Admittance Meter without any corrections. At 375 and 425 mc/sec, the stub could not be adjusted short enough to antiresonate the large C_0 . The large value of C_0 was due to the large conducting area of the electrodes and the small thickness of the quartz blank (approximately 0.002 inch).

The spurious responses as well as the main responses were obtained at each crystal overtone response as shown in the figures. The spurious responses were again severe, although slightly less so than for previous tests.

The data from Figures 54, 55, and 56 are summarized in Table 6.

Overtone responses for quartz blank W351, with a fundamental frequency of 35 mc/sec, are shown in Figure 57. The capacitance, C_0 , because of its increased size due to a thinner quartz blank, could be antiresonated

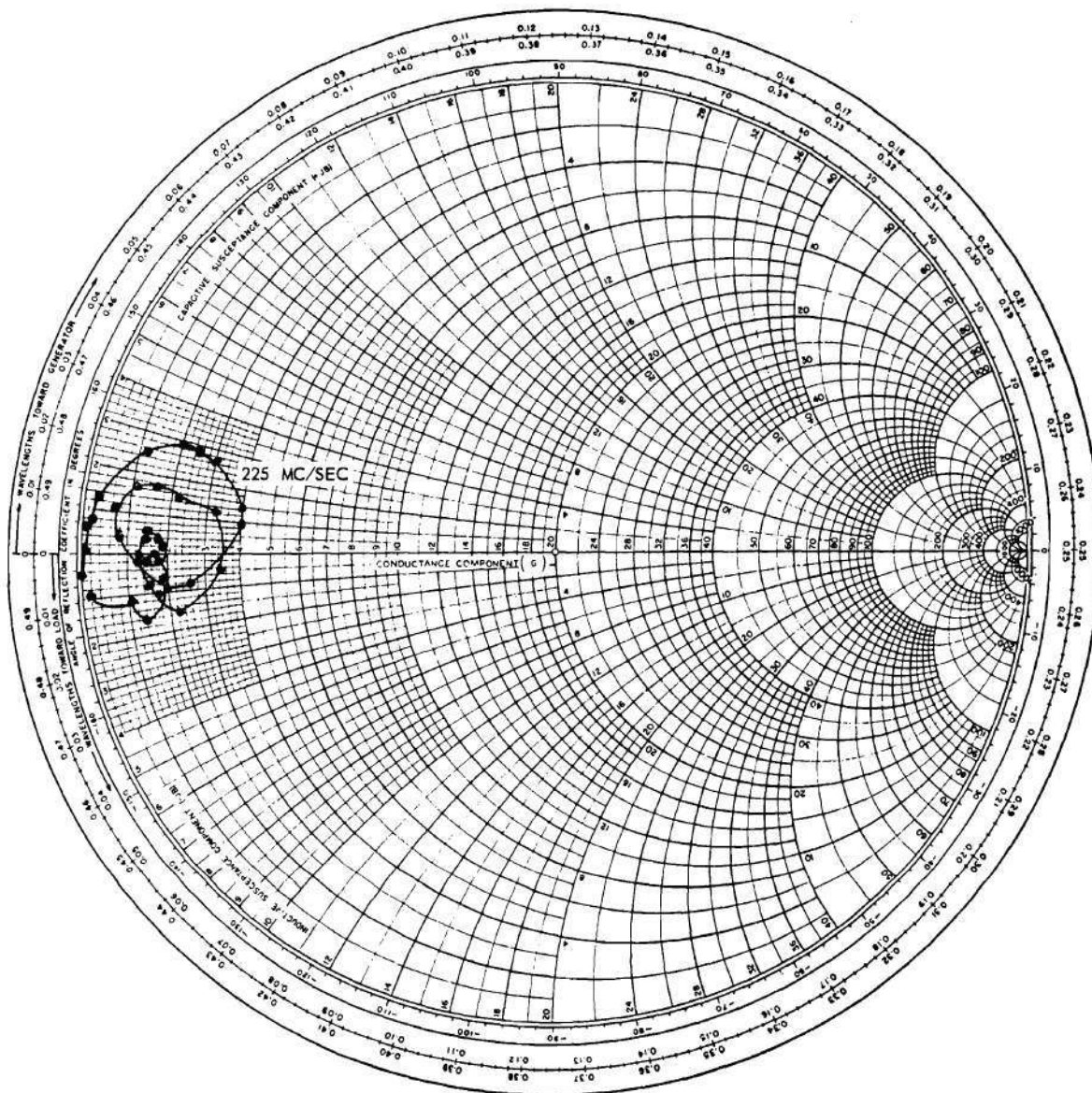


Figure 54. Responses of Crystal W254 in the Model 3 Holder at 225 Mc/Sec.

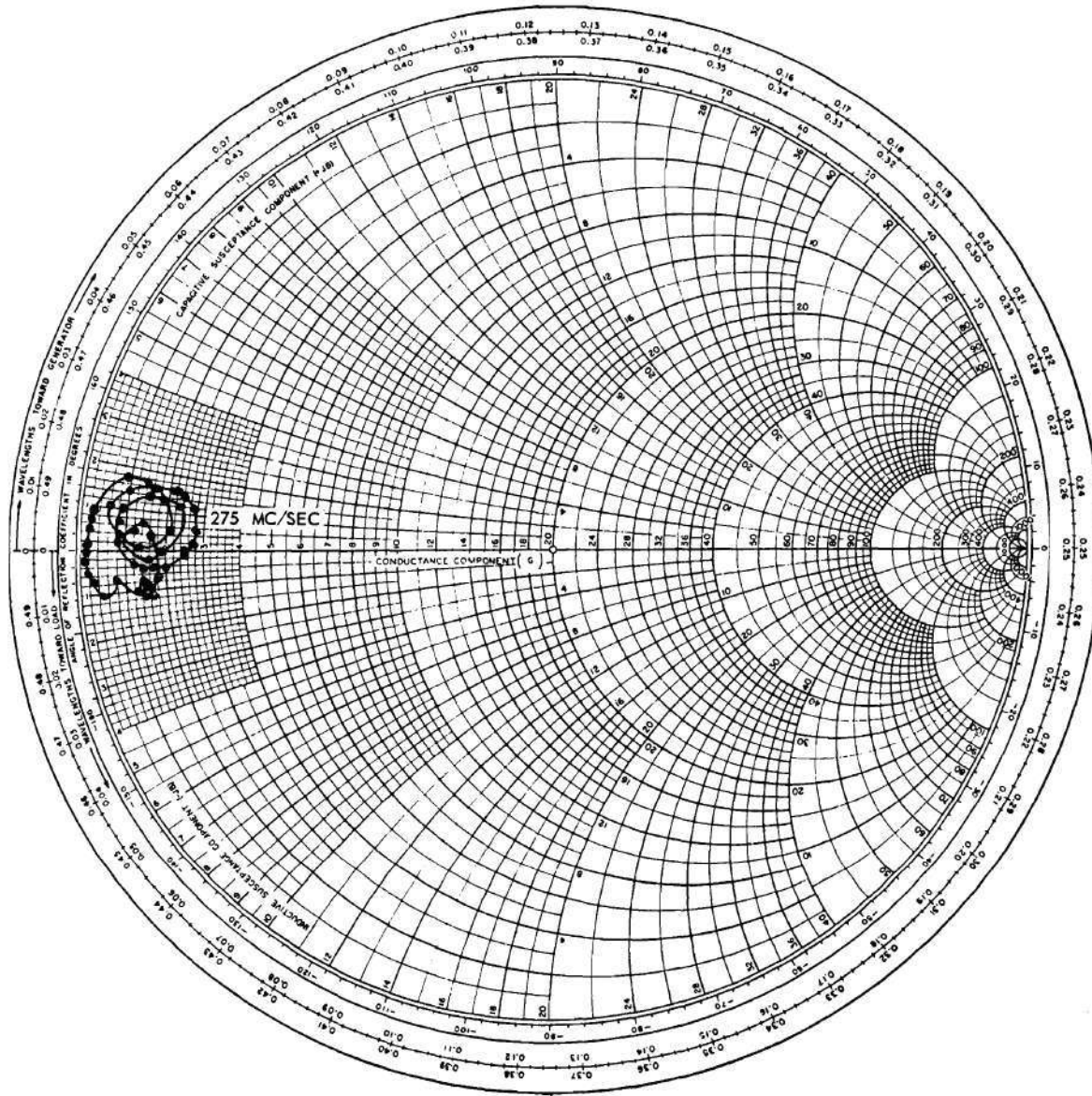


Figure 55. Responses of Crystal W254 in the Model 3 Holder at 275 Mc/Sec.

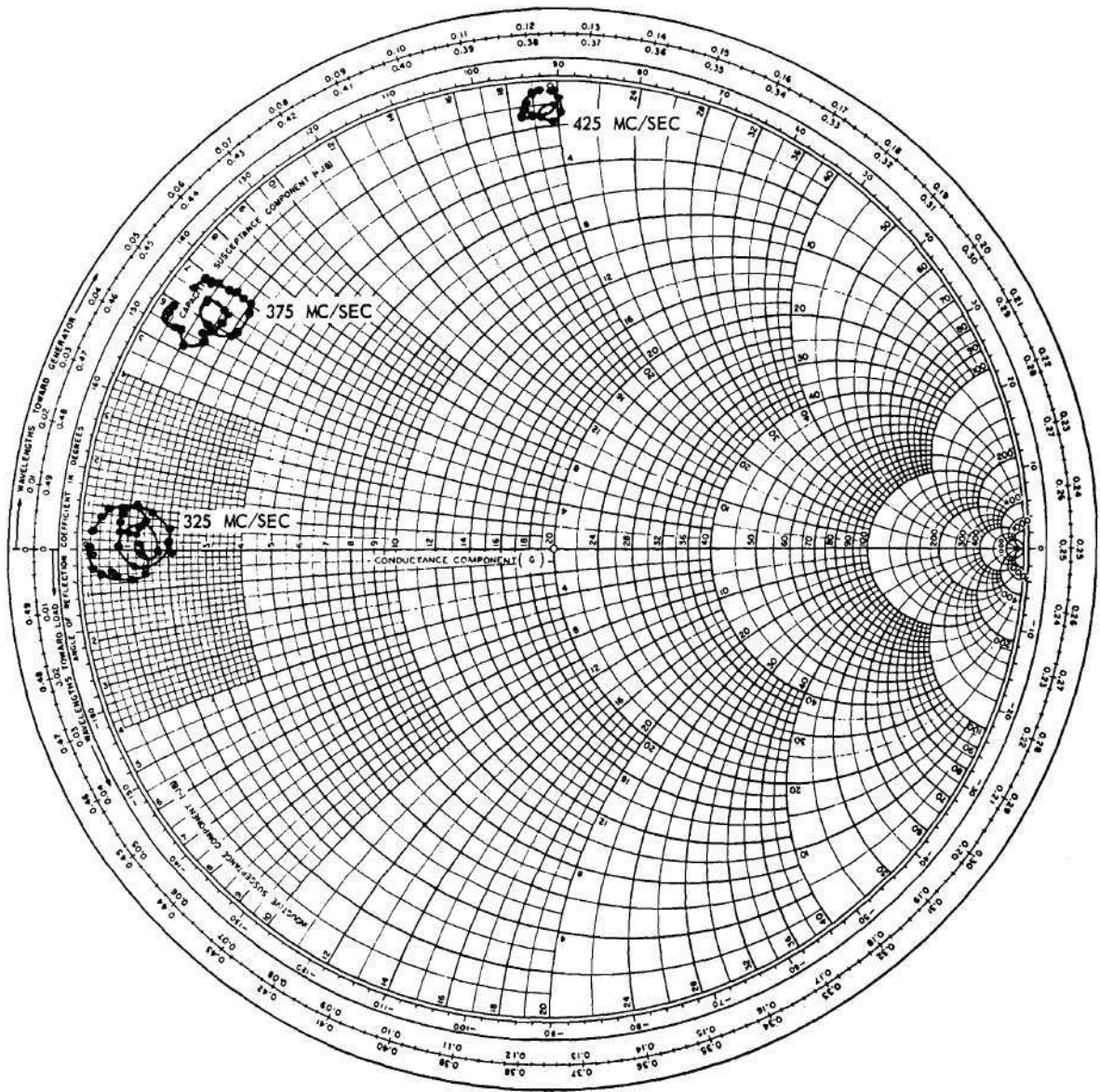


Figure 56. Responses of Crystal W254 in the Model 3 Holder at 325, 375, and 425 Mc/Sec.

Table 6. Crystal W254 in the Model 3 Holder.

Overtone Frequency (Mc/Sec)	Overtone Number	Resistance, R_1 (Ohms)
225	9	250
275	11	355
325	13	500
375	15	500
425	17	650

only at the lower overtone frequency. The data on this crystal are summarized in Table 7.

Table 7. Crystal W351 in the Model 3 Holder.

Overtone Frequency (Mc/Sec)	Overtone Number	Resistance, R_1 (Ohms)
318	9	140
389	11	130
460	13	80

The reason for the lowest value of R_1 being indicated at the highest frequency and the reason for the indicated holder losses at this frequency appeared to be the large shunt susceptance of the holder, which necessitated the use of a high multiplying factor with the Admittance Meter, thus contributing large errors.

Quartz blank W504, with a fundamental frequency of 50 mc/sec, was mounted and tested in the Crystal Measurements Standard at three overtone frequencies. The results are shown in Figure 58. Again, C_0 could not be

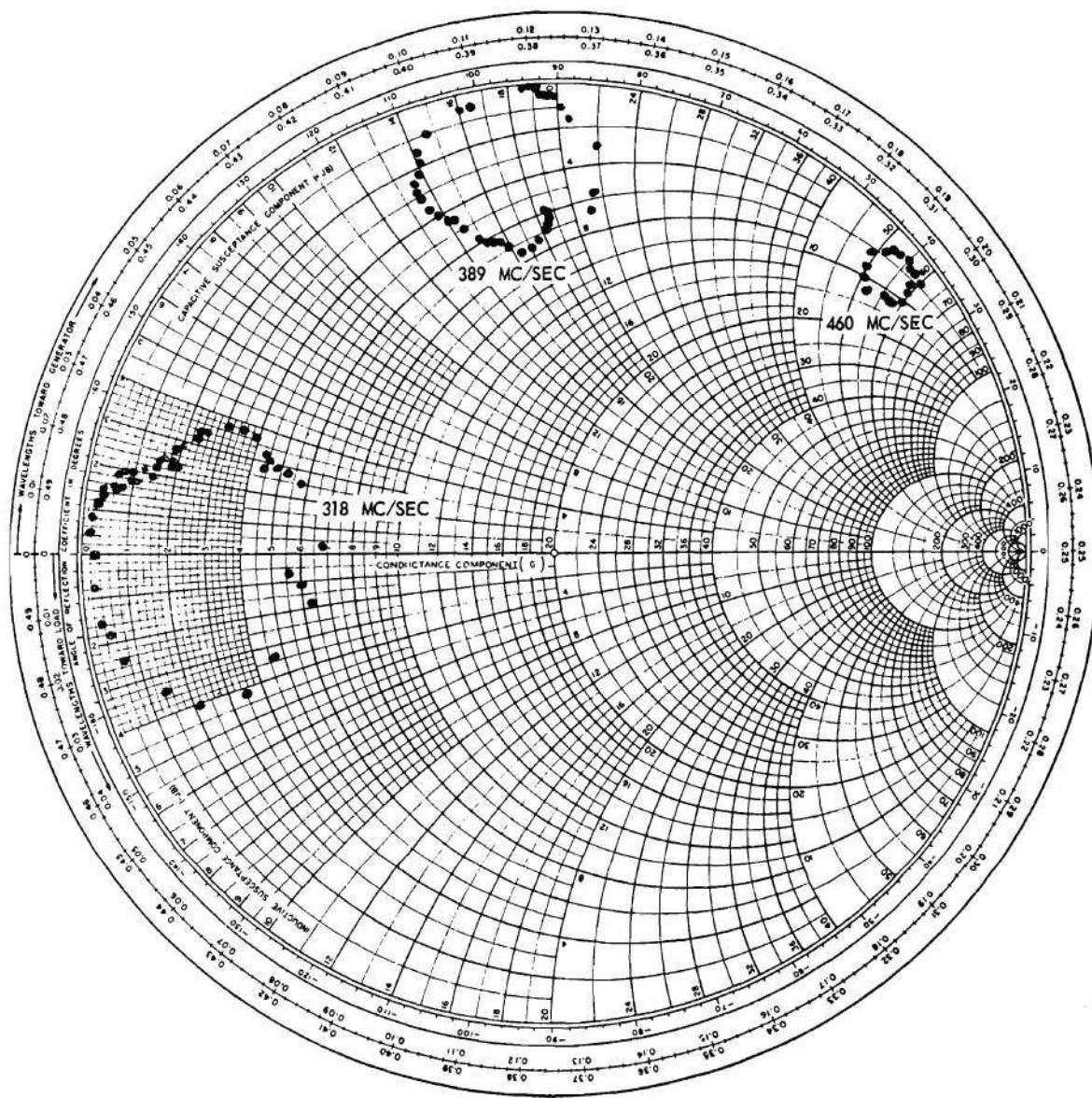


Figure 57. Responses of Crystal W351 in the Model 3 Holder.

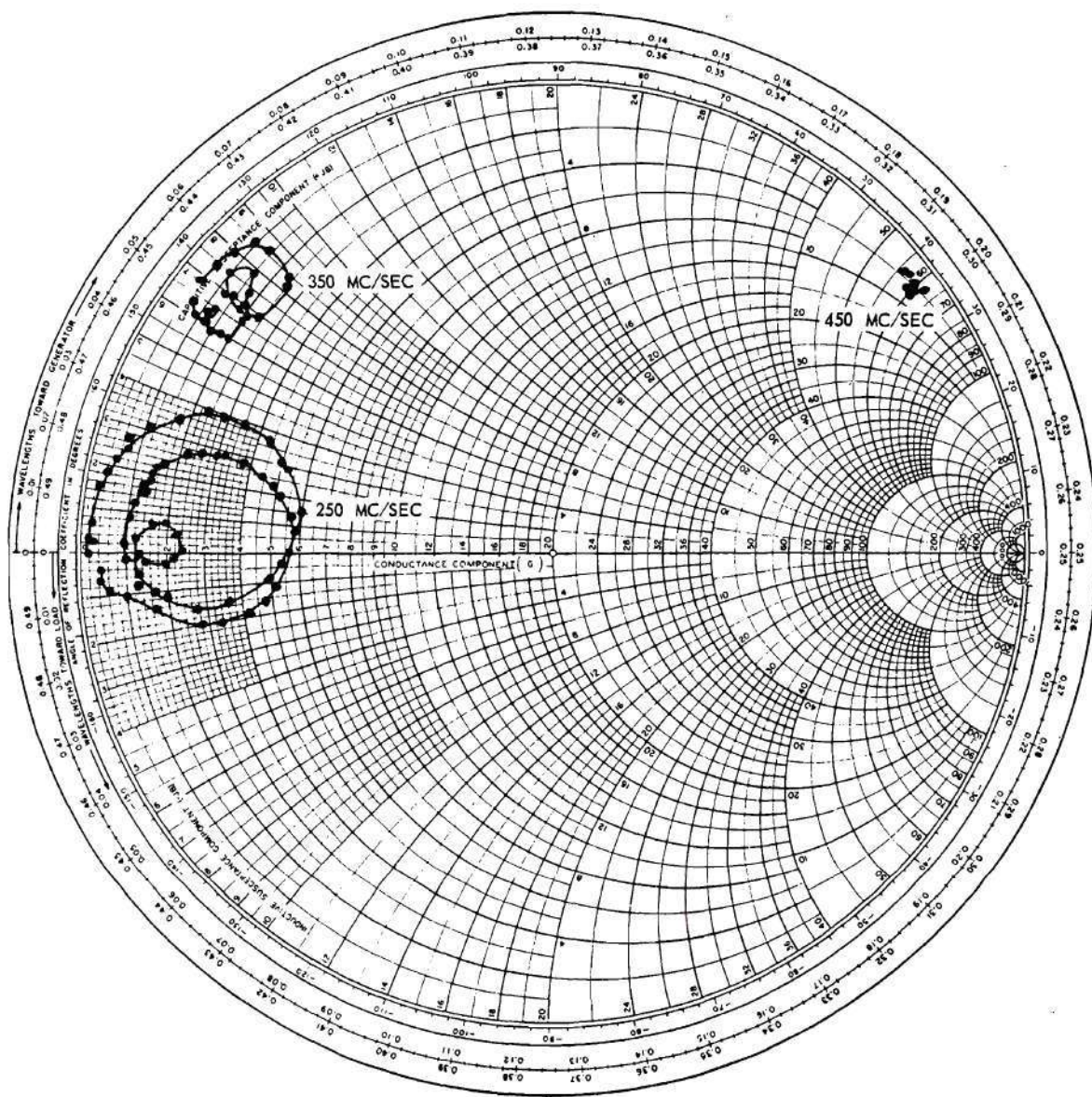


Figure 58. Responses of Crystal W504 in the Model 3 Holder.

completely antiresonated at the two higher overtone frequencies. A summary of the test data appears in Table 8.

Table 8. Crystal W504 in the Model 3 Holder.

Overtone Frequency (Mc/Sec)	Overtone Number	Resistance, R_1 (Ohms)
250	5	166
350	7	400
450	9	147

The indicated resistance at the highest overtone frequency was again believed to be greatly in error for reasons previously indicated.

In all of the above tests, the large size of C_0 greatly reduced the accuracy of the measurements since holder antiresonance could not be obtained at the higher overtone frequencies. Therefore, the parts E and F of Figure 53 were again redesigned to the final form shown in Figure 59 (and also as sketched in Figure 52). The large cross-sectional area, responsible for the large shunt capacitance, was reduced by recessing the parts to leave only a center stud and an outer ring. The center stud was then recessed to 0.0002 inches below the ring. The amount of recess was measured by focusing a calibrated microscope, having an extremely small depth of field, alternately on the ring and on the center stud.

Crystal blank W504 was tested with the new electrodes in the holder. The data shown in Figures 60 and 61 were obtained. The motional-arm resistance was somewhat higher than had been obtained previously with the same blank; however, the spurious responses had been eliminated from the region of the main response. With the reduced capacitance of the new

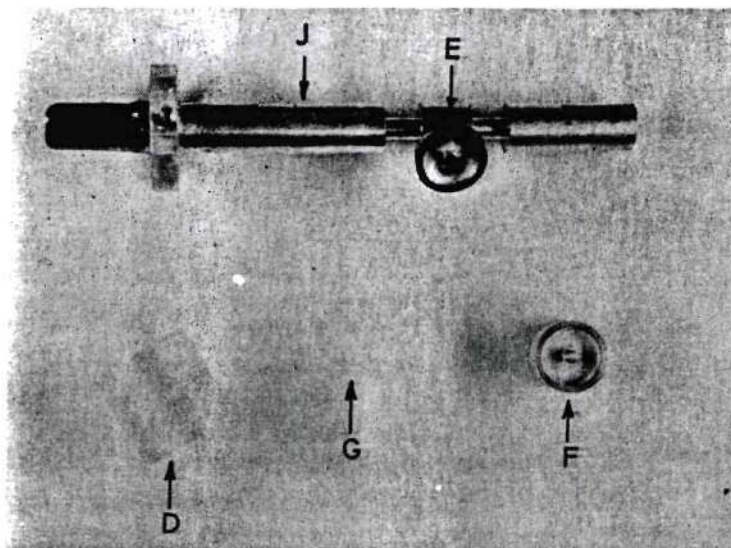


Figure 59. The Recessed Metal Electrodes for the Model 3 Holder.

holder, antiresonance could now be obtained at 350 mc/sec. Complete holder antiresonance was still not possible at 450 mc/sec.

The test data for crystal W507, with a fundamental frequency of 50 mc/sec, are shown in Figures 62 and 63 for four overtone frequencies. At the lower frequency, 150 mc/sec, the maximum inductance of the stub was not sufficient to obtain antiresonance. At 450 mc/sec, the minimum inductance of the stub was too great to obtain antiresonance.

A summary of the test data, including the calculated Q , is presented in Table 9.

Table 9. Crystal W507 with the Recessed Electrodes.

Overtone Frequency (Mc/Sec)	Overtone Number	Resistance, R_1 (Ohms)	Q
150	3	143	45,000
250	5	356	29,800
350	7	555	35,000
450	9	730	-----

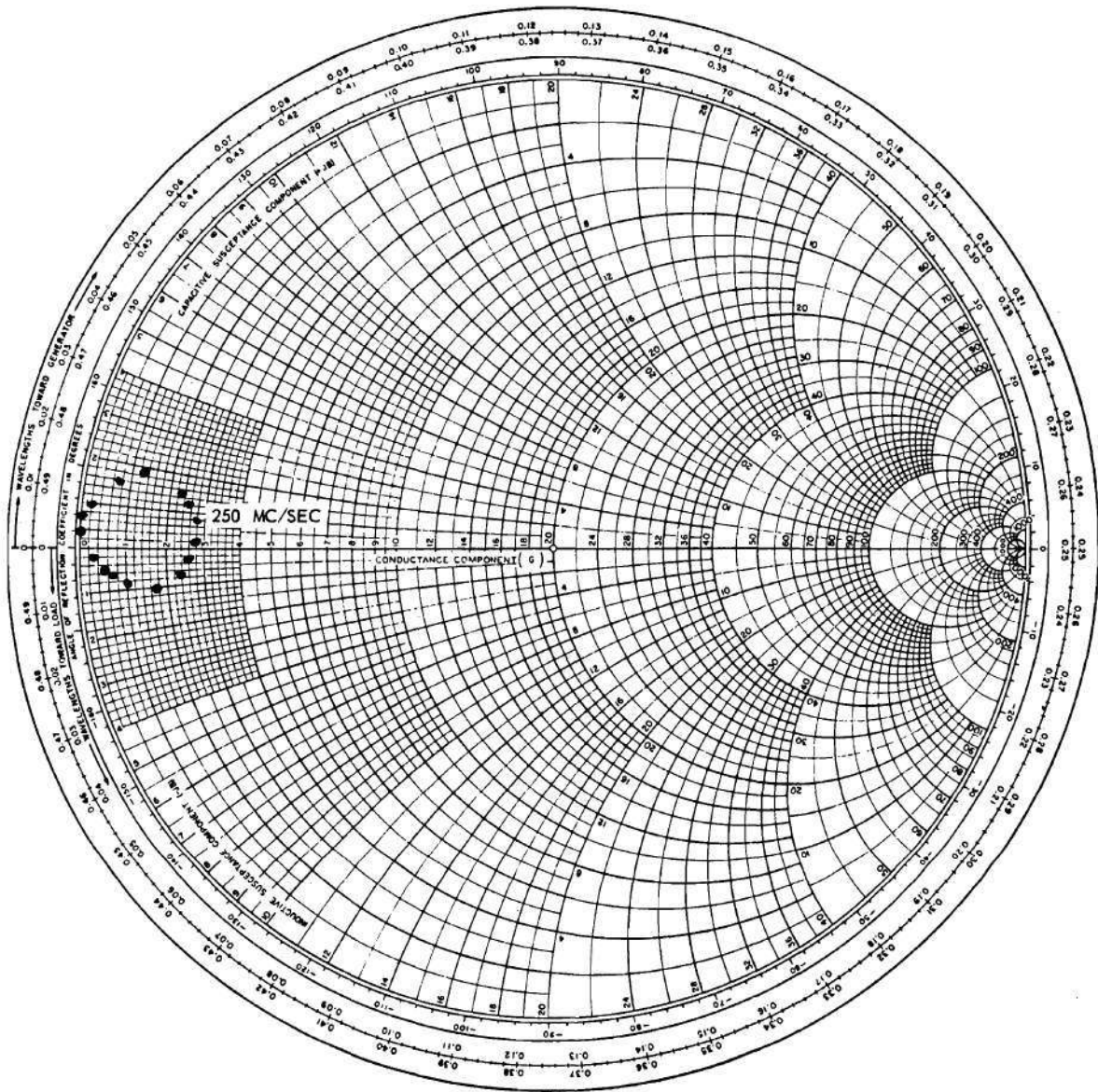


Figure 60. Responses of Crystal W504 at 250 Mc/Sec with the Recessed Electrodes.

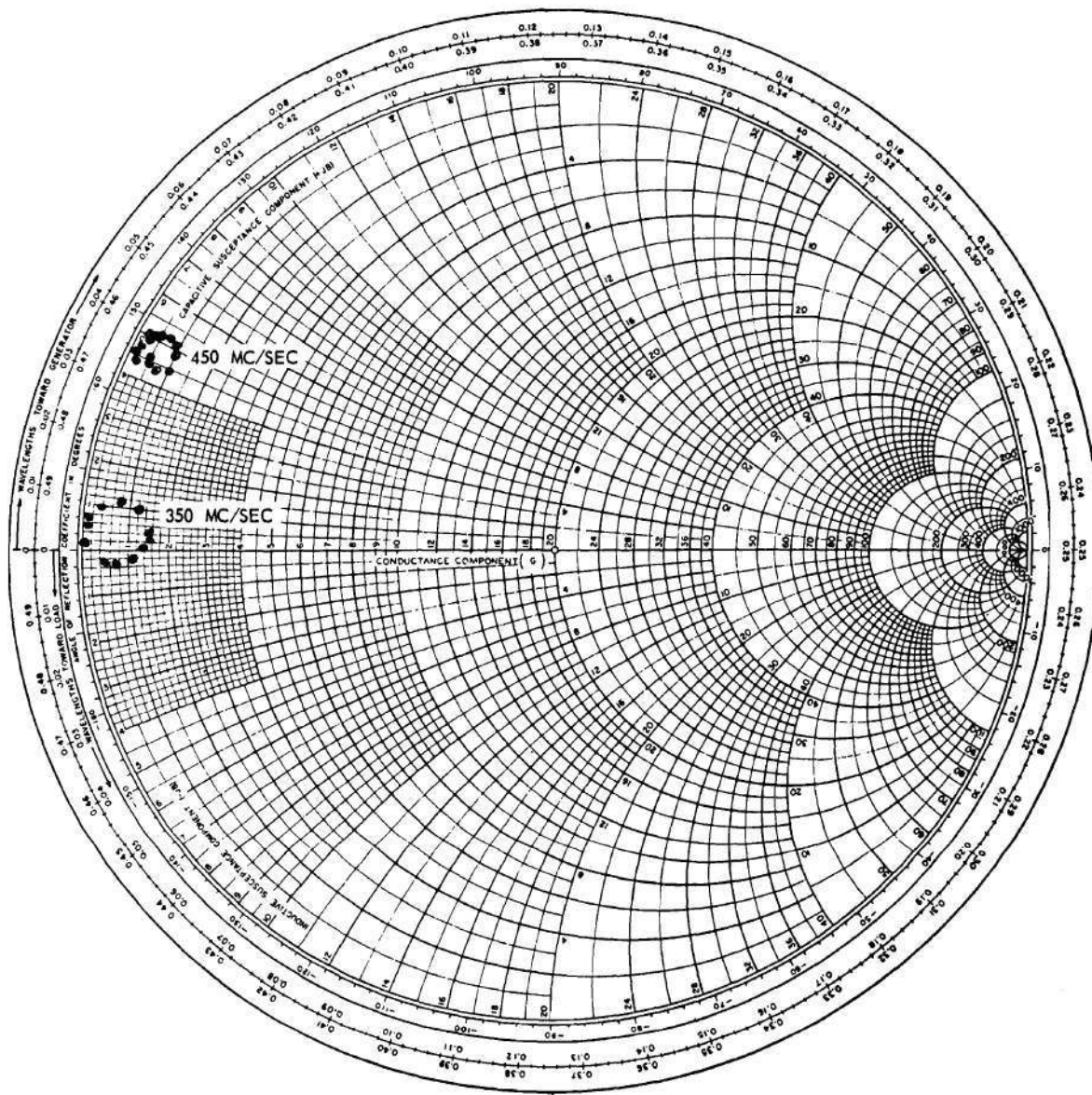


Figure 61. Responses of Crystal W504 at 350 and 450 Mc/Sec with the Recessed Electrodes.

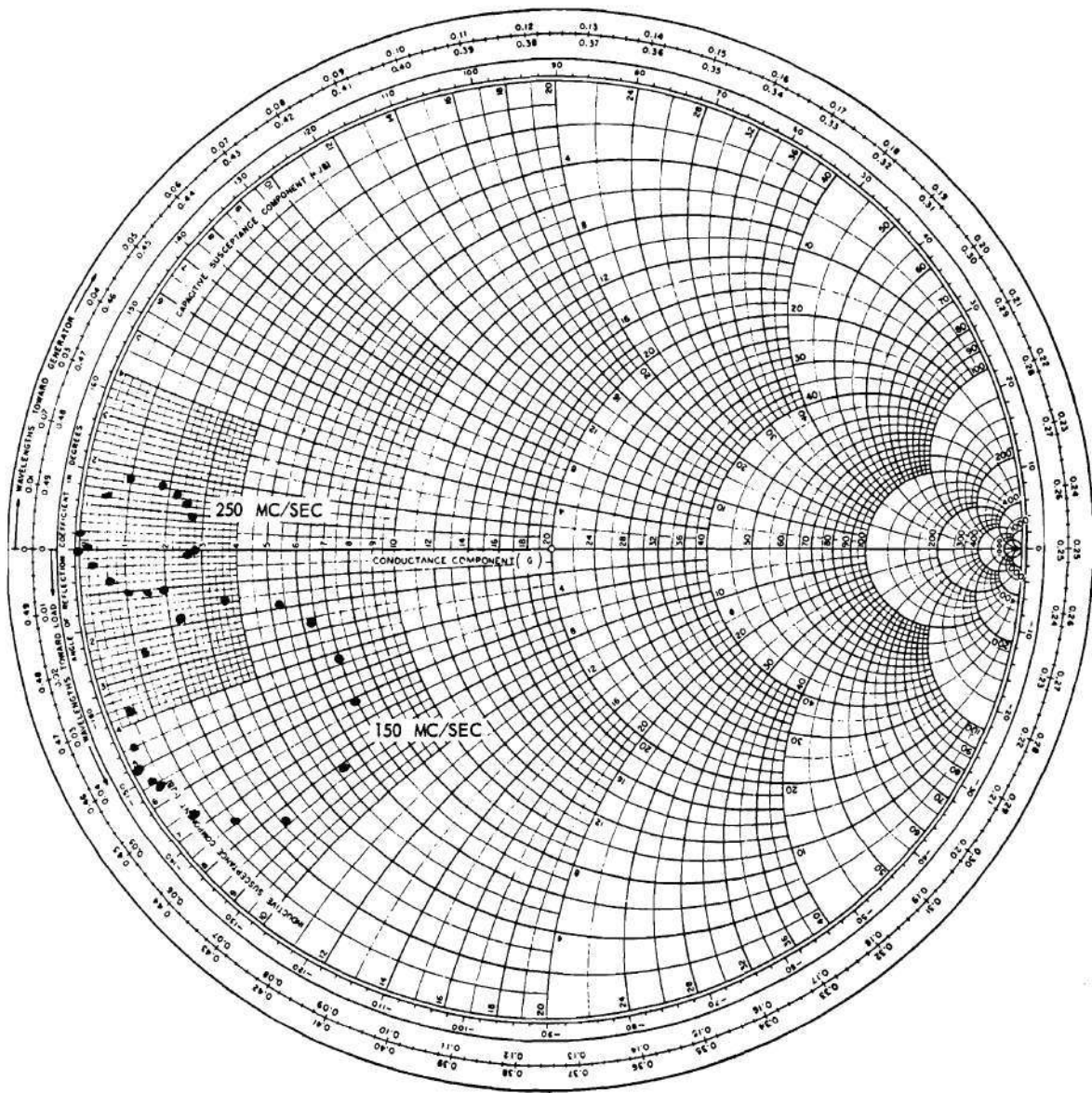


Figure 62. Responses of Crystal W507 at 150 and 250 Mc/Sec with the Recessed Electrodes.

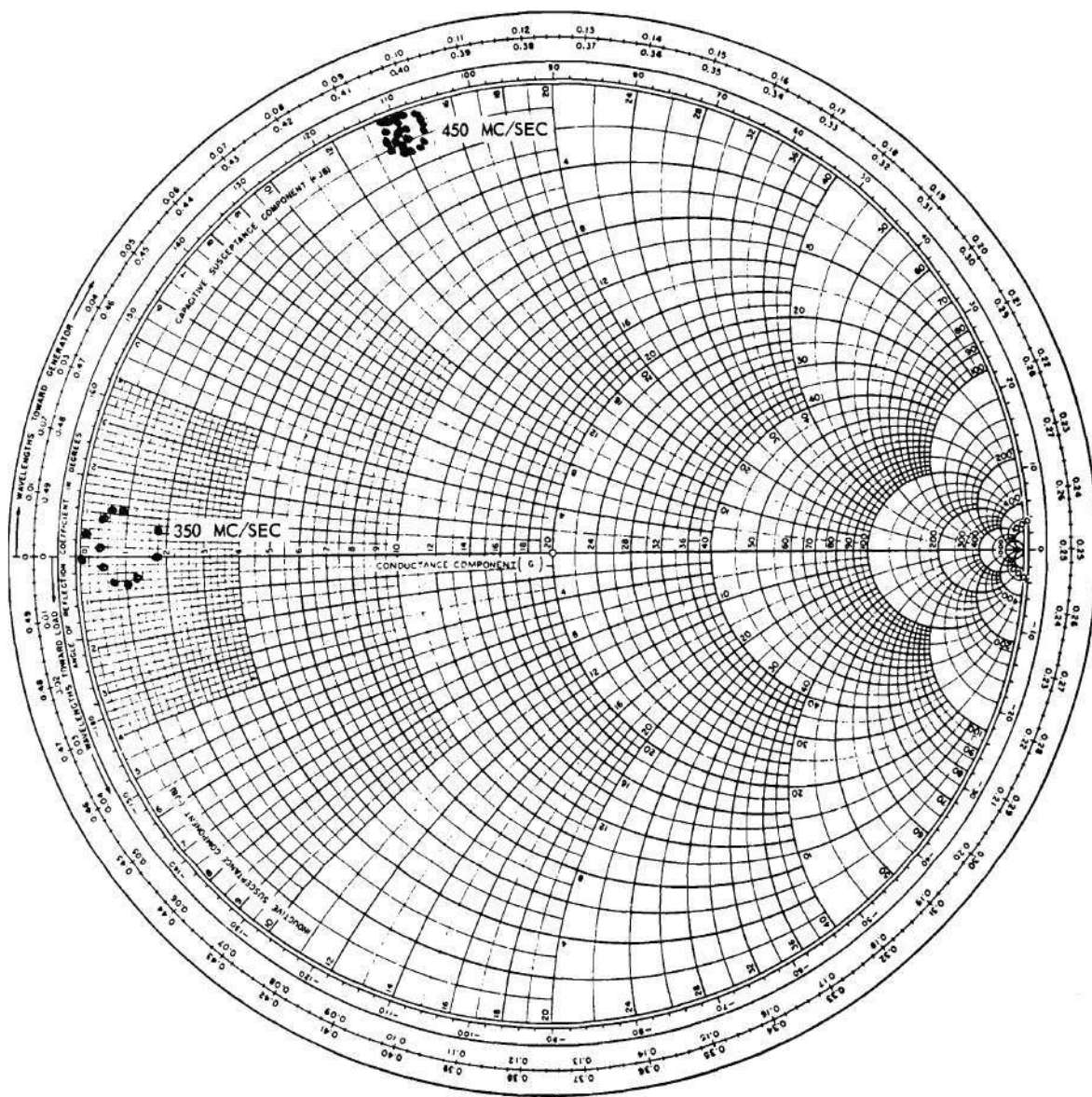


Figure 63. Responses of Crystal W507 at 350 and 450 Mc/Sec with the Recessed Electrodes.

The Q could not be calculated at the higher overtone frequency since facilities were not available at that time for accurately measuring such frequencies.

Since quartz plate W507 showed the best overtone responses which had been obtained and since its characteristics were considered sufficient to prove the usefulness of the coaxial holder through oscillator applications, the unit was left mounted and the coaxial crystal construction and testing phase of the work was terminated.

The Smith Chart data which have been presented imply that because of the circular shapes of the responses, the coaxially mounted crystals can be represented by simple series resonant circuits. That this is true was confirmed by frequency distribution analyses. Thus, the original purpose of this portion of the research had been accomplished. Because of the single valued conductance and susceptance characteristics in the vicinity of resonance, as contrasted with the multivalued characteristics often obtained with conventional crystals, and because of the absence of Q degradation by the holder, the coaxially mounted crystal is well suited to oscillator applications at high frequencies.

Several improvements in the holder are still possible. For example, the shunt capacitance, C_0 , can be further reduced by replacing the metallic electrodes with quartz electrodes which have been recessed by a small amount at the center and plated to form a proper electrode. The conducting area at the outer edge of the quartz blank is not necessary since its only purpose is to provide mechanical support for the blank.

Calculations indicate that a new shorted transmission line stub can be designed which will permit holder antiresonance to be obtained over the

frequency range from 150 to above 450 mc/sec. Integral construction of the electrode and stub assembly, rather than the use of standard General Radio coaxial components, would be required. The reduction in C_0 mentioned above would also be necessary to readily accomplish this objective. The reduction of crystal resistance, R_1 , by optimizing the air-gap electrode diameter should be possible. Previous tests have indicated that both of these factors are of importance in determining the characteristics of the complete crystal assembly.

The most important factor in eliminating spurious responses seems to be the symmetry of the mounting and electrode structure. A high degree of symmetry would be possible if machining facilities of greater precision were available.

The necessary facilities for the additional experiments indicated above were not available locally; however, such facilities are in existence at other research installations. Another reason for not presently pursuing these additional investigations was the present unavailability of additional high-quality quartz blanks. Most of the blanks which were used in the tests described above have been broken in repeated attempts at improving the results.

The test results which have been described together with the known state of the art of machining and the known state of the art of quartz crystal blank production clearly indicate that applications of quartz crystals at frequencies as high as 500 mc/sec are presently possible.

CHAPTER IV

CRYSTAL CONTROL OF OSCILLATORS AT VHF AND UHF

A secondary, but nevertheless important, purpose of this research was to investigate the behavior of crystals, both conventional and coaxial, in high-frequency oscillator circuits. The design of low-frequency (below about 25 mc/sec) crystal controlled oscillator circuits has been well described in the literature. The applications of quartz crystals at higher frequencies have received general attention only within the past decade. Edson (26) describes some of the earlier attempts at designing crystal-controlled oscillators in the frequency range from 50 to 150 mc/sec. The practical design of oscillators for this frequency range has been more recently described by Gruen and Flait (27). Applications at higher frequencies have been only briefly mentioned by these and other researchers (28).

One series of oscillator circuits covering the frequency range from 150 to 300 mc/sec was developed on a Signal Corps sponsored project at Georgia Tech (28). Two triode vacuum tubes and a two-gang variable inductor were used with conventional crystals to obtain crystal control in a circuit known as a Plate Degenerative Oscillator. The stability was only moderate and the power output was very small. Another circuit, developed on the same project, maintained feeble crystal control at frequencies as high as 420 mc/sec with highly selected crystals (only one crystal could be found to operate at the highest frequency). This circuit applied the capacitance-bridge principle.

At frequencies below about 50 mc/sec, a crystal can be represented by a simple series resonant circuit shunted by a small capacitor (or as a parallel circuit when properly terminated by a suitable capacitor); thus, the design of crystal-controlled oscillators is relatively simple. The design procedure is primarily a problem of properly loading the crystal to maintain a reasonably effective Q . At frequencies between 100 and 150 mc/sec, neither the crystals nor other circuit components can be represented by simple electrical equivalences and adequate mathematical descriptions of the circuits become very difficult. However, with suitable high-quality crystals, satisfactory crystal control can often be obtained. At frequencies above 150 mc/sec, presently known mathematical descriptions of the circuits fail to fully explain the observed behaviors. Although the physical circuits may contain relatively few components, such components can be adequately described only by complicated equivalent circuits. For example, the series reactance of a physical resistor may be greater than the resistance; likewise, an inductor may appear as a lossy capacitor in the equivalent circuit. Thus, although the design theories still apply in principle, the physical construction of workable oscillator circuits becomes difficult.

Since one of the purposes of the oscillator study was to compare the performances of the conventional and coaxial crystal units, a single circuit which could be controlled by either of the crystal units was desirable. Of the known types of oscillator circuits, the capacitance-bridge configuration was chosen for this study since: (1) it provided better stabilities with conventional crystals than did other types; (2) one terminal of the crystal unit was at ground potential, thus providing

ready adaptation to coaxial crystals; and (3) a prototype oscillator unit which had been constructed on a previous Georgia Tech research project, and which had been optimized for use with conventional crystals, was available. A photograph of this oscillator with a conventional crystal in position is shown in Figure 64. The schematic diagram of the oscillator is shown in Figure 65.

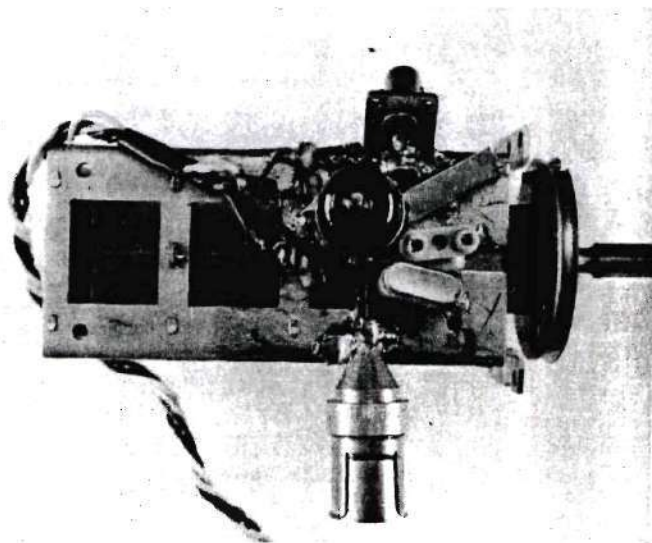


Figure 64. The Capacitance-Bridge Oscillator.

This oscillator is basically a Hartley oscillator with provisions for including the crystal in the cathode feed-back circuit. Since non-crystal-controlled oscillations would normally result from feedback through the shunt capacitance, C_o , of the crystal, a second feedback path with an opposite phase relation was provided through a variable capacitor, C_a . At frequencies other than crystal overtone responses, oscillations were prevented from occurring by adjusting the variable capacitor to equal the C_o of the crystal. Thus the feedback path actually consisted of a four-arm bridge, two arms being the two halves of the

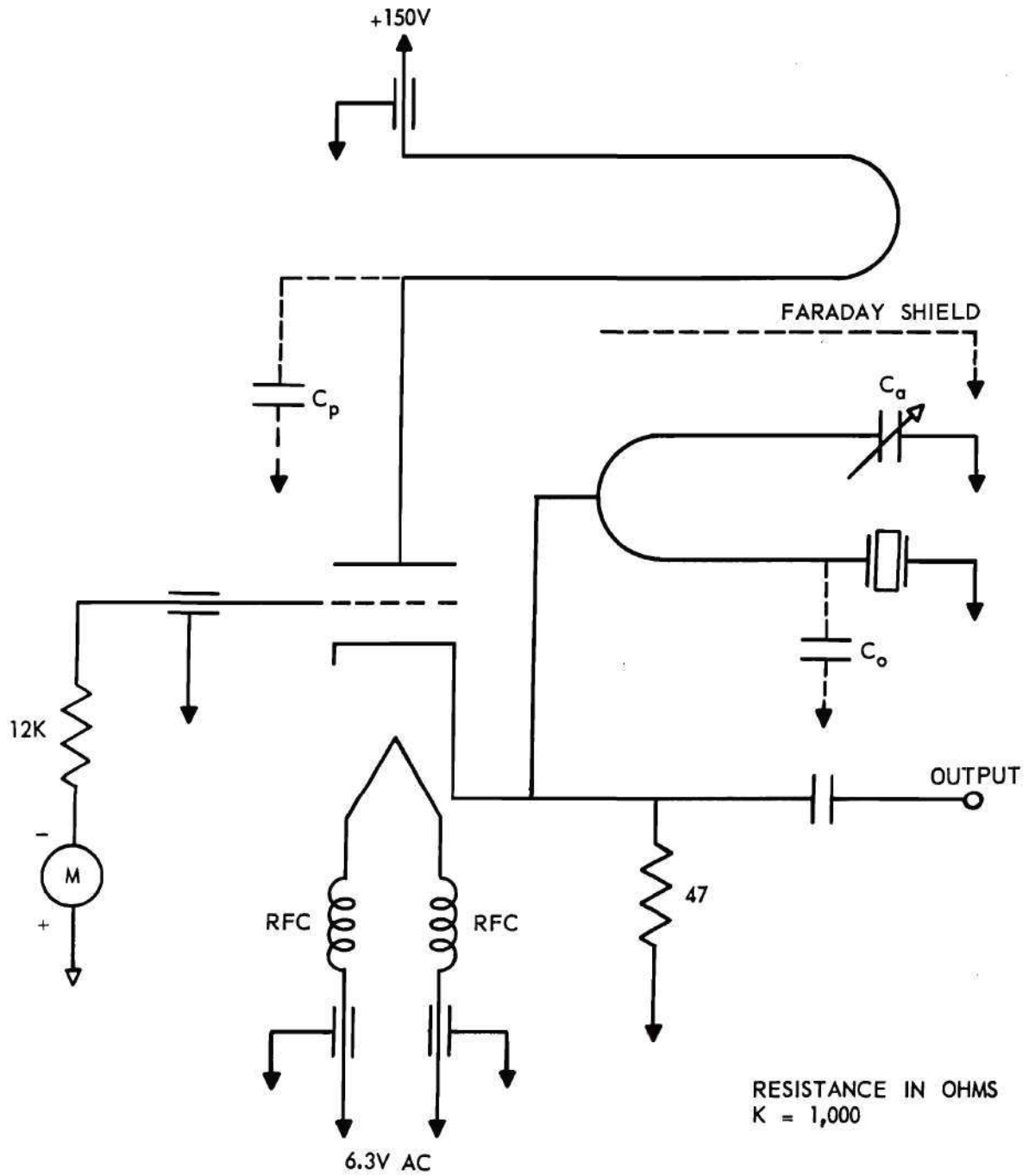


Figure 65. The Circuit Diagram of the Capacitance-Bridge Oscillator.

transformer winding and the other two arms being the crystal C_o and the variable capacitor. At a crystal overtone response, the balance of the bridge was upset by the crystal conductance, thus providing positive feedback through the cathode.

The primary of the transformer was placed in the plate circuit of the vacuum tube and was resonated by the tube and stray capacitances, C_p . The transformer consisted of two sections of a modified Mallory Inductuner, closely coupled but separated by a Faraday shield to prevent direct capacitance feedback to the cathode circuit. A grid current meter was provided to indicate the presence of oscillations and to facilitate tuning. A socket was provided for the conventional crystal paralleled by a coaxial connector for the coaxial crystal. The variable bridge capacitor, C_a , was also mounted by means of a crystal socket to provide for wide variations in the capacitance required for the two types of crystals.

This oscillator was tested with several conventional crystals at frequencies between 350 and 375 mc/sec. No attempts were made to control the temperature of the crystals or the filament voltage of the oscillator; however, a regulated plate voltage source was used. Figure 66 shows the typical frequency variations with the best of the conventional crystals over a period of four hours. The typical frequency extremes over a one-hour period were separated by approximately 5 parts in 10^6 . The long-term drift rate was approximately 3 parts in 10^6 per hour and was probably caused by temperature changes. During any period of one minute, the frequency could be expected to change by not more than about 3 parts in 10^6 .

Coaxial crystal number W507, as described in the previous chapter, was attached to the oscillator by means of a full-wavelength coaxial line

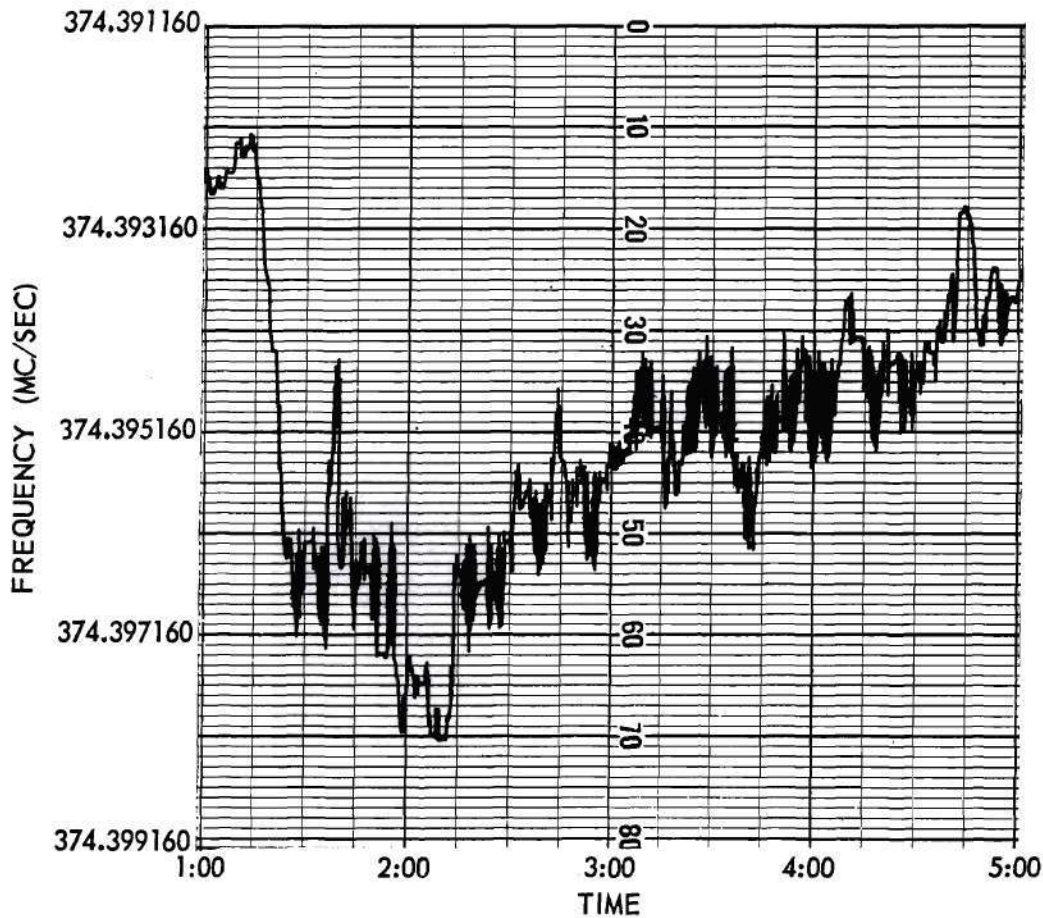


Figure 66. Typical Frequency Variations of the Capacitance-Bridge Oscillator with a High Quality Conventional Crystal.

(an adjustable line that could be shortened to one-half-wavelength was not available). The variable bridge capacitor was removed from the circuit since any undesired reactance could be canceled by the adjustment of the coupling line. The shorted coaxial stub of the crystal unit was adjusted to cancel the crystal shunt capacitance at a frequency of 350 mc/sec and the length of the coupling line was adjusted to obtain crystal controlled oscillations with the plate inductuner resonated at 350 mc/sec. Typical frequency variations over a period of 4 hours are shown in Figure 67. Approximately the same long-term frequency drift was observed since the

temperature of the coaxial crystal was not controlled. (The changes in the direction of drift shown in the figure were probably caused by reversals in the direction of temperature change.) During most periods of one minute, the frequency changed by less than 1 part in 10^6 . (Note the difference in frequency scales of Figures 66 and 67). Some larger changes were apparently caused by vacuum-tube filament temperature variations due to line voltage variations.

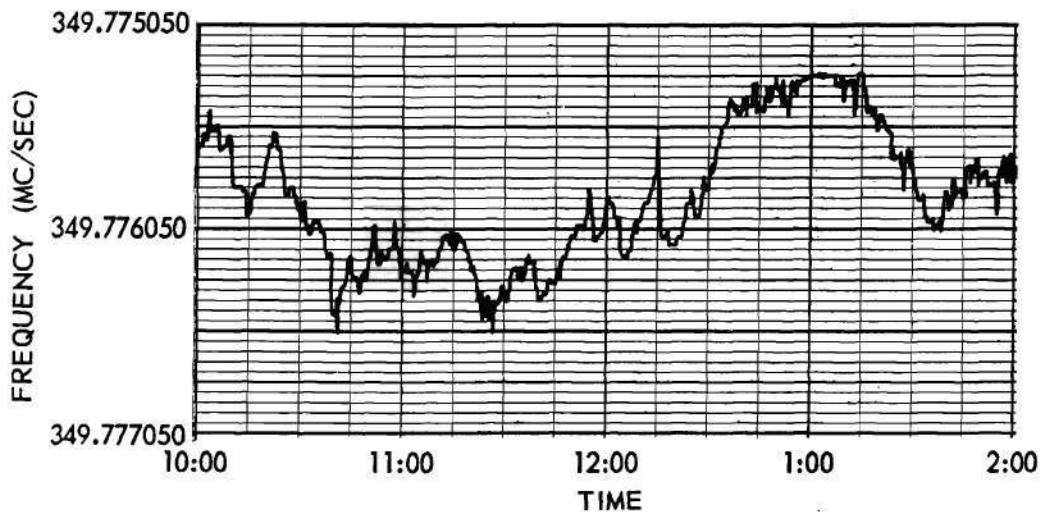


Figure 67. Typical Frequency Variations of the Capacitance-Bridge Oscillator with the Model 3 Coaxial Crystal.

While comparing the conventional crystal with the coaxial crystal, the following should be considered:

- (1) The oscillator circuit was designed and optimized for use with conventional crystals.
- (2) The conventional crystal was a unique unit in that it was the only one out of many which provided the stability needed.
- (3) The conventional crystal can was evacuated to increase its Q by a factor as great as 2, while the coaxial crystal was operated under normal atmospheric pressure.

- (4) Although this particular coaxial crystal was the best unit which had been produced, it was only slightly superior to several others described in the previous chapter.

This test, together with several other similar tests, indicated that, at high frequencies, the coaxial crystal is superior to the conventional crystal, even in circuits designed especially for the conventional crystals. The coaxial crystal should show even greater superiority in circuits specially designed for it.

A comparison between the coaxial crystal and the conventional crystals was also desirable at the lower frequencies. For this comparison, a Plate Degenerative Oscillator, constructed by Robertson (28) was chosen. A photograph of this oscillator is shown in Figure 68, and the circuit diagram is shown in Figure 69. The type N coaxial connector, visible in

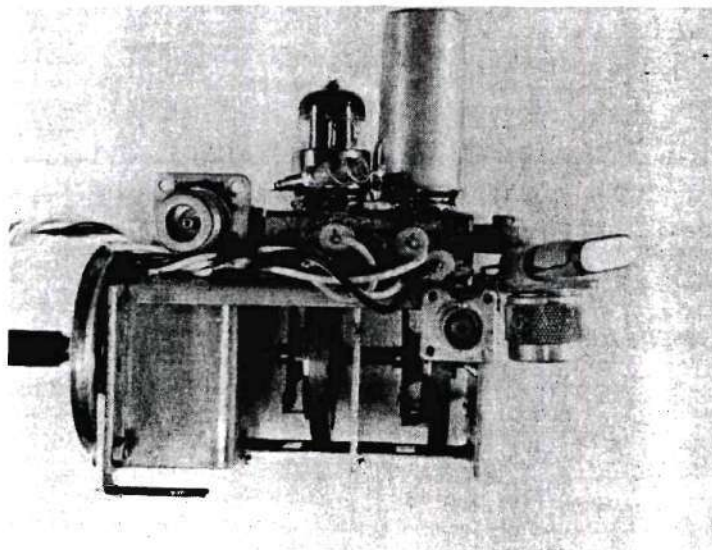


Figure 68. The Plate-Degenerative Oscillator.

the photograph, was provided for attaching the coaxial crystal. The best conventional crystal which provided crystal control at frequencies near 250 mc/sec was chosen. The frequency variations due to ambient conditions

ALL CAPACITANCE VALUES IN MICROMICROFARADS.
 ALL RESISTANCE VALUES IN OHMS.
 K = 1000

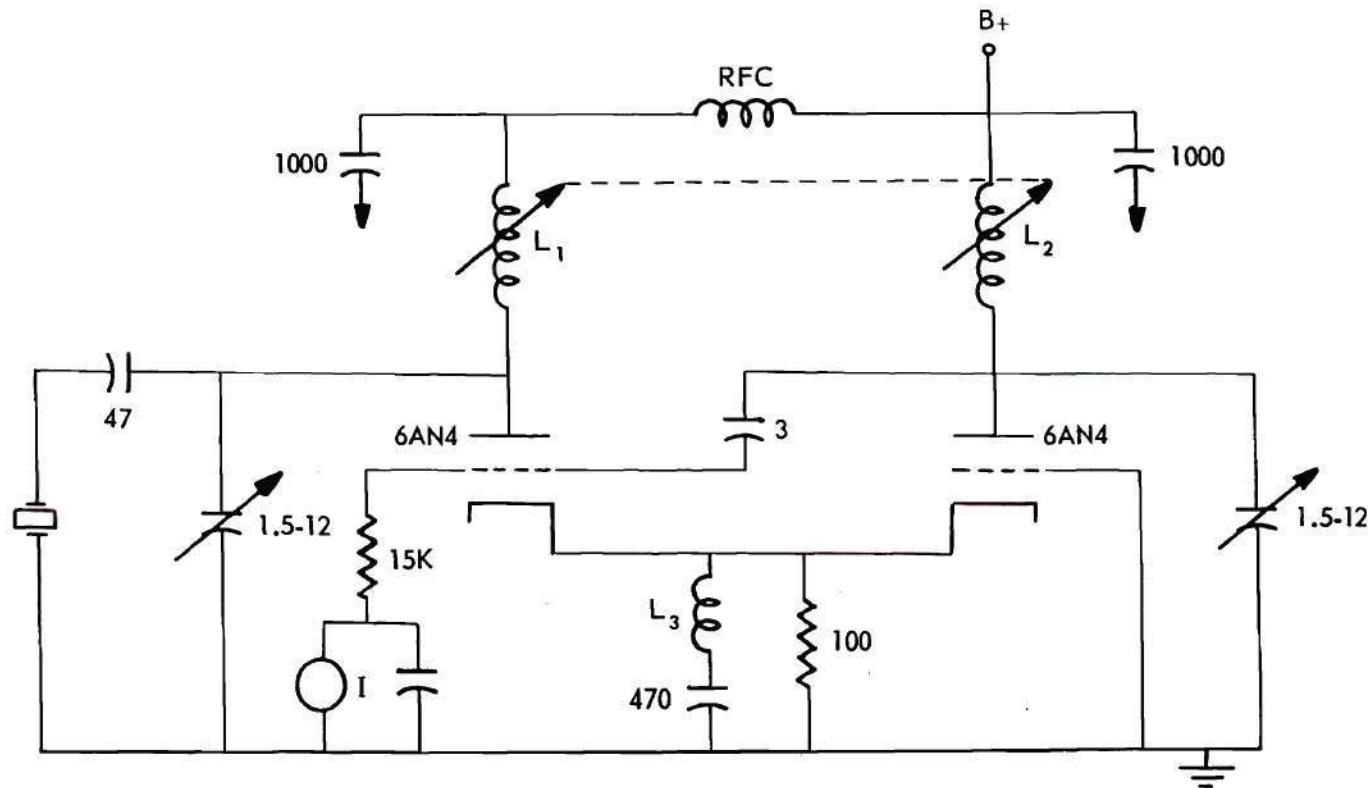


Figure 69. The Circuit Diagram of the Plate-Degenerative Oscillator.

were so small that they could not be conveniently recorded as for the previous tests at 350 mc/sec; therefore, the plate supply voltage was varied by 25 volts and the resulting frequency variation was observed. The typical frequency variations for this crystal was 5100 cps as the voltage was changed from 200 to 175 volts.

Coaxial crystal number W507 was substituted in the oscillator with the proper coaxial line and stub settings for operation at 250 mc/sec. As the voltage was changed from 200 to 175 volts, the frequency typically changed by 2500 cps. Thus, the coaxial crystal was only slightly superior to the best obtainable conventional crystal for this particular frequency and oscillator circuit. This condition was to be expected since the holder losses of the particular conventional crystal were not severe at this frequency.

The stabilities obtained in neither of these tests can be considered acceptable where a high order of frequency stability is required. The purpose of the tests was to compare the two types of crystals and not to determine the ultimate stability obtainable.

Several factors contribute to the poor stabilities of the oscillators described. For example, with the capacitance-bridge oscillator circuit of Figure 65, in theory, crystal control should not be obtainable if the crystal and capacitor C_a are interchanged, since negative rather than positive feedback should occur through the crystal resistance. However, in practice, crystal control can be obtained almost as readily with one connection as with the other, indicating that small changes in frequency are accompanied by large changes in oscillator loop phase shift. For large changes in phase shift to be possible, several circuit elements

must contribute to the phase shift (indicating that the circuit of Figure 65 is only an approximation to the electrical circuit of the actual physical unit). The presence of several elements which can contribute to the phase shift would in turn imply that the frequency stability may be expected to be poor since all circuit elements, at the higher frequencies, are generally susceptible to changes due to environmental conditions. With the Plate Degenerative Oscillator, an even larger number of circuit elements can contribute to changes in phase shift, which accounts for the relatively poorer stabilities which were observed in experiments not described here. One method of improving the stability of high-frequency oscillators would, therefore, be to eliminate as many as possible of the elements which contribute to oscillator phase shifts. In particular, such elements as r-f chokes and r-f by-pass capacitors should be carefully chosen and their positions in the circuits carefully located. One aid in accomplishing these objectives is the adoption of coaxial configurations for the tuned circuit elements. A disadvantage of the coaxial configurations is, however, the difficulty involved in the physical construction of the necessary elements, especially the elements required to provide crystal control.

The design and construction of stable crystal-controlled coaxial oscillators was beyond the scope of this research; however, to determine the relative advantages of the coaxial oscillator configurations, several free-running coaxial oscillators were constructed. With each oscillator, better stabilities were obtained than with the lumped element counterparts. Elementary attempts at crystal controlling these oscillators were only partially successful because of the lack of time and facilities for con-

structuring the necessary special coaxial components. Complete crystal control was never obtained with a coaxial configuration. Nevertheless, the investigations indicated that full crystal control should be possible by employing special coaxial lines and couplings of appropriate impedances.

One of the typical coaxial oscillator configurations which operated without crystal control is shown in Figure 70. Some degree of crystal stabilization could be obtained by replacing the grid by-pass capacitor with the coaxial crystal; however, the control was poor. Also, the number of tuned elements required by this configuration was excessive.

An oscillator which employs only a single tuned transmission line is shown in Figure 71. Attempts at crystal controlling this oscillator were unsuccessful. A reason for the poor characteristics of this oscillator appeared to be the physical length between the plate and cathode taps on the coaxial line. If the line were curved so that these points were near each other, better operation would be expected.

Figures 70 and 71 are only examples of some of the types of circuits which were investigated. Other circuits, however, showed similar characteristics.

From the brief investigations of oscillator circuits, the following conclusions were indicated:

- (1) The coaxial crystal provides better frequency stabilities than were obtainable with conventional crystals, even in conventional lumped element circuits.
- (2) Coaxial oscillator circuits provided better free-running stabilities than did conventional lumped element circuits.
- (3) If the coaxial crystal can be properly coupled to the coaxial oscillator circuits, greatly improved stabilities should be obtained.

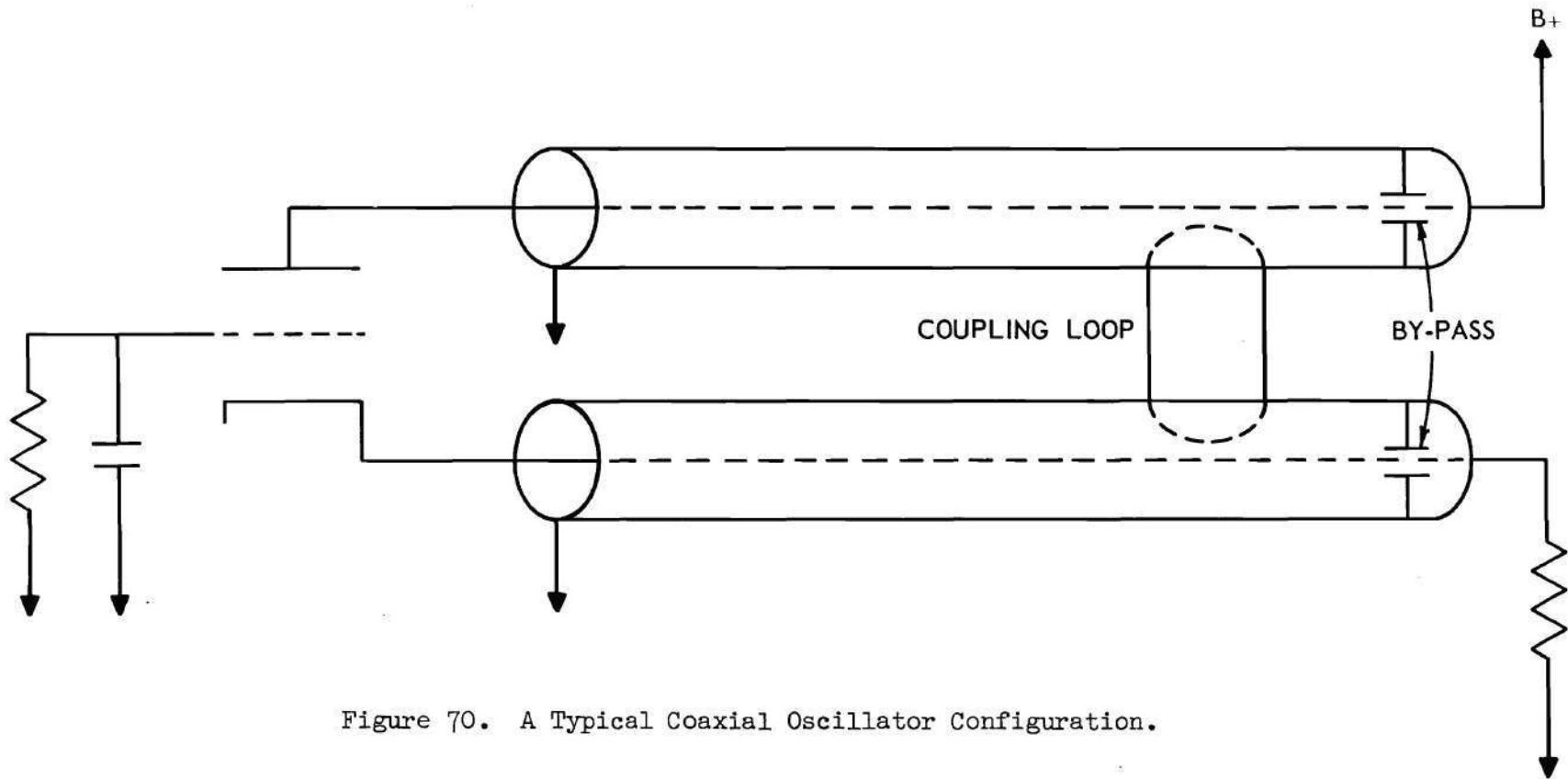


Figure 70. A Typical Coaxial Oscillator Configuration.

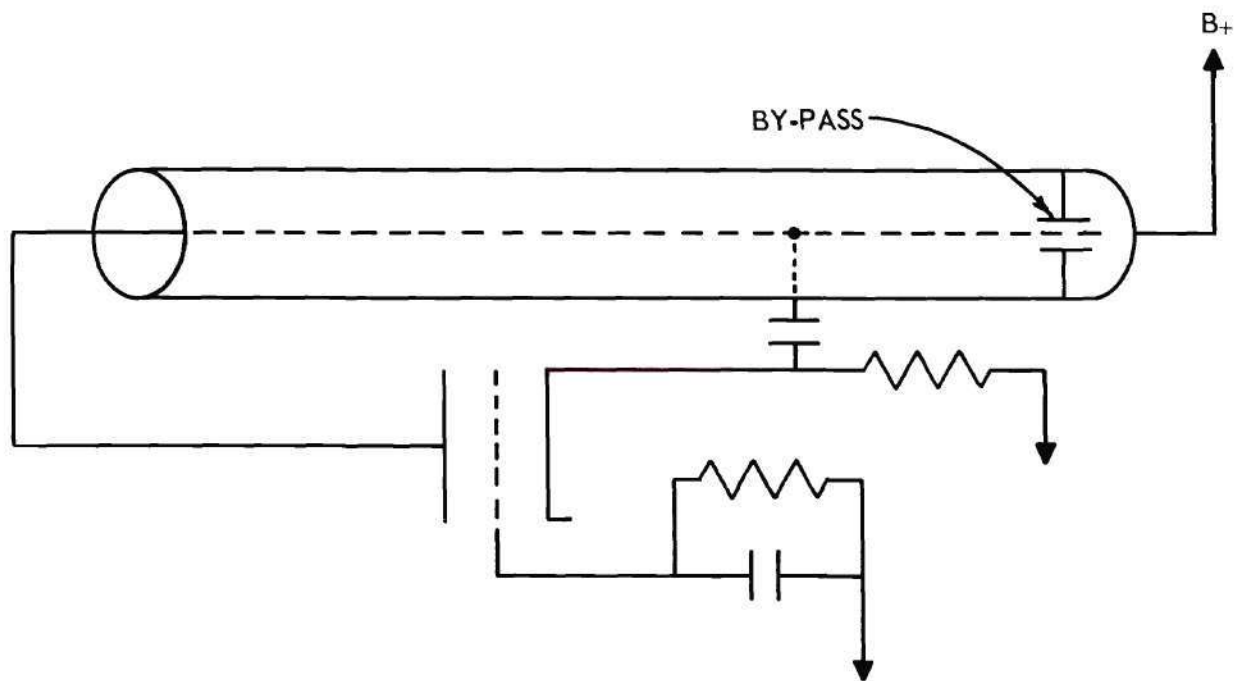


Figure 71. A Transmission-Line Oscillator.

CHAPTER V

CONCLUSIONS AND RECOMMENDATIONS

The initial investigations under this research were primarily concerned with the investigation of properties of conventionally mounted quartz crystals. A measurement system, capable of providing the necessary data, was first developed. Subsequently, large volumes of data were obtained on several high-quality HC-6 crystals which had measurable overtone responses at frequencies as high as 500 mc/sec. An equivalent circuit, to represent the electrical behavior of the crystals, was analyzed to determine its applicability to high-frequency, conventionally-mounted crystals. A statistical study of such crystals was then made on the basis of the collected data to enable the typical characteristics to be determined.

Both during and after the termination of the studies of the conventionally-mounted crystals, various coaxial crystal mounting techniques were investigated. Mechanical and electrical configurations and suitable mounting techniques were developed to enable useable high-frequency overtone crystal responses to be obtained. Typical coaxial holder characteristics were measured by mounting the few available crystal blanks. One coaxial unit, consisting of a coaxial holder and a crystal blank having a fundamental frequency of 50 mc/sec, was left assembled for elementary oscillator studies.

Some simple crystal-controlled oscillator circuits were investigated at frequencies as high as 375 mc/sec to provide direct comparisons

of the useable characteristics of the conventionally-mounted and the coaxially-mounted crystals.

The principal accomplishments of the research were:

1. The development of a measurement system for measuring the parameters of resonant systems having relatively high Q 's in the frequency range from 150 to above 400 mc/sec.
2. The development of measurement and analysis procedures to permit the determination of typical characteristics of conventionally-mounted quartz crystals including methods for assigning element values to a suitable electrical equivalent circuit.
3. The collection and analysis of a sufficiently large volume of data on conventionally-mounted crystals to permit the specification of typical characteristics at frequencies as high as 500 mc/sec. (These data should aid greatly in the design of oscillators using such crystals.)
4. The development of a coaxial crystal holder having desirable characteristics superior to those of the conventional holders.
5. The limited investigation of oscillator circuits which substantiated the claimed superiority of the coaxial holder and provides a basis for future oscillator work.

Because of the rapidly changing state of the art, some of the measured and calculated data may soon become obsolete. For example, as better techniques for grinding and polishing quartz blanks are developed, the typical characteristics of conventionally-mounted crystals may be improved.

When sufficient improvements become a reality, the typical characteristics, such as described in Chapter II, must be reevaluated. Also, as the quality of quartz blanks is improved, the quality of the characteristics as obtained with the coaxial holder will be proportionally improved.

Component advances such as transistors and tunnel diodes should play an important role in the improvement of crystal-controlled oscillator characteristics. Techniques for the application of such devices as well as for the application of vacuum tubes and conventional circuit elements can be greatly improved.

Thus, the following areas are believed to be worthy of further investigations:

1. The continued analyses of conventionally-mounted crystals as sufficient improvements are made.
2. The continued investigations of coaxial holder configurations as improvements in the quality of quartz blanks are made. In particular, the further investigation of such parameters as electrode air gaps and electrode sizes and shapes may lead to greatly improved characteristics.
3. The further investigation of oscillator circuits (Continued investigations (29) by the author and others subsequent to the experimental work under this research have shown that very substantial improvements in oscillator stabilities are possible).

APPENDIX II

MEASUREMENT SYSTEMS AND PROCEDURES

A. Introduction.--Several methods exist for measuring the parameters of quartz crystals at low frequencies. These include various bridge and substitution methods as well as a number of novel circuit measurement methods. Crystal Impedance Meters are available for use at frequencies from 75 kc/sec to 175 mc/sec. At frequencies above 20 mc/sec, the Crystal Impedance Meters are the only currently used instruments. These instruments are capable of measuring only a limited number of parameters of quartz crystals such as frequency and impedance at resonance. Such limited information is not sufficient for analyzing the complete characteristics of crystals even at frequencies below 200 mc/sec.

For frequencies above 200 mc/sec, no standard crystal measurement equipment exists. The development of a special measurement system was, therefore, necessary (21,22,30,31,32,33,34,35). Standard commercial equipment was used in the measurement system insofar as possible. Special calibration and modification of the equipment was required in some cases. The complete collection of equipment is collectively called the Crystal Measurements Standard since a part of its design purpose was to provide calibration facilities for the Crystal Impedance Meters currently under development.

A block diagram of the Crystal Measurements Standard is shown in Figure 72. The basic measurement instrument is the General Radio Admittance Meter Type 1602B. This instrument is used with a signal source,

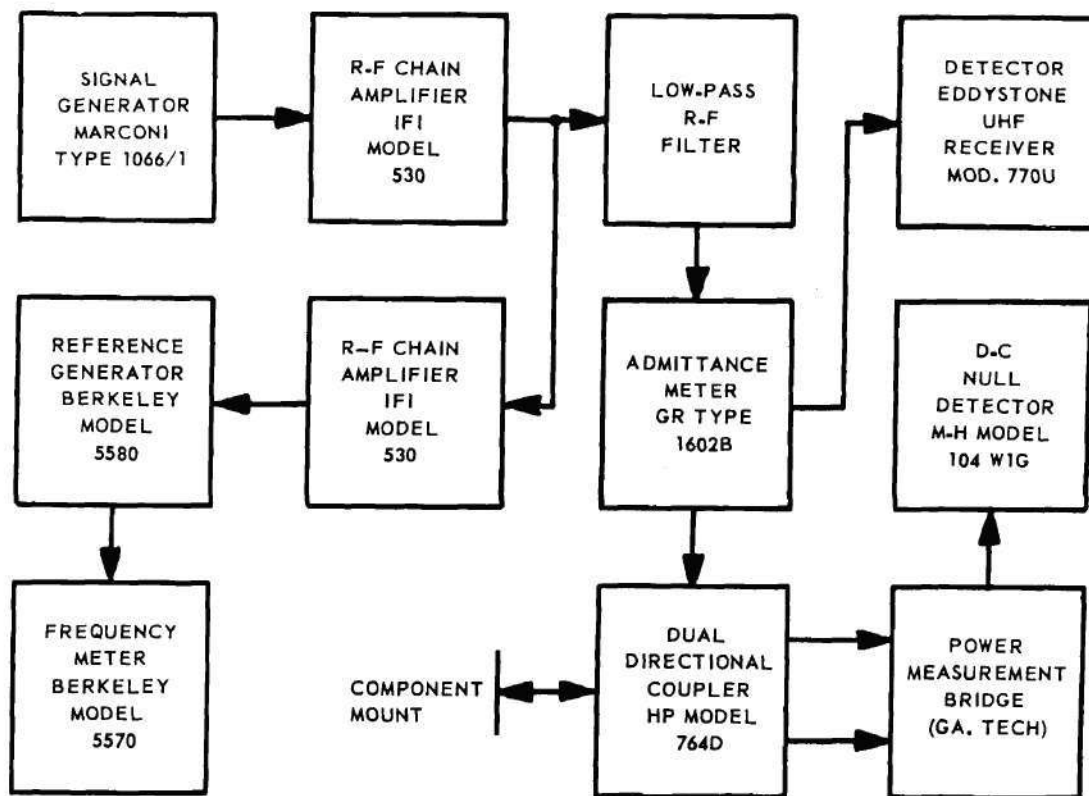


Figure 72. The Block-Diagram of the Crystal Measurements Standard System.

null detection system, frequency measuring system, and power measuring system to measure the admittance-versus-frequency characteristics of a test crystal.

The signal source is a Marconi AM-FM Signal Generator Type 1066/1 which was selected for its excellent short-term stability. Very good short-term stability is necessary because of the relatively high Q of the test crystals. Instruments for Industry, Inc., Wide-Band Amplifier Model 530 is used following the signal generator to provide sufficient signal amplitude and isolation at frequencies below 300 mc/sec. Suitable commercial amplifiers are not yet available for use at higher frequencies.

The low-pass filter is sometimes required because of harmonic frequencies generated in the wide-band amplifier.

The frequency-measuring system consists of an additional chain amplifier to provide adequate signal amplitude to drive a Berkeley Reference Generator Model 5580 which, in turn, drives a Berkeley Frequency Meter Model 5570. The Reference Generator converts the r-f energy to lower frequencies (between 2 and 35 mc/sec). The Frequency Meter is a digital instrument with a maximum frequency range of from zero to 42 mc/sec. Both instruments are supplied with a standard 1 mc/sec reference signal from a Western Electric D175730 secondary-standard oscillator. This oscillator is periodically calibrated against the standard broadcasts from radio station WWV. The over-all accuracy of frequency measurement is of the order of one part in 10^7 .

The r-f null detector is an Eddystone UHF Receiver Model 770U. The receiver was modified and shielded for this application.

The power measurement system consists of a Hewlett-Packard Dual Directional Coupler Model 764D, a Georgia Tech constructed power measurement bridge and a Minneapolis-Honeywell Electronik Null Indicator Model 104 WIG.

The various components of the Standard are described in greater detail on the following pages.

B. The General Radio Admittance Meter.--In the early stages of development of the Crystal Measurement Standard, a General Radio Admittance Meter Type 1602B and a Hewlett-Packard Model 803A VHF Bridge were available. Numerous crystal measurement runs were made using each instrument. A variety of calibration tests were also performed. Neither instrument was found to have sufficient accuracy for the intended purpose. No

instruments having greater accuracy were commercially available. Thus, an investigation was instigated to determine which of the two instruments could be readily calibrated to greater accuracy. Because of the lack of local calibration facilities and because of the willingness of the General Radio Company to perform additional calibrations on their type 1602B instrument, a new specially-calibrated Admittance Meter was purchased. Purchased with the instrument were specially calibrated resistive terminations and a special component mount.

The resistive terminations used in the early calibration tests were the General Radio Type 874-W50, 874-W100, and 874-W200 terminations which were claimed to have an impedance magnitude accuracy of one per cent with a very small phase angle at frequencies below 300 mc/sec. No provisions were available locally for checking the calibration of these terminations. However, one sample of the GR-874-W100 termination was submitted to the National Bureau of Standards by the United States Army Signal Research and Development Laboratories at Fort Monmouth, New Jersey, for calibration purposes. The resulting data are given in Table 10.

In the calibration of the W100 termination, a General Radio Type 874-WN3 Short-Circuit Termination was used to establish the reference plane. A difference in length of approximately 0.8 cm between the W100 termination and the short-circuit termination was not taken into account by the National Bureau of Standards. These data were subsequently corrected by means of a digital computer at Georgia Tech. Both the original data and the corrected data are included in Table 10. If the assumption is made that this sample of the W100 type termination is typical, then the validity of previous work based upon this type of termination is verified.

Table 10. Electronic Computer Corrections of National Bureau of Standards Data on General Radio Termination Type 874-W100, Serial No. 111.

Frequency (mc/sec)	NBS DATA		CORRECTED DATA	
	Impedance Magnitude (ohms)	Impedance Angle (degrees)	Impedance Magnitude (ohms)	Impedance Angle (degrees)
50	99.9	-0.8	99.91	-0.096
60	99.8	-0.9	99.82	-0.057
70	99.8	-1.1	99.83	-0.116
80	99.8	-1.2	99.83	-0.076
90	99.7	-1.4	99.74	-0.137
100	99.7	-1.5	99.75	-0.097
110	99.7	-1.7	99.77	-0.156
120	99.6	-1.8	99.68	-0.118
130	99.6	-2.0	99.70	-0.178
140	99.6	-2.1	99.71	-0.138
150	99.5	-2.3	99.63	-0.201
160	99.5	-2.4	99.64	-0.160
170	99.4	-2.6	99.57	-0.224
180	99.4	-2.7	99.58	-0.184
190	99.3	-2.9	99.51	-0.248
200	99.3	-3.0	99.52	-0.208
210	99.3	-3.2	99.55	-0.268
220	99.2	-3.3	99.47	-0.233
230	99.2	-3.5	99.50	-0.293
240	99.1	-3.6	99.42	-0.258
250	99.0	-3.8	99.36	-0.324
260	99.0	-3.9	99.38	-0.284
270	98.9	-4.1	99.32	-0.350
280	98.9	-4.2	99.34	-0.311
290	98.8	-4.4	99.28	-0.377
300	98.8	-4.5	99.31	-0.337

Note: The nominal impedance of this termination is 100 ohms. The data are corrected for an effective difference in length of 0.783 cm between the termination and the reference short.

The new General Radio Admittance Meter was calibrated before shipment to within a claimed accuracy of approximately one per cent of this nominal admittance over the frequency range from 175 to 300 mc/sec. This accuracy applied to an admittance level of 20 millimhos and was expected to be somewhat poorer at greatly different admittances.

The calibration charts which were supplied with the Admittance Meter by the General Radio Company are shown in Figures 73 and 74 to illustrate the types of corrections and the order of accuracy to be expected both with and without the application of corrections. These charts are valid only for the particular Admittance Meter with the serial number indicated. This instrument is a standard production-run instrument and was not modified in any way to obtain this accuracy.

Also ordered and received with the Admittance Meter were three resistive terminations and one component mount. The component mount together with its open and short terminations were specially adjusted in length by the General Radio Company to equal the length of the standard resistive terminations (approximately 3.5 cm). Calibration data on the resistive terminations are shown in Figure 75.

Extensive efforts were made to determine the accuracy of the new General Radio Admittance Meter. With the available equipment, no precise data concerning the expected over-all accuracy of the Crystal Measurements Standard using this instrument could be obtained; however, some of the more important calibration data are presented here.

The system was expected to be accurate to within about one per cent for magnitude and one degree for phase angle, when measuring admittance near 20 millimhos. This accuracy of agreement was almost obtained as shown in Figure 76 for three different terminations mounted directly on the Admittance Meter. The accuracy with the 50-ohm termination is well within one per cent for magnitude and one degree for phase angle. The accuracy with the 100-ohm termination is slightly poorer than was obtained with the 50-ohm termination. For the 200-ohm termination, the

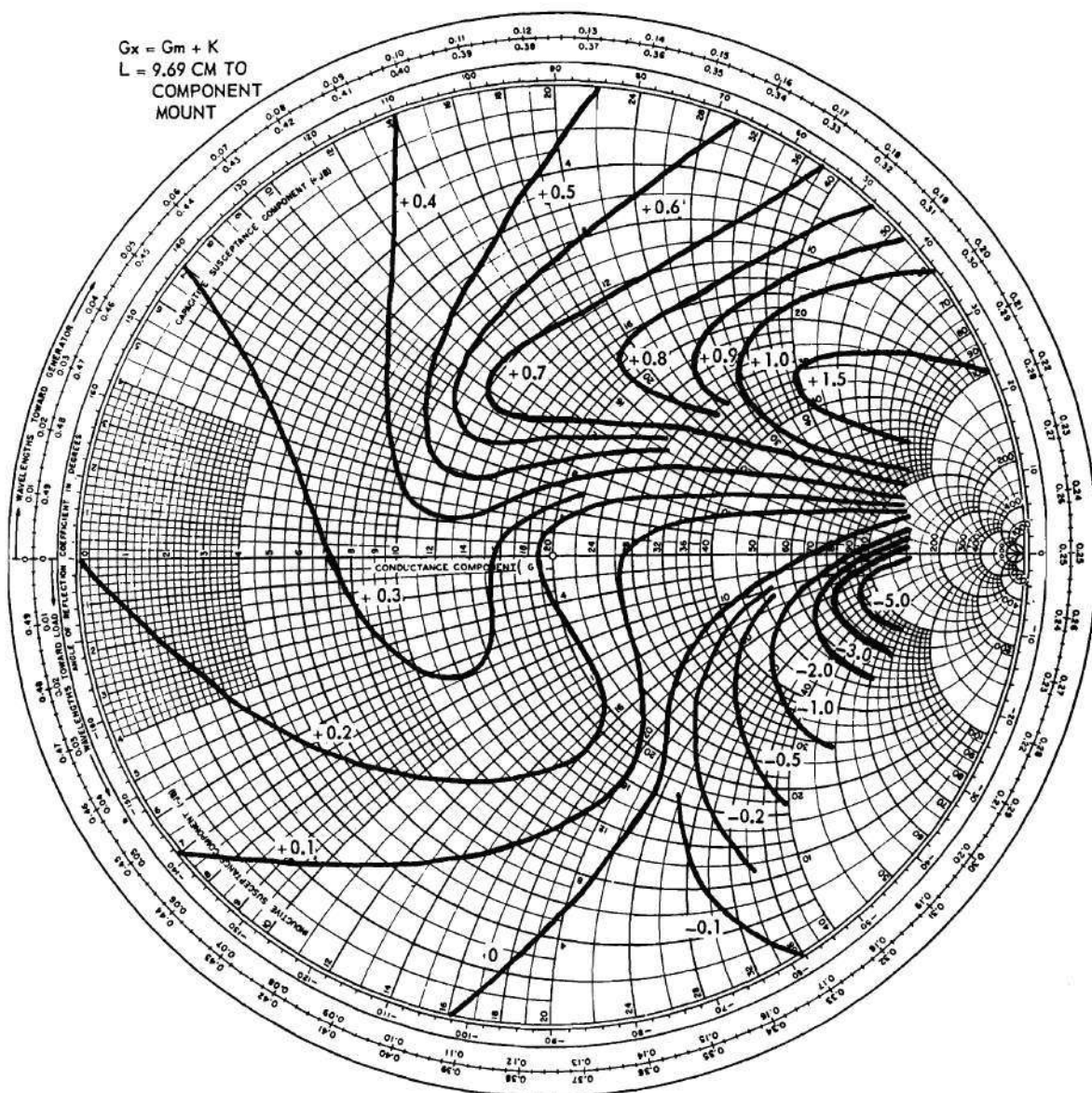


Figure 73. Conductance Corrections for General Radio Admittance Meter, Serial Number 1401.

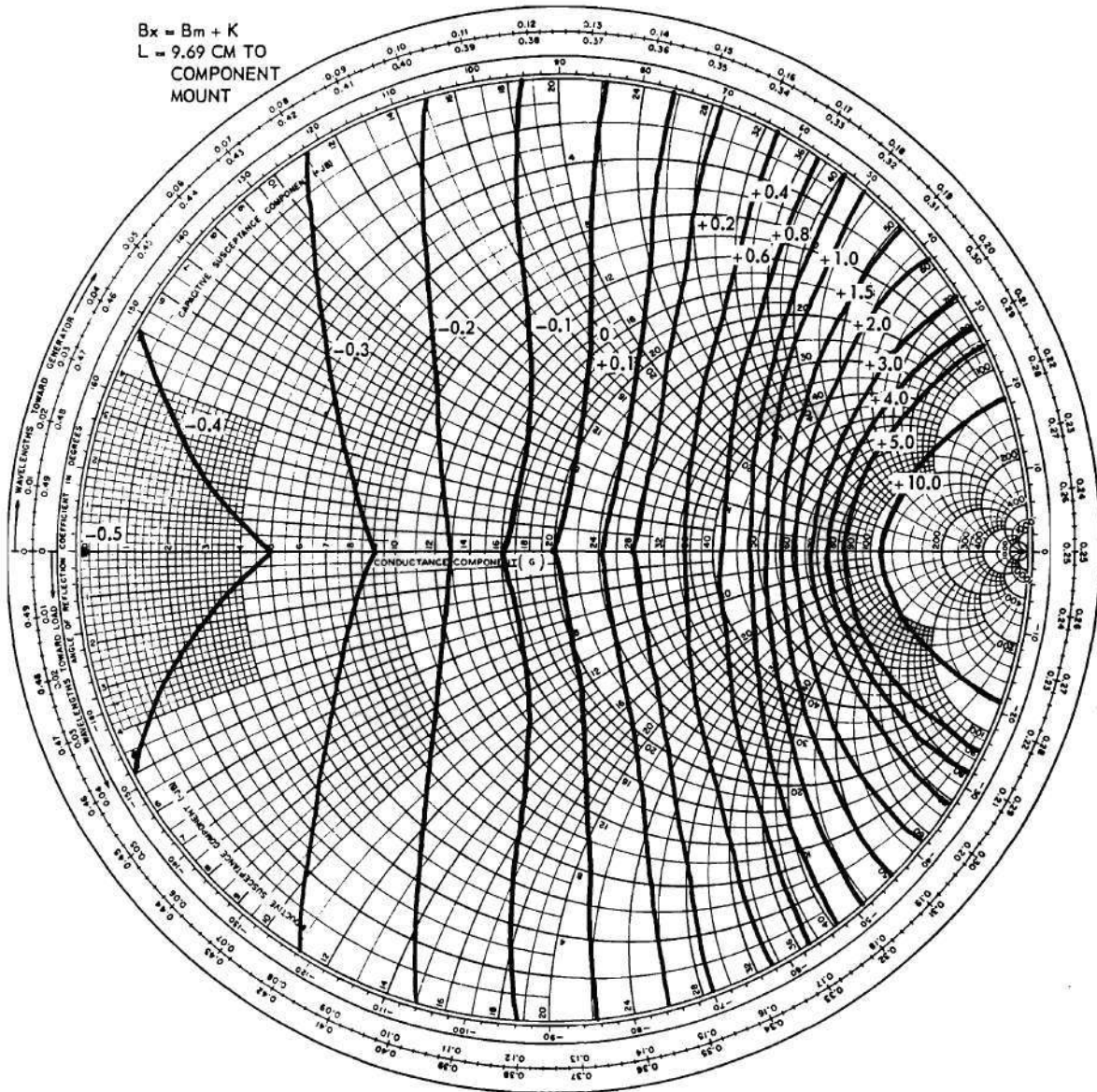


Figure 74. Susceptance Corrections for General Radio Admittance Meter, Serial Number 1401.

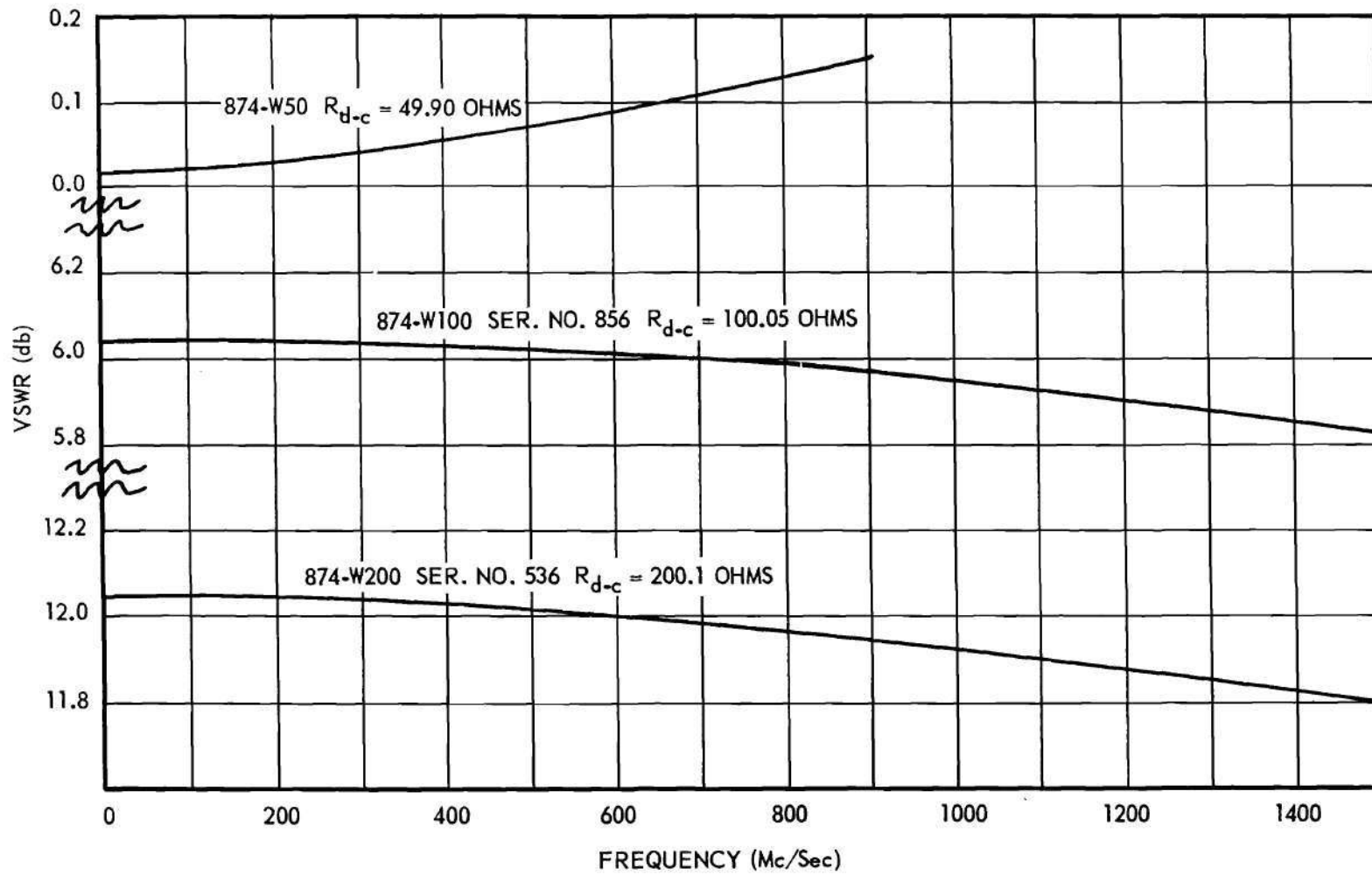
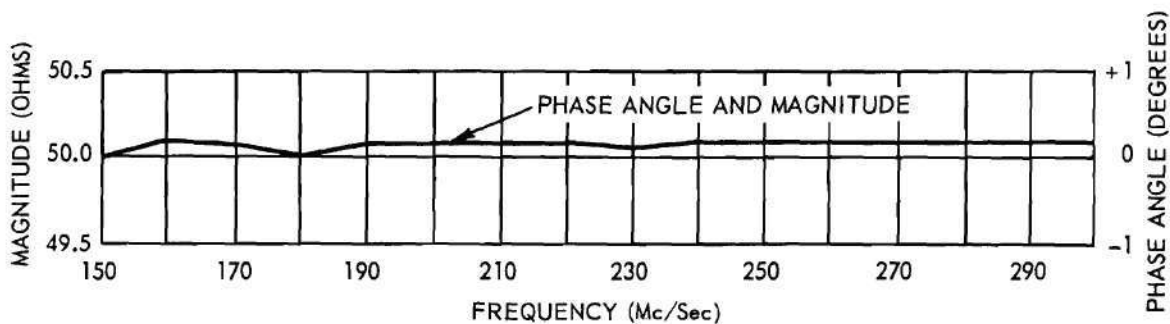
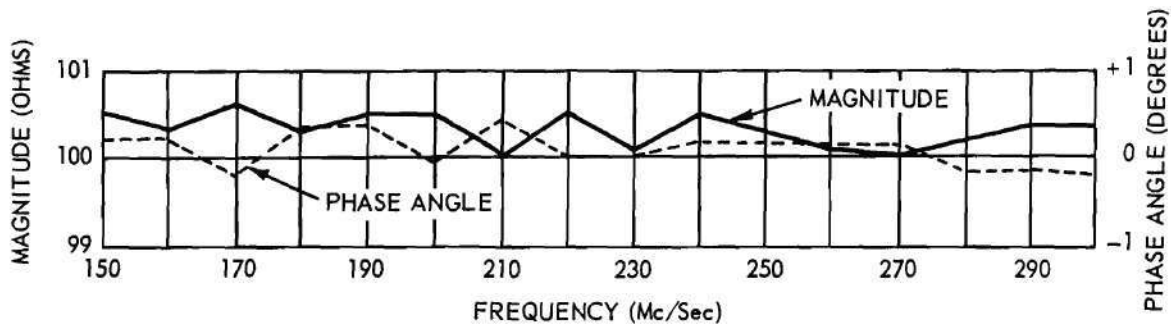


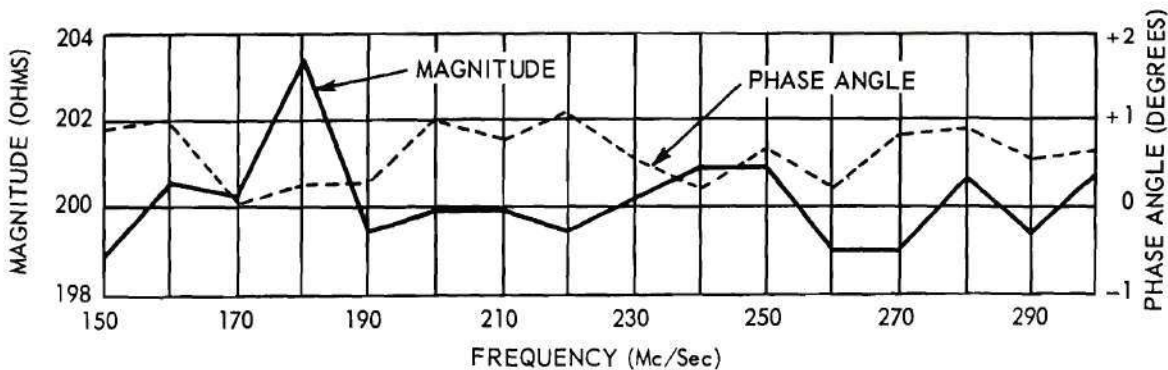
Figure 75. Calibration of General Radio Resistive Terminations with Serial Numbers as Shown.



(a) 50-OHM TERMINATION



(b) 100-OHM TERMINATION



(c) 200-OHM TERMINATION

Figure 76. Admittance Meter Measurements on Resistive Terminations with Minimum Line Length.

error exceeds one per cent for magnitude but is almost within one degree for phase angle. This data run was repeated on two other occasions with approximately the same results.

A study of the Admittance Meter dials partially explains the errors shown in Figure 76. For example, the resolution at 5 millimhos on the dials (200 ohms) is only one per cent if the readings can be made to one-tenth of the smallest division. This precision in reading is generally not possible without optical aids.

The data shown in Figure 76 were obtained with the terminations mounted directly on the Admittance Meter. The calculated electrical separation between the termination and the internal bridge terminals was 9.69 cm. The Admittance Meter readings were first corrected by using Figures 73 and 74. The 9.69 cm of 50-ohm transmission line were then subtracted by a digital computer using a specially prepared program. No line losses were considered since the correction charts included such effects.

The particular terminations, line lengths, and frequencies used in the above run are capable of checking the calibration of the Admittance Meter only over a very limited range of the Smith chart, as shown by the heavy lines in Figure 77. As a result, the data presented cannot lead to any general conclusions concerning the overall accuracy of the instrument.

Since the procedure for measuring the drive level of a crystal involves the insertion of a Hewlett-Packard Dual Directional Coupler Model 764D between the component mount and the Admittance Meter, additional data runs were made with the coupler in position but using the standard

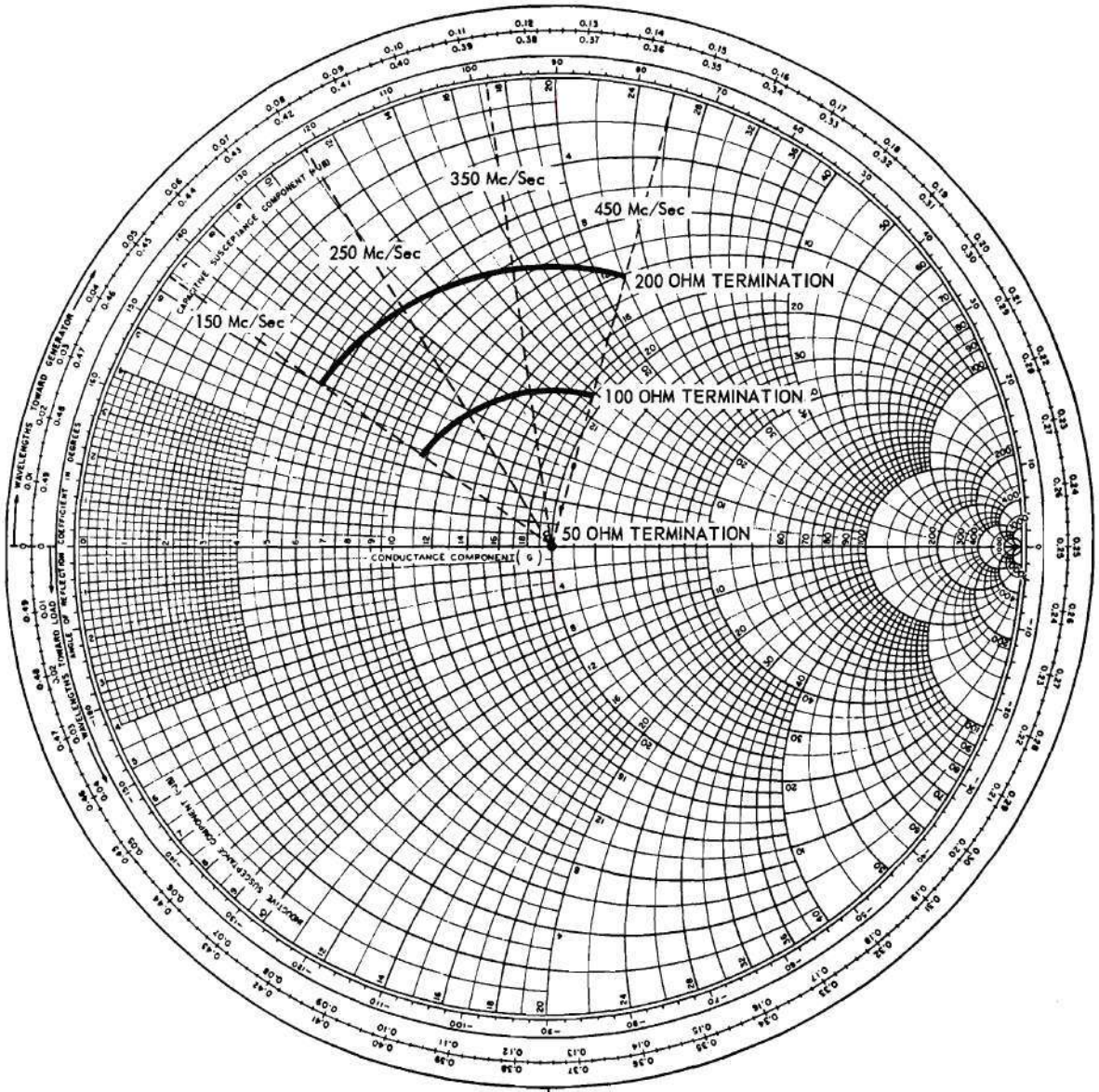


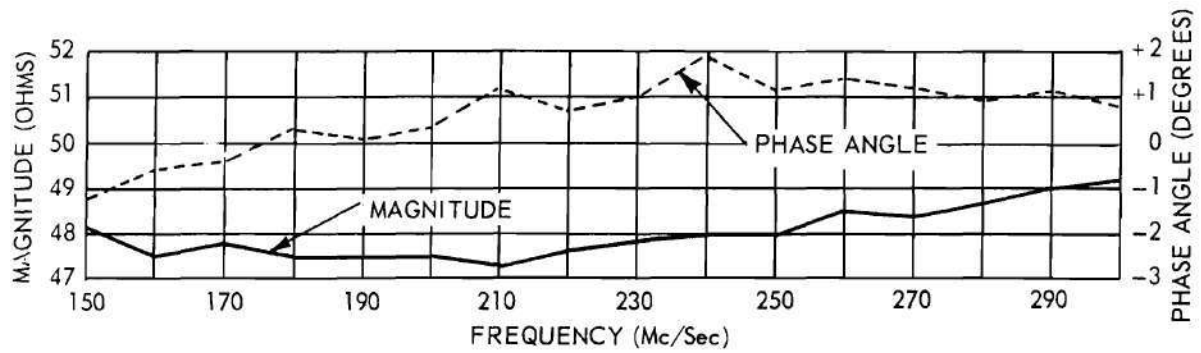
Figure 77. Loci of Points which can be Calibrated with a 9.69 Cm Line Length.

terminations to replace the component mount. The results are shown in Figure 78. The data for these curves were again obtained by applying the instrument corrections and then subtracting the electrical length of the complete transmission line. This electrical length was determined by a series of open- and short-circuit measurements over the frequency range. As the calculated lengths showed wide variations under various conditions, an average value was determined. The accuracy of the choice can be evaluated from the phase angle curves of Figure 78.

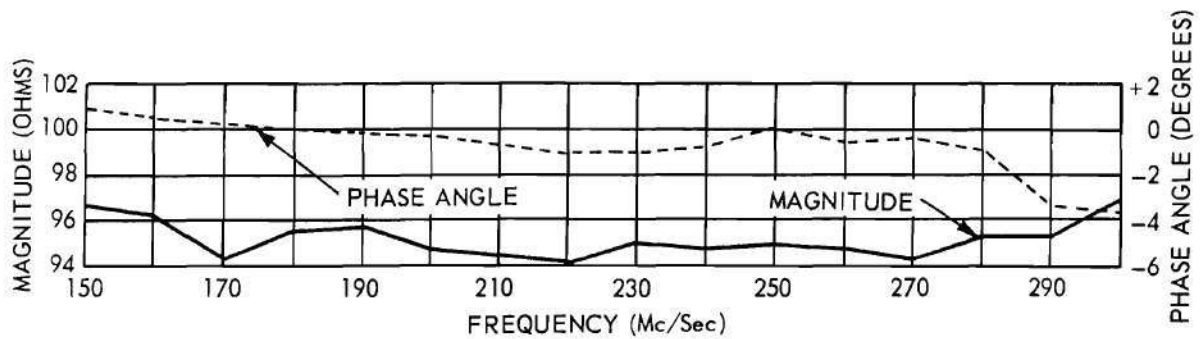
The large errors indicated by Figure 78 were first assumed to be due to excessive losses in the directional coupler. The coupler was, therefore, replaced by an approximately equal (40-cm) length of air-dielectric transmission line. A repeat of the data run yielded the results shown in Figure 79. The errors were generally less than with the directional coupler.

A series of evaluation tests were initiated to determine the sources of error when the directional coupler or additional transmission line was in use. First considered was the effect of the multiplier dial of the Admittance Meter. The main conductance and susceptance dials of the Admittance Meter are calibrated from zero to 20 millimhos. For larger admittances, a multiplier dial is used. This dial multiplies the readings of both main dials simultaneously. Thus poorer over-all accuracy is obtained when either the conductance or the susceptance is large and the other is small.

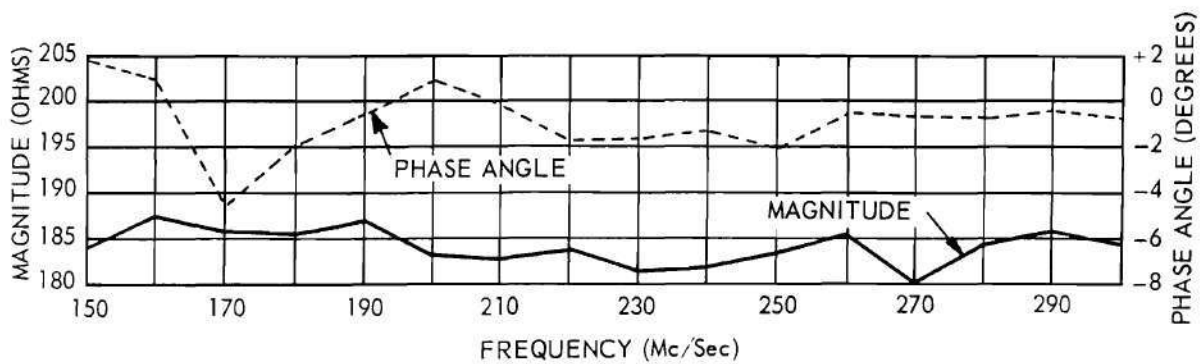
With the choice of terminations and frequencies used with the 9.69 cm line length as shown in Figure 77, the multiplying dial would remain at unity. However, when the longer line lengths were used,



(a) 50-OHM TERMINATION



(b) 100-OHM TERMINATION



(c) 200-OHM TERMINATION

Figure 78. Admittance Meter Measurements on Resistive Terminations with a Dual Directional Coupler Inserted in the Coaxial Line.

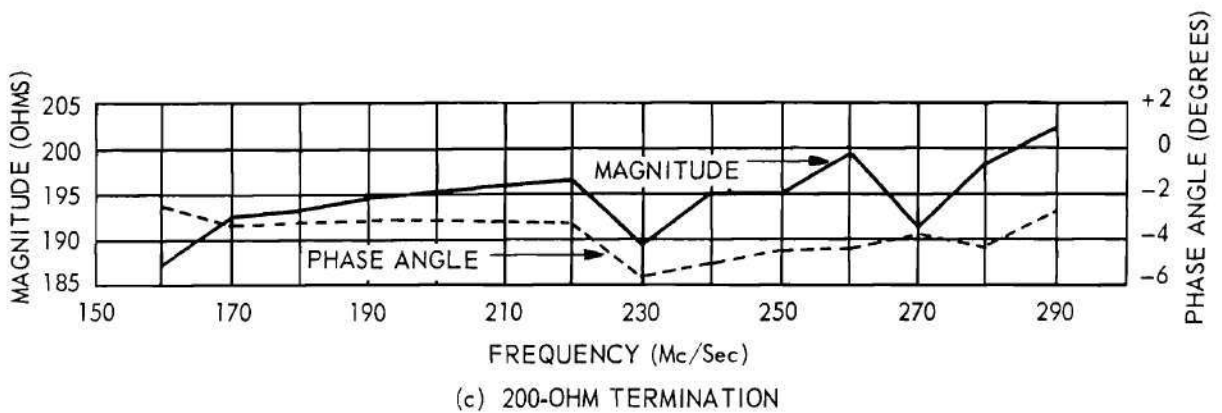
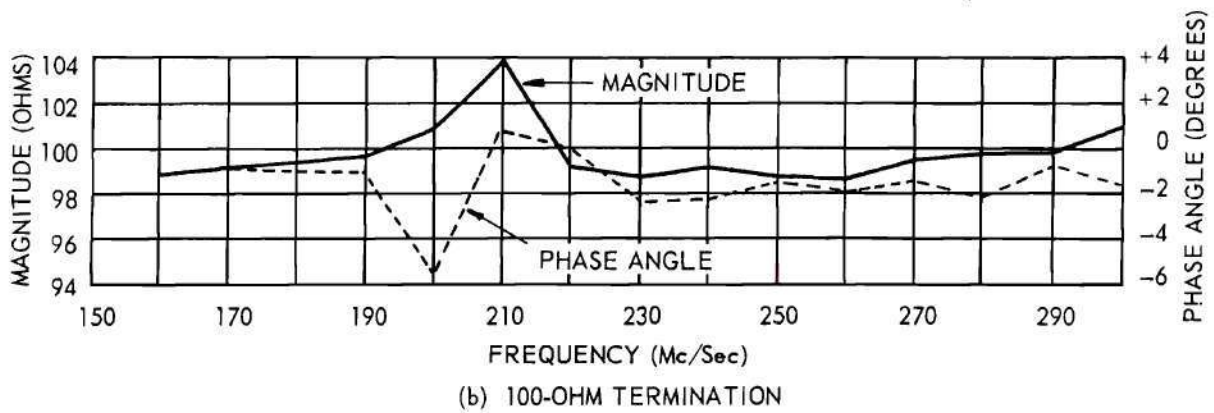
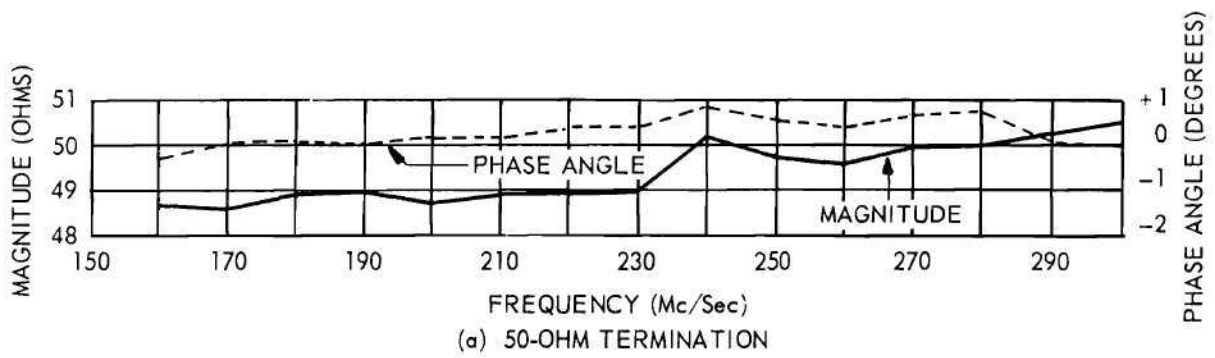


Figure 79. Admittance Meter Measurements on Resistive Terminations with a 40-Cm Line Length.

multiplying factors as high as 5 were required. To determine the magnitude of errors introduced by the multiplier dial, a series of measurements were made by setting the multiplier to discrete values between one and two and recording the conductance and susceptance readings. Errors greater than one per cent were thus attributed to the multiplier dial. A recheck of the data of Figures 78 and 79, however, showed no general correlation between the multiplying factor and the observed errors. Although this source of error is important, it is not considered to be the major factor in this particular case.

Probably the most logical sources of error are transmission-line deficiencies of various types. The following method was considered for correcting some of these deficiencies.

At any single frequency, a transmission line of arbitrary length may be represented as a two-terminal pair network as shown in Figure 80. Since the line is symmetrical, both shunt admittances may be labeled Y_a . Y_b is the series admittance of the equivalent pi-circuit. Y_L represents

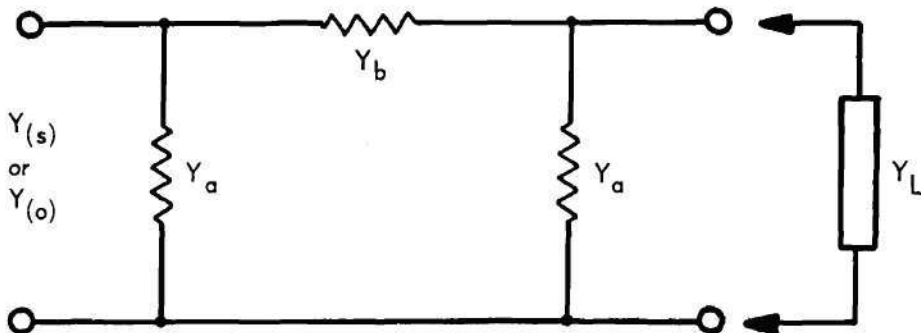


Figure 80. Network Approximation of a Transmission Line.

an arbitrary load. If $Y_{(s)}$ and $Y_{(o)}$ are used to represent the sending-end admittance with the load terminals respectively shorted and opened,

the conventional transmission line equation,

$$Z = Z_o \frac{Z_R + Z_o \tanh \gamma l}{Z_o + Z_R \tanh \gamma l}, \quad (1)$$

becomes

$$Y_{(s)} = \frac{1}{Z_o} \coth \gamma l \quad (2)$$

for the short-circuit condition and

$$Y_{(o)} = \frac{1}{Z_o} \tanh \gamma l \quad (3)$$

for the open-circuit condition, where Z_R represents the receiving-end condition, γ is the propagation constant, l is the line length, and Z_o is the characteristic impedance of the line.

But, from Figure 80,

$$Y_{(s)} = Y_a + Y_b \quad (4)$$

and

$$Y_{(o)} = Y_a + \frac{Y_a Y_b}{Y_a + Y_b}. \quad (5)$$

Substituting Y_a from Equation 4 into Equation 5 yields

$$Y_{(o)} = Y_{(s)} - Y_b + \frac{(Y_{(s)} - Y_b)Y_b}{Y_{(s)}} \quad (6)$$

or

$$Y_{(o)} Y_{(s)} = (Y_{(s)} - Y_b)(Y_{(s)} + Y_b) = Y_{(s)}^2 - Y_b^2, \quad (7)$$

from which

$$Y_b^2 = Y_{(s)}^2 - Y_{(o)} Y_{(s)}. \quad (8)$$

Letting $Y_0 = 1/Z_0$ in Equation 8 and substituting $Y_{(s)}$ and $Y_{(o)}$ from Equations 2 and 3 gives

$$\begin{aligned} Y_b^2 &= Y_0^2 \coth^2 \gamma l - Y_0^2 \tanh \gamma l \coth \gamma l \\ &= Y_0^2 (\coth^2 \gamma l - 1) = Y_0^2 \operatorname{csch}^2 \gamma l . \end{aligned} \quad (9)$$

or

$$Y_b = \frac{Y_0}{\sinh \gamma l} . \quad (10)$$

From Equation 4

$$\begin{aligned} Y_a &= Y_{(s)} - Y_b = Y_0 \coth \gamma l - \frac{Y_0}{\sinh \gamma l} \\ &= Y_0 \left(\frac{\cosh \gamma l - 1}{\sinh \gamma l} \right) . \end{aligned} \quad (11)$$

But

$$\cosh X - 1 = 2 \sinh^2 \frac{X}{2} \quad (12)$$

and

$$\sinh X = 2 \sinh \frac{X}{2} \cosh \frac{X}{2} \quad (13)$$

or

$$\frac{\cosh X - 1}{\sinh X} = \frac{\sinh X/2}{\cosh X/2} = \tanh \frac{X}{2} . \quad (14)$$

Therefore,

$$Y_a = Y_0 \tanh \frac{\gamma l}{2} . \quad (15)$$

When the load, Y_L , of Figure 80 is connected, the input admittance, Y , becomes

$$\begin{aligned}
 Y &= \bar{Y}_a + \frac{(Y_a + Y_L) Y_b}{Y_a + Y_b + Y_L} \\
 &= \frac{Y_a(Y_a + Y_b) + Y_L(Y_a + Y_b) + Y_a Y_b}{(Y_a + Y_b) + Y_L} . \quad (16)
 \end{aligned}$$

Equation 16 may be simplified by replacing $(Y_a + Y_b)$ by $Y_{(s)}$, as in Equation 4,

$$Y = \frac{Y_{(s)}(Y_a + Y_L) + Y_a Y_b}{Y_{(s)} + Y_L} = \frac{\frac{Y_a Y_b}{Y_{(s)}} + Y_a + Y_L}{Y_{(s)} + Y_L} \cdot Y_{(s)} . \quad (17)$$

Further simplification results from substituting Equation 5 into Equation 17 to obtain

$$Y = Y_{(s)} \frac{Y_{(o)} + Y_L}{Y_{(s)} + Y_L} \quad (18)$$

or

$$Y_L = Y_{(s)} \frac{Y_{(o)} - Y}{Y - Y_{(s)}} . \quad (19)$$

For a half-wavelength line, since $Y_{(s)}$ is very large,

$$Y_{\lambda/2} = Y_{(s)} \frac{Y_{(o)} + Y_L}{Y_{(s)} + Y_L} \Bigg|_{Y_{(s)} \rightarrow \infty} = Y_{(o)} + Y_L \quad (20)$$

or

$$Y_L = Y_{\lambda/2} - Y_{(o)} . \quad (21)$$

Equation 19 was programmed on a digital computer and used to correct the original data of Figures 78 and 79. The results were approximately the same as obtained from line subtractions. Even greater errors were obtained in some cases near quarter- and half-wavelength points

where either $Y_{(o)}$ or $Y_{(s)}$ became very large. This method of line-length correction was cross-checked with the 9.69-cm data of Figure 76 and showed very good agreement. Of interest is the fact that this method of line-length subtraction does not require a knowledge of the actual line length or of the frequency. The method should also compensate for some, if not all, of the line deficiencies; however, in a practical example, it did not accomplish this purpose.

In an attempt to reduce some of the errors encountered when using the directional coupler or a coaxial-line section between the Admittance Meter and the termination, several sources of error were considered.

The first consideration concerned the admittance calculation procedure just described. As mentioned above, when the frequency is such that the line length is near a quarter- or half-wavelength, the admittance of either the short- or open-circuit termination is very large and, therefore, requires a large multiplying factor on the Admittance Meter dial. At such lengths, if the conductance with the open- or short-circuit termination were actually zero, as it would be for a perfect termination and perfect coaxial line, but were recorded as 0.1 millimho (one-fifth of the smallest division on the conductance scale), a multiplying factor of ten would make the conductance appear to be 1 millimho instead of zero. This becomes an appreciable conductance, when compared with the readings with the resistive terminations, and would introduce large errors in the calculations of the impedances of the terminations. In an attempt to eliminate this possible error, the line was assumed to be lossless and the conductive readings of either the open-circuit termination, the short-circuit termination, or both were assumed to be

zero. The directional coupler and 40-cm line data were rerun on the computer with each of these three assumptions and the results replotted. The accuracies were improved near 150 and 300 mc/sec, but the over-all accuracy was as poor or poorer than that of the line-subtraction methods. This result would seem plausible since under the above assumptions, the admittance-calculation method reduces to a line-subtraction method and thus defeats its originally intended purpose.

One possible source of error in the measurement system is incorrect characteristic impedances. Accordingly, the diameters of the center conductor of several samples of coaxial line were measured. The variations found in the diameters were large enough to produce variations in the impedance of the lines as great as one per cent.

On the assumption that the lines were lossless, but of the wrong impedance, three samples of the 40-cm line data, one for each of the resistive terminations, were selected for further study. By trial and error, a resistive impedance ($Z_0 = 51.39$ ohms) was found which, when used in conjunction with the transmission-line equation, resulted in impedance magnitudes of 50, 100, and 200 ohms respectively for the three terminations. The remaining 40-cm line data were then run on the computer using 51.39 ohms for Z_0 instead of 50 ohms. The results are shown in Figure 81. This type of compensation is not adequate since the magnitude of the impedance of the terminations is increased too much at the lower frequencies while it is not increased enough at the higher frequencies, as may be seen from this figure. The data indicated that the errors in the 40-ohm line run and the directional coupler run were caused by line losses in addition to a possible impedance error.

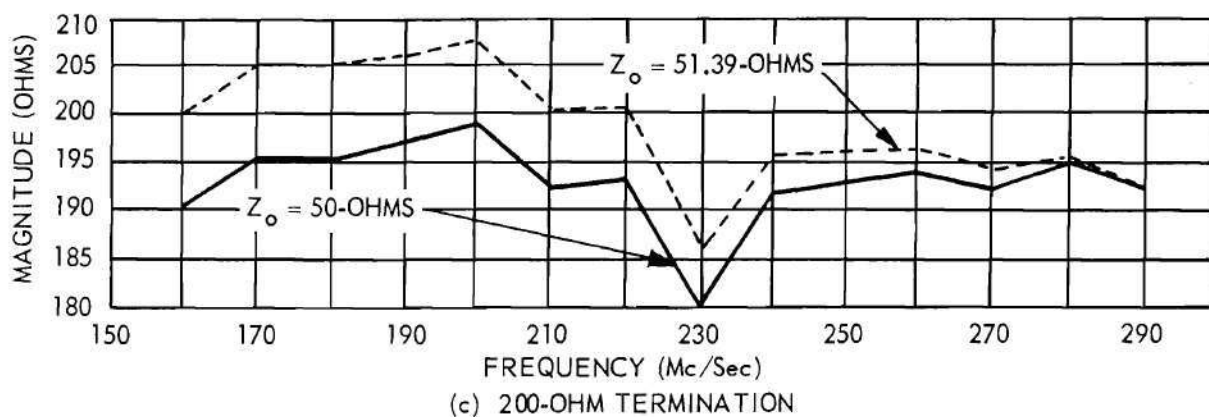
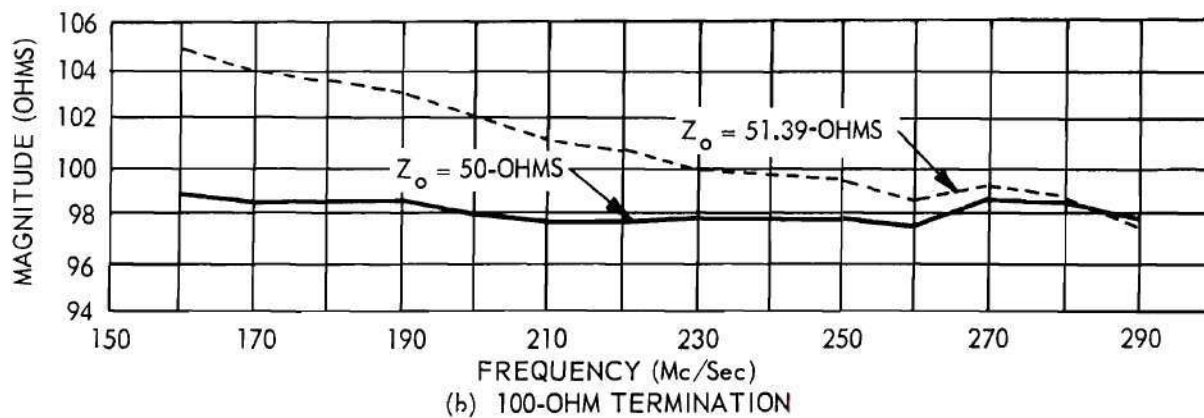
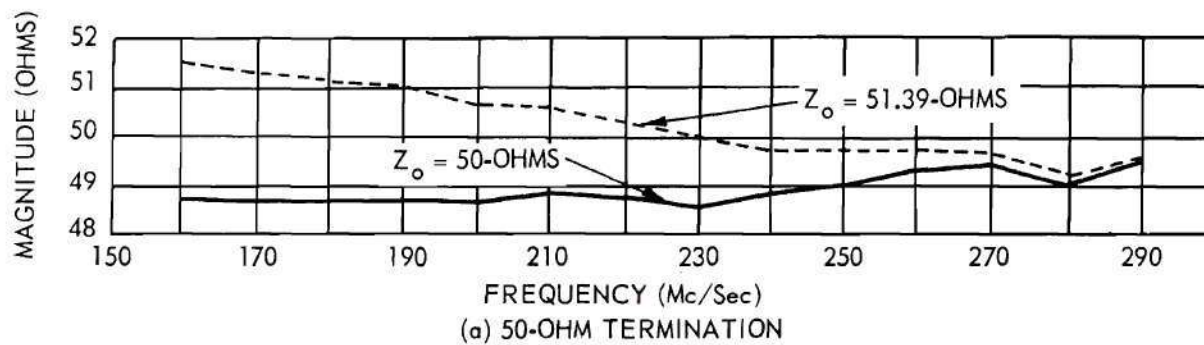


Figure 81. Impedance Level Compensation of 40-Cm Transmission Line Data.

An alternate method of improving the measurement accuracy with the directional coupler is to place the coupler in a half-wavelength transmission line. This method has the advantage that the Admittance Meter directly reads the actual admittance of the crystal or termination after dial corrections have been made, thus eliminating the necessity of using the computer for line subtractions. Also, if the total line is lossless, the actual physical length and impedance of the line need not be known. The disadvantages of the half-wavelength method are threefold: (1) line-loss compensations are inconvenient to make, (2) the method requires more personnel time for obtaining the same amount of data than does the fixed-line method due to the time required to set up the half-wavelength line for each frequency, and (3) Admittance Meter calibrations cannot be readily checked since only one point is represented on a Smith Chart for each termination as frequency is varied.

The normal procedure used in setting up a half-wavelength line is to place an open-circuit termination on the end of the coaxial line and vary the length of the line until the Admittance Meter and detector system null at zero susceptance. When this setup procedure was used, phase angles of the order of 3 or 4 degrees were obtained for the terminations. However, an inspection of Figure 74 showed the susceptive correction for a reading of $0 + j0$ to be $-j0.5$. The line was, therefore, not set at an exact half-wavelength. In a second run, the Admittance Meter was set to a reading of $0 + j0.5$ and the line adjusted so that the detector indicated a null. After corrections then, the susceptance of the open-circuit termination was zero, indicating a half-wavelength line. The results for such a run with the three terminations using a coaxial

air line are shown in Figure 82. The directional coupler was not used in the line for this run because of the desirability of determining the best possible accuracy.

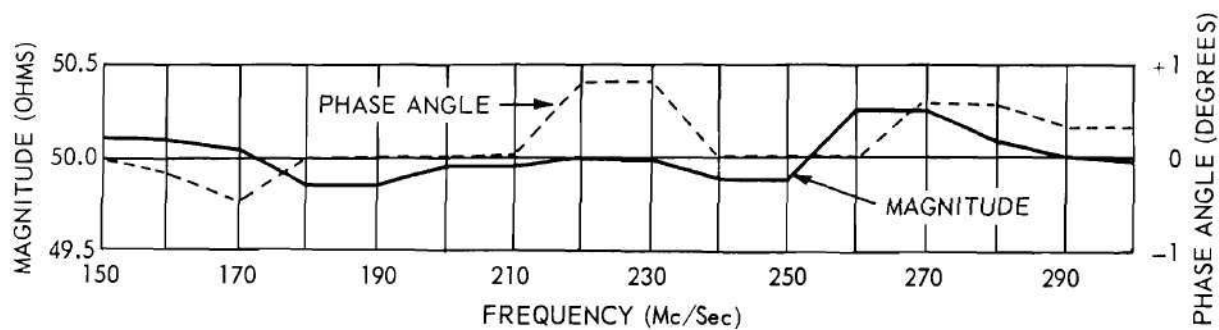
The accuracies with the 50- and 100-ohm terminations are comparable to that for the 9.69-cm run, while the accuracy with the 200-ohm termination, although better than with arbitrary line lengths, was not as good as with the 9.69-cm line.

Measurements were made using the directional coupler as a part of a half-wavelength line. The data were only slightly poorer than for the half-wavelength line without the directional coupler.

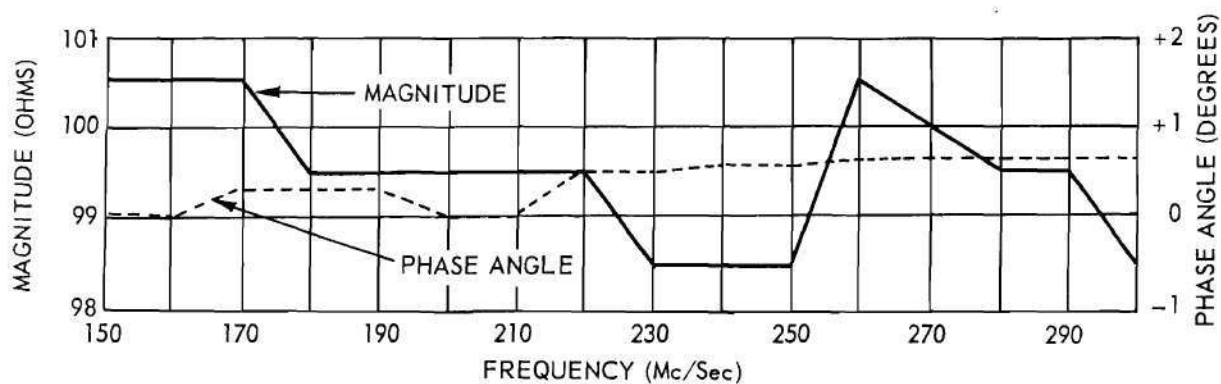
The following conclusions may be drawn from the preceding data:

(1) measurement errors of less than one per cent for impedance magnitude and one degree for phase angle are possible when the terminations are placed directly on the Admittance Meter terminals (9.69 cm line length) and when the impedance magnitude is of the order of 50-ohms, (2) both the directional coupler and arbitrary lengths of coaxial line introduce appreciable errors in measurements, (3) half-wavelength lines introduce less errors, generally, than do random line lengths and, (4) the directional coupler introduces only slightly greater errors than does an equal length of air-dielectric transmission line.

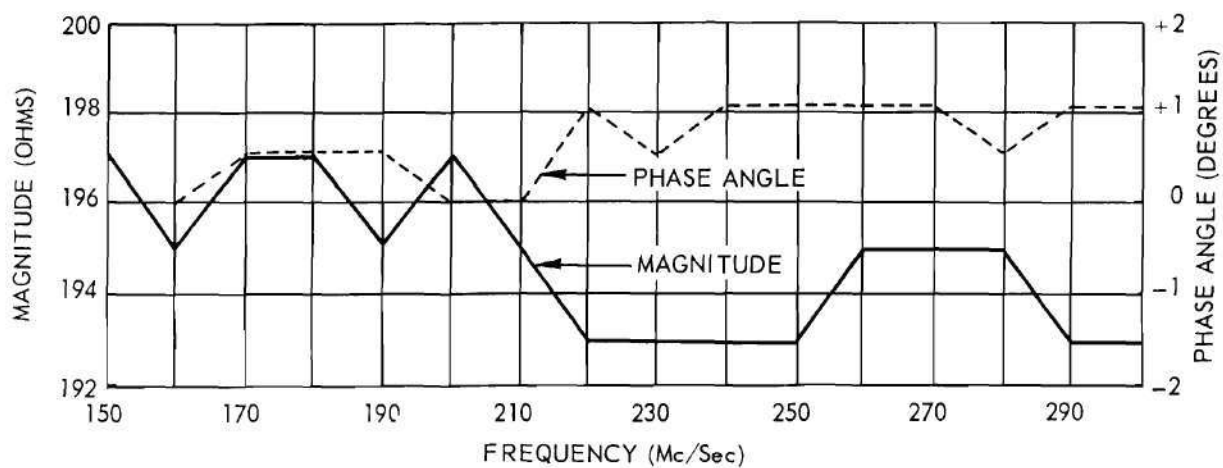
Neither mechanical nor mathematical methods were found to compensate for the additional errors introduced by the directional coupler and arbitrary transmission-line lengths, apparently because of the complicated way in which the losses occur. The fact that each line connector introduces a discontinuity also complicates the mathematical analysis of the system. Since the importance of immediate results outweighed the



(a) 50-OHM TERMINATION



(b) 100-OHM TERMINATION



(c) 200-OHM TERMINATION

Figure 82. Admittance Meter Measurements on Resistive Terminations with a Half-Wavelength Line.

advantages of greater accuracy, further efforts to determine the exact sources of errors were discontinued.

An alternate solution to the calibration problem would be to calibrate the Admittance Meter with the directional coupler and component mount in position. This calibration would be possible only if a sufficiently great number of accurately calibrated standards were available and if the standards were compatible with the component mount. Such standards are available at the National Bureau of Standards, Boulder, Colorado. The calibration procedure would involve obtaining sufficient data to cover a Smith Chart with closely spaced correction contours which could then be used to correct the crystal admittance data.

C. Radio-frequency amplifiers.--Initial tests of the Crystal Measurements Standard System indicated that the Marconi Signal Generator could not provide sufficient drive to test all crystals at the desired maximum drive level. Also, the stability of the generator was degraded when it was operated without isolation from the Admittance Meter. Thus, several attempts were made to construct satisfactory r-f amplifiers to be inserted between the generator and the Admittance Meter. Before a successful model was developed, commercial amplifiers suitable for the purpose became available. Thus two Instruments for Industry Model 530 wide-band chain amplifiers were purchased. Originally, only one amplifier was ordered, but the gain of one amplifier alone was not sufficient for some crystal measurement applications, particularly under mismatched conditions.

The manufacturer specifies that the bandpass of the amplifier is 10 kc to 300 mc/sec, with 18 db voltage gain into a matched load. The

input and output impedances of the amplifier are 135 and 150 ohms, respectively.

Since the Crystal Measurements Standard System uses 50-ohm coaxial components, the input and output terminals of the amplifiers are mismatched and the gain of each amplifier is reduced. A matching network could be placed on each of the inputs and outputs to match the amplifiers; however, the loss due to the insertion of the networks is often greater than the loss due to mismatched conditions.

In initial tests of the amplifiers, the output voltage was not constant for constant input voltage. The output variations were assumed to be due to variations in grid bias. Thus, the internal bias sources of the amplifiers were disconnected and replaced by a 6-volt dry cell. The output fluctuations continued, but were not as severe. The internal B^+ supply was then replaced by an external regulated supply. The fluctuations were thus reduced to a negligible amount.

A plot of the power gain for various load conditions is given for one of the amplifiers in Figure 83. Also included is a plot of the power gain for the other amplifier working into a 50-ohm load, and a plot of the two amplifiers in cascade working into the same load. The cable impedance in all cases was 50 ohms.

The apparent cycling of the gain as the frequency was varied was due to the mismatch of the coaxial line at both input and output of the amplifier. Since the minimum gain of the two amplifiers in cascade, as shown in Figure 83, is greater than the original requirement of 20 db, and since the power must be adjusted to predetermined values at each frequency and load as indicated by the power measurement system, constant gain over the entire frequency range was not considered necessary.

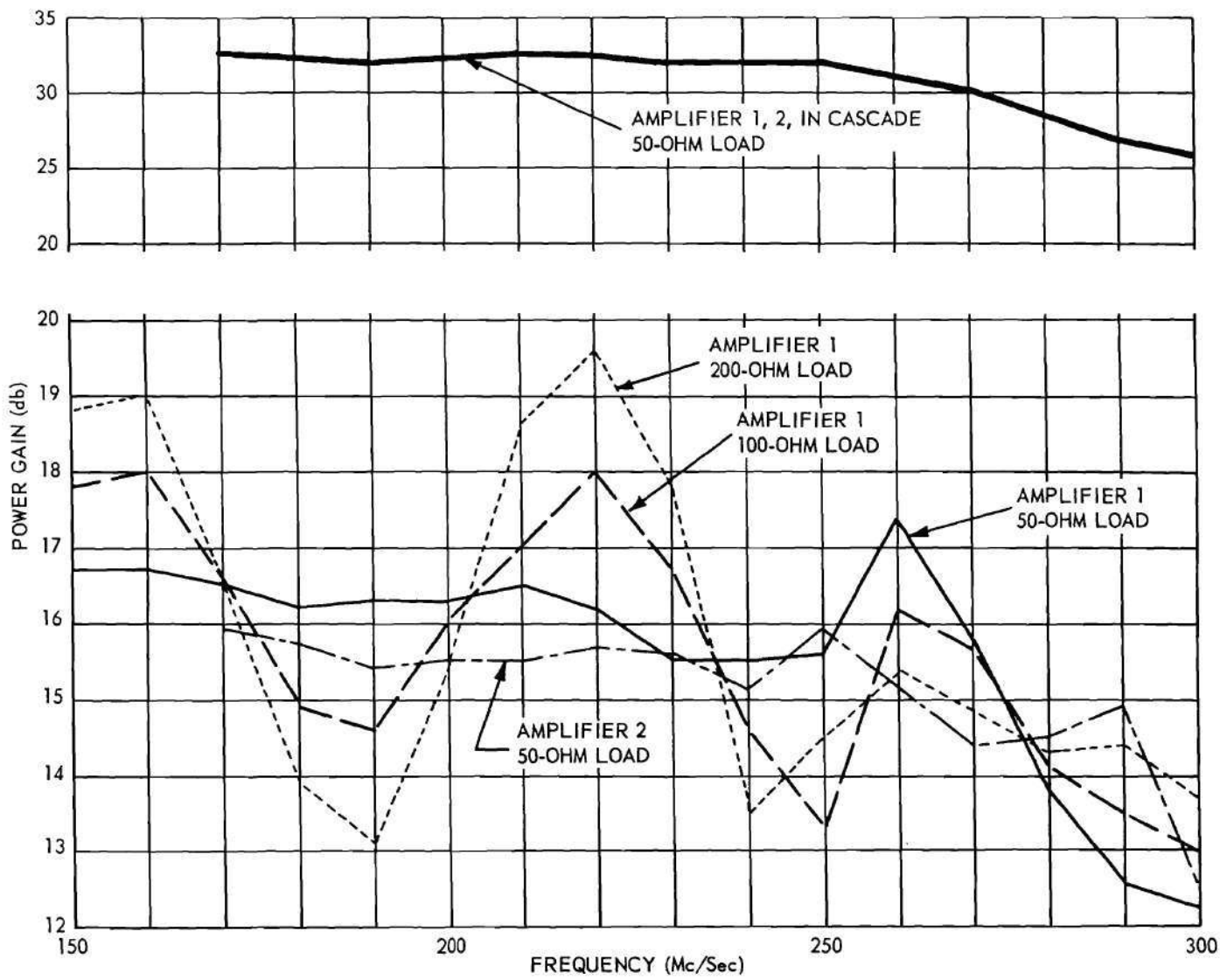


Figure 83. Power Gain Characteristics of the Instruments for Industry Wide-Band Amplifiers Model 530.

A test run was made on one of the amplifiers to determine the magnitude of harmonic distortion that would be introduced into the system. The Marconi Signal Generator was adjusted to a frequency of 90 mc/sec and data were obtained as shown in Table 11. The data are only approximate and depend on the dial calibration of an AN/APR-4 radar receiver which was used as an output indicator.

Table 11. The Harmonic Generation of a Radio-Frequency Amplifier

Fundamental Frequency (Mc/Sec)	Amplifier Input Level (Mv)	Harmonic Frequency (Mc/Sec)	Harmonic Output (Db Below Fundamental)	
			Signal Gen. (Db)	Amplifier (Db)
90	2	180	44	44
90	2	270	36	36
90	100	180	48	27
90	100	270	40	40

With an input of 2 mv, the amplifier does not introduce appreciable harmonic distortion. However, as can be seen, more distortion is introduced with an input of 100 mv. To eliminate possible errors in crystal measurements due to harmonic excitation, two Microlab Corporation low-pass filters were purchased. The cutoff frequencies specified by the manufacturer are 300 mc/sec for the Model FL-301, and 400 mc/sec for the Model FL-401. Microlab specifies that the stop band limit of their filters is greater than six times the cutoff frequency. A 200 mc/sec low-pass filter (Model LP-200, Microphase Corporation) was already available. The characteristics of the three filters are shown in Figure 84. For any frequency in the range 175 to 300 mc/sec, the use of the various

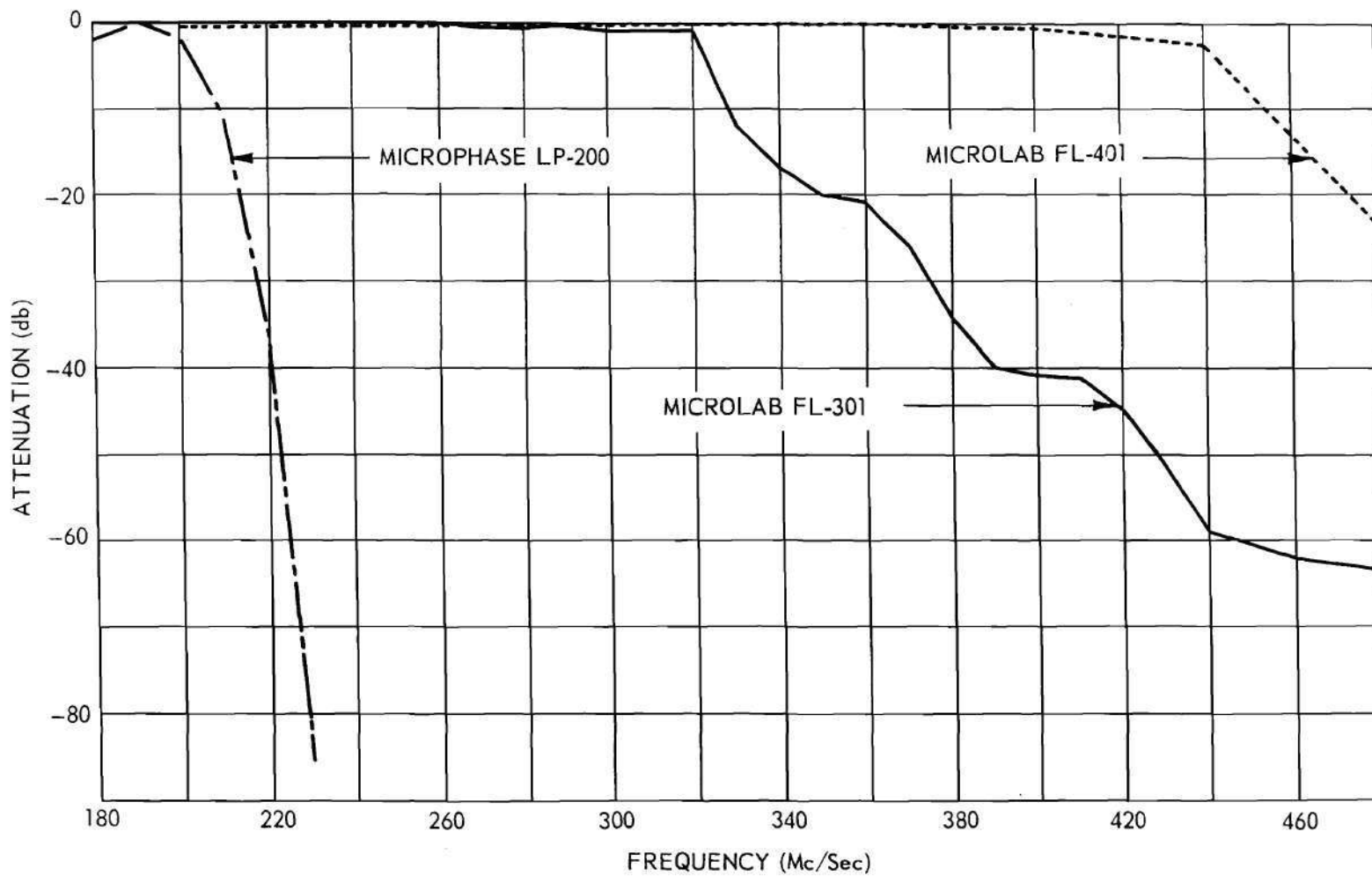


Figure 84. Frequency Characteristics of Three Low-Pass Radio-Frequency Filters.

filters will provide harmonic rejection of at least 40 db up to the sixth harmonic of the fundamental, if a stop-band limit is assumed as specified.

The filters are not normally required for crystal measurements when using the Crystal Measurements Standard, since the harmonic output from the amplifiers is relatively small and since the crystals are relatively linear. For accurate power measurements, however, the filters are sometimes required since the Power Measurement System does not include provisions for frequency discrimination.

D. Detector systems.--A source of error in the Crystal Measurements Standard System was the lack of sufficient null-detection sensitivity to permit accurate null adjustment of the Admittance Meter. This difficulty arises from the requirements that the crystal drive remain at very low levels (between 0.2 and 4 mw). Previous data indicated that none of several commercial null detectors tested had sufficient sensitivity. The possibility of using commercial high-frequency communication receivers was considered. However, a very limited number of such receivers were being manufactured. Of those available, only one, the Eddystone Model 770C, was found which was both reasonably priced and covered all of the desired frequency range. This receiver was purchased after the distributor provided data which indicated that it would offer appreciable improvement over previous detection systems.

The null-detection sensitivity curve for the Eddystone receiver is presented in Figure 85.

One difficulty encountered with the Eddystone receiver was that of r-f leakage from external sources. This leakage was objectionable only at frequencies where television stations or other strong signals were

present. However, the source of leakage could provide direct coupling between the signal generator or other instruments and the receiver.

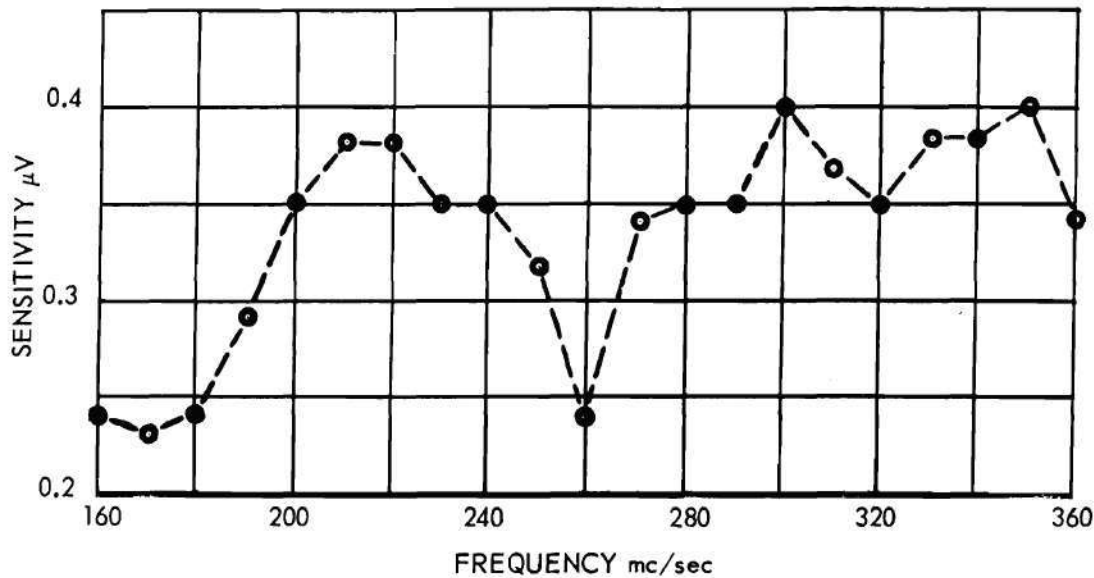


Figure 85. Null-Detection Sensitivity of the Eddystone Receiver Type 770U.

The a-c power cable appeared to be the principal source of leakage. Thus a filter consisting of two feed-thru capacitors and an r-f choke was installed in each power connection at the receiver.

In order to use the receiver as a null detector, the internal signal level meter was replaced with an external meter of greater sensitivity. The connection of these additional leads to the receiver became another source of r-f leakage. Thus, choke-capacitor filters were installed in these leads also.

Even with the filter installations indicated above, the r-f leakage was still appreciable, due to the relatively large openings in the case of the receiver. Because of the difficulty of installing copper screening in the receiver case, a small double shielded screen box was constructed

to house the entire receiver. Additional filters were added at each of the external connections. The resulting total signal leakage was reduced by more than 40 db.

Further evaluation data indicated that the first filters installed between the outer shield box and the receiver did not provide sufficient isolation. To further improve the filtering, these components were replaced by four Tobe Filterettes as shown in Figure 86. The manufacturer's specifications state that this filter has a 45-db attenuation at 150 kc/sec and greater than 45-db attenuation from 150 kc/sec to 1000 mc/sec.

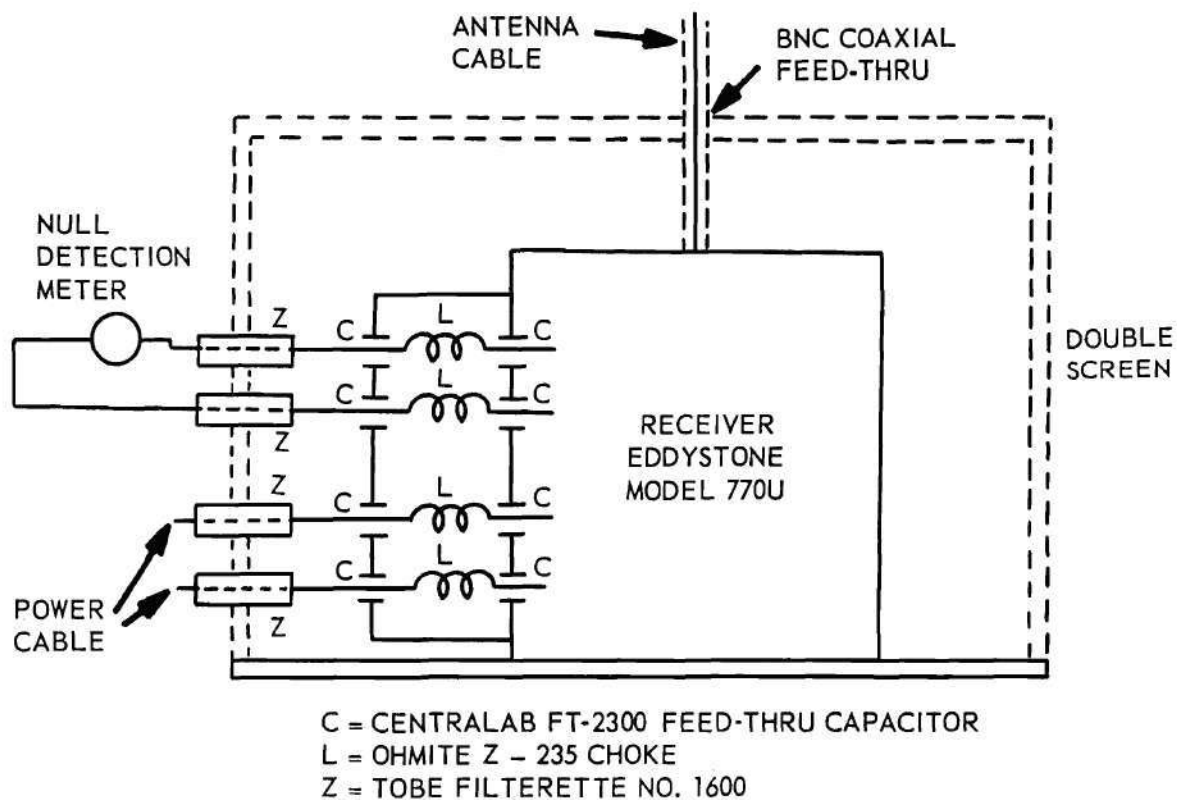


Figure 86. Stray-Signal Shielding Used with the Eddystone Receiver Type 770U.

Also, the standard RG-58 BNC cable used between the receiver antenna terminal and the Admittance Meter was not sufficiently shielded to eliminate it as a source of stray-signal pickup. Tests were made with other types of commercial cable, with the same results. A special cable was finally made up by inserting an RG-58 cable into a copper tube and soldering both ends to BNC connectors. This modified cable provided adequate shielding.

To determine the effectiveness of the various shieldings, several data runs were made. The first run was performed with all shieldings in use and with no external signal source. The receiver remained in the shield box with the cover closed. One end of the special copper-covered cable was placed on the antenna terminal and the other end was terminated with a short-circuit. A plot of the output current versus frequency is given in Figure 87(a). Except for two isolated responses, one at 225 mc/sec, and the other at 270 mc/sec, the signal-level-meter output current was less than 40 ua. These two isolated responses did not change in magnitude when the door of the shield box was opened. The responses were, therefore, assumed to be of internal origin.

For comparison, the responses of the receiver with the shield box door open are shown in Figure 87(b).

In a third run, the receiver remained in the shield box with the door closed, but the copper-covered cable was replaced by the standard RG-58/U cable. The increased responses, as shown in Figure 87(c), at 155, 198, and 204 mc/sec may be noted, with the latter two due to television Channel 11. Two interesting phenomena occurred during this run. The first was the reduction of the magnitude of the spurious responses

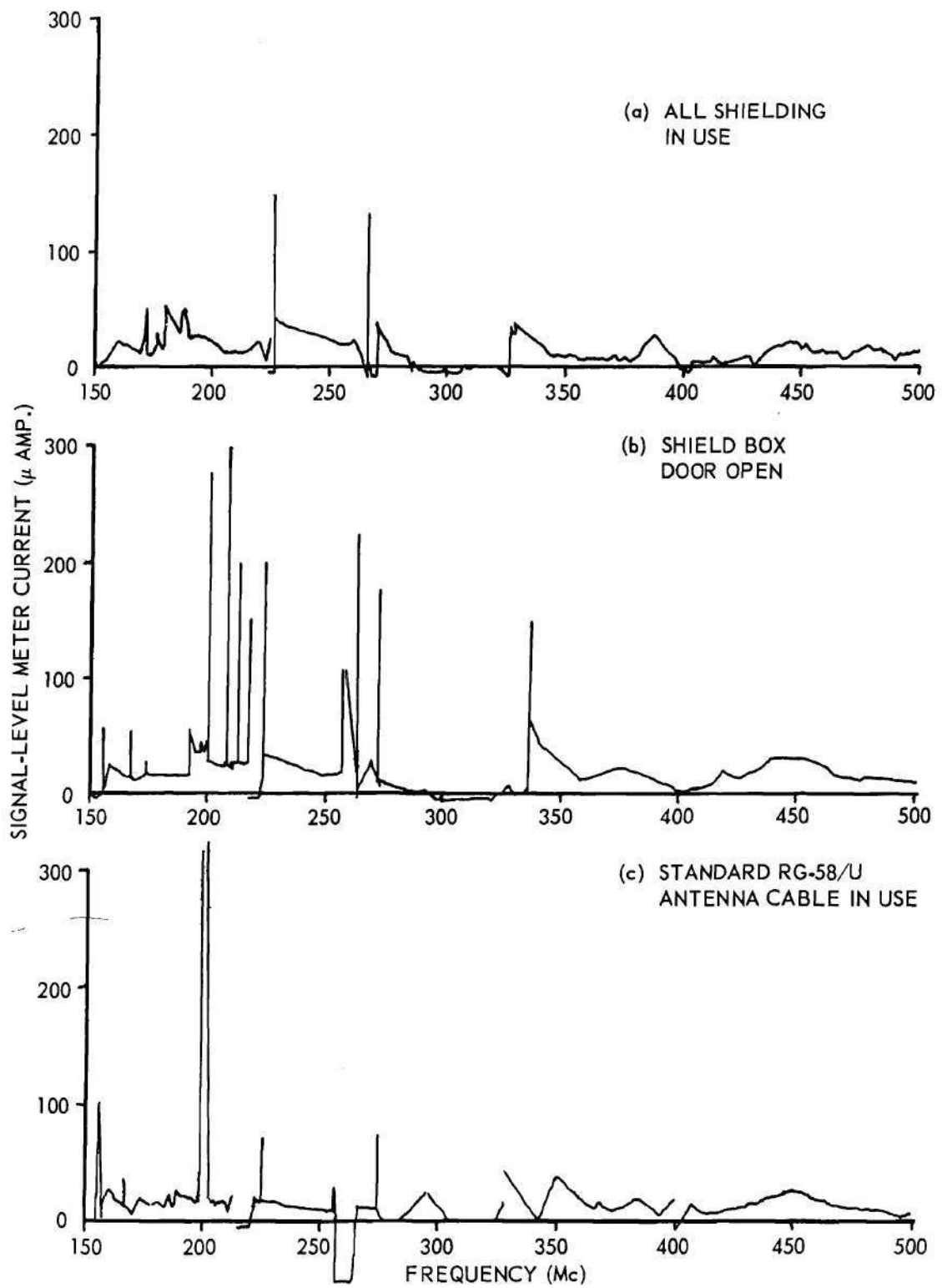


Figure 87. Spurious-Signal Reception of the Eddystone Receiver Type 770U.

at 225 and 270 mc/sec. The length of cable used on the antenna input was first believed to have caused the occurrence of these spurious responses. Therefore, a matching network consisting of a 22-ohm series resistor and a 220-ohm shunt resistor was put in series with the antenna cable at the input of the receiver. The spurious responses still remained, however, with the same magnitude as before and were still a function of the type and length of cable used. Because of the decreased sensitivity of the system, the matching network was removed.

The second interesting phenomena was the extreme negative reading of the d-c milliammeter in the frequency range from 262 to 267 mc/sec. This negative reading was caused by the r-f section of the receiver going into oscillation. The oscillation was directly attributed to the BNC cable used in the third run. At the frequency of oscillation, the length of the cable was such as to reflect an impedance into the antenna terminals which caused the receiver to oscillate. The oscillation and negative reading of the milliammeter were eliminated by simply changing the length of cable used at the antenna input. The special copper-covered cable was of such a length that oscillations did not occur at any frequency within the range of the receiver.

Two sensitivity runs, one with the AVC on and the other with the AVC off, as shown in Figure 88, were made at 250 mc/sec to determine the relation between the signal-level meter reading and the r-f signal-input voltage. As may be noted from the graph, the curve is much steeper with the AVC turned off than it is when the AVC is on; however, the dynamic range of the curve is much less. For initial measurements in locating a null, the AVC should be left on, but as the exact null is reached,

better resolution may be obtained with the control turned off. The occurrence of the negative reading of the milliammeter due to excessive input signal may also be noted from this graph.

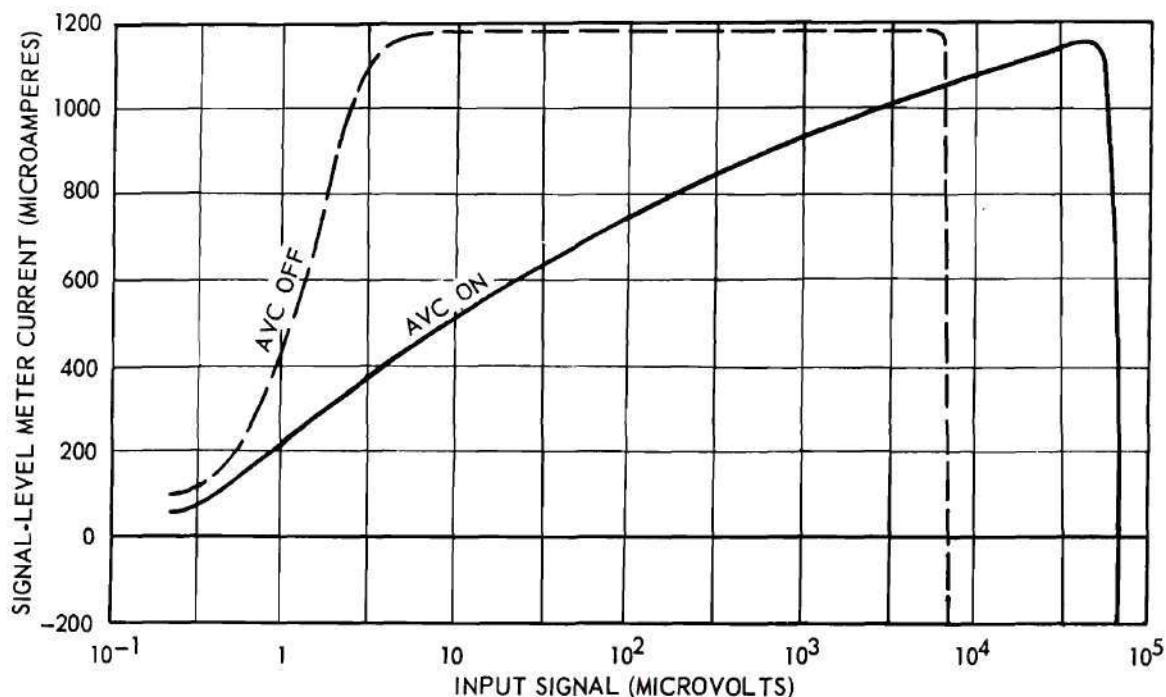


Figure 88. Signal-Level Meter Sensitivity of the Eddystone Receiver at 250 Mc/Sec.

Figure 88 also aids in estimating the amplitudes of the responses shown in Figure 87. No efforts were made to determine the amplitudes of the various responses in microvolts since day-to-day changes produce variations by factors as great as five. Also, the sensitivity curve of Figure 88 is subject to some variation with ambient conditions and is valid only at the frequency specified.

Other tests indicated that the equivalent noise at the input of the receiver is less than 0.3 μv at all frequencies.

The two occurrences of negative signal-level-meter reading referenced above are due to excessively large signals (such as may be produced by oscillations in the r-f sections) in the i-f channel of the receiver. When very large signals are applied to the receiver, the AVC diode is overloaded and draws excessive current from the delay bias source. The delay bias is obtained from a voltage divider between the receiver's plate supply line and ground. The same divider is used in the signal-level meter bridge circuit. Thus, when the AVC diode is overloaded, the negative reading of the signal level meter results. The modification of the receiver to eliminate this negative reading was not considered necessary since the condition in no way limits the usefulness of the receiver as a null detector.

E. The power measurement system.--The incorporation of means for measuring the drive level to a crystal under test into the Crystal Measurement Standard was originally considered necessary because of reported dependence of crystal parameters upon the drive level (36). Accordingly, a system capable of directly indicating the power dissipation in the crystal was developed. The system consisted of a Hewlett-Packard Dual Directional Coupler Model 764D inserted between the Admittance Meter and the component mount as shown in Figure 72. Associated with the directional coupler were two specially calibrated detector diodes, a d-c bridge, and a Minneapolis-Honeywell Electronik Null Detector Model 104 WIG. The system was calibrated by means of a sensitive termination type power level meter. The over-all error in measuring crystal drive level is less than ± 10 per cent for voltage standing-wave ratios between 1.0 and 6.5, for power levels from 0.1 to 10.0 mw, and frequencies

from 175 to 300 mc/sec. At the normal 2 mw crystal drive level, the errors were less than 20 per cent over the frequency range and admittance levels of interest. Complete details of the Power Measurement System have been reported elsewhere (22).

Previous data in this chapter have shown that the introduction of the directional coupler into the Crystal Measurements Standard System decreases the accuracy of admittance measurements. Further studies indicated that the errors in data due to variations in power level were less than the errors introduced by the insertion of the directional coupler. Thus the Power Measurement System was generally not used in obtaining crystal data. As a substitute, the voltage across the crystal was determined by replacing the crystal by a resistor having approximately the same resistance as the crystal at its resonant frequency and then measuring the voltage across the resistor with a high-frequency voltmeter.

F. Other instrumentation.--No modifications of the Marconi Signal Generator for use with the Crystal Measurements Standard were found necessary. Some initial modifications to improve the stability were made but were later removed as the improvements did not warrant the inconveniences of the changes. A complete description of the performance of this instrument has been reported elsewhere (22).

The frequency measurement equipment consisted of a Berkeley Model 5580 Converter and a Berkeley Model 5570 Frequency Meter. This equipment was used without modification except for the substitution of a more accurate frequency standard signal for the internal crystal oscillator.

The component mount indicated in the block diagram of Figure 72 was a modified General Radio Type 874-M Component Mount. The length of

the mount was adjusted to equal the electrical length of the standard terminations. Crystal pin connectors consisting of drilled binding-head screws were inserted in the component mount as may be seen in the typical setup of the Crystal Measurements Standard System shown in Figure 89.

G. Measurement procedures.--The complete Crystal Measurements Standard may be used to measure the admittance characteristics of both conventionally mounted crystals and prototype coaxially mounted crystals. The former must be plugged into the component mount described above. The latter is plugged directly onto the Admittance Meter.

Since the above calibration data indicated that greatest accuracy was obtained with minimum line length between the Admittance Meter and the crystal, the component mount and coaxial crystals were both connected directly to the Admittance Meter without any intervening transmission line. The standard line-length separation from the Admittance Meter when the component mount was used was stated by the manufacturer to be 9.69 cm. The line-length separation with coaxially mounted crystals depended upon the particular mount being used.

After all of the equipment (except the power measurement system which, as previously stated, was not generally employed) indicated in the block diagram of Figure 72 was properly interconnected, special r-f shields were installed at all junctions of coaxial cables. These shields were provided by the General Radio Company.

An equipment warm-up time of approximately one hour was generally required for the equipment to stabilize sufficiently for a crystal data run. During this time, some of the equipment could be used, however, in the block diagram of Figure 90 for locating the overtone responses of

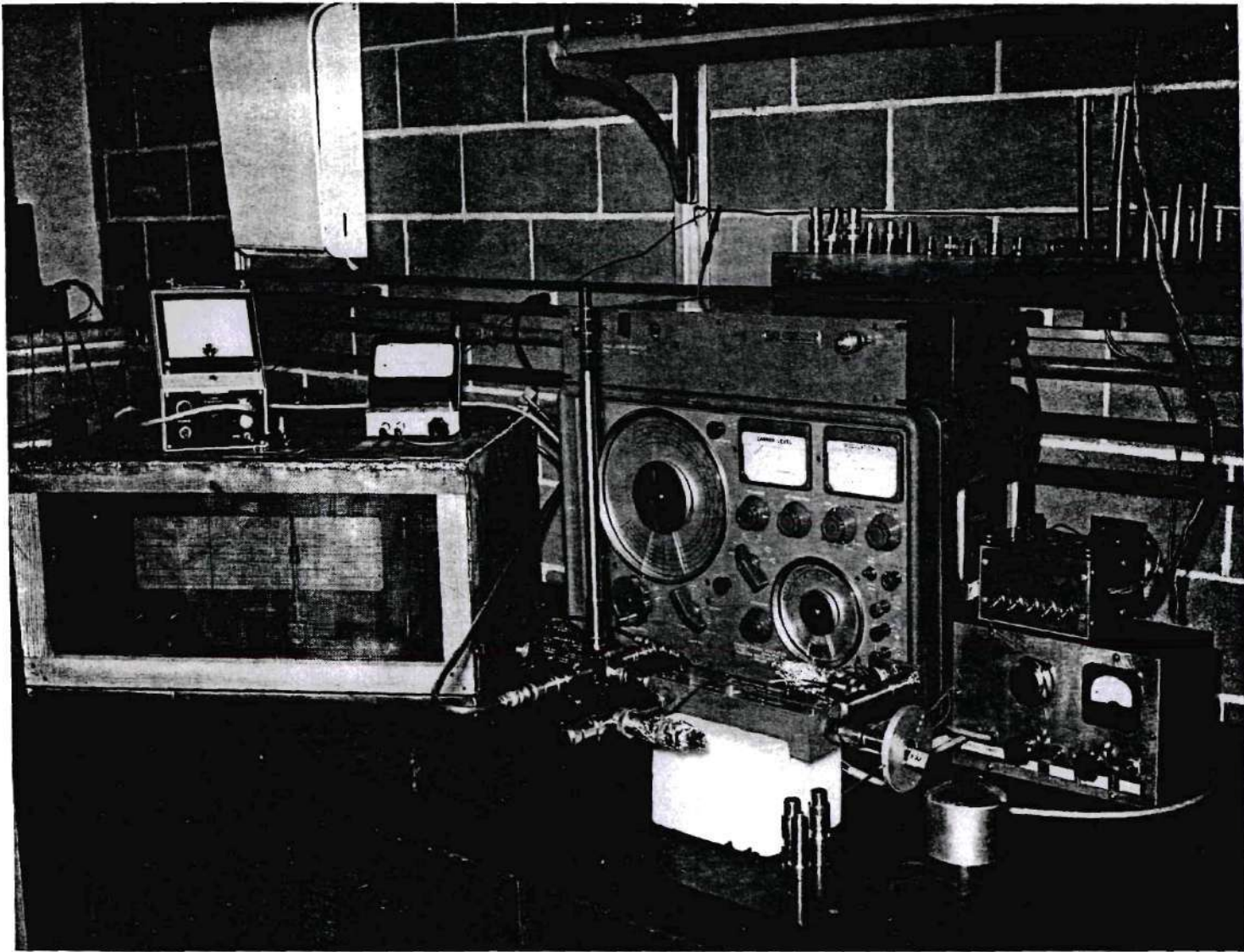


Figure 89. A Typical Setup of the Crystal Measurements Standard.

crystals for which previous data were not available. With this setup, as the signal generator is swept through the range of frequencies, the presence of an overtone response is indicated by a dip in the null-detector reading.

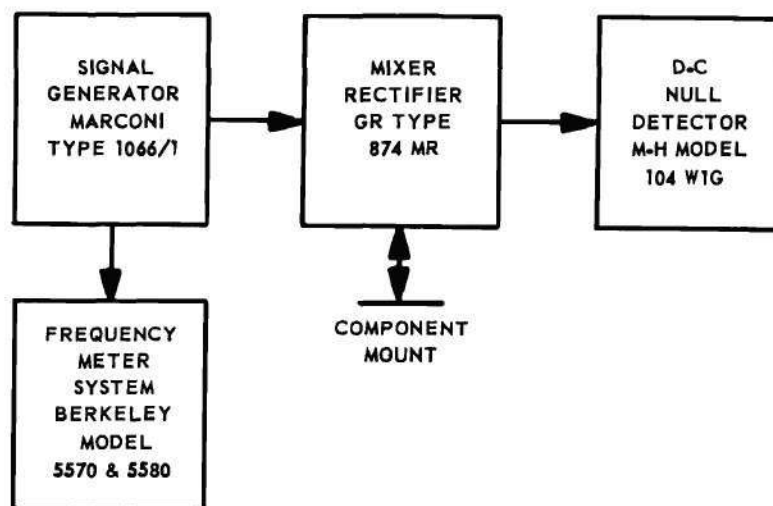


Figure 90. System for Locating Crystal Overtone Responses.

After all of the equipment is properly reconnected as shown in Figure 72 and the test crystal is installed, the operation procedure for the Crystal Measurements Standard is as follows:

- (1) adjust the signal generator frequency to the required overtone frequency,
- (2) adjust the frequency measuring equipment to read the required frequency,
- (3) adjust the receiver tuning for maximum indication on the signal-level meter,
- (4) adjust the conductance and susceptance dials of the Admittance Meter for a minimum receiver signal-level meter indication,
- (5) immediately energize the frequency measuring equipment for a single count, and

(6) record the conductance, susceptance, and frequency.

To determine the beginning (lower frequency limit) of an overtone response, the initial conductance reading is considered. If the conductance reading is essentially zero, the correct frequency may be either higher or lower. If the initial conductance reading is appreciable, the frequency should be decreased approximately 50 kc/sec and another reading made as indicated above. The procedure is then repeated as required.

After the beginning of the overtone response is found, the frequency is increased while retuning the receiver and at the same time observing the reading of the signal-level meter. When an appreciable change in the signal-level meter reading has occurred, the null is again obtained with Admittance Meter dials and the readings recorded. In this way, a smooth distribution of points, when plotted on a Smith Chart, may be obtained. The change in signal-level meter reading which is permitted before successively nulling the Admittance Meter will determine the number of data points which will be obtained per overtone response.

Generally, the data points must be plotted on a Smith Chart as they are read to serve as a guide for determining when the data is complete. Such a procedure readily indicates the presence of spurious responses, data for which may or may not be required.

Time required to obtain data for one overtone response varies from 15 minutes to one hour or more, depending upon the number of data points required. Each overtone data run should be completed as rapidly as possible to prevent drifts due to temperature changes.

When a data run is made on the holder only of a crystal, the general procedure is the same except that the frequencies for which data is desired are generally predetermined.

APPENDIX II

MATHEMATICAL PROCEDURES AND COMPUTER PROGRAMS

During the performance of this research, extensive use was made of the digital computer facilities of the Rich Electronic Computer Center. Some of the original programs were written for the Remington Rand ERA 1101 computer but were later rewritten for the IBM 650 computer because of a greater facility for handling the particular type of input and output data. Since the quantity of mathematical calculations was not considered extensive from the standpoint of the capabilities of the computer, most of the programs were written for use with the Bell General Purpose Interpretive System for the IBM 650. As the number of different programs required was large, the time saved in programming in the interpretive system rather than in machine language more than offset the small additional machine time required.

Approximately 20 different programs were written for use with the Bell System. Some of these programs were only of temporary usefulness, while others were used only once to prove or disprove a particular point in question. Only the programs which were used extensively will be described here.

Program 1. Mathematical subtraction of a transmission-line length.--This program was used to subtract predetermined lengths of lossless transmission line from any arbitrary impedance function at any arbitrary frequency. Its most extensive application was to subtract the 9.69 cm length

of transmission line between the crystal component mount and the Admittance Meter of the Crystal Measurements Standard System.

The equation for the sending-end impedance, Z_s , of a transmission line of electrical length, \underline{d} , terminated at the receiving end by an impedance, Z_r , is

$$Z_s = Z_o \frac{Z_r + j Z_o \tan 2\pi d/\lambda}{Z_o + j Z_r \tan 2\pi d/\lambda}, \quad (22)$$

where Z_o is the characteristic impedance of the line and λ is the free-space wavelength at the frequency specified.

The impedance determined by the Admittance Meter is Z_s while the desired impedance is Z_r . The solution of equation 22 for Z_r yields

$$Z_r = Z_o \frac{Z_s - j Z_o \tan (1.2 \underline{f} \underline{d} \cdot 10^{-8})}{Z_o - j Z_s \tan (1.2 \underline{f} \underline{d} \cdot 10^{-8})}, \quad (23)$$

where the appropriate constant has been included so that \underline{f} may be expressed in cycles per second and \underline{d} in centimeters.

The equation may be rewritten in a more appropriate form for the computer as

$$\begin{aligned} Z_r = R + j X &= C \frac{(A + j B) - j C E}{C - j (A + j B) E} \\ &= C \frac{A + j(B - CE)}{(C + BE) + j(-AE)} = \frac{C(f + jG)}{H + jI} \end{aligned} \quad (24)$$

where $A = \text{Re}(Z_s)$, $B = \text{Im}(Z_s)$, $C = Z_o$, $E = \tan 1.2 \underline{f} \underline{d} \cdot 10^{-8}$, $F = A$, $G = B - CE$, $H = C + BE$, and $I = -AE$.

The equation may be rationalized to yield

$$\begin{aligned} Z_r &= C \frac{(FH + GI) + j(GH - FI)}{H^2 + I^2} = C \frac{(J + jK)}{H^2 + I^2} \\ &= \frac{CJ}{H^2 + I^2} + j \frac{CK}{H^2 + I^2}, \end{aligned} \quad (25)$$

where $J = FH + GI$ and $K = GH - FI$.

Therefore,

$$R_r = \frac{CJ}{H^2 + I^2} \quad \text{and} \quad X_r = \frac{CK}{H^2 + I^2}. \quad (26)$$

The receiving-end admittance, Y_r , is

$$Y_r = 1/Z_r = \frac{H^2 + I^2}{C(J + jK)} = \frac{L}{C} \frac{J}{M} - j \frac{L}{C} \frac{K}{M} = G_r + jB_r \quad (27)$$

where $L = H^2 + I^2$ and $M = J^2 + K^2$.

Since the laboratory data are generally in admittance form, the initial portion of the program makes the necessary input conversions. The program provides output both in impedance rectangular, R_r and X_r , and admittance rectangular, G_r and B_r , form.

The machine running time is approximately 3.5 seconds per data card. The program for these equations in the Bell General Purpose System for the IBM 650 is shown in Table 12.

Program 2. Determine the driving-point admittance characteristic of a crystal network.--This program was used to calculate the driving-point admittance characteristics of a complete crystal and holder over several

Table 12. Transmission Line Subtraction Program

Card No.	Order	Description
0	- - - - -	Problem No. Card
1	9 800 001 000	Program Point No. 1
2	7 000 525 527	Read input data, See Note 1
3	2 525 525 000	$G_s \times G_s$
4	4 526 526 500	$(G_s \times G_s) + (B_s \times B_s)$
5	3 525 000 524	Compute A
6	-3 526 500 523	Compute B
7	2 527 600 000	Compute df
8	2 000 602 501	Compute $1.2 df \cdot 10^{-8} = \theta$
9	0 353 501 502	Compute $\sin \theta$
10	0 354 501 000	Compute $\cos \theta$
11	3 502 000 503	Compute $\tan \theta = E$
12	5 523 601 506	Compute H
13	-2 524 503 507	Compute I
14	2 503 601 000	Compute EC
15	-1 523 000 505	Compute $G = B - EC$
16	2 524 506 000	Compute $AH = FH$
17	4 505 507 508	Compute $FH + GI = J$
18	-2 524 507 000	Compute $-FI$
19	4 505 506 509	Compute $GH - FI = K$
20	2 506 506 000	Compute $H \times H$
21	4 507 507 512	Compute $H \times H + I \times I = L$
22	2 508 508 000	Compute $J \times J$
23	4 509 509 514	Compute $J \times J + K \times K = M$
24	3 601 512 513	Compute $C / (H \times H + I \times I) = C/L$
25	2 000 508 528	Compute $CJ / (H \times H + I \times I) = R_r$
26	2 513 509 529	Compute $CK / (H \times H + I \times I) = X_r$
27	2 513 514 516	Compute CM/L
28	3 508 000 530	Compute $LJ/CM = G_r$
29	-3 509 516 531	Compute $-LK/CM = B_r$
30	7 300 527 531	Punch output
31	8 000 000 001	Return to program point 1
32	- - - - -	Constant Card, See Note 2
33	- - - - -	Start Compute Card

Note 1: Input cards contain frequency (cps) in 527, G_s (mhos) in 525, and B_s (mhos) in 526.

Note 2: Constant card inserts d in 600, $Z_0 = C$ in 601, and $1.2 \cdot 10^{-8}$ in 602.

frequency ranges. The particular usefulness was for reconstructing an ideal crystal characteristic from a set of calculated crystal parameters. The program permitted a direct comparison of the theoretical data with the original Crystal Measurements Standard data. This comparison method was often used as a guide for making vernier corrections in holder calculations to improve the accuracy of the resulting motional-arm data.

The equivalent circuit, which is the basis for the program, is shown in Figure 91. Any reasonable finite element values may be assigned to the parameters with the exception that neither C_0 nor C_1 may be zero. The same program may be used to calculate the admittance function for the holder only by making R_0 , R_1 , and L_1 zero and dividing the desired value of C_0 between C_0 and C_1 .

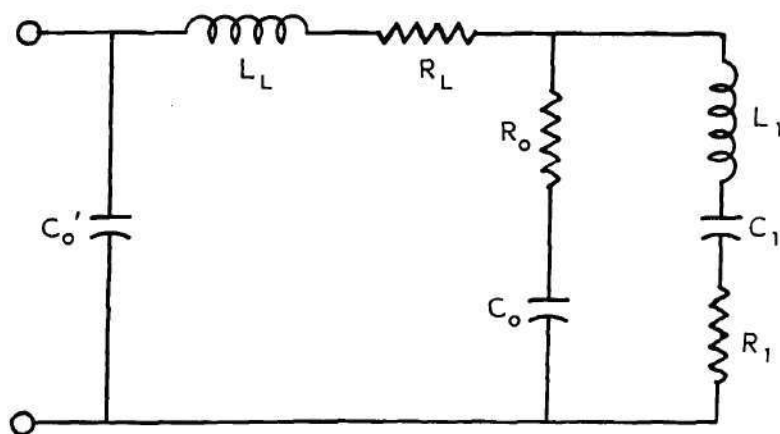


Figure 91. Circuit Diagram for Computer Program 2.

The program is arranged to calculate any number of complete crystal or holder only responses over any combination of frequency increments without reloading the program into the computer. This facility is accomplished by using two classes of input data cards:

Class 1 specifies all of the parameter values of Figure 91 and

Class 2 specifies the frequency range over which calculations are to be made, beginning at f_o , increasing the frequency by Δf for each new calculation, and restarting the program after N calculations (one or more cards of this type may be used).

A code number on the class 2 card indicated whether a new class 1 card or a new class 2 card is to follow. The computer will stop if the class 2 card is incorrectly coded. The computer also stops when no more input cards remain or when a class 2 card does not follow a class 1 card.

All data units are in ohms, mhos, henries, farads, or cycles per second.

The machine running time is determined by the number of data points to be calculated. The program in the Bell General Purpose System is shown in Table 13.

Program 3. Crystal holder analysis.--After appropriate crystal holder data have been obtained and the perfect circle approximations made to determine the data points which typically represent the holder, the parameters of the holder may be calculated by the following method.

The holder is assumed to be representable by the circuit of Figure 92. The impedance, Z_1 , is

$$Z_1 = R_L + j(\omega L_L - 1/\omega C_o) \quad (28)$$

and

$$\begin{aligned} Y_1 &= \frac{R_L}{R_L^2 + (\omega L_L - 1/\omega C_o)^2} - j \frac{L_L - 1/\omega C_o}{R_L^2 + (\omega L_L - 1/\omega C_o)^2} \\ &= G_1 + j\omega B_1. \end{aligned} \quad (29)$$

Table 13. Calculate Network Admittance Function Program

Card No.	Order	Description
0	- - - - -	Problem number card.
1	9 800 001 000	Program point no. 1.
2	7 000 500 508	Read class 1 cards. See note 1.
3	9 800 002 000	Program point no. 2.
4	7 000 508 511	Read class 2 card or cards. See Note 2.
5	1 508 900 525	Transfer f_o to output.
6	9 800 003 000	Program point no. 3.
7	2 525 904 400	Calculate $2\pi f_o$.
8	2 000 500 401	Calculate $2\pi f_o L_1$.
9	2 400 501 000	Calculate $2\pi f_o C_1$.
10	-3 901 000 402	Calculate $-1/2\pi f_o C_1$.
11	1 000 401 403	Calculate $-1/2\pi f_o C_1 + 2\pi f_o L_1 = X_1$.
12	2 000 000 000	Calculate $(X_1)^2$.
13	4 502 502 404	Calculate $(R_1)^2 + (X_1)^2$.
14	3 502 000 405	Calculate $R_1 / ((R_1)^2 + (X_1)^2) = G_1$.
15	-3 403 404 406	Calculate $-X_1 / ((R_1)^2 + (X_1)^2) = B_1$.
16	2 400 503 000	Calculate $2\pi f_o C_o$.
17	-3 901 000 407	Calculate $-1/2\pi f_o C_o = X_o$.
18	2 000 000 000	Calculate $(X_o)^2$.
19	4 504 504 408	Calculate $(R_o)^2 + (X_o)^2$.
20	3 504 000 409	Calculate $R_o / ((R_o)^2 + (X_o)^2) = G_o$.
21	-3 407 408 410	Calculate $-X_o / ((R_o)^2 + (X_o)^2) = B_o$.
22	1 406 000 412	Calculate $B_o + B_1 = B_2$.

Table 13. Calculate Network Admittance Function Program (Continued)

Card No.	Order	Description
23	1 405 409 411	Calculate $G_0 + G_1 = G_2$.
24	2 000 000 000	Calculate $(G_2)^2$.
25	4 412 412 413	Calculate $(G_2)^2 + (B_2)^2$.
26	3 411 000 414	Calculate $G_2 / ((G_2)^2 + (B_2)^2) = R_2$.
27	1 000 506 416	Calculate $R_2 + R_L = R_3$.
28	-3 412 413 415	Calculate $-B_2 / ((G_2)^2 + (B_2)^2) = X_2$.
29	4 400 505 417	Calculate $X_2 + 2\pi f_o L_L = X_3$.
30	2 000 000 000	Calculate $(X_3)^2$.
31	4 416 416 418	Calculate $(R_3)^2 + (X_3)^2$.
32	3 416 000 526	Calculate $R_3 / ((R_3)^2 + (X_3)^2) = G_3 = G_4$ $= G_1$.
33	-3 417 418 419	Calculate $-X_3 / ((R_3)^2 + (X_3)^2) = B_3$.
34	4 400 507 527	Calculate $B_3 + 2\pi f_o C_o = B_4 = B$.
35	7 300 525 527	Punch output. See note 3.
36	1 525 509 525	Increase f_o by Δf .
37	-1 510 901 510	Decrease N by 1.
38	8 600 510 003	Transfer to P.P. no. 3 if $N \neq 0$.
39	8 600 511 002	Transfer to read class 2 card if 511 $\neq 0$.
40	8 000 000 001	Transfer to read class 1 card.
41	- --- --- ---	Start compute card.

Note 1: Class 1 cards contain element values as follows: L_1 in 500, C_1 in 501, R_1 in 502, C_o in 503. R_o in 504, L_L in 505, R_L in 506,

C'_o in 507. At least 2 cards must be used since one card can contain at most 6 input data.

Note 2: Class 2 cards contain f_o in 508, Δf in 509, N in 510, and either zero or non-zero in 511. If 511 is zero, class 1 cards must follow. If 511 is non-zero, class 2 cards must follow.

Note 3: Output cards contain f in 525, G in 526, and B in 527.

Thus

$$Y_2 = G_2 + j B_2 \quad (30)$$

where

$$G_2 = G_1$$

and

$$B_2 = - \frac{L_L - 1/\omega C_o}{R_L^2 + (\omega L_L - 1/\omega C_o)^2} + \omega C'_o. \quad (31)$$

The maximum value of G_1 occurs when $\omega L_L = 1/\omega C_o$. Since $G_2 = G_1$ and is unaffected by the addition of the element C'_o , the maximum value of G_2 also occurs when $\omega L_L = 1/\omega C_o$ and is equal to $1/R_L$. Thus G_2 at any frequency is determined as a function only of frequency, L_L , and C_o according to the first term of equation 29 where R_L is simply $1/G_{2max}$.

The first half of equation 29 may be rewritten as

$$G_2 R_L^2 + G_2 (\omega L_L - \frac{1}{\omega C_o})^2 = R_L, \quad (32)$$

which becomes

$$\omega L_L - 1/\omega C_o = \pm \sqrt{\frac{R_L - G_2 R_L^2}{G_2}}. \quad (33)$$

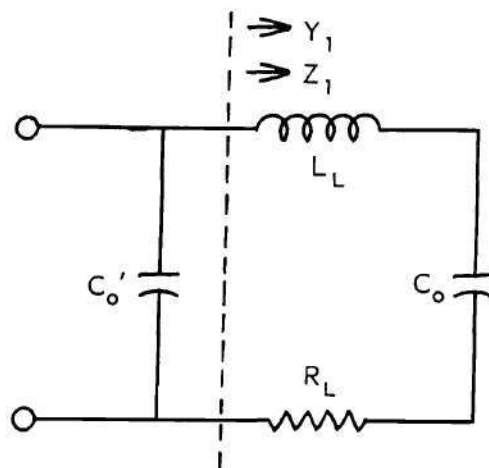


Figure 92. Circuit Diagram for Computer Program 3.

Let ω_1 be a frequency below $\omega_0 = 1/\sqrt{L_L C_o}$ and ω_2 be a frequency above ω_0 .

Then

$$\omega_1 L_L - 1/\omega_1 C_o = - \sqrt{\frac{R_L (1 - G_{2(1)} R_L)}{G_{2(1)}}} \quad (34)$$

and

$$\omega_2 L_L - 1/\omega_2 C_o = + \sqrt{\frac{R_L (1 - G_{2(2)} R_L)}{G_{2(2)}}} \quad (35)$$

The radicals of equations 34 and 35 must always be real since $G_{2\max} R_L = 1$.

Let K_1 be defined as

$$K_1 = \sqrt{\frac{R_L (1 - G_{2(1)} R_L)}{G_{2(1)}}} \quad (36)$$

and K_2 be defined as

$$K_2 = \sqrt{\frac{R_L (1 - G_{2(2)} R_L)}{G_{2(2)}}} \quad (37)$$

Then

$$\omega_1 L_L - 1/\omega_1 C_o = -K_1 \quad (38)$$

and

$$\omega_2 L_L - 1/\omega_2 C_o = K_2 \quad (39)$$

Multiply equation 38 by $-\omega_2$ and equation 39 by ω_1 and add to obtain

$$\frac{\omega_2}{\omega_1 C_o} - \frac{\omega_1}{\omega_2 C_o} = \omega_2 K_1 + \omega_1 K_2 \quad (40)$$

or

$$\frac{1}{C_o} = \frac{\omega_2 K_1 + \omega_1 K_2}{\frac{\omega_2}{\omega_1} - \frac{\omega_1}{\omega_2}} \quad (41)$$

or

$$C_o = \frac{\frac{\omega_2}{\omega_1} - \frac{\omega_1}{\omega_2}}{\omega_2 K_1 + \omega_1 K_2} \quad (42)$$

From equation 39

$$L_L = \frac{K_2 + 1/\omega_2 C_o}{\omega_2} \quad (43)$$

and from equation 31

$$C_o' = \frac{B_2 + \frac{\omega L_L - 1/\omega C_o}{R_L^2 + (\omega L_L - 1/\omega C_o)^2}}{\omega} \quad (44)$$

All quantities on the right side of equation 44 are known and C_0' may thus be evaluated at any value of ω . For convenience, either ω_1 or ω_2 is generally used for this evaluation.

Two variations of program 3 were written based upon equations 42, 43, and 44 and the fact that $R_L = 1/G_{2max}$. The program for the first variation in the Bell General Purpose System sets ω equal to ω_2 in equation 44. This program is listed in Table 14. The second variation sets ω equal to ω_1 in equation 44 and thus differs only to a minor extent.

Table 14. Crystal Holder Analysis

Card No.	Order
1	9 800 005 000
2	7 000 550 556
3	3 901 556 501
4	2 000 551 000
5	-1 901 000 000
6	2 000 501 000
7	3 000 551 000
8	0 300 000 557
9	2 501 554 000
10	-1 901 000 000
11	2 000 501 000
12	3 000 554 000
13	0 300 000 558
14	3 553 550 559
15	3 550 553 000
16	-1 559 000 560
17	2 904 550 561
18	2 904 553 562

Table 14. Crystal Holder Analysis (Continued)

Card No.	Order
19	2 000 557 000
20	4 561 558 000
21	3 560 000 503
22	2 562 000 000
23	3 901 000 563
24	1 000 558 000
25	3 000 562 502
26	2 562 000 000
27	-1 000 563 564
28	2 000 000 000
29	4 501 501 000
30	3 564 000 000
31	1 000 555 000
32	3 000 562 500
33	7 300 500 503
34	7 300 551 556
35	8 000 000 005

Note: The detailed operation of the program as well as the locations of the inputs, outputs, and constants can be traced by anyone sufficiently familiar with the Bell General Purpose System.

Program 4. Crystal holder subtraction.--This program was designed to subtract a holder equivalent circuit from a set of composite crystal admittance data. The program was used extensively for determining the motional-arm characteristics after the holder parameters had been calculated. The Hafner crystal equivalent circuit is the basis for the computations. Each of the holder elements may be assigned any finite value with the exception that C_0 must not be zero. The principal outputs are the conductance and

susceptance values for the motional arm. An additional output is provided, permitting the program to be used for the simultaneous subtraction of C'_0 only while the other calculations are being made.

The listing of the program is shown in Table 15.

Table 15. Crystal Holder Subtraction

Card No.	Order
01	7 000 500 504
02	9 800 001 000
03	7 000 527 531
04	2 527 904 510
05	2 000 500 000
06	-1 531 000 532
07	2 000 000 000
08	4 530 530 512
09	3 530 000 000
10	-1 000 501 513
11	2 510 502 514
12	-3 532 512 000
13	-1 000 514 515
14	2 000 000 000
15	4 513 513 516
16	2 510 503 517
17	-3 901 517 517
18	2 000 000 000
19	4 504 504 518
20	3 504 000 519
21	3 513 516 000
22	-1 000 519 528
23	3 517 518 520
24	-3 515 516 000
25	1 000 520 529

Table 15. Crystal Holder Subtraction (Continued)

Card No.	Order
26	7 300 527 532
27	8 000 000 001

Note: The detailed operation of the program as well as the locations of the inputs, outputs, and constants can be traced by anyone sufficiently familiar with the Bell General Purpose System.

Program 5. Crystal analysis composite.--Program 5 is a combination of programs 1, 2, 3, and 4 used to, first, subtract a transmission line length and, from the resulting data, determine the holder parameters, second, to calculate the holder admittances for later comparison with the original data, and third, to subtract the holder from the overtone responses, leaving only the motional-arm admittance data. This program will not be described in detail here since it can be readily reconstructed by anyone familiar with the previously described programs and the Bell General Purpose System.

This program was used extensively for rapid calculations of motional-arm parameters. The program 3 portion was modified on occasions to permit the holder parameters to be calculated by different methods.

APPENDIX III

SYMBOLS AND ABBREVIATIONS

The following symbols and abbreviations are used throughout this thesis with the meanings indicated:

B - a general or specific susceptance

B^+ - the plate supply voltage for a vacuum-tube circuit

C - a general or specific capacitance

C_o - the shunt holder capacitance of a crystal unit appearing across the motional arm

C'_o - the shunt capacitance at the external terminals of a crystal unit

C_1 - the capacitance of the motional arm of a crystal unit

G - a general or specific conductance

K - a multiplier of 1000

Kc or Kc/Sec - kilocycles per second

L - a general or specific inductance

L_L - the series holder inductance of a crystal unit

L_1 - the inductance of the motional arm of a crystal unit

Mc or Mc/Sec - megacycles per second

Q - the quality factor of a resonant circuit

R - a general or specific resistance

RFC - radio-frequency choke

R_o - a resistance sometimes placed in series with C_o

R_L - the series holder resistance of a crystal unit

R_1 - the resistance of the motional arm of a crystal unit

X - a general or specific reactance
Y - a general or specific admittance
Z - a general or specific impedance
 Z_0 - the characteristic impedance of a transmission line
 Z_R - the terminating impedance on a transmission line
avc - automatic volume or gain control
a-c - alternating-current
cm - centimeter
d-c - direct-current
f - frequency
l - the length of a transmission line
mw - milliwatt
r-f - radio-frequency
v - volt
 γ - the propagation constant of a transmission line
 Δ - an increment
 θ - an angle
 μv - microvolt
 λ - wavelength

APPENDIX IV

LITERATURE CITED

1. Havel, J. M., "Crystal Requirements for Future Military Equipment," Proceedings of the Tenth Annual Symposium on Frequency Control, Signal Corps Engineering Laboratories, Fort Monmouth, N. J., 1956, p. 440.
2. Edson, William A., Vacuum-Tube Oscillators, New York: John Wiley and Sons, Inc., 1953, p. 122.
3. Gruen, H. E., "Design Criteria for Vacuum-Tube Crystal Oscillators," Proceedings of the Eleventh Annual Symposium on Frequency Control, United States Army Signal Research and Development Laboratories, Fort Monmouth, N. J., 1957, p. 503.
4. Buchanan, John P., Handbook of Piezoelectric Crystals for Radio Equipment Designers, Wright-Patterson Air Force Base, Ohio: Wright Air Development Center, 1954, p. 38.
5. Cady, W. G., Piezoelectricity, New York: McGraw-Hill Book Company, Inc., 1946.
6. Buchanan, op. cit., p. 12.
7. Currie, J. and Currie, P., "Development by Pressure of Polar Electricity in Hemihedral Crystals with Inclined Faces," societe mineralogique de France, 3 (1880), pp. 90-93.
8. Voigt, W., "General Theory of the Piezo- and Pyroelectric Properties of Crystals," Abhandlungen der Gesellschaft der Wissenschaften zu Gottingen, 36 (1890), pp. 1-99.
9. Buchanan, op. cit., p. 17.
10. Van Dyke, K. S., "The Electric Network Equivalent of a Piezoelectric Resonator (abstract)," Physical Review, 25 (1925), p. 895.
11. Van Dyke, K. S., "The Piezoelectric Resonator and Its Equivalent Network," Proceedings of the Institute of Radio Engineers, 16 (1928), pp. 742-764.
12. Van Dyke, K. S., "The Electric Network Equivalent of a Piezoelectric Resonator (abstract)," Physical Review, 40 (1932), p. 1026.

13. Butterworth, S., Proceedings of the Physical Society, London, 27 (1915), pp. 410-424.
14. Dye, D. W., "Piezoelectric Quartz Resonator and Equivalent Electrical Circuit," Proceedings of the Physical Society, London, 38 (1926), pp. 399-458.
15. Cady, W. G., Piezoelectricity, New York: McGraw-Hill Book Company, Inc., 1946, p. 334.
16. Smith, P. H., "Transmission Line Calculator," Electronics, January 1939, p. 29.
17. King, R. W. P., Transmission-Line Theory, New York: McGraw-Hill Book Company, Inc., 1955.
18. Pochmerski, D., "VHF Crystal Impedance Meter AN/TSM-15," Proceedings of the Eleventh Annual Symposium on Frequency Control, United States Army Signal Engineering Laboratories, Fort Monmouth, N. J., 1957, p. 463.
19. Robertson, D. W., "A New Method for Measuring the Equivalent Parameters of VHF Quartz Crystals," Proceedings of the Tenth Annual Symposium on Frequency Control, Signal Corps Engineering Laboratories, Fort Monmouth, N. J., 1956, p. 323.
20. Gerber, E. A., and Koerner, L. F., "Methods of Measurement of the Parameters of Piezoelectric Vibrators," Proceedings of the Institute of Radio Engineers 46, No. 10, October 1958.
21. Robertson, D. W., Scott, T. R., and Wrigley, W. B., Investigation of Methods for Measuring the Equivalent Electrical Parameters of Quartz Crystals, Final Report, Project A-151, Engineering Experiment Station, Georgia Institute of Technology, May 1956.
22. Witt, S. N., Jr., and Woodcox, V. K., Investigation of Methods for Measuring the Equivalent Electrical Parameters of Quartz Crystals, Final Report, Project A-362, Engineering Experiment Station, Georgia Institute of Technology, October 1958.
23. Buchanan, op. cit., pp. 109-113.
24. Hafner, E., Measurements of VHF Crystal Parameters-A Graphical Method of Data Reduction, Engineering Report No. E-1216, United States Army Signal Engineering Laboratories, Fort Monmouth, N. J., September 1957.
25. Buchanan, op. cit., p. 474.

26. Edson, W. A., Clary, W. T., and Hogg, J. C., Jr., High-Frequency Crystal-Controlled Oscillator Circuits, Final Report, Project 131-45, Engineering Experiment Station, Georgia Institute of Technology, December 1950.
27. Gruen, H. E., and Plait, A. O., A Study of Crystal Oscillator Circuits, Final Report, Project E-050, Armour Research Foundation, Illinois Institute of Technology, Chicago, August 1957.
28. Robertson, D. W., Witt, S. N., Jr., and Free, W. R., Investigation of Methods for Measuring the Equivalent Electrical Parameters of Quartz Crystals, Progress Report No. 2, Project A-271, Engineering Experiment Station, Georgia Institute of Technology, October 1956.
29. Witt, S. N., Jr., and Denny, H. W., VHF and UHF Crystal Controlled Oscillators, Final Report, Project A-511, Engineering Experiment Station, Georgia Institute of Technology, June 1961.
30. Robertson, D. W., Witt, S. N., Jr., and Free, W. R., Investigation of Methods for Measuring the Equivalent Electrical Parameters of Quartz Crystals, Progress Reports No. 1, 3, and 4, Project A-271, Engineering Experiment Station, Georgia Institute of Technology, 1956-1957.
31. Witt, S. N., Jr., and Woodcox, V. K., Quartz Crystal Studies and Measurements, Phase II, Final Report, Projects No. A-402-1, -2, and -3, Engineering Experiment Station, Georgia Institute of Technology, February 1959.
32. Witt, S. N., Jr., "Crystal Measuring Techniques Above 200 Mc/Sec," Proceedings of the Eleventh Annual Symposium on Frequency Control, United States Army Signal Engineering Laboratories, Fort Monmouth, N. J., 1957, p. 478.
33. Witt, S. N., Jr., "VHF Crystal Parameter Measurements," Proceedings of the Twelfth Annual Symposium on Frequency Control, United States Army Signal Research and Development Laboratories, Fort Monmouth, N. J., 1958, p. 383.
34. Witt, S. N., Jr., "Methods for Measuring Quartz Crystal Units at VHF," Proceedings of the Thirteenth Annual Symposium on Frequency Control, United States Army Signal Research and Development Laboratories, Fort Monmouth, N. J., 1959, p. 137.
35. Witt, S. N., Jr., and Woodcox, V. K., Quartz Crystal Studies and Measurements, Final Report, Projects A-402-11, -12, and -13, Engineering Experiment Station, Georgia Institute of Technology, August 1960.
36. McKeown, D., "Design Parameters for VHF Crystal Units," Proceedings of the Twelfth Annual Symposium on Frequency Control, United States Army Signal Research and Development Laboratories, Fort Monmouth, N. J., 1958, p. 317.

VITA

Samuel N. Witt, Jr. was born in Seminole, Oklahoma, on January 29, 1928. He is the son of Samuel N. and Mary Mable Witt. He was married in 1947 to Miss Knoxie Stocker of Whitwell, Tennessee, and has three children.

He attended public schools in Madisonville, Tennessee; Murphy, North Carolina; Jasper, Tennessee; and Whitwell, Tennessee, and was graduated from the Whitwell High School as Valedictorian of his class in 1944. He attended the Tennessee Polytechnic Institute at Cookeville, Tennessee, as an undergraduate and received the Bachelor of Science in Electrical Engineering degree in 1950, after a two year period in the U. S. Navy from 1946 to 1948. He received the Engineering Medal for the highest four-year undergraduate average in engineering. He received the Master of Science in Electrical Engineering degree from the Georgia Institute of Technology at Atlanta, Georgia, in 1953.

His experience includes one year as Instructor at the Tennessee Polytechnic Institute from 1950 to 1951, two years as Research Assistant at the Engineering Experiment Station of the Georgia Institute of Technology from 1951 to 1953, nine years as Research Engineer at the Engineering Experiment Station from 1953 to 1962, and five years of part-time teaching in the School of Electrical Engineering of the Georgia Institute of Technology as Lecturer from 1956 to 1961. Since June, 1961, he has been employed as Vice President, Engineering, at RMS Engineering, Incorporated, Atlanta, Georgia. At the Engineering Experiment Station,

he has engaged in research activities in radar circuitry, transistor oscillators, cavity resonator systems, quartz crystal measurements, and quartz crystal oscillator design. He has directed several projects sponsored by the U. S. Army Signal Corps. He has presented and published several papers relating to frequency control and quartz crystal measurements. He is a member of Kappa Mu Epsilon, Eta Kappa Nu, Sigma Xi, a Senior Member of the Institute of Radio Engineers, and a Registered Professional Engineer in the State of Georgia.